

Some pages of this thesis may have been removed for copyright restrictions.

If you have discovered material in AURA which is unlawful e.g. breaches copyright, (either yours or that of a third party) or any other law, including but not limited to those relating to patent, trademark, confidentiality, data protection, obscenity, defamation, libel, then please read our [Takedown Policy](#) and [contact the service](#) immediately

SYNTHESIS AND SCREENING OF POTENTIAL ANTIMICROBIAL COMPOUNDS

PREETI PRAMOD GUNTHEY

Doctor of Philosophy

ASTON UNIVERSITY

December 2013

©Preeti Gunthey, 2013 asserts her moral right to be identified as the author of this thesis.

This copy of the thesis has been supplied on condition that anyone who consults it is understood to recognise that its copyright rests with its author and that no quotation from the thesis and no information derived from it may be published without appropriate permission or acknowledgement.

ASTON UNIVERSITY

SYNTHESIS AND SCREENING OF POTENTIAL ANTIMICROBIAL COMPOUNDS

A thesis submitted by Preeti Gunthey, for the degree of Doctor of Philosophy

December 2013

Abstract

Tuberculosis (TB), an infection caused by human pathogen *Mycobacterium tuberculosis*, continues to kill millions each year and is as prevalent as it was in the pre-antimicrobial era. With the emergence of continuously-evolving multi-drug resistant strains (MDR) and the implications of the HIV epidemic, it is crucial that new drugs with better efficacy and affordable cost are developed to treat TB. With this in mind, the first part of this thesis discusses the synthesis of libraries of derivatives of pyridine carboxamidrazones, along with cyclised (1,2,4-triazole and 1,2,4-oxadiazole) and fluorinated analogues. Microbiological screening against *M. tuberculosis* was carried out at the TAACF, NIAID and IDRI (USA). This confirmed the earlier findings that 2-pyridyl-substituted carboxamidrazones were more active than the 4-pyridyl-substituted carboxamidrazones. Another important observation was that upon cyclisation of these carboxamidrazones, a small number of the triazoles retained their activity while in most of the remaining compounds the activity was diminished. This might be attributed to the significant increase in logP value caused by cyclisation of these linear carboxamidrazones, resulting in high lipophilicity and decreased permeability. Another reason might be that the rigidity conferred upon the compound due to cyclisation, results in failure of the compound to fit into the active site of the putative target enzyme. In order to investigate the potential change to the compounds' metabolism in the organism and/or host, the most active compounds were selected and a fluorine atom was introduced in the pyridine ring. The microbiological results shows a drastic improvement in the activity of the fluorinated carboxamidrazones amides as compared to their non fluorinated counterpart. This improvement in the activity could possibly be the result of the increased cell permeability caused by the fluorine.

In a subsidiary strand, a selection of long-chain α , β -unsaturated carboxylic esters, α -keto, β -hydroxy carboxylic esters and β -keto, α -hydroxy carboxylic esters, structurally similar to mycolic acids, were synthesised. The microbiological data revealed that one of the open chain compound was active against the *Mycobacterium tuberculosis* H37Rv strain and some resistant isolates. The possible compound activity could be its potential to disrupt mycobacterial cell wall synthesis by interfering with the FAS-II

pathway.

Keywords : *Mycobacterium tuberculosis*, carboxamidrazone, cyclisation, fluorination, Horner-Wadsworth-Emmons modification to Wittig's reaction.

Acknowledgements

The work presented in this thesis would not have been possible without my close association with many people who were always there when I needed them the most. I take this opportunity to acknowledge them and extend my sincere gratitude for helping me make this PhD thesis a possibility.

First and foremost, I would like to thank my supervisor Dr. Daniel Rathbone for all his friendly guidance and patience. I am indebted to him for arranging several mechanisms sessions that helped me to gain a better understanding of chemistry. I am grateful to him for carrying out a painstaking task of proofreading this thesis.

I would like to thank the School of Life and Health Sciences and The Sir Richard Stapley Educational Trust for providing me financial support. I am grateful to EPSRC National Mass Spectrometry Service Centre (Swansea University) for providing the mass spectrometry data for the compounds synthesised in this thesis.

This work was supported by National Institutes of Health and the National Institute of Allergy and Infectious Diseases (NIAID), Contract No. HHSN272201100009I, Tuberculosis Antimicrobial Acquisition and Coordinating Facility (TAACF) through a research and development contract with the NIAID, Contract No. HHSN27200001 and Infectious Disease Research Institute (IDRI), Contract No. HHSN272201100009I / HHSN27200001.

A special word of thanks for Dr. Mike Davis, Karen Farrow and Tom Hinton for the help and continuous technical assistance during my PhD. I owe a sincere thanks to Gill Pilfold (Senior research administrator) and my colleagues Ren, Soumick, Alex, Matt, Pranav, Kshama, Cornelius and Shibu for always being there and bearing with me the good and bad times during my wonderful days of PhD.

Finally, I would like to thank my mom (Shubhada), dad (Pramod) and little sister (Supriya) for being very supportive and patient with me. To my uncle (Avinash) and aunt (Neelima) and my in-laws, thank-you for always being so wonderful and encouraging. And last but not the least I would like to thank my husband Ganesh. He was always there cheering me up and has been my rock throughout.

Contents

1	Introduction	22
1.1	Evolutionary history of tuberculosis and its discovery	23
1.2	TB epidemiology	24
1.3	Mechanisms of disease and immunological response	27
1.3.1	Overview of TB disease	27
1.3.2	Diagnosing TB	28
1.3.3	<i>M. tuberculosis</i> infection	28
1.3.4	Other mycobacteria causing the disease	29
1.4	The mycobacterial cell wall	30
1.4.1	General structure and functions	30
1.4.2	Peptidoglycan-arabinogalactan	31
1.4.3	Mycolic acids and their biosynthesis	32
1.4.4	Intercalation of free-outer lipids	39
1.5	Control of TB	41
1.5.1	Vaccines	41
1.5.2	WHO initiatives	42
1.5.3	Currently-used drugs	43
1.6	Treatment regimen	51
1.7	Drug resistance	52
1.8	Project aims	53
2	Chemistry and synthesis of heteroaryl amidrazone compounds	54
2.1	Introduction	54
2.2	Structure activity relationship studies	59

2.2.1	Imines	59
2.2.2	Ureas	60
2.2.3	Sulphonamides and <i>N</i> -oxides	60
2.2.4	Amides	60
2.2.5	General carboxamidrazone amide structure	61
2.3	Lead Optimisation	62
2.3.1	Intended variations of the building blocks in synthesis of carboxamidrazone	63
2.3.2	COMPOUND A (Carboxamidrazone amide)	65
2.3.3	COMPOUND B (<i>N</i> ¹ -[(alkyl)oxy]pyridyl carboximidamide)	66
2.3.4	COMPOUND C (Bis-amide version of carboxamidrazone)	66
2.4	Results and Discussion	67
2.4.1	COMPOUND A (Carboxamidrazone amide)	67
2.4.2	COMPOUND B (<i>N</i> ¹ -[(alkyl)oxy]pyridyl carboximidamide)	72
2.4.3	COMPOUND C (Bis-amide carboxamidrazone)	75
2.4.4	Purity	76
2.4.5	Solubility	77
2.4.6	NMR Data	77
2.4.7	Melting point data	79
2.4.8	Microbiological results	79
2.4.9	Structure activity relationship	84
2.5	Summary and Conclusion	84
2.5.1	Summary	84
2.5.2	Conclusion	95
2.6	EXPERIMENTAL	96
2.6.1	Chemicals	96
2.6.2	Instrumentation	96
2.6.3	Preparation of pyridine-2-carboxamidrazone (85)	97
2.6.4	Preparation of pyridine-4-carboxamidrazone (86)	97
2.6.5	Preparation of pyridine-2-amidoxime (87)	98
2.6.6	Preparation of pyridine-4-amidoxime (88)	99
2.6.7	General procedure for carboxamidrazone synthesis from acid chlorides	99
2.6.8	General procedure for synthesis of carboxamidrazone from acids	100

2.6.9	General method for preparation of Lithocholic acid derivatives	143
3	Cyclisation of carboxamidrazone amides	146
3.1	Introduction	146
3.2	Lead optimisation	148
3.2.1	Synthesis of the intended triazoles and oxadiazoles	149
3.2.2	COMPOUND D (1,2,4-triazole compounds)	151
3.2.3	COMPOUND E (1,2,4-oxadiazole compounds)	152
3.2.4	Cyclisation of urea compounds	152
3.2.5	Cyclisation of <i>N</i> -oxide compounds	153
3.3	Results and Discussion	153
3.3.1	COMPOUND D (1,2,4-triazole compounds)	153
3.3.2	COMPOUND E (1,2,4-oxadiazole compounds)	158
3.3.3	Attempted cyclisation of carboxamidrazone urea compounds	162
3.3.4	Cyclisation of <i>N</i> -oxide compounds	163
3.3.5	Purity	163
3.3.6	Solubility	164
3.3.7	NMR Data	164
3.3.8	Melting point data	166
3.3.9	Microbiological results	166
3.3.10	Structure activity relationship	169
3.4	Summary and Conclusion	170
3.5	EXPERIMENTAL	171
3.5.1	Chemicals	171
3.5.2	Instrumentation	171
3.5.3	General procedure for synthesis of 1,2,4-triazole from carboxamidrazone amide	171
3.5.4	General procedure for synthesis of 1,2,4-oxadiazole from aldoxime	202
4	Fluorinated Carboxamidrazone Derivatives	220
4.1	Introduction	220
4.2	Lead optimisation	222
4.3	Results and Discussion	223
4.3.1	Trifluoromethylation of heteroaryl amidrazone compounds using Langlois reagent	223

4.3.2	Trifluoromethylation of heteroaryl amidrazone compounds by photoredox catalysis method	225
4.3.3	Trifluoromethylation of heteroaryl amidrazone compounds using the Togni reagent	231
4.3.4	Synthesis of fluorinated carboxamidrazone amides	232
4.3.5	Purity	235
4.3.6	Solubility	235
4.3.7	Microbiological results	235
4.4	Summary and Conclusion	236
4.5	Experimental	238
4.5.1	Preparation of pyridine(2-fluoro)-4-carboxamidrazone (167)	238
4.5.2	Preparation of pyridine(5-fluoro)-2-carboxamidrazone (168)	238
4.5.3	Preparation of pyridine(3-fluoro)-2-carboxamidrazone (169)	239
4.5.4	General procedure for fluorinated carboxamidrazone amide synthesis from acid chlorides	240
4.5.5	General procedure for synthesis of fluorinated carboxamidrazone amide from acids	240
4.5.6	General procedure for trifluoromethylation of heteroaryl amidrazone compounds using Langlois reagent	244
4.5.7	General procedure for trifluoromethylation of heteroaryl amidrazone compounds by photoredox catalysis method	244
4.5.8	General procedure for trifluoromethylation of heteroaryl amidrazone compounds using the Togni reagent	245
5	Analogues of mycolic acids as potential inhibitors of mycobacterial cell wall synthesis	246
5.1	Introduction	246
5.2	Lead optimisation	248
5.3	Results and Discussion	249
5.3.1	Synthesis of α , β -unsaturated esters (alkene) by HornerWadsworthEmmons modification to Wittig's reaction	249
5.3.2	Synthesis of long chain aldehydes using Swern oxidation	252
5.3.3	Synthesis of β -hydroxy esters by Reformatsky reaction	254
5.3.4	Synthesis of 2-alkyl-2-hydroxy-3-oxocarboxylic esters	256
5.3.5	Attempted tertiary ketol rearrangement of 2-hydroxy-3-oxocarboxylic esters by di-n-butyltin oxide catalyst method	258

5.3.6	Microbiological results	258
5.4	Summary and Conclusion	260
5.5	Experimental	261
5.5.1	General preparation of α, β -unsaturated esters	261
5.5.2	General procedure for synthesis of aldehydes using Swern oxidation	264
5.5.3	General procedure for oxidation of α, β -unsaturated carboxylic esters	265
5.5.4	General procedure used for Reformatsky reaction	270
5.5.5	General procedure for tertiary ketol rearrangement using di-n-butyltin oxide catalyst	272

List of Figures

1.1	Tuberculosis epidemiology in 2011: World map of prevalence of all forms of TB per 100,000 inhabitants (WHO (2013))	25
1.2	Cases of tuberculosis worldwide, 1840 – 2010. Graph showing the decline in mortality due to <i>M. tuberculosis</i> infection from 1840 to today and enlarged version showing the graph of TB cases reported between 1980 to 2005 (McKeown et al. (1966), WHO (2009))	26
1.3	The mechanism of TB infection of macrophages in the broader view of tubercle formation in the lung. Adapted from Ben (2006).	29
1.4	The mycobacterial cell wall: structure and sites of drug action. The cell wall primarily consists of peptidoglycan layer (yellow & brown hexagons) which are in turn connected to the arabinogalactans (blue pentagons) by the galactan linkers (orange lines) These arabinogalactans are attached directly to the mycolic acids (red flagella like structures). The surface free lipids (green ovals) is made up of complexes like sulfatides, diacyltrehalose, phthiocerol dimycocerosates and polyacyltrehalose which are attached to the mycolic acids. The figure also depicts the site of action of some of the known anti-mycobacterial drugs. Assembled from Chatterjee (1997) and Crellin et al. (2013)	31
1.5	Structures of the main mycolic acids of <i>M. tuberculosis</i> H37Rv. The mero chain is longer than the alpha chain. Assembled from Barry III et al. (1998)	33
1.6	Mycolic acids subclasses from <i>M. tuberculosis</i> H37Rv. Assembled from Barry III et al. (1998)	34
1.7	The stereochemistry of the hydroxyl group and the α -methyl- β -methoxy group	34

1.8	The reaction sequence in FAS I: In step 1 the acetyl-CoA and malonyl-CoA covalently binds to the FAS-I enzyme. In step 3, β -ketoacyl-CoA synthase (elongase) condenses a long-chain acyl-CoA with two carbons from malonyl-CoA to form β -ketoacyl-CoA. The next step involves a three step reactions β -keto reduction, dehydration and enoyl reduction which produces the saturated butyryl-S-FAS-I molecule. Repeating these four steps for 9 and 12 cycles leads to C20- and C26-chains respectively, which are the main precursors of FAS-II. Assembled from Barry III et al. (1998)	35
1.9	The reaction sequence in FAS II: In step 1 the acetyl-CoA binds covalently to the FabH (FAS-II enzyme) active site cysteine. The next step involves decarboxylation of the malonyl-CoA, leaving a reactive carbon atom. The final step reaction is condensation of the malonyl-CoA with the fatty acyl chain and the β -ketoacyl-AcpM product is released. This reaction is catalysed by FabH. Assembled from Barry III et al. (1998)	36
1.10	An overview of mycolic acid synthesis. Assembled from Barry III et al. (1998) and van Roermund et al. (1998)	37
1.11	Example showing that a small change in the structure can alter the entire biosynthetic pathway.	38
2.1	The most active compounds synthesised by Mamolo et al. (1992).	55
2.2	List of the most active compounds synthesised by Billington et al. (2000)	56
2.3	N^1 -[3, 5-di-(tert-butyl)-2-hydroxybenzylidene]-pyridine-4-carboxamidrazone	56
2.4	Pyridine-2-carboxamidrazone N^1 -[3, 5-di-(tert-butyl)-2-hydroxybenzoyl] amide	57
2.5	General structures of the compounds synthesised by Ren (2009)	57
2.6	Two of the most active imines, a: N^1 -[(<i>E</i>)-[4-(1, 1-dimethylpropyl) phenyl] methyleneamino] pyridine-2-carboxamidine, b: N^1 -[(<i>E</i>)-(3, 5-ditert-butyl-2-hydroxy-phenyl) methyleneamino] pyridine-4-carboxamidine	59
2.7	Two examples of the urea derivatives, a: 1-[(<i>Z</i>)-[amino (4-pyridyl) methylene] amino]-3-(4-nitrophenyl) urea, b: 1-[(<i>Z</i>)-[amino (4-pyridyl) methylene] amino]-3-cyclohexyl-urea	60
2.8	List of amides, a: N^1 -[(<i>Z</i>)-[amino(4-pyridyl) methylene] amino]-4-heptyl-benzamide, b: N^1 - (4-Pentylbenzoyl)-pyridine-2-carboxamidrazone, general structures of azobenzoyl amide and general structure of benzoyloxybenzoyl amide carboxamidrazone	61
2.9	General structure of carboxamidrazone amide	62
2.10	Summary of previous work carried out in carboxamidrazone at Aston university.	62
2.11	General structures of the intended lead compounds to be synthesised	63

2.12	General structures of the Compound A (carboxamidrazone amides)	65
2.13	General structure of Compound B	66
2.14	General structure of Compound C	66
2.15	General structure of Compound C	75
2.16	Structure of <i>N</i> ¹ -(4-(10-Undecenoyl))-pyridine-4-carboxamidrazone	78
2.17	The comparison of partial NMR spectra of compound (39) shows the disappearance of the smaller peak in the nmr spectrum taken at 50°C.	78
2.18	The global minimum version of the linear side chain and cyclised side chain carboxamidrazone amide was generated using Cache program and van der Waal's surface was calculated on the compounds	79
2.19	Pyridine-2-carboxamidrazone	97
2.20	Pyridine-4-carboxamidrazone	97
2.21	Pyridine-2-amidoxime	98
2.22	Pyridine-4-amidoxime	99
3.1	Two structures for 1,2,4-triazole. A: the widely accepted structure of triazole. B: the structure of the pyrrodiazole.	147
3.2	Summary of the changes made in this study to the original lead compound.	148
3.3	Superimposed structures of the linear and cyclised compounds; (a) carboxamidrazone amide; (b) cyclised carboxamidrazone amide; The highlighted atoms were the superimpositioning sites; (c) superimposed; (d) superimposed side view.	149
3.4	General structure of 1,2,4-triazole compounds	151
3.5	General structure of Compound B	152
3.6	General structure of Compound C	152
3.7	General structure of Compound D	153
3.8	The two form of 1,2,4-triazole compound	164
3.9	Structure of 2-[5-(4-butoxyphenyl)-1H-1,2,4-triazol-3-yl]pyridine	165
3.10	A comparison of NMR spectra representing two forms of 2-[5-(4-butylphenyl)-4H-1,2,4-triazol-3-yl]pyridine.	165
3.11	MIC value as a function of logP	170
4.1	Ezetimibe: an example representing the significant contribution of fluorine substitution on metabolic stability.	221

4.2	Active compounds for CF ₃	222
4.3	Structure of the proposed fluorine containing compounds	223
4.4	Proposed mechanism for direct trifluoromethylation of arenes by photoredox catalysis. Assembled from Nagib & MacMillan (2011)	226
4.5	Fluorine NMR showing the ratio of desired product to impurities.	229
4.6	Fluorine NMR showing increase in the desired product.	230
4.7	Pyridine(2-fluoro)-4-carboxamidrazone	238
4.8	Pyridine(5-fluoro)-2-carboxamidrazone	238
4.9	Pyridine(3-fluoro)-2-carboxamidrazone	239
5.1	The key intermediate in mycolic acid pathway and its analogue	247
5.2	Generic structure of the proposed compounds	248

List of Tables

1.1	Common treatment regimens for patients suffering from drug-resistant tuberculosis. . . .	43
1.2	Commonly used TB drugs and their mechanisms.	44
1.3	Treatment regimens for Latent TB infection.	51
1.4	Basic treatment regimens for TB infection.	52
2.1	The list of the most active compounds against <i>M. tuberculosis</i> along with their IC ₅₀ and IC ₉₀ values synthesised by Ren (2009)	58
2.2	List of acid chlorides and acids used in the synthesis of carboxamidrazone amides	64
2.3	List of analogues of compound A	71
2.4	List of analogues of compound B	75
2.5	The MIC values and IC ₅₀ and IC ₉₀ values of the most active compounds	82
2.6	The MIC values and IC ₅₀ and IC ₉₀ values of the most active compound	83
2.7	The Macrophage assays values and MTT values of the most active compound	83
2.8	List of the carboxamidrazone amide compounds synthesised at Aston laboratory along with their biological activity.	90
2.9	List of the carboxamidrazone amide compounds synthesised at Aston laboratory along with their biological activity.	94
3.1	Comparison of three nomenclature systems.	147
3.2	Acid chlorides and acids used in synthesis of cyclised compounds	151
3.3	List of analogues of compound D	158
3.4	List of analogues of compound E	161
3.5	The IC ₅₀ and IC ₉₀ values of the triazole compounds when tested against <i>Mycobacterium tuberculosis</i> at the NIAID	168

3.6	The MIC, IC ₅₀ and IC ₉₀ values of the oxadiazole compounds when tested against <i>Mycobacterium tuberculosis</i> at the NIAID	169
4.1	Table of experiments for cyclisation	231
4.2	List of analogues of fluorinated carboxamidrazones.	234
4.3	The first stage microbiological data summary of the fluorinated carboxamidrazone amides.	235
4.4	Microbiological data for the Control drug used in the first stage analysis.	236
4.5	The second stage MIC data summary of the fluorinated carboxamidrazone amides.	236
5.1	Aldehyde and ketones used in synthesis of α, β -unsaturated esters	249
5.2	Summary of alkenes prepared along with their yields	252
5.3	List of analogues of 2-alkyl-2-hydroxy-3-oxocarboxylic esters and 3,3-dialkyl-3-hydroxy-2-oxocarboxylic ester.	257
5.4	Table representing the first stage microbiological data for the 2-alkyl-2-hydroxy-3-oxocarboxylic esters.	259
5.5	The second stage MIC data summary of the 2-alkyl-2-hydroxy-3-oxocarboxylic esters.	259
5.6	The second stage MIC data summary of the fluorinated carboxamidrazone amides.	260

List of Schemes

2.1	Synthetic scheme A for Compound A	67
2.2	Synthetic scheme B for Compound A	67
2.3	Synthetic scheme C for Compound A	68
2.4	Synthetic scheme A for Compound B	72
2.5	Synthetic scheme B for Compound B	72
2.6	Synthetic scheme for Compound C	76
3.1	Scheme for the synthesis of 1,2,4-triazole compound from condensation of carboxamidrazone amide.	153
3.2	Scheme for the attempted synthesis of 1,2,4-triazole compound from condensation of bile acid related carboxamidrazone amide.	154
3.3	Scheme for the synthesis of 1,2,4-oxadiazole compound from condensation of aldoxime.	158
3.4	Scheme for the cyclisation of urea derivative of carboxamidrazone amides.	162
4.1	Scheme for the trifluoromethylation of the heteroaryl amidrazone compounds using Langlois reagent. Adapted from Ji et al. (2011)	224
4.2	Scheme for the trifluoromethylation of the heteroaryl amidrazone compounds using Togni reagent	232
4.3	Scheme for the synthesis of fluorinated caxboxamidrazone amide.	232
5.1	A complete synthetic scheme for the proposed target compounds	248
5.2	Scheme for synthesis of α, β -unsaturated esters (alkene) by HornerWadsworthEmmons modification to Wittig's reaction	249
5.3	Scheme for synthesis of long chain aldehydes and ketones from primary alcohols using Swern oxidation	253
5.4	Scheme for synthesis of β hydroxy esters by Reformatsky reaction	255

5.5	Scheme for synthesis of 2-alkyl-2-hydroxy-3-oxocarboxylic esters by direct oxidation method by potassium permanganate	256
5.6	Attempted scheme for synthesis of 2-alkyl-2-hydroxy-3-oxocarboxylic esters by catalytic rearrangement method	258

Abbreviations

2PY 2-Pyridine carboxamidrazone

4PY 4-Pyridine carboxamidrazone

M. tuberculosis *Mycobacterium tuberculosis*

AG Arabinogalactan

AIDS Acquired immunodeficiency disease

AMK Amykacin

ART Antiretroviral therapy

BCG Bacille Calmette-Guérin

bTG Beta-Thromboglobulin

CDCP Centres for disease control and prevention

CDI 1,1'-Carbonyldiimidazole

CNS Central nervous system

CYS Cycloserine

DCM Dichloromethane

DIM Phthiocerol dimycocerosate

DMAP 4-Dimethylaminopyridine

DME Dimethyl ether

DMF Dimethylformamide

DMSO Dimethyl sulfoxide

DNA Deoxyribonucleic acid

DOTS Directly observed therapy short course

EMB Ethambutol

FabH Malonyl-CoA ACP transacylase

FAS-I Fatty acid synthesis-I

FAS-II Fatty acid synthesis-II

FATP Fatty acyl-tetrapeptide

GIT Gastrointestinal tract

GMM Glucose monomycolate

GPL Glycopeptidolipid

HIV Human immunodeficiency virus

HTS High throughput screening

HWE Horner-Wadsworth-Emmons

IC Inhibitory concentration

IDRI Infectious Disease Research Institute

INH Isoniazid

InhA Enoyl-ACP reductase

IR Infrared spectroscopy

KM Kanamycin

LORA Low Oxygen Recovery Assay

LOS Lipooligosaccharide

LTBI Latent TB infection

MA Mycolic acid

MABA Microplate Alamar Blue Assay

MAC *Mycobacterium avium* complex

mAGP Mycolyl-arabinogalactan-peptidogalactan complex

MBC Minimal Bactericidal Concentration

MDG Millennium development goal

MDR Multidrug resistant

MIC Minimum inhibitory concentration

MOPAC Molecular orbital package

MRSA Methicillin-resistant *Staphylococcus aureus*

MS Mass spectrum

NAG *N*-acetylglucosamine

NAM *N*-acetylmuramic acid

NIAID National Institute of Allergy and Infectious Diseases

NMR Nuclear magnetic resonance

PASA *p*-Aminosalicylic acid

PG Peptidogalactan

PGL Phenolic glycolipid

PZA Pyrazinamide

R_f value Retention factor

rBCG Recombinant Bacille Calmette-Guérin

RMP Rifampicin

RNA Ribonucleic acid

SL Sulfolipid

SRI Southern Research Institute

STM Streptomycin

TAACF Tuberculosis Antimicrobial Acquisition and Coordinating Facility

TB Tuberculosis

TDM Trehalose 6,6-dimycolate

THF Tetrahydrofuran

TLC Thin layer chromatography

TMM Trehalose monomycolate

UV Ultra violet

WHO World health organization

XDR Extensively drug-resistant

Chapter 1

Introduction

"I have no business to live this life if I cannot eradicate this scourge from mankind" -Robert Koch (1882)

Ever since the human history is recorded Tuberculosis (TB) has been a curse to mankind. TB is a highly contagious, air-borne disease. The TB bacilli upon entering the lungs trigger the immune system and get trapped in granulomas. It is a chronic granulomatous disease mainly affecting the respiratory tract, however, sometimes it may also affect the lymphatic, uro-genital, or nervous system or even the gastrointestinal tract in some critical cases (Raviglione et al. (1995)). TB is caused by the *Mycobacterium tuberculosis*. The early detection of TB is difficult since no symptoms are usually observed in initial stages. However in the later stage of the disease cough is the most common symptom. The other symptoms include low blood pressure, dyspnea, tachycardia and cyanosis.

TB accounts for numerous deaths each year. In the recent times followed by AIDS, TB is reported to be one of the major reasons for the deaths. The World Health Organization (WHO) and the Centres for Disease Control and Prevention (CDCP) have predicted 3.5 million deaths each year in the early decades of 2000. Figures stated in the WHO reports suggests that about one third of the population is already infected by TB with about 8 million more people developing active disease each year. It is estimated that about two million people die each year due to TB. However about 90 – 95% of the infections remain asymptomatic as they are contained by the immune system. The TB bacillus is opportunistic and can stay dormant for years in a healthy body. The chances of developing active TB increase in these patients if the immune system is weakened, for example by an HIV infection or treatment with immuno-suppressants like in the case of the organ transplants also indirectly contribute to developing

TB (Comstock (2000)).

The continued high burden of fighting TB in the developing countries has less to do with a biomedical understanding of the disease and treatment and more to do with the failure to understand the social conditions of the disease. The inequality in TB occurrence around the world highlights the importance of understanding the disease within social, cultural and historical contexts of these populations. In all the developing countries social determinants of health including poor housing conditions, unemployment, and inferior health care experiences are involved in contributing to the high disparity of disease (Reading & Wien (2009)). Some other reasons are minimal exposure to sun light and excessive exposure to ultraviolet light.

1.1 Evolutionary history of tuberculosis and its discovery

Terms like consumption, phthisis, scrofula, Pott's disease, tabes, bronchitis, inflammation of lungs, hectic fever, gastric fever, lupus and the white plague observed in ancient literature refer to TB. TB is also called Koch's disease, named after a German scientist Robert Koch (1843 – 1910), who in 1882 first discovered *M. tuberculosis*, the bacterium which causes TB in humans and mammals.

The TB bacterium has co-evolved with humans for several thousands or perhaps millions of years (Rothschild et al. (2001), Hershkovitz et al. (2008)). Although it is still unclear how humans were infected, a popular belief suggests that the TB originated in the bovine and then transferred to the humans through domestication of these animals. However recent studies have found that the *M. tuberculosis* complex (MTBC) obtained from the animals and humans did not match and suggests that it originated from a common ancestor. Hershkovitz et al. (2008) discovered the 9,000 years old Neolithic era human skeletal remains infected with TB. The evidence of TB has also been found in Egyptian mummies dating from 2400 – 3000 BC (Zink et al. (2003)). The oldest known fossil remains showing signs of TB infection are 500,000 years old Homo erectus skeleton in Turkey (Kappelman et al. (2008)).

Although the mention of TB has been observed in ancient literature of Hippocrates and Aristotle in the early 400 BC, it was the Roman doctor, Caelius Aurelianus who made the first accurate description of the disease making detailed observations of his patients in the 5th century AD. In early 18th century the English physician Benjamin Marten (c.1690 – 1756) wrote a book 'A New Theory of Consumptions' in 1720 in which he correlated the 'phthisis' a greek term for the disease consumption as it was then

called with the 'animalcules' that lived in the lungs and caused lesions. He also proposed a theory that 'phthisis' was the highly contagious disease as opposed to it being hereditary which was a popular belief back then (Doetsch (1978)).

The term 'tuberculosis' was coined by the German scientist Johann Lukas Schönlein (1793 – 1864) in 1839 who thought of TB as cancer like tumour. The word tuberculosis was derived from tubercles a word introduced by an English physician Richard Morton (1637 – 1698) to describe the lesions of the disease 'consumption'. In 1843 Philipp Klencke (1813 – 1881) carried out an experiment to demonstrate the contagiousness of TB, whereby a rabbit was injected with a tubercle material and it contracted the disease and subsequently died. The 'animalcule' described by Marten was not discovered until 1882, when Robert Koch isolated a bacillus within tubercles. He developed a tuberculin skin test, from the extracts of tuberculin from the dead *M. tuberculosis* cells, which was used to identify the TB patients, a work for which he received a Nobel Prize in 1905 (Herzog (1998)).

1.2 TB epidemiology

The World Health Organization (WHO) presented a Global Tuberculosis Report in 2012. On a positive note, the Millennium Development Goal (MDG) target to arrest the TB epidemic by the year 2015 has already been achieved. The development of new cases of TB have gone down to 2.2% between 2010 to 2011. The last few decades since 1990's, the mortality rate has decreased by 41% and the worldwide target of 50% reduction in mortality rate by 2015 is on track. However the global TB burden remains gigantic. In 2011, approximately 8.7 million new cases of TB were reported of which 13% were co-infected with HIV and 1.4 million people died from TB. TB continues to remain one of the top reasons for death among women, with 500,000 deaths in 2011 (WHO (2013)).



The boundaries and names shown and the designations used on this map do not imply the expression of any opinion whatsoever on the part of the World Health Organization concerning the legal status of any country, territory, city or area or of its authorities, or concerning the delimitation of its frontiers or boundaries. Dotted lines on maps represent approximate border lines for which there may not yet be full agreement.

Figure 1.1: Tuberculosis epidemiology in 2011: World map of prevalence of all forms of TB per 100,000 inhabitants (WHO (2013))

The report also suggests that the African and European regions are not on track to reduce the mortality rate to 50% of the 1990's by 2015. While the mortality and incidence rates are falling, the multidrug-resistant TB (MDR-TB) cases are increasing. About 19% i.e. one among every five TB patient is estimated to have MDR-TB. The countries like India and China where the largest number of TB cases are observed the number is less than one in ten, however this figure is expected to go up in next three years (WHO (2013)). Of the top fifteen countries with highest TB incidences, thirteen are in Africa, of which most are sub-Saharan (see Fig. 1.1). The developing countries face huge problems with regard to affording large quantities of antibiotics and logistically dispensing the drugs due to huge number of incidences of TB.



Figure 1.2: Cases of tuberculosis worldwide, 1840 – 2010. Graph showing the decline in mortality due to *M. tuberculosis* infection from 1840 to today and enlarged version showing the graph of TB cases reported between 1980 to 2005 (McKeown et al. (1966), WHO (2009))

The global threat caused by TB was once again brought forward in late 1980s after about a period of two decades due to HIV (see Fig. 1.2). The 2009 WHO report estimated that of total TB cases reported about 14.8% were coincident with HIV infection and majority of the incidences occurred in Africa. Since the probability of TB infection is greatly increased in immuno-compromised people, HIV added a new dimension to the TB epidemic. One such research has shown an interesting observation between TB and HIV. The *M. tuberculosis* bacteria modifies chemokine and cytokine concentrations, as well as their

receptors, in such a way that it not only permits but also boosts viral replication (Hanna et al. (2005), Toossi (2003)).

WHO in 2004 first recommended collaborative TB/HIV activities to combat the disease. This implementation of collaborative TB/HIV activities saved an estimated 1.3 million lives between 2005 and the end of 2011. In 2011 the number of TB patients tested for HIV went up from 3% in 2004 to 69% in the African Region. Globally, 48% of the TB patients known to be HIV positive were started on antiretroviral therapy (ART) in 2011. To meet WHO's recommendation all TB patients living with HIV are promptly started on ART.

1.3 Mechanisms of disease and immunological response

1.3.1 Overview of TB disease

TB disease primarily affects the lungs and about 75% of the cases reported are pulmonary. In about 15 – 20% of active cases, the infection spreads outside the respiratory organs, causing other kinds of TB. These are collectively denoted as 'extrapulmonary tuberculosis'. It is usually observed in immunosuppressed persons and young children. Most commonly it is observed in the lymphatic system, pleura, bones and joints (most often the spine), the nervous system, liver and spleen. In some rare cases the TB is dispersed widely throughout the body and it called as 'Miliary TB'.

The symptoms of TB do not appear until the infection reaches the lungs. Unlike the other bacteria *M. tuberculosis* has a slower replication process and hence the symptoms precipitate years after the individual was infected by the disease. The symptoms of active TB are not very specific and depend on the localization of the disease. The most evident symptom is in the lungs (pulmonary TB), but can affect other organs such as the lymph nodes, the spine, the pleura, bones, abdomen or meninges (extrapulmonary TB). The most common symptoms for pulmonary TB include productive cough (for more than 2 weeks), weight loss, fever (night sweats), haemoptysis and breathlessness (Miller et al. (2000)). In addition to this, symptoms can occur that are not related to the site of infection, for instance haematological abnormalities such as anaemia, as well as electrolyte imbalance and psychological effects (Chung & Hubbard (1969), Ebrahim et al. (1995), Sukhova (Sukhova)).

1.3.2 Diagnosing TB

An accurate and speedy detection of TB is required to halt the spread of disease and start the treatment immediately. This is especially important in cases of the patients who have TB coincident with the HIV infection. Since this disease is more prevalent in third world countries, cost effectiveness is an important factor to be considered while developing diagnostic equipments. The present methods to detect TB are tuberculin skin test, chest X-ray and/or microscopy, culturing and biopsy of the affected tissue. Another technique is using sputum smear test which is based on Ziehl-Neelsen staining technique and direct microscopy (Kim et al. (1984), Toman & Frieden (2004)). The use of this test is strongly advocated by WHO as it is cheap and a quick method. However this method is less sensitive as compared with culturing which can detect active disease from as few as 10 cells. The culturing method generates more data such as drug resistance and can also be used to detect extra-pulmonary disease, however its major drawback is the extensive time required for the cultures to grow (about 3-6 weeks).

1.3.3 *M. tuberculosis* infection

A person with active pulmonary TB expels infectious aerosol droplets when he coughs, spits or sneezes. With each sneeze or bout of cough about 40,000 droplets are released which can remain in the air for up to several hours hence increasing the chances of infection. The infectious dose of TB is very low hence fewer than 10 bacteria can cause infection thus further adding to the problem.

People who are in close or prolonged contact like family or the caretakers of the patient, are more prone to infection. Statistics suggest that each person with active untreated disease can infect about 10 – 15 other people each year (Organization et al. (2011)). Healthcare professionals, medical practitioners and laboratory scientists who are in close contact with the organism are also at high risk. The chances of TB infection is greatly increased in patients with HIV infections because of the compromised cell-mediated immune system which is essential for the defence against TB. Other factors include use of immunosuppressant drugs for the treatment of illnesses like diabetes, anti-cancer therapy etc. which can also increase the risk of infection. Young children and elderly people are also susceptible to TB owing to the underdeveloped or weaker immune system.

TB infection is developed by the ingestion of *M. tuberculosis* cells in the form of droplets in air which are engulfed by the macrophages that reach the alveoli. This triggers a series of events where due to

replication of the tubercle bacilli additional macrophages are brought into the area. This mass forms an early tubercle (see Fig. 1.3). After a few weeks many macrophages die and release the bacilli forming a caseous centre in the tubercle. In another few weeks a large cystic tubercle is formed which has an enlarged air filled caseous centre where the bacilli multiply extracellularly. This tubercle is surrounded by the infected macrophages and lymphocytes. When the tubercle matures it ruptures into a bronchiole and spills the bacilli which spreads the pathogen throughout the respiratory and other systems.

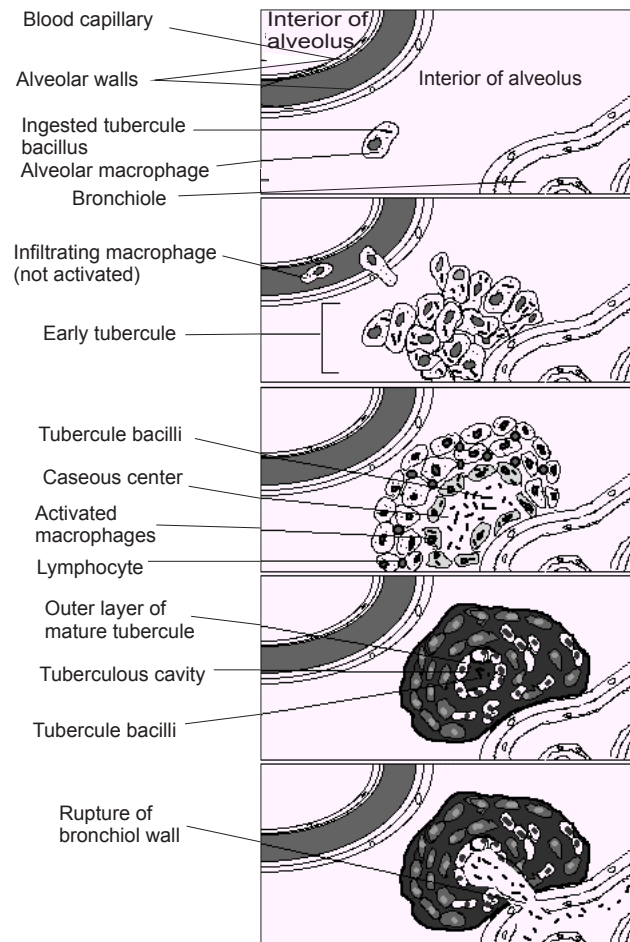


Figure 1.3: The mechanism of TB infection of macrophages in the broader view of tubercle formation in the lung. Adapted from Ben (2006).

1.3.4 Other mycobacteria causing the disease

The other pathogenic members of the *M. tuberculosis* complex causing TB are *Mycobacterium bovis*, *Mycobacterium africanum*, *Mycobacterium microti* and *Mycobacterium pinnipedii*. The *M. bovis* cause TB in animals, especially cattle, buffalo, and some wild animals like lion and baboon. *M. microti* causes TB in small mammals. *M. africanum* was isolated from ancient human remains in equatorial Africa. The *Mycobacterium pinnipedii* primarily infects seals. The other mycobacteria include *Mycobacterium*

avium complex (the avium tubercle bacillus), *Mycobacterium kansasii*, *Mycobacterium marinum* which cause granulomatous skin disease in humans, *Mycobacterium fortuitum* and *Mycobacterium chelonae*. Most of these mycobacteria cause TB or TB like diseases and are opportunistic in nature affecting the immuno-deficient people like young children, elderly people and those suffering from AIDS.

There are some other pathogenic mycobacteria which cause non tubercular diseases like *Mycobacterium leprae* which cause leprosy, *Mycobacterium ulcerans* which cause Buruli ulcers and *Mycobacterium avium paratuberculosis* which cause Crohn's disease.

1.4 The mycobacterial cell wall

1.4.1 General structure and functions

M. tuberculosis is a rod-shaped aerobic bacterium. Although *M. tuberculosis* does not fit into conventional Gram-positive or Gram-negative classification as its cell wall is resistant to Gram-staining techniques due to high lipid content, they are still classified as acid-fast Gram-positive bacteria due to their lack of an outer cell membrane (Wheeler & Ratledge (1994)). The primary function of this cell wall is to provide a permeability barrier for both the host's immune system and the anti-TB drugs (Brennan & Nikaido (1995)). It also acts as a protective shell around the bacterium that helps the bacteria to survive the cluttered environment inside infected macrophages (Takayama et al. (2005), Wang et al. (2000)). The unique cell wall of mycobacteria confers a characteristic acid-fast staining property to the bacteria. Additionally, the cell wall also interacts with the host cell causing immune modulation and virulence (Bhatt et al. (2007), Cox et al. (1999), Kan-Sutton et al. (2009)). It is believed that the close interaction of the complex high molecular weight lipids and polysaccharides within the cell wall renders the *M. tuberculosis* its characteristic pathogenesis (Minnikin et al. (2002)). The cell envelope consists of upper and lower segment. Beyond the membrane is a thin layer of peptidoglycan (PG) which is covalently linked to arabinogalactan (AG), which is in turn attached to mycolic acids with their long meromycolate and short α -chains. This complex structure is termed as the cell wall core the mycolyl-arabinogalactan-peptidoglycan (mAGP) complex and forms the lower segment. The upper segment is composed of free lipids interspersed with proteins and carbohydrates (Crick et al. (2001)) (see Fig. 1.4).

The bio-synthetic pathways in the synthesis of cell wall have been an attractive target for quite a long time for many anti-mycobacterial drugs like Isoniazid (INH) targets the enoyl-ACP reductase (InhA) in

fatty acid synthesis – II (FAS-II) pathway in mycolic acid bio-synthesis (Rozwarski et al. (1998), White et al. (2005)), Ethambutol (EMB) targets an arabinosyltransferase in arabinan biosynthesis (Belanger et al. (1996), Telenti et al. (1997)). A good understanding of the structure and bio-synthesis of the cell wall will not only enable the scientist to develop newer anti-mycobacterial drug targets but also help to puzzle out the mycobacterium and the host cell interaction.

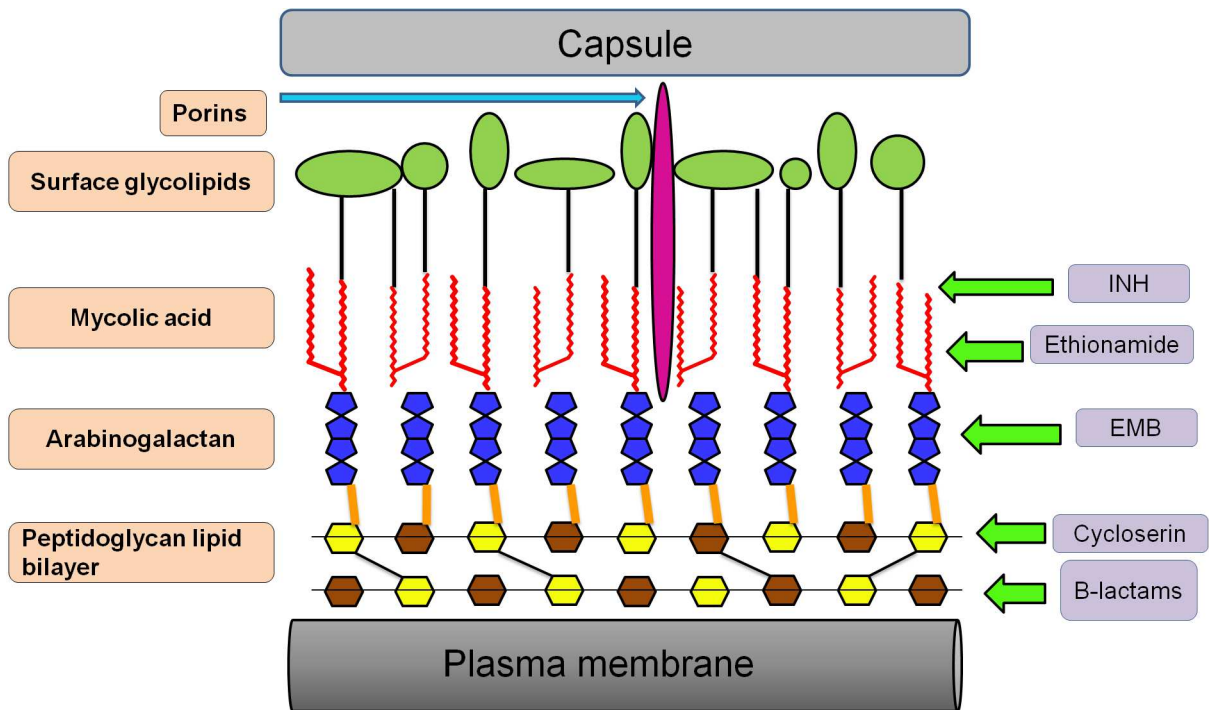


Figure 1.4: The mycobacterial cell wall: structure and sites of drug action. The cell wall primarily consists of peptidoglycan layer (yellow & brown hexagons) which are in turn connected to the arabinogalactans (blue pentagons) by the galactan linkers (orange lines) These arabinogalactans are attached directly to the mycolic acids (red flagella like structures). The surface free lipids (green ovals) is made up of complexes like sulfatides, diacyltrehalose, phthiocerol dimycocerosates and polyacyltrehalose which are attached to the mycolic acids. The figure also depicts the site of action of some of the known anti-mycobacterial drugs. Assembled from Chatterjee (1997) and Crellin et al. (2013)

1.4.2 Peptidoglycan-arabinogalactan

The principle part of the mycobacterial cell wall is composed of an insoluble cross-linked peptidoglycan layer (see Fig. 1.4) (Alderwick et al. (2007)). The PG layer consists of β -(1,4) linked *N*-acetylglucosamine (NAG), *N*-acetylmuramic acid (NAM) residues, and a tetra-peptide chain. These tetra-peptide chains form a three dimensional mesh like structure (Madigan (2005)). The bio-synthetic pathway of the PG is well delineated in *Escherichia coli* and it is believed that the biosynthetic process is similar between these two species (Goffin & Ghuysen (2002), van Heijenoort (2001)). The PG is not grafted into the cell membrane but is covalently bound to the arabinogalactan layer; a branched poly-

mer of arabinose and galactose, with a unique linker which forms a disaccharide bridge between the NAG end of PG and galactose containing non-reducing end of AG (McNeil et al. (1990)). The growth and the survival of mycobacteria depends heavily on the AG biosynthesis. The AG is situated right above the PG layer (see Fig. 1.4) and is formed of approximately 30 β -D-galactofuranose residues which is further elaborated by the arabinan chains (Alderwick et al. (2007)). Almost two third of these chains are esterified by the mycolic acids (Daffe et al. (1990)). This entire sandwich model of PG and AG esterified with mycolic acid is together known as mycolyl-arabinogalactan-peptidoglycan (mAGP) complex.

1.4.3 Mycolic acids and their biosynthesis

The cell wall in mycobacteria is unusual in that it consists of 60% lipids. In the early 1990s, scientists while isolating materials from the cell wall of *M. tuberculosis*, came across a mixture of many high molecular weight hydroxyl acids. The wax – like mass was then termed ‘mycolic acid’ by Anderson & Chargaff (1929). Though it has no direct relation to the anti-fungal agents, however it was named so, due to its structure which has long chains that appears like flagella. It was predicted that mycolic acid was mixture of lipids containing long chain molecules, liberating hexacosanoic acid following pyrolytic cleavage (Barry III et al. (1998)). Due to the lack of sophisticated analytical equipment, the exact structure was not known, however, the approximate empirical formula was suggested as $C_{88}H_{172}O_4$ or $C_{88}H_{176}O_4$. The once predicted as a single component mass, has now been identified as a component made up of over 500 closely related structures (Barry III et al. (1998)). This astounding number reflects the biological importance in the cell wall of *M. tuberculosis*.

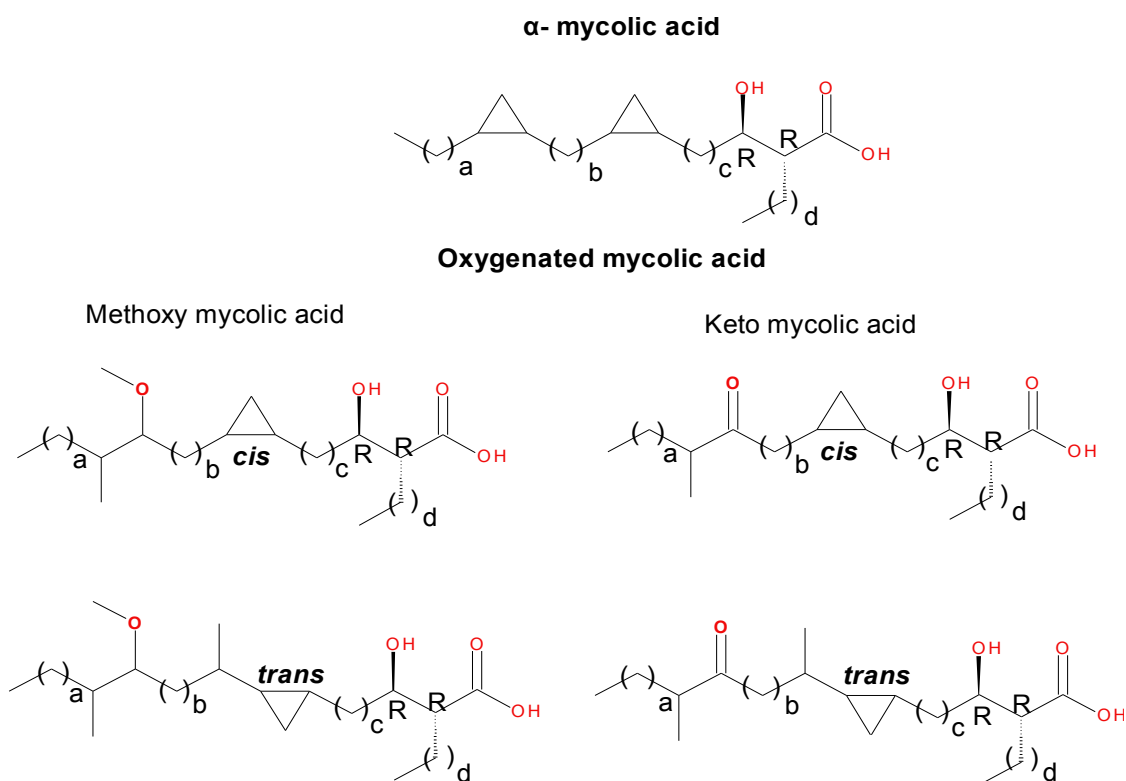


Figure 1.5: Structures of the main mycolic acids of *M. tuberculosis* H37Rv. The mero chain is longer than the alpha chain. Assembled from Barry III et al. (1998)

Mycolic acids (MA) are defined as β -hydroxy fatty acids with a long α -alkyl side chain. MA obtained from *M. tuberculosis* can be further divided into three classes: α -MA, methoxy-MA and keto-MA (see Fig. 1.5). The nomenclature of these mycolates have been assigned on the positioning of the oxygen function in the mero chain (see Fig. 1.6) (Asselineau et al. (1998), Minnikin (1982)). The term ' α ' has been assigned to the acid that lacks the oxygen function in addition to the 3-OH acid units. The α -MA consists of two cyclopropane groups in the mero chain: one is positioned in the proximal end (closer to the hydroxyl group) and other at the distal end (away from the hydroxyl group). Both the methoxy and keto MA have a *cis*- or *trans*-cyclopropane ring in the proximal end, however a methoxy MA have α -methyl- β -methoxy group at the distal end while keto MA has α -methyl- β -keto group at the distal end (see Fig. 1.5). When the methoxy and keto MA are in a *trans* position they have a methyl branch adjacent to the cyclopropane ring (Minnikin & Polgar (1967a), Minnikin & Polgar (1967b)).

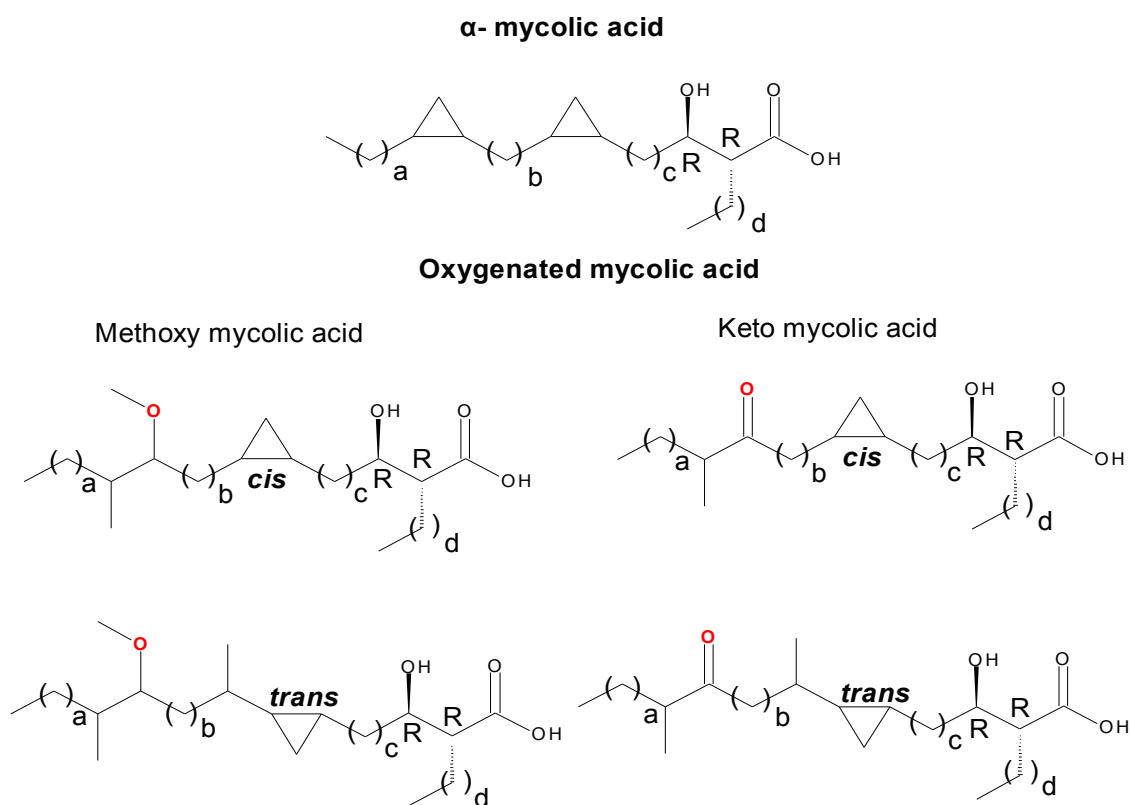


Figure 1.6: Mycolic acids subclasses from *M. tuberculosis* H37Rv. Assembled from Barry III et al. (1998)

Mycolic acids occur as a mixture of various chain lengths. These acids are formed as a result of combination of various fragments in the meromycolate chains like the *cis*- and *trans*- orientations of the cyclopropane group and the fragments like α -methyl- β -methoxy, α -methyl- β -keto, *cis*-alkene, α -methyl-*trans*-alkene, and α -methyl-*trans*-epoxy (Minnikin (1982)). A very little is known about the absolute stereo-chemistry of these compounds. However some evidence suggests that the hydroxyl group assumes *R,R* configuration and the α -methyl- β -methoxy at the distal end from the hydroxyl group assumes *S,S* configuration (see Fig. 1.7 (Daffe et al. (1991), Dubnau et al. (2000))).

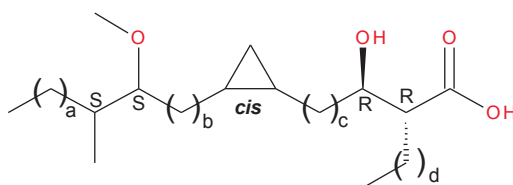


Figure 1.7: The stereochemistry of the hydroxyl group and the α -methyl- β -methoxy group

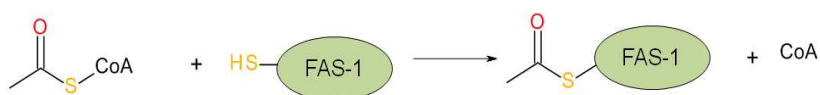
Different mycobacteria contain different sets of MA. The α -MA and α' -MA, with either *cis*- or *trans*- configuration with either one or two double bond and epoxy-MA (in *M. smegmatis* and *M. fortuitum*) (Lacave et al. (1987), Daffé et al. (1981)) to wax esters, ω -carboxy-MA, ω -1-methoxy-MA (Luquin et al.

(1990)) were isolated from other mycobacteria. The structure of the MA is closely related to the functions of these lipids; a small change in the structure can alter the entire functioning of the bacilli (Dubnau et al. (2000)). For example the cyclopropane ring is responsible for the cord formation which are toxic to humans (Minnikin et al. (2002)). The *cis* orientation of the cyclopropane ring encourages rapid growth of the bacteria in the macrophages (Rao et al. (2005)), while the *trans* orientation causes suppressive effects on the *M. tuberculosis* induced inflammation and virulence (Rao et al. (2006)).

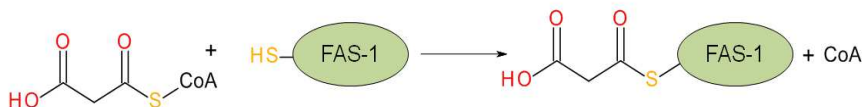
To synthesize these lipids mycobacteria employ two fatty acid synthases (FAS) namely FAS-I and FAS-II. FAS-I are multienzyme complexes found in the advanced prokaryotes and eukaryotes, and FAS-II is a disaggregated synthetase generally found in plants and bacteria (Raman et al. (2005))

FAS-I

1. Acetyl transacylation



2. Malonyl transacylation



3. Condensation



4. Reduction - Dehydration - Reduction

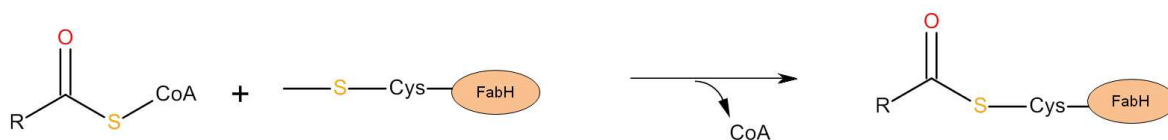


Figure 1.8: The reaction sequence in FAS I: In step 1 the acetyl-CoA and malonyl-CoA covalently binds to the FAS-I enzyme. In step 3, β -ketoacyl-CoA synthase (elongase) condenses a long-chain acyl-CoA with two carbons from malonyl-CoA to form β -ketoacyl-CoA. The next step involves a three step reactions β -keto reduction, dehydration and enoyl reduction which produces the saturated butyryl-S-FAS-I molecule. Repeating these four steps for 9 and 12 cycles leads to C20- and C26-chains respectively, which are the main precursors of FAS-II. Assembled from Barry III et al. (1998)

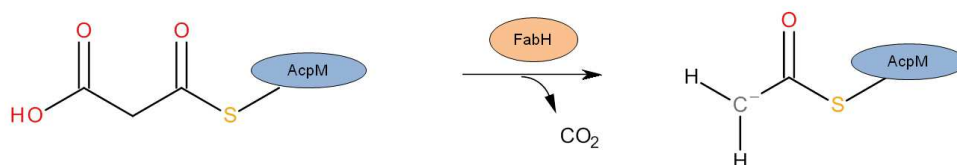
The synthesis of mycolic acid is initiated in the cell wall through the FAS I system where a multienzyme system causes elongation of the chain by two carbon atoms. The repetition of the four steps gives the desired long chain compounds. As step 1 acetyl-CoA and malonyl-CoA are converted to complexes acetyl-S-Enz and malonyl-S-Enz. In the step 2, condensation of these complexes takes place and a β -ketoacyl-C4-S-Enz is obtained, which after reduction, dehydration and enoyl reduction gives a butyryl-S-Enz. After repeating these steps several times C20 and C26 fatty acids are formed (see Fig. 1.8). Barry III et al. (1998) proposed that from this step the FAS II system is actively involved in the mycolic acid formation. A very long acid of α , methoxy and keto mycolic acids are synthesized. The C26 fatty acids i.e. hexacosanoyl –CoA produced in FAS-I become short α -alkyl chain and methyl carboxyl segments in all the three α , methoxy and keto mycolic acids. These are called merosegments. Barry III et al. (1998) defined meroacids as long α -alkyl chains of mycolic acids which are released in the form of meroaldehydes on pyrolytic cleavage.

FAS-II

1. Acyl transfer



2. Decarboxylation



3. Condensation

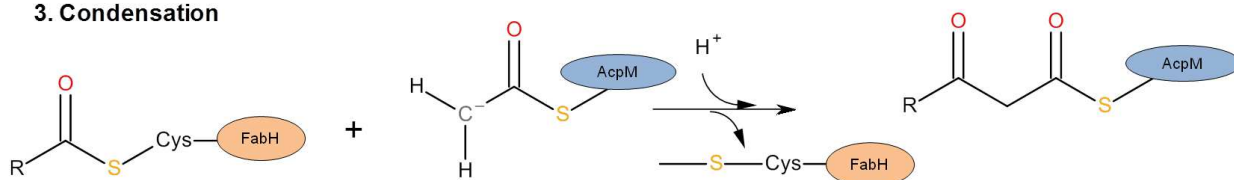


Figure 1.9: The reaction sequence in FAS II: In step 1 the acetyl-CoA binds covalently to the FabH (FAS-II enzyme) active site cysteine. The next step involves decarboxylation of the malonyl-CoA, leaving a reactive carbon atom. The final step reaction is condensation of the malonyl-CoA with the fatty acyl chain and the β -ketoacyl-AcpM product is released. This reaction is catalysed by FabH. Assembled from Barry III et al. (1998)

Followed by the FAS I, FAS II reactions take place where the malonyl-S-CoA is converted to malonyl-S-acyl carrier protein i.e. malonyl-S-ACP by the enzyme malonyl-CoA:ACP transacylase (FabD). The R-CO-S-ACP is converted to R-CHO-CH₂-CO-S-ACP in presence of two enzymes, β -ketoacyl ACP synthase (KasA/KasB) which is further reduced by the β -ketoacyl ACP reductase to R-CHOH-CH₂-CO-S-ACP. The third step is dehydration. R-CHOH-CH₂-CO-S-ACP is converted to R-CH=CH-CO-S-ACP (trans position) by β -hydroxyacyl ACP dehydrase. Step 4 is reduction. The product is then reduced to R-CH₂-CH₂-CO-S-ACP by 2-trans enoyl ACP reductase (InhA) (see Fig. 1.9). In this step a chain elongation takes place and then product is two carbons longer. This β -ketoacyl-AcpM product is again taken to be the part of reaction one and after several repetitions of all the steps a long chain compound is obtained. Claisen condensation: this is the last step and involves the final assembly of the mycolic acid in *M. tuberculosis* (see Fig. 1.10).

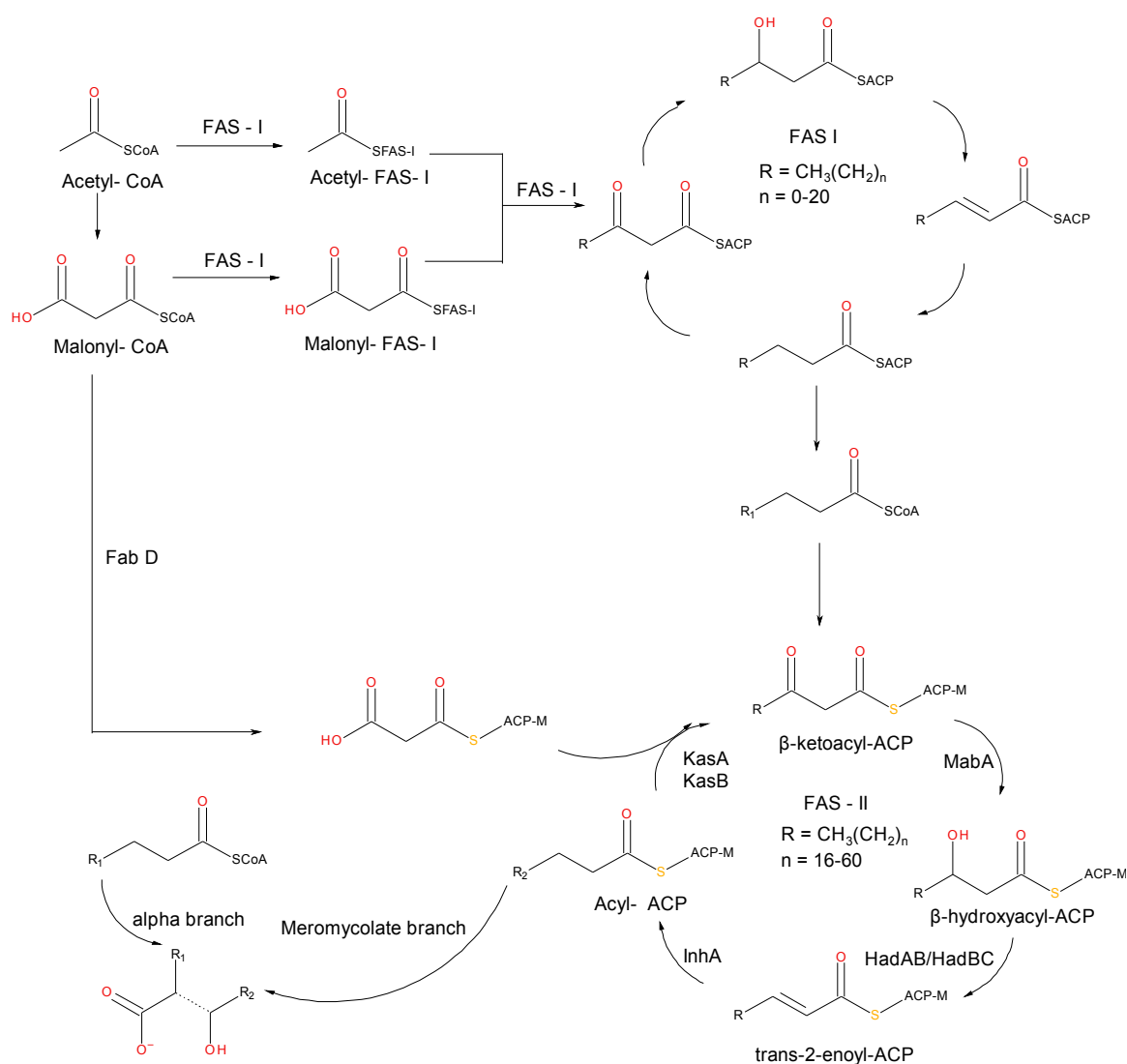


Figure 1.10: An overview of mycolic acid synthesis. Assembled from Barry III et al. (1998) and van Roermund et al. (1998)

Mycolic acid functions

The fundamental function of the mycolic acids, like all the fatty acids is to give a rigid shape to the cell, protection from external forces and a basic barrier function. In addition to this, mycolic acids provide resistance to chemicals causing dehydration or damage and thus improving its adeptness in surviving in unfavourable environment (Barry III et al. (1998)). It is almost impermeable to hydrophilic compounds and has very low permeability to hydrophobic compounds thus negating the use of common antibiotics (Barry III et al. (1998)).

Site of inhibition

Many of the present first line anti tuberculosis agents like Isoniazid, Pyrazinamide etc act on the mycolic acid pathways. Thus for many years scientists have considered the mycolic acid synthetic pathway of significant important potential site of inhibition. Many publications suggest that the in the first step of FAS II of mycolic acid synthesis there is uptake of long chain analogs of mycolic acids with the interrupter group present at the carboxyl end. This results into termination of the further synthesis of mycolic acid pathway. Thus it acts as an inhibitor.

Qureshi et al. (1994) suggests that (*Z*)-tetracos-5-enoic acid (1) is the key intermediate in the mycolic acid pathway; it stimulates α -mycolic acid synthesis. The cyclopropane analog of (*Z*)-tetracos-5-enoic fatty acid (2) was found to inhibit α -mycolate synthesis in *M. smegmatis* (see Fig. 1.11).

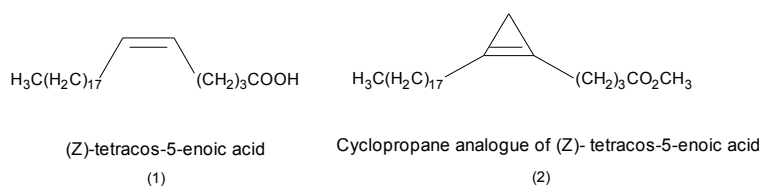


Figure 1.11: Example showing that a small change in the structure can alter the entire biosynthetic pathway.

Based on the above arguments, a study was carried out in Aston university, where long chain 2-hydroxy-3-oxocarboxylic esters were synthesized which are structurally similar to the mycolic acids. This is discussed in detail in Chapter 5.

1.4.4 Intercalation of free-outer lipids

As shown in the Fig. 1.4, the mycobacterial cell envelope is intercalated with various free glycolipids that are attached to the mAGP complex. This lipid rich outer layer is composed of complex lipids that have multiple methyl branched-fatty acids esterified to their backbone and various large molecules based on trehalose and phthiocerol like phthiocerol dimycocerosate (PDIM), phenolic glycolipid (PGL), mycolic acid containing lipids (TMM, TDM and GMM) and other kinds of complex lipids, such as glycopeptidolipids (GPLs) and lipooligosaccharides (LOSs).

Phthiocerol dimycocerosate (PDIM)

The PDIM is formed by esterification of long-chain phthiocerol or phthiodiolone with multiple methyl branched fatty acids like mycocerosic acids (Minnikin et al. (2002)). This lipid plays an important role in the early stages of the *M. tuberculosis* infection with macrophages. It also participates in receptor-dependent phagocytosis, phagosome acidification arrest, protecting the bacilli from reactive nitrogen intermediates and host cell membranes modification (Astarie-Dequeker et al. (2009), Rousseau et al. (2004)).

Phenolic glycolipid (PGL)

The PGL and PDIM are structurally similar molecules with the only difference being that the PGL has a glycosylated phenolic moiety at the end of the phthiocerol chain. PGL was generally observed in slow growing pathogenic mycobacteria such as *M. kansasii*, *M. gastri*, *M. ulcerans*, *M. leprae*, *M. marinum* and *M. tuberculosis* (Daffé & Lanéelle (1988)) and was classified under the class mycoside (Gastambide-Odier et al. (1967)). PGL is reported to possess several immuno-modulatory properties (Prasad et al. (1987), Vachula et al. (1989)) like the release of pro-inflammatory chemokines and cytokines (Reed et al. (2004)). Collins et al. (2005) carried out an experiment which demonstrates that decrease in the production of PGL decreases the virulence of the *M. bovis* in a Guinea pig infection model.

Mycolic acid containing lipids

Some mycolates can be extracted as free lipids; these lipids are covalently bound to trehalose or glucose to form trehalose monomycolate (TMM), trehalose 6,6"-dimycolate (TDM) and glucose monomycolate (GMM). GMM is synthesized by using the glucose from the host cell and can be an indicator of infection (Enomoto et al. (2005), Moody et al. (1997)). The TDM also known as the cord factor, is responsible for the convoluted growth of the *M. tuberculosis* as well as its virulence (Ryll et al. (2001)). The TDM also induces the release of chemokines and cytokines which contributes to its immuno-modulatory properties (Lima et al. (2001)). The other functions of TDM include enabling the bacterium to enter the host cell macrophages (Yasuda (1999)) and inducing the formation of granulomas (Behling et al. (1993), Borders et al. (2005)). TMM, a precursor of TDM, is responsible for the transport of mycolic acid to the cell wall AG (Katsube et al. (2007), Belisle et al. (1997)) and then gets converted to TDM before being ejected from the cytoplasm (Takayama et al. (2005)).

Sulfolipid (SL)

SL is composed of trehalose 2-sulfate core modified with 4 fatty acyl substituents and is found in some virulent strains of *M. tuberculosis* (Goren et al. (1976)). The exact function of this glyco-lipid is still unclear; it has been experimentally demonstrated that loss of SL has no impact on the bacilli replication (Kumar et al. (2007)).

Glycopeptidolipids (GPLs)

GPLs are a principle constituent in the outer layer cell wall of several species of mycobacteria. All the mycobacteria share a common structure of fatty acyl-tetrapeptide (FATP) and the pathogenicity of the mycobacteria is determined by the glycosylations of FATP (Chatterjee & Khoo (2001), Patterson et al. (2000)). A recent study has shown that GPLs participate in receptor-dependent phagocytosis of *Mycobacterium* by macrophages (Villeneuve et al. (2005)).

Lipooligosaccharides (LOS's)

LOSs are highly antigenic glycoconjugates present on the cell surface and are used as targets for serotyping. They are usually found in following members of the *M. tuberculosis* class *M. kansasii*, *M. gastri*, *M. marinum* and *M. Canetti* (Burguière et al. (2005), Daffe et al. (1991)). The biosynthesis and role of LOSs is still unclear.

1.5 Control of TB

The TB treatment has come long way since treating the unknown deadly disease to the patient specific chemotherapy. The use of drugs like sulphonamide and penicillins for the treatment of the infectious diseases had been around for a while, but these drugs were ineffective against TB bacteria. However after years of research Selman A. Waksman in 1944 successfully isolated an antibiotic streptomycin from *Streptomyces griseus*, the first anti-TB drug. A discovery for which he was awarded the Nobel prize in medicine in 1952. Although this drug had serious side-effects and within a few months of use had developed resistance against mutant strains, it proved that *M. tuberculosis* was no bacteriological exception and paved a way for further research in TB chemotherapy. The present day TB control involves two way attack through the use of vaccines and anti-TB drugs.

1.5.1 Vaccines

Currently only one vaccine against TB is available: Bacille Calmette-Guérin also called BCG vaccine; it is an attenuated live vaccine obtained from *Mycobacterium bovis*. In the early 1900s a French bacteriologist Albert Calmette along with Camille Guérin observed that under specific laboratory conditions and specific culture media the virulence of *Mycobacterium bovis* strain, which caused bovine TB, was reduced. An intensive research involving *in vitro* passaging of this strain and trials on different animal models were carried out for about 13 years, before they did the first human trial in 1921, which showed positive results (Behr (2002)). This BCG strain was then distributed around the world to various laboratories, where addition of different strains to the vaccines resulted in continued evolution of BCG. The present day vaccine dose not represent a single strain but a group of sub-strains. In 1974 the organisations like WHO, UNICEF and GAVI started a collaborative project called Expanded Programme on

Immunization. The project aimed to immunise every child across the world against fatal disease TB by 1990 (UNICEF 2010). The BCG vaccine has a highly variable efficacy, it reduces the risk of TB by about 50% in new borns and children (Colditz et al. (1995)). However its efficiency in adults ranges from 0-83% (Brewer (2000)).

This limited protection by BCG has encouraged the development of newer vaccines. Based on our current understanding of *M. tuberculosis* infection, and the use of specific genetic tools two main approaches are considered for development of new vaccines (i) boosting the BCG vaccination by expressing recombinant *M. tuberculosis* antigenic protein (known as recombinant BCG, rBCG) (Reed et al. (2009), Tchilian, Desel, Forbes, Bandermann, Sander, Hill & McShane (Tchilian et al.)) and (ii) creating attenuated strains of *M. tuberculosis* by deleting the genes responsible for replication or virulence (Aguilar et al. (2007), Waters et al. (2007)). Currently two rBCG candidates are in phase 1 clinical trials (Walker et al. (2010), Horwitz (2005)).

1.5.2 WHO initiatives

TB is generally treated with a combination of different drugs as a mono-drug therapy results into resistance to the drugs (Wang et al. (2006)). The standard TB treatment involves chemotherapy using isoniazid (INH), rifampicin (RMP), pyrazinamide (PZA) and ethambutol (EMB) for two months then it is followed up by INH and RMP for next four months. In the case of latent TB, WHO recommends a follow up by INH and RMP for two months after the standard treatment (Organization et al. (2010)). However the long duration of the course results in poor patient compliance, which is one of causes of drug resistance.

To overcome this problem, in 1991, the WHO introduced DOTS an acronym for Directly Observed Therapy Short-course and this scheme is adopted by many countries. In addition to DOTS the WHO also started a 'Stop TB' campaign in 2006 (Organization et al. (2010)). The six main aims of this campaign for 2006-2015 to promote the advantages of DOTS and create awareness about MDR. To reduce the prevalence of TB by 50% of the total cases observed in 1990. According to WHO the prevalence between the year 1990 to 2007 has dropped from 300 to 206 per 100,000 population. The target for 2050 is to reduce this to 1 case per million per year (WHO (2009)).

Even the short course like DOTS requires a minimum six months strict regimen of chemotherapy with a various combination of first line and second line drugs (see 1.5.3). In the DOTS treatment, a com-

plete patient profiling is done right from the screening for the disease to the chemotherapy and to the monitored outcome (Obermeyer et al. (2008)). The present DOTS treatment involves a daily course of rifampicin, isoniazid, ethambutol, pyrazinamide and (in some cases) streptomycin for the first two months and then isoniazid and rifampicin thrice a week for four months (Cox et al. (2006)). Should the bacteria cell develop resistance to one or more drugs, the medication course is altered as needed by changing drugs and extending the period of treatment (see Table. 1.1) (Campbell & Bah-Sow (2006)).

The major problem with this scheme is the long duration of the treatment. The initial few weeks of the treatment reduce the symptoms and cause many patients to discontinue the DOTS course. This non-completion of course not only causes the TB to relapse but also result in drug resistance.

Rifampicin-resistant TB	Isoniazid-resistant TB	Multidrug-resistant TB
Isoniazid 18 months	Rifampicin 12 months	Five drugs initially (Rifampicin, isoniazid, ethambutol, pyrazinamide and streptomycin) for 12 months
Ethambutol and/ or pyrazinamide 18 months	Ethambutol or pyrazinamide 12 months	then three drugs (Isoniazid, ethambutol and pyrazinamide) for 18 – 24 months

Table 1.1: Common treatment regimens for patients suffering from drug-resistant tuberculosis.

1.5.3 Currently-used drugs

In 1947, the introduction of Streptomycin as anti-tubercular agent has seen significant progress in TB chemotherapy. Later in 1952 the discovery of isoniazid enhanced its therapeutic potential to the fullest. The early 1960s were marked for introducing ethambutol and rifampin. Later the discovery of pyrazinamide completely changed the strategy of the chemotherapy. The recent additions to these drugs are fluoroquinolones, macrolides, and rifampin congeners.

According to the WHO guideline the anti-TB drugs can in classified in three broad classes based on their mechanism of action, side-effects and clinical utility. The first line agents (essential drugs), they have the most efficacies and least toxicity: isoniazid (INH), rifampin (RMP), pyrazinamide (PZA), etham-

butol (EMB) and streptomycin (STM). The second line agents (reserved drugs) include six different classes like aminoglycosides (e.g. amikacin (AMK), kanamycin (KM)), polypeptides (e.g. viomycin, capreomycin), fluoroquinolones (e.g. ciprofloxacin, levofloxacin), thioamides (e.g. ethionamide), cycloserine, *p*-aminosalicylic acid. These compounds generally have fewer efficacies and more toxicity or both as compared to the first line agents. These agents are rarely used as a single drug in treatment and are mostly used in combination with the first line agents. The last class of compounds, the third line agents, comprise of rifabutin and macrolides. These compounds have very less efficacy or the effectiveness is yet to be proven.

The *M. tuberculosis* cell is unique and involves large number of genes in lipid synthesis, the enzymes employed in these pathways provide an excellent drug target. The most common drugs include those that disrupt the DNA replication, translation and cell wall lipid synthesis. Table. 1.2 list the commonly used TB drugs and their mechanisms of action.

Drugs	Mechanisms of Action
Isoniazid	Inhibition of cell wall mycolic acid synthesis; effects on DNA, lipids, carbohydrates and NAD metabolism
Rifampin	Inhibition of RNA synthesis
Pyrazinamide	Disruption of membrane transport and energy depletion
Ethambutol	Inhibition of cell wall arabinogalactan synthesis
Streptomycin	Inhibition of protein synthesis
Kanamycin	Inhibition of protein synthesis
Quinolones	Inhibition of DNA synthesis
Ethionamide	Inhibition of mycolic acid synthesis
PAS	Inhibition of folic acid and iron metabolism
Cycloserine	Inhibition of peptidoglycan synthesis

Table 1.2: Commonly used TB drugs and their mechanisms.

Nicotinamides.

The nicotinamide discovery was made in the year 1912. However its antitubercular activity was not discovered till early 1950's. The French scientist, Chorine in 1945, first reported the antitubercular

activity of nicotinamide. However it was later discovered that the tuberculostatic activity observed was not due to the nicotinic acid and the anti-tubercular activity was not related to vitamin function. Thus the nicotinic acid itself was never used but its clinically active analogs were created, which form the basis of today's chemotherapy.

Isoniazid

After extensive research, Fox in 1952, first isolated an intermediate product, hydrazide of isonicotinic acid (Isoniazid), which was the most active compound known (Fox & Gibas (1952)). INH is an essential component of every drug therapy unless the bacterium has become resistant or the patient is intolerant to the drug. The exact mechanism of action is unknown however it is primarily tuberculocidal. It acts on both intra and extra cellular bacilli. INH is a prodrug and is activated by the mycobacterial KatG, a catalase peroxidase enzyme, the drug undergoes a series of highly reactive transition states before oxidising (Suarez et al. (2009)). It is proposed that activated INH might act on the cell wall synthesis by displacement of the nicotinamide and hence causing an inactive enzyme drug complex which further triggers changes in protein, lipid and nucleic acid metabolism. Thus causing inhibition of mycolic acid synthesis and resulting into cell wall rupture.

Pyrazinamide

Pyrazine carboxamide is another active analogue of nicotinamide which was developed in parallel to INH (Kushner et al. (1952)). It is used along with INH and STM to shorten the DOTS course from one year to six months. It has a weak tuberculocidal activity and is specifically active against semi-dormant bacilli in the acidic conditions of phagosome and hence is used to treat intracellular bacterial infections. Akin to INH, PZA is a prodrug and gets converted to the pyrazinoic acid due to the enzymatic actions of pyrazinamidase (Zimhony et al. (2007)). This active form of the PZA when accumulated causes disruptions in membrane potential and eventually leads to cell lysis. It is also believed to have a similar target to INH i.e. inhibition of mycolic acid bio-synthesis. It acts by preventing the elongation of the fatty acid C₆ to C_{24/26} in FAS I (Fox & Gibas (1952), Zimhony et al. (2000)). It is used in combination with other drugs as it develops resistance rapidly.

Ethionamide

Ethionamide (2-ethyl thioisonicotinamide), is a second line agent, most active derivative of nicotinamide and is used against the drug-resistant TB bacteria (Wang et al. (2007)). It is structurally similar to INH

and hence it was observed that both the compounds target InhA. Ethionamide is similar to INH in another way in that it is also a prodrug. A flavin mono-oxygenase, ethA, is identified as the activator gene, that catalyses the cleavage of a carbon-carbon bond next to carbonyl, thus using a Baeyer-Villiger oxidation reaction it converts ketones to esters and cyclic ketones to lactones. Winder et al. (1971) established that ethionamide acts by obstructing the binding of arabino residue to the PG causing disruption in mycolic acid pathway. It is used when the bacteria develops resistance to the first line agents like INH and RMP. Ethionamide is known to develop a rapid resistance and hence it is used in combination with other first or second line drugs.

General SAR of nicotinamides

The pyridine ring is essential in all the above drugs for the activity, replacing the ring with heterocyclic rings like furan, thiazole, pyrimidine and pyrazine causes loss of activity. The position of hydrazine in INH, thioamide in ethionamide, and carboxamide in PZA is optimum at 4, moving to 2nd or 3rd position results in reduced or complete loss of activity (Foye et al. (2008)).

Aminoglycoside antibiotics

Aminoglycosides are produced by soil actinomycetes. This class of compounds are result of deliberate research against gram-positive bacteria. In 1944, Waksman first introduced streptomycin which was active against *M. tuberculosis* in both the *in vitro* and *in vivo* studies (Schatz et al. (1944)). Subsequently many compounds were synthesized like neomycin, gentamycin, tobramycin and paromomycin. But these drugs were not active against *M. tuberculosis*.

Streptomycin

Streptomycin is the oldest aminoglycoside antibiotic obtained from *Streptomyces griseus*. STM was the first drug clinically available for the treatment of TB and was first used in 1947. It inhibits both gram-positive and gram-negative bacteria. It was a drug of choice in the past for the treatment of TB. However large doses were required which gave undesirable side effects like ototoxicity. It mainly acts on extracellular bacilli, due to poor penetration into the cells. The mechanism of action is transportation of STM across the cell wall and cytoplasmic membrane, and binding to the P 10 protein of the 30S ribosomal subunit which causes inhibition of the protein bio-synthesis due to the formation of abnormal protein. However a recent study has suggested that STM also inhibits the enzymatic polymerisation of

the amino acids, which is responsible for the bactericidal action (Spotts & Stanier (1961), Foye et al. (2008)). The aldehyde in the streptose ring when reduced to primary alcohol gives dihydrostreptomycin which has same activity as STM but the toxicity to auditory branch increases. Conversion of aldehyde to acids, oxime, semicarbazone, phenylhydrazone results in inactivity (Foye et al. (2008)).

Other aminoglycoside compounds like kanamycin and amikacin are more toxic antibiotics and rarely used to treat atypical mycobacteria and people who do not respond to the usual therapy.

Salicyclates and benzoates

***p*-Aminosalicylic acid**

Lehmann in 1946 discovered that the salicyclates and benzoates elevate the respiration of tubercle bacillus and hence it was proposed that these compounds are important for the normal metabolism of the organisms and hence they can be used as anti-tubercular target. *p*-Aminosalicylic acid (PASA) was discovered in an attempt to find compounds that have antitubercular activity. However it was later observed that PASA shows little effect on the respiration of *M. tuberculosis* and hence it established that the initial hypothesis was flawed (Kobarfard & Kauffman (2003)). It is not active against any bacteria other than TB, this selectivity could be attributed to the differences in the affinity of folate synthetase of TB and other bacteria for PASA (Kobarfard & Kauffman (2003), Foye et al. (2008)). It is one of the least active compounds and acts as a tuberculostatic drug. It is given in rare cases along with other first line drugs where it delays the resistance to these drugs. It is effective only against the growing bacilli, thus indicates a mechanism of action similar to that of sulfonamides. The tuberculostatic activity of the PASA can be reversed by administration of *p*-aminobenzoic acid. Substitution of the amino group with hydroxy, alkoxy, tertiary amines or amides causes loss of activity. Conversion of the acid group to esters, amides or nitrates resulted in inactivity. Conversion of the hydroxyl group to ester or ether results in loss of activity (Foye et al. (2008)).

Cyclic polypeptides

Capreomycin

It is a cyclic polypeptide and resembles viomycin structurally and pharmacologically. It is effective *in vitro*

hence used mostly for treatment of experimental TB. It develops resistance when administered alone, also cross resistance has been noted with kanamycin, neomycin and viomycin but none is reported with INH and STM (Georghiou et al. (2012)). The drug shows clinical efficacy along with INH or PASA.

Oxazolidone

Cycloserine

Cycloserine (CYS), (D-4-amino-3-isoxazolidone), was first isolated in 1955 from *S. orchidaceus* and is a chemical analogue of D-alanine. This is one of the simplest broad spectrum antibiotic to have anti-tubercular activity. CYS acts by interfering in several steps of protein synthesis in the *M. tuberculosis*. During the early stages of cell wall synthesis L-alanine is converted to D-alanine and then two molecules of D-alanine are in turn linked together and incorporated into the cell wall. CYS competitively inhibit the D-alanine incorporation into the cell wall and also inactivates the enzymes which recemise L-alanine, resulting in its antibiotic property (Prosser & Carvalho (2013), Foye et al. (2008)). Resistance to this compound is developed slowly and also no cross resistance is observed. Yet this compound is rarely used in case of resistant bacteria due to the high risk of CNS toxicity. The L-isomer is more active than the D-isomer. The 4-amino group is essential for the activity. Removing the 4-amino group makes the compound inactive and converting it to 4-amino-oxy retains the activity (Foye et al. (2008)).

Ethylenediamines

During the screening of compounds for antimycobacterial property N,N'-diisopropylethylenediamine was found to be active. Subsequently several analogs of this compound were tested against mycobacteria and (+)-2,2'-(ethylenediimino)di-1-butanol (ethambutol, EMB) was found to be the most active compound.

Ethambutol

Ethambutol is selectively tuberculostatic and clinically as active as STM. It acts prevalently on fast multiplying bacteria and atypical mycobacteria. The mechanism of action of this drug is not fully understood, however few theories have been proposed that it interferes in the RNA synthesis and prevents protein and DNA synthesis by forming complexes with divalent cations which inhibits the functions of amines

like spermidine and spermine which are involved in maintaining the integrity of nucleic acids (Tripathi (2013)). Another theory suggests that it inhibits the arabinogalactan synthesis and thus disrupts the mycolic acid incorporation in cell wall (Takayama & Kilburn (1989)). Although ethambutol develops a slow resistance as compared to other first line agents and no cross resistance has been reported, combination therapy is still recommended to prevent resistance from occurring. It is mostly used against the organisms that are resistant to STM and INH. The distance between the two nitrogen atoms is optimum for the activity, any alteration to this by addition of carbon, oxygen or sulfur atom results in loss of activity. Replacing the alcohol function with phenoxy, thio or amino group renders the compound inactive. Replacing the *sec*-butyl group with *tert*-butyl or hydroxy isopropyl group eliminates the activity. The D-isomer is 200 to 500 times more active than L-isomer. The ethoxy and methoxy derivatives of EMB have similar activity as the parent compound when tested *in vivo*, this is due to the enzymatic dealkylation action (Foye et al. (2008)).

Rifamycin antibiotics

The Rifamycin antibiotics are highly substituted derivatives of naphthalene, obtained from *Streptomyces mediterranei*. This group of compounds have broad spectrum of activity.

Rifampin (Rifampicin, RMP)

Rifampin is a semisynthetic derivative of rifamycin B discovered in 1957 and was clinically available in Europe in 1966 and was released in US in 1971. It has bactericidal action and acts on both extra and intracellular organisms. It primarily acts on slow or intermittently dividing bacilli, but generally covers all the sub-population of TB bacteria including atypical mycobacteria. Its efficacy is similar to INH. It is thought to interfere selectively with the mycobacterial RNA polymerase and not with the mammalian RNA, thus inhibiting the DNA dependent RNA synthesis. Mono-drug therapy of RMP develops rapid resistance due to mutation in the *rhoB* gene (RMP target) (Wehrli (1983), Foye et al. (2008)). No cross resistance is reported. Modifications on the aliphatic portion of the rifampin molecule results in inactive compound (Foye et al. (2008)).

Another drug from the rifamycin group is rifabutin. It is structurally similar to RMP and has the same mechanism of action. It is comparatively less active than RMP and is rarely used in treatment of TB. It is reported to have only a partial cross resistance (Tripathi (2013)).

Thiosemicarbazones

During the screening of compounds sulfathiadiazoles an intermediate benzaldehyde thio-semicarbazone was found to be active against TB. The exact mechanism of action is unknown, however no cross resistance is observed with INH thus indicating that thio-semicarbazones do not act by the same mechanisms as INH or sulfonamides. Replacement of the thio-semicarbazone group with a semicarbazone, hydrazone or oxime yields inactive compounds.

Thioureas

During the screening of some anti-fungal compounds some di-phenylthioureas demonstrated tuberculostatic activity. 4,4'-disubstituted diphenylthioureas were shown to have good activity. The mechanism of action is unclear, however some evidence suggests that it interferes with protein biosynthesis. The substitution of electron donating group at para position on both the rings is essential for the activity. Moving the substitution to the ortho or meta position abolishes the activity. Increased substitution also reduces the activity. Replacing the phenyl ring by a cyclohexyl ring or replacing the thiourea group with urea, guanidine, pseudothiourea etc diminishes the activity (Foye et al. (2008)).

Fluoroquinolones

The quinolones class was introduced in the mid 1960s for the treatment of urinary tract or GIT infections, ever since many generations of this class of compound have been synthesized. However these compounds had limited use due to high risk of resistance, low potency and limited spectrum. A breakthrough was achieved when a new class of fluorinated quinolones was synthesized. These compounds had better penetrability, broad spectrum, high potency, and slow development of resistance. The most commonly used drugs from this class are ciprofloxacin, ofloxacin, sparfloxacin, moxifloxacin, levofloxacin, and lomefloxacin. These compounds interfere with the DNA replication and transcription processes by inhibiting the bacterial DNA gyrase and topoisomerase IV enzyme (Ginsburg et al. (2003)). Ciprofloxacin, ofloxacin etc are commonly used in the treatment of TB in combination therapy. Some third generation fluoroquinolones like temafloxacin, a ciprofloxacin analogue, are used widely in treatment of TB infection and levofloxacin have efficacy similar to EMB against TB bacteria. Another member of the fourth generation fluoroquinolones used in treatment of TB includes moxifloxacin. However due to

the broad spectrum, they possess a high risk of resistance and hence are used in combination with the first line agents (Ginsburg et al. (2003)). Recent studies have shown that the anti bacterial activity of the compound is attributed to the basic pharmacophore, the quinoline ring system. With the evidence that suggests that the C-6 fluorine enhances the cell penetration and also improves the DNA gyrase complex binding. It was observed that the activity of these compounds was greatly affected by the substitution at C-7. The five or six membered heterocyclic rings increased the activity and piperazinyl ring substitution demonstrated maximum activity (Foye et al. (2008)).

1.6 Treatment regimen

The TB bacteria usually attacks the lungs, however if the infection goes untreated for a long time, it can attack other organs like brain, kidney and spine and can be fatal. Both the TB-related conditions like the latent TB infection (LTBI) and the TB disease are treated using a condition specific regimen.

The treatment of LTBI is essential as it helps in controlling and eliminating the disease. After ensuring that the risk of developing an active disease is ruled out one of the four suitable regimen as discussed in Table. 1.3 is recommended by the Centers for Disease Control and Prevention ¹.

Drugs	Duration	Interval	Minimum doses (mg)
Isoniazid	9 months	daily	270
		twice weekly*	76
Isoniazid	6 months	daily	180
		twice weekly*	52
Isoniazid and Rifapentine	3 months	once weekly*	12
Rifampin	4 months	daily	120

* Use Directly Observed Therapy (DOT)

2

Table 1.3: Treatment regimens for Latent TB infection.

The treatment of TB disease is more complicated than LTBI and requires an extensive regimen of 6 to

¹ <http://www.cdc.gov/>

² <http://www.cdc.gov/>

nine months. Once tested positive on the smear test a basic 2 month treatment is recommended with first line agents (INH, RMP, PZA, EMB) ³. Based on the degree of infection various continuation phases are used as discussed in table. 1.4.

Preferred Regimen	Alternative Regimen	Alternative Regimen
<i>Initial Phase</i> Daily INH, RIF, PZA, and EMB* for 56 doses (8 weeks)	<i>Initial Phase</i> Daily INH, RIF, PZA, and EMB* for 14 doses (2 weeks), then twice weekly for 12 doses (6 weeks)	<i>Initial Phase</i> Thrice-weekly INH, RIF, PZA, and EMB* for 24 doses (8 weeks)
<i>Continuation Phase</i> Daily INH and RIF for 126 doses (18 weeks) or Twice-weekly INH and RIF for 36 doses (18 weeks)	<i>Continuation Phase</i> Twice-weekly INH and RIF for 36 doses (18 weeks)	<i>Continuation Phase</i> Thrice-weekly INH and RIF for 54 doses (18 weeks)

4

Table 1.4: Basic treatment regimens for TB infection.

1.7 Drug resistance

According to the 2009 WHO report, out of the total 10.4 million cases of TB nearly 5% were MDR-TB. Statistics demonstrated that more than half of the cases were new incidences while only 1.9% of the cases were previously treated for TB. A clear correlation between incidence of MDR-TB and newly diagnosed disease was observed especially in the high incidence countries like India and China. Due to the high number of multidrug-resistant (MDR) and extensively drug-resistant cases (XDR) of TB there is an immense need for new drugs. The worldwide spread of AIDS has added a new aspect to the TB problem. According to WHO more the 10 million people each year are infected with HIV. These patients are more prone to develop active TB disease and MAC (*Mycobacterium avium* complex) infections.

Resistance can be developed by various means such as the target gene undergoing a self-generated chromosomal mutation, gene over-expression, drug efflux or inactivation mechanisms, and affecting

³<http://www.cdc.gov/>

⁴<http://www.cdc.gov/>

the drug permeability (Zhang & Yew (2009)). Drug resistant TB strains first arose shortly after the introduction of STM in 1944, when the mono-drug therapy of STM resulted in relapse of TB due to gene mutation. The rationale for combination therapy, therefore, is to employ two or three drugs acting on various targets, as the chances of the cell acquiring mutation at two or three unlinked target genes is less likely and thus reduces the probability of drug resistance. The process of genetic mutation is accelerated by mono-drug therapy, poor drug prescription, shortfalls in drug distribution and most importantly patient drug non-adherence.

With newer publications providing deeper insights of *M. tuberculosis* H₃₇Rv genome originally isolated in 1905 has vastly increased the understanding of the organism biology, mechanisms of drug action and resistance. This paved the way for the development of newer drug leads like 2-aminothiazoles, oxadiazolythio, thiadiazolythio and triazolylthio derivatives (Ananthan et al. (2009)), carboxamidrazones (Billington et al. (2000)) etc.

1.8 Project aims

Statistics showing an increase in the MDR cases of TB and the reports of continuously evolving resistant strains, the present chemotherapy is in jeopardy and thus the need for newer, effective and cheap drugs is as high as it was a century ago. Therefore there are two main aims of this PhD project:

1. To synthesize libraries of analogues and derivatives of carboxamidrazone, a known active compound and its derivatives and its cyclized and fluorinated analogues. And to test for their biological activity against the *M. tuberculosis* H₃₇Rv strain.
2. To synthesize target specific compounds like long chain 2-hydroxy-3-oxocarboxylic esters which are structurally similar to the mycolic acids and might act on the FAS-II mechanism and test for their biological activity against the *M. tuberculosis* H₃₇Rv strain.

Chapter 2

Chemistry and synthesis of heteroaryl amidrazone compounds

2.1 Introduction

This chapter describes and discusses the generation of a library of heteroaryl compounds and their analogues to screen for their activity against Mycobacteria especially *Mycobacterium tuberculosis*. In the following some of the contributions towards the synthesis of the amidrazone class and its derivatives are briefly reviewed. The amidrazone compounds have been known for a long time to possess anti-tubercular activity. Thiele (1892) generated aminoguanidine by reduction of nitroguanidine, a present day amidrazone class of compound. Numerous scientists have developed the chemistry to make several new amidrazones (Neilson et al. (1970), Mihina & Herbst (1950), Libman & Slack (1956), Doyle & Kurzer (1976)). However, its anti tubercular activity was not discovered until the mid 1950s. The high tuberculostatic activity of carboxyhydrazide of 4-pyridine led to the discovery of many of its analogues. The next two decades saw further research into the synthesis of hydrazones (Kitaev et al. (1970)), 2-benzimidazolyl derivatives (Vereshchagina et al. (1973)), imidic acid derivatives (Grout (1975)) and triazolepropionic acids (Buckler et al. (1978)) along with the investigation into their anti inflammatory and anti tubercular activities.

In the last two decades significant work has been carried out in this area. The Mamolo group in the 1990s has synthesised 2-pyridyl and 4-pyridyl carboxamidrazone compounds and their derivatives. These compounds were further tested against *M. tuberculosis* H37Rv and *M. tuberculosis* isolated

from human bronchial aspirates (Mamolo et al. (1992), Mamolo et al. (1993), Mamolo & Vio (1996)). The compounds shown in Fig. 2.1 exhibited some interesting inhibitory activity against some of the *M. tuberculosis* organisms that were resistant to isoniazid, rifampicin and ofloxacin.

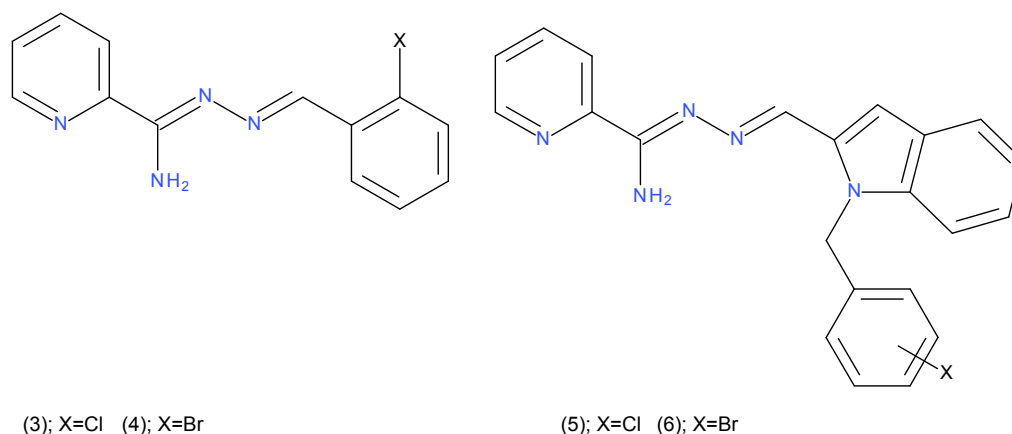


Figure 2.1: The most active compounds synthesised by Mamolo et al. (1992).

The structure activity relationship studies by Mamolo et al. (1992), Mamolo et al. (1993), Mamolo & Vio (1996) suggested that it is essential for the amidrazone group to be attached at the 2-position ortho position of the pyridine ring. It is also suggested that a substituent should be attached to the benzylidene end as opposed to the pyridine ring, as this combination is optimum for the penetration of the entire molecule into the highly lipophilic mycobacterial cell membrane. However, the conclusion drawn by the Mamolo group was based on a small size data set of 21 compounds of N^1 -benzylideneheteroaryl carboxamidrazones.

A further investigation in this field was carried out at Aston University by the Rathbone group. A large library of carboxamidrazones and their derivatives Fig. 2.2 were synthesised using robotic equipments, which were then subjected to a preliminary testing at Aston University, on *M. fortuitum*. This organism was selected since it is much safer and grows faster as compared to *M. tuberculosis*.

The toxicity levels of the compounds shown in Fig. 2.2 were then tested on the rat liver metabolism system, human erythrocytes and mononuclear leucocytes using INH as the reference (Coleman et al. (1999), Coleman et al. (2000), Coleman et al. (2001)). In this study the compounds were incubated in two ways i) direct and ii) metabolising system controlled. It was observed that the compounds (7), (8), and (10) were less toxic than INH at same concentration on direct incubations. However compound (9) exhibited a high level of toxicity towards the human mononuclear leucocytes (Coleman et al. (1999), Coleman et al. (2000), Coleman et al. (2001)).

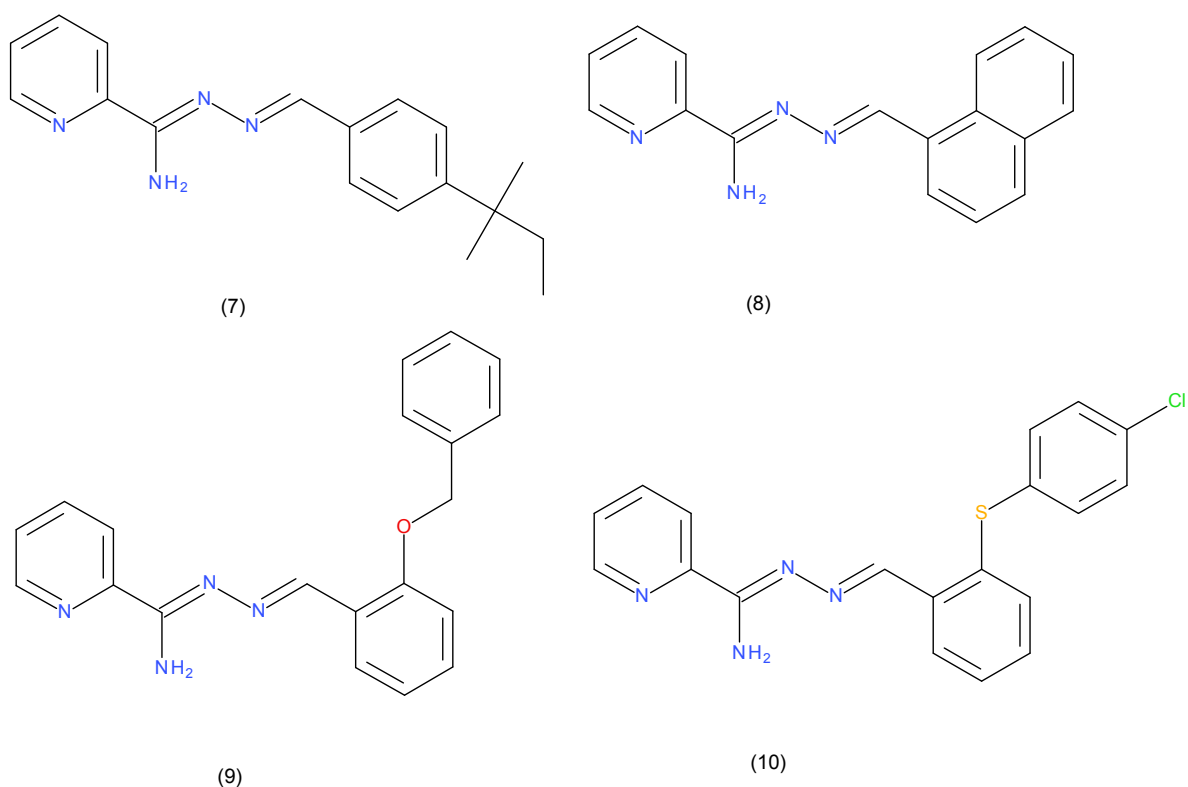


Figure 2.2: List of the most active compounds synthesised by Billington et al. (2000)

Rathbone et al. (2006) took this study further by synthesising a new series of phenolic N^1 -benzylidene-pyridinecarboxamidrazones. In this study, many active compounds were synthesised, but the most active of them all against *M. tuberculosis* was N^1 -[3, 5-di-(tert-butyl)-2-hydroxybenzylidene]-pyridine-4-carboxamidrazone (11) (see Fig. 2.3). It was observed that the compound (11) was active against most gram positive bacteria, including MRSA strains, and MIC values in the range of 6.50 – 12.99 μM . In contrast, the compound was found to be completely inactive against gram negative bacteria. However, compound (11) failed the direct leucocyte toxicity test causing 100% human leucocytes cell lysis.

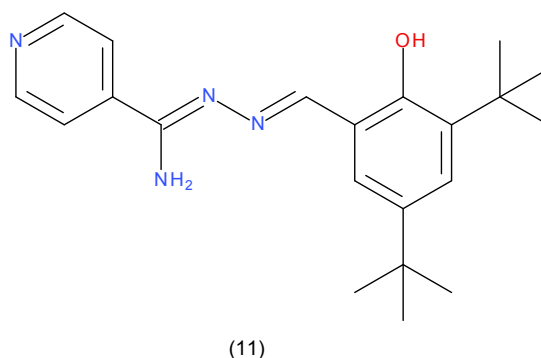
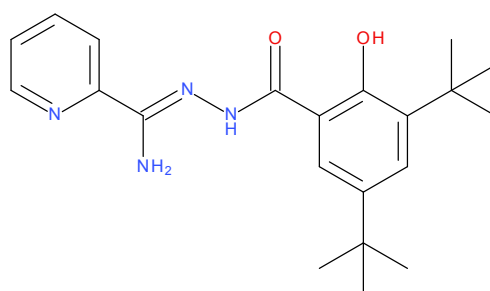


Figure 2.3: N^1 -[3, 5-di-(tert-butyl)-2-hydroxybenzylidene]-pyridine-4-carboxamidrazone

The compound (11) shown in Fig. 2.3 was used as a lead compound by Khan (2008). Her work involved mainly synthesis of carboxamidrazone derivatives including amides, ureas, sulphonamides, and methyl ketimines. The sulphonamides derivatives were difficult to isolate, urea derivatives were generally found to be inactive, except for the few 4-pyridine-substituted compound derivatives, and methyl ketimines were also mostly inactive. Amongst all the compound groups, amides were found to be the most active group against *M. tuberculosis*. The compound pyridine-2-carboxamidrazone N^1 [3, 5-di-(tert-butyl)-2-hydroxybenzoyl] amide (see Fig. 2.4) was found to be of special interest, since it had an MIC value $<20.29 \mu\text{M}$ causing a 100% inhibition.



(12)

Figure 2.4: Pyridine-2-carboxamidrazone N^1 –[3, 5-di-(tert-butyl)-2-hydroxybenzoyl] amide

Ren (2009), carried out further research using the compound shown in Fig. 2.4 as a lead compound to synthesis a new series of compounds by modifying the aryl moieties. His work mainly emphasised amides and imines.

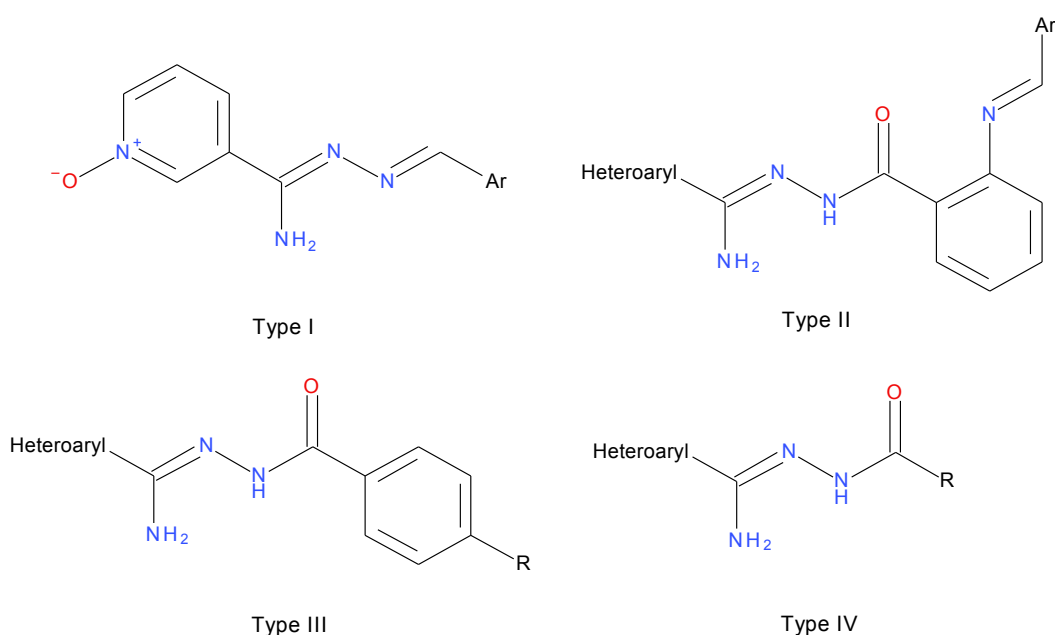


Figure 2.5: General structures of the compounds synthesised by Ren (2009)

The biological data obtained from Ren's compounds Type III and IV (see Fig. 2.5) suggested that the compounds with long alkyl chain substitutions at the benzoyl end were the most active compounds as shown in Table. 2.1. These results are in agreement with Mamolo et al. (1992) and Billington et al. (2000), where it is suggested that the increase in the lipophilicity of the molecule increases the permeability of the bacterial cell wall, thus increasing the activity of the molecule.

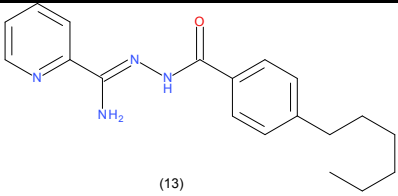
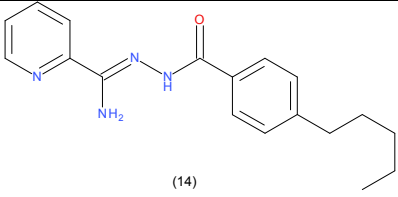
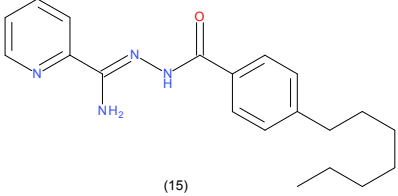
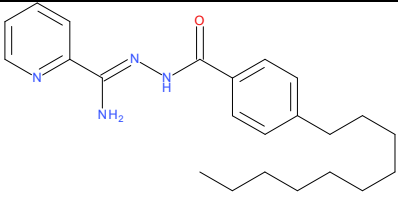
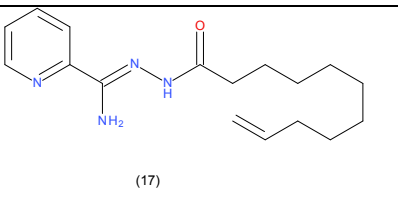
Compound Name	Compound Structure	IC ₅₀ μM	IC ₉₀ μM
<i>N</i> ¹ -(4-Hexylbenzoyl)-pyridine-2-carboxamidrazone	 (13)	3.23	4.32
<i>N</i> ¹ -(4-Pentylbenzoyl)-pyridine-2-carboxamidrazone	 (14)	2.88	4.50
<i>N</i> ¹ -(4-Heptylbenzoyl)-pyridine-2-carboxamidrazone	 (15)	4.58	4.96
<i>N</i> ¹ -(4-Decylbenzoyl)-pyridine-2-carboxamidrazone	 (16)	17.75	19.44
<i>N</i> ¹ -(4-(10-Undecenoyl))-pyridine-2-carboxamidrazone	 (17)	14.37	23.97

Table 2.1: The list of the most active compounds against *M. tuberculosis* along with their IC₅₀ and IC₉₀ values synthesised by Ren (2009)

Sikdar (2010) investigated the carboxamidrazone mostly by modifying the central chain. The pyridyl moiety was connected with the substituted benzyl moiety using three atoms instead of four to study the optimum chain length required for the compound activity. However these compounds were found to have only moderate to low activity.

2.2 Structure activity relationship studies

2.2.1 Imines

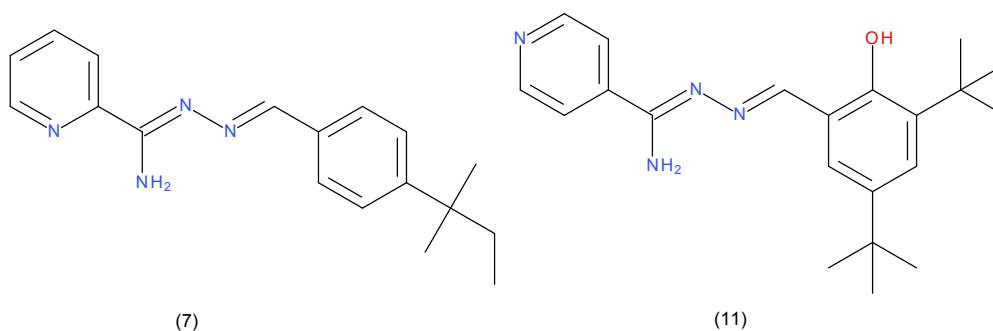


Figure 2.6: Two of the most active imines, a: N^1 -[(*E*)-[4-(1,1-dimethylpropyl)phenyl]methyleneamino]pyridine-2-carboxamide, b: N^1 -[(*E*)-(3,5-ditert-butyl-2-hydroxy-phenyl)methyleneamino]pyridine-4-carboxamide

The compounds (7) and (11) were the most active compounds of the imine series against *M. tuberculosis* with the MIC of 25.98 – 32.47 μM (Billington et al. (2000) (see Fig. 2.6)). The 4-pyridyl substituted compound (11) was the most active compound with MIC of 6.50 – 12.99 μM . Replacing the 4-pyridine ring in compound (11) with 2-pyridine, 3-pyridine, 2-pyrazinyl or 2-quinolyl rendered the compound inactive (Tims (2002)). The tert. butyl groups on the compound (11) were found to be essential for the activity. Substitution of tert. butyl group with a methyl group caused loss of activity. The introduction of a halogen group like Iodine in the compound (11) caused the activity to diminish and the compound was four times less potent (Rathbone et al. (2006)). Replacing the hydroxyl group in (11) with ether completely abolished the activity. However replacing the hydroxyl group in (11) with acetate slightly lowered the activity; this anomaly suggested that the acetate derivative might be acting as a pro-drug for the parent compound. The poly-hydroxylation of compound (11) exhibited moderate activity (Rathbone et al. (2006)).

Coleman et al. (1999) has shown that the amidrazone nucleus is extremely toxic to the human mononu-

clear leucocytes. Hence in an attempt to reduce the toxicity a further research was carried out at Aston University by the Rathbone group, which involved synthesis of urea, sulphonamide, methyl ketimines and amide derivatives.

2.2.2 Ureas

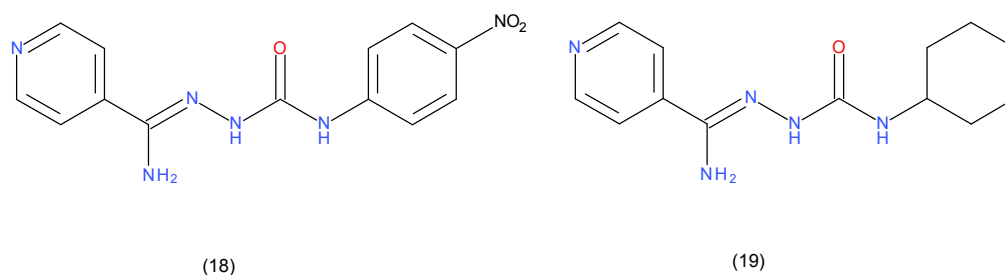


Figure 2.7: Two examples of the urea derivatives, a: 1-[(Z)-[amino (4-pyridyl) methylene] amino]-3-(4-nitrophenyl) urea, b: 1-[(Z)-[amino (4-pyridyl) methylene] amino]-3-cyclohexyl-urea

The urea derivatives were generally inactive against *M. tuberculosis*. The 4-pyridyl compounds were found to be active compared to 2-pyridyl compounds. The methoxy and halogen substitution resulted in the loss of activity. Nitro group substitution at para position (18) increased the activity, however substitution at the ortho position caused loss of activity. The substitution of cyclohexane ring at the benzoyl end (19) caused an increase in activity ((see Fig. 2.7) Khan (2008)). This further supported the argument that a large alkyl group increased the lipophilicity which was beneficial for the complete penetration into the bacterial cell and thus increased the activity (Mamolo et al. (1993), Mamolo & Vio (1996)).

2.2.3 Sulphonamides and N-oxides

The compounds with the sulphonamide nucleus were inactive. The 4-pyridyl-4-N-oxide compounds were also inactive (Khan (2008)).

2.2.4 Amides

Based on the previous work carried out at Aston university it was observed that the amide derivatives of carboxamidrazones were the most active compounds against *M. tuberculosis*. For this study only a

subset of carboxamidrazone amides with a substituted benzoyl and aliphatic substitutions are considered. The 2-pyridyl compounds were generally more active as compared to the 4-pyridyl compounds. Replacing the 2-pyridyl with 3-pyridyl diminished the activity. A large alkyl chain substitution at the benzoyl end enhanced the activity. It was observed that the compounds (13), (14) and (15) containing the alkyl chain substitution of five to seven carbons on the benzoyl ring was active against *M. tuberculosis* (Ren (2009)).

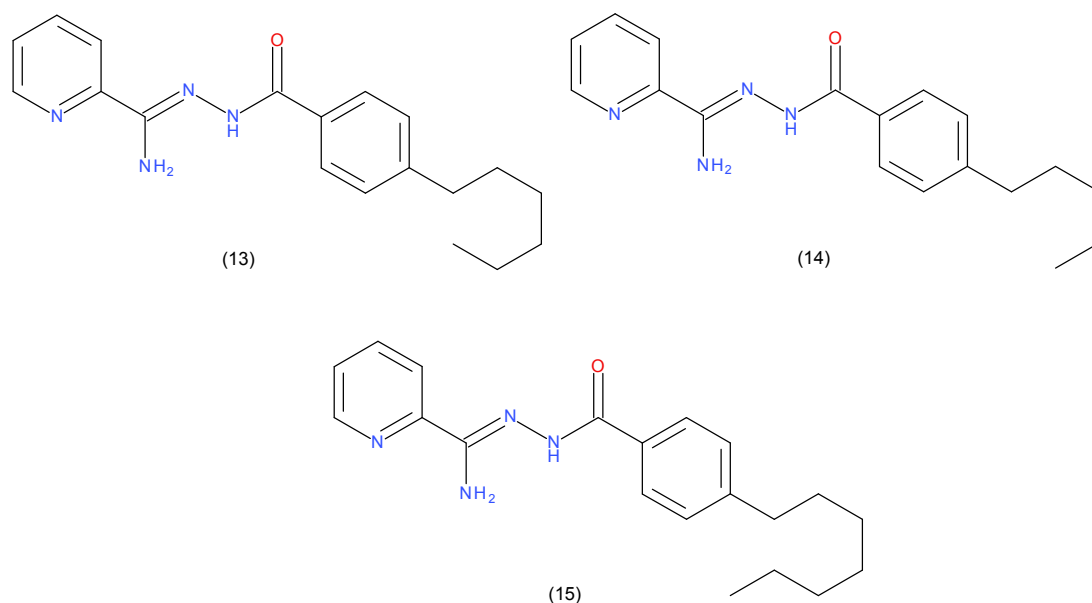
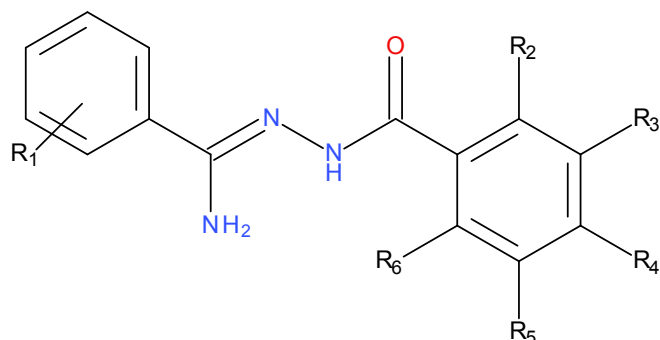


Figure 2.8: List of amides, a: N^1 -[(*Z*)-[amino(4-pyridyl) methylene] amino]-4-heptyl-benzamide, b: N^1 -(4-Pentylbenzoyl)-pyridine-2-carboxamidrazone, general structures of azobenzoyl amide and general structure of benzoyloxybenzoyl amide carboxamidrazone

2.2.5 General carboxamidrazone amide structure

The five atom carboxamidrazone chain connecting the pyridyl moiety to the benzoyl moiety is essential for the activity as reducing the chain length caused loss of activity. The 2-pyridyl-substituted carboxamidrazone amides were found to be generally more active than the 4-pyridyl or 3-pyridyl substituted compounds. The alkyl chain substitution at R4 position on the benzoyl ring enhances the activity of compounds (13), (14) and (15)(Ren (2009)). The tert. butyl groups at R3 and R5 along with a hydroxy group attached at R2 renders the compound active (12). The hydroxy group at R2 (ortho) position is essential for the activity. Shifting the hydroxy from R2 to R4 (para) (20) position diminishes the activity (Sikdar (2010)). Halogens other than iodine like bromine or chlorine causes loss in activity. The presence of electronegative substitution is favourable for activity, but the compounds were found to be highly

toxic (Sikdar (2010)).



(13); R₁= 2-Pyridyl
R₄= 6 carbon alkyl chain

(15); R₁= 2-Pyridyl
R₄= 7 carbon alkyl chain

(20); R₁= 2-Pyridyl
R₃ and R₅= tert. butyl
R₄= OH

(14); R₁= 2-Pyridyl
R₄= 5 carbon alkyl chain

(12); R₁= 2-Pyridyl
R₃ and R₅= tert. butyl
R₂= OH

Figure 2.9: General structure of carboxamidrazone amide

2.3 Lead Optimisation

The Fig. 2.10 summarises the previous work carried out at Aston university in the carboxamidrazone and the changes made to optimise the compound for antimycobacterial activity.

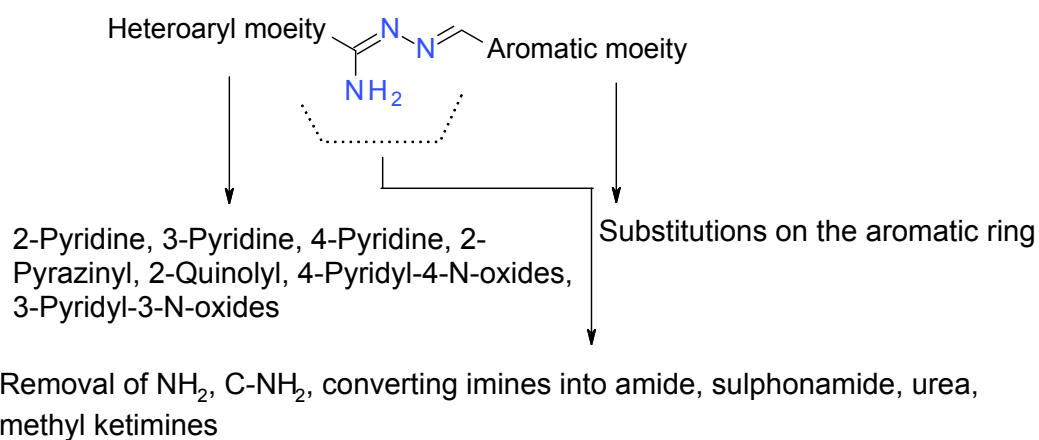


Figure 2.10: Summary of previous work carried out in carboxamidrazone at Aston university.

2.3.1 Intended variations of the building blocks in synthesis of carboxamidrazone

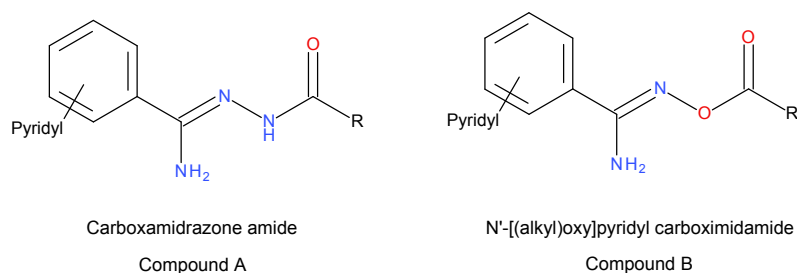


Figure 2.11: General structures of the intended lead compounds to be synthesised

Aryl building block

A library of compounds was synthesised in an attempt to increase the antimycobacterial activity while decreasing the toxicity of the compounds. To achieve this various building blocks were altered.

In the previous research (Ren (2009)) have synthesised carboxamidrazones with alkyl chains attached to the benzoyl group and tested them for anti tubercular activity. It was observed that the compounds with 5 and 6 alkyl chains were the most active compounds followed by the 7 alkyl chain. To take this research forward a matrix was created where some of the carboxamidrazones missing in the (Ren (2009)) library were synthesised using different alkyl chain lengths. Table. 2.2 shows the list of various acid chlorides used to modify the compound A (Fig. 2.11). The acid **da** was used to study the effect of cyclic substrate on the activity as opposed to the 6-hexylbenzoyl chloride which has flexible side chain. Some of the acid chlorides were selected to study the effect absence of a benzoyl ring has on activity. Some of the acid chlorides selected have an alkoxy group attached to the benzoyl group. Alkyl and alkoxy both are electron donating groups and are structurally similar and hence were selected for the present study.

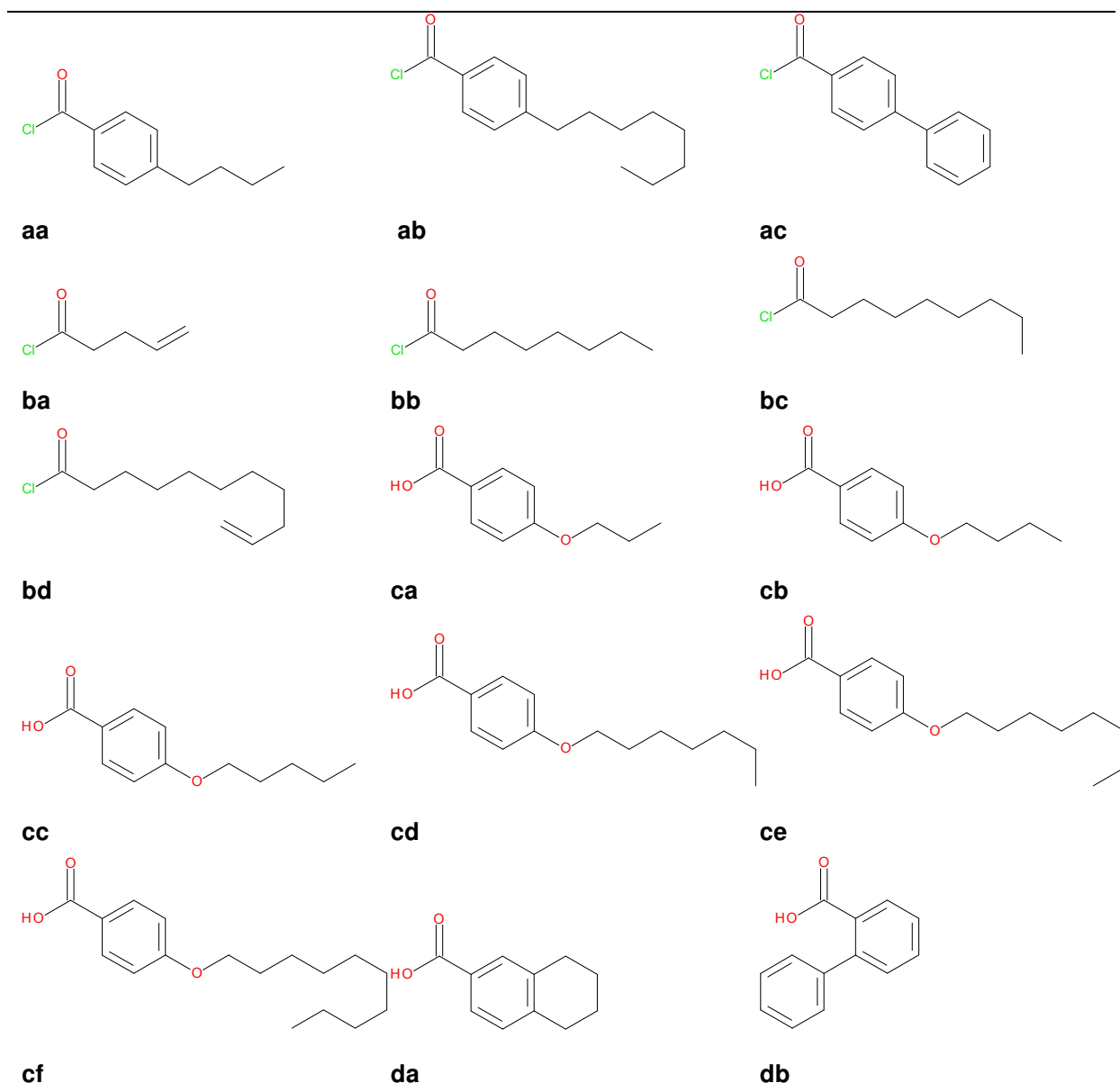


Table 2.2: List of acid chlorides and acids used in the synthesis of carboxamidrazone amides

Pyridyl building block

The hydrazine monohydrate on reacting with the cyano pyridines gave subsequent pyridyl carboxamidrazones (Tanaka et al. (1994)). Rathbone et al. (2006) have tested the pyridine carboxamidrazone against *Mycobacterium tuberculosis* and is known to possess antimicrobial activity. Many amidrazones like imines, 2, 3 and 4 -pyridyl carboxamidrazones and benzilidines were synthesised to create a library of compounds in the earlier research (Tims (2002)). However based on previous studies carried out by Tims (2002), Ren (2009), Sikdar (2010) it was observed that only 2-pyridyl and 4-pyridyl carbox-

amidrazone were active. Therefore, in the present study only 2 and 4 pyridyl carboxamidrazone were selected.

In the following sections, the analogues of the lead compounds are listed.

2.3.2 COMPOUND A (Carboxamidrazone amide)

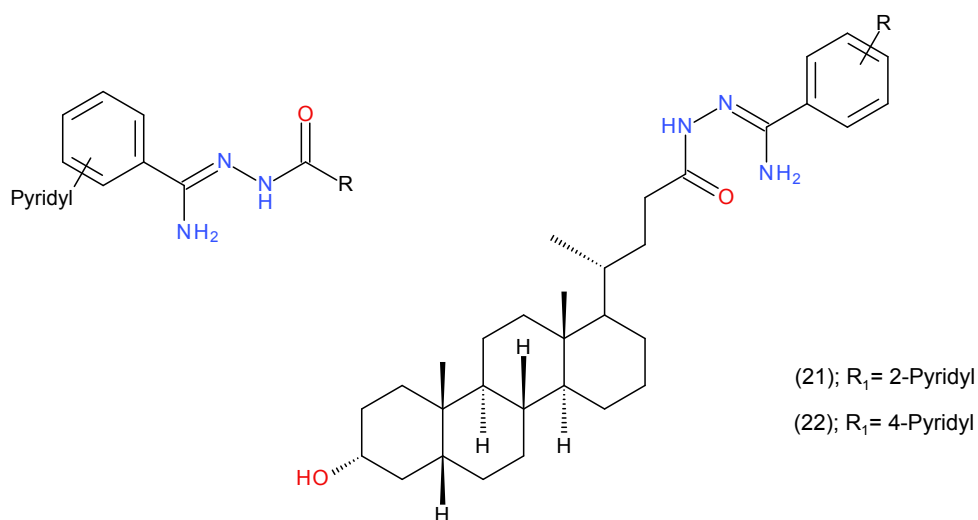


Figure 2.12: General structures of the Compound A (carboxamidrazone amides)

The carbamidrazone amides were tested at Aston university against *E.coli* and *S.aureaus* but failed to exhibit any activity. Further biological testing of this class of compounds against *M. tuberculosis* H37Rv at TAACF, US exhibited some promising results. Five of these compounds were found to be active while five of them were weakly active Ren (2009). Hence a library of analogues of these compounds was synthesised to explore this class of compounds.

Compounds (21) and (22) are part of the larger ongoing project at Aston University, 'Germination to termination'. The concept is to attach the antimicrobial compound to the bile salt. The bile salt is known to possess the activity to germinate spores into the fully grown microbes (Sorg & Sonenshein (2008)). At this point the antimicrobial attached to the bile salt can act on the microbes and cause the lysis of microbial cells.

2.3.3 COMPOUND B (N^1 -[(alkyl)oxy]pyridyl carboximidamide)

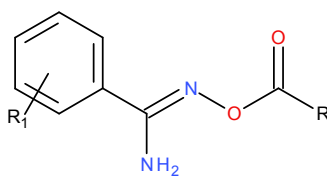
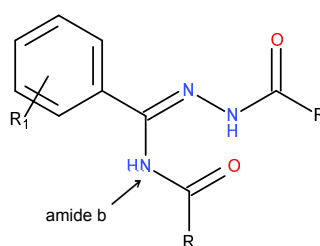


Figure 2.13: General structure of Compound B

The N^1 -[(alkyl)oxy]pyridyl carboximidamide compound is structurally similar to carboxamidrazone amide and has the same number of atoms in the central chain except that the nitrogen atom adjacent to the carbonyl group is replaced by oxygen. This class was synthesised to study the effect the increase in electro-negativity has on the compound's activity and to investigate the removal of a hydrogen bond donor at that position.

The biological data from carboxamidrazone amide suggests that compounds having alkyloxy groups attached to the benzene ring and the alkyl chain attached directly to the carboxyl group do not show much activity. Hence the substrates ba to bd as listed in Table. 2.2 were omitted while synthesising this class of compounds.

2.3.4 COMPOUND C (Bis-amide version of carboxamidrazone)



Compound C

Figure 2.14: General structure of Compound C

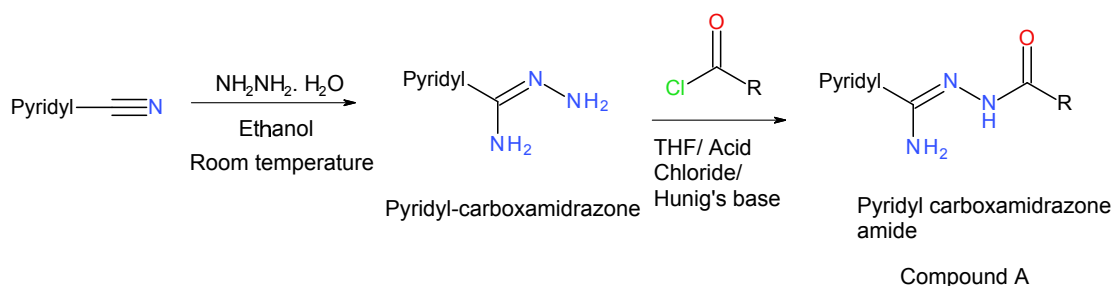
The synthesis of bis-amide carboxamidrazone was attempted to introduce a second point of variation in the molecule to block the amide b with acetate group. The idea behind the synthesis of this compound was that if both the amide groups could be made reactive, two anti-mycobacterial groups can potentially be attached on single compound which can attack two resistant strains of bacteria for which at present a combination therapy is used.

2.4 Results and Discussion

2.4.1 COMPOUND A (Carboxamidrazone amide)

Scheme A for Compound A

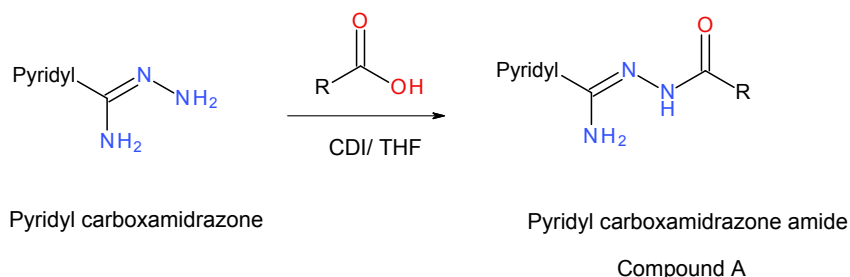
This is a two step reaction sequence. The first step involves preparation of carboxamidrazone. The respective cyanopyridine was reacted with hydrazine in ethanol to give carboxamidrazone (Case (1965)). These compounds were then reacted with acid chlorides in presence of Hünig's base to give the desired product (Khan (2008)).



Scheme 2.1: Synthetic scheme A for Compound A

Scheme B for carboxamidrazone amide

A few analogues of carboxamidrazone amides, where the acid chlorides were unavailable, were synthesised from carboxylic acids as shown in Scheme. 2.2.



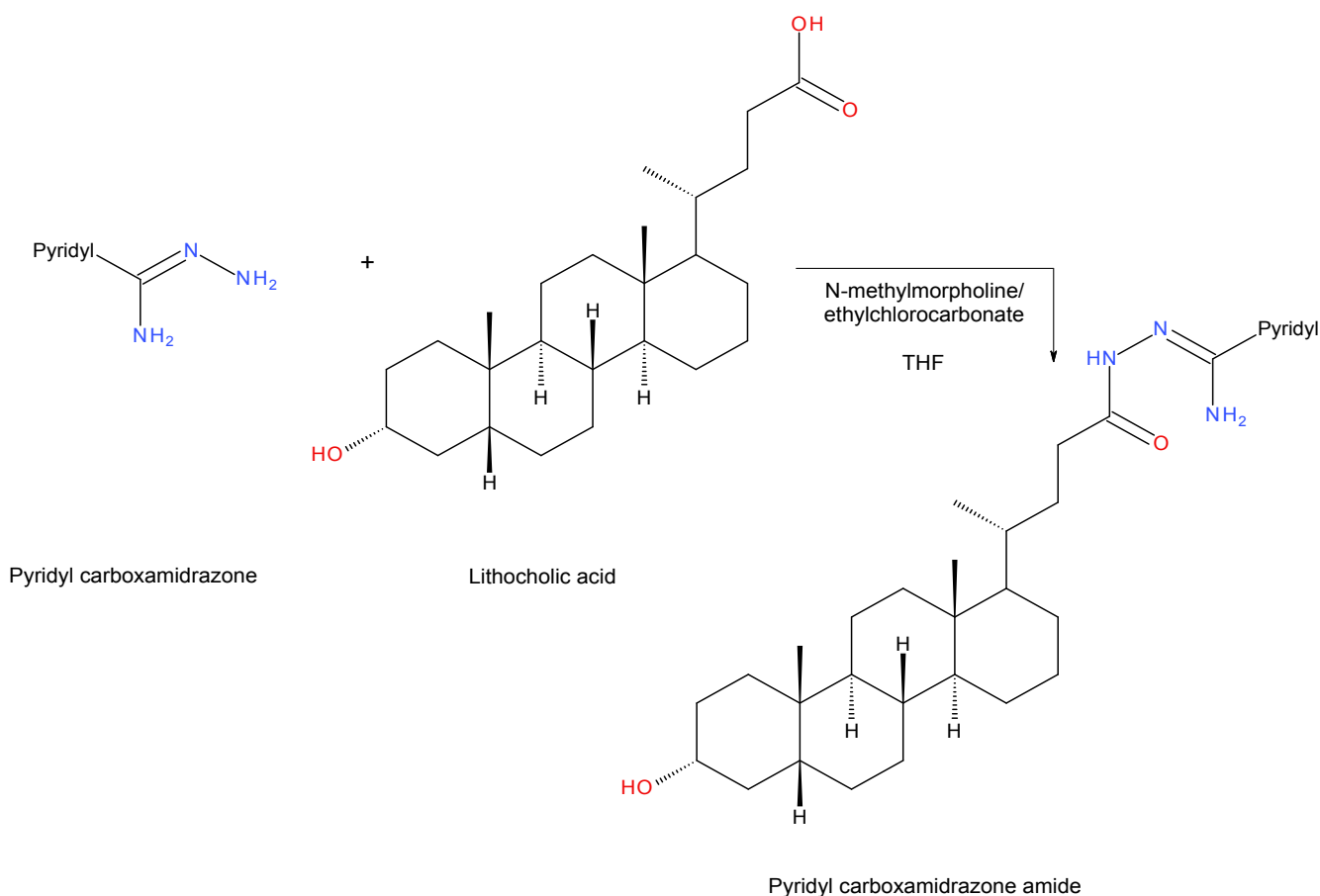
Scheme 2.2: Synthetic scheme B for Compound A

This is a three step reaction sequence. The carboxamidrazone was prepared as discussed in Scheme. 2.1. The solution of required carboxylic acid and N, N' -carbonyldiimidazole (CDI) were stirred together in THF which formed an intermediate. This intermediate was then treated with an appropriate solution

of carboxamidrazone to give the desired product. The crude compound thus obtained was washed with water and sat. sodium bicarbonate solution. In this reaction the CDI, a coupling agent, promotes the transacylation reaction in acids.

Scheme C for carboxamidrazone amide

Another set of analogues of carboxamidrazone amides were synthesised from bile acids.

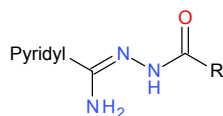


Scheme 2.3: Synthetic scheme C for Compound A

This was a two step reaction sequence. The carboxamidrazone was prepared as discussed in Scheme 2.1. This amide was then reacted with the lithocholic acid and *N*-methylmorpholine and ethylchlorocarbonate, in presence of THF to give the desired product.

The analytical data, namely, mass spectrum, NMR, IR were found to be consistent with the proposed structure. The NH bond suggests the compound formation as it joins the two starting materials. The IR shows a broad peak in the range of $1665 - 1760 \text{ cm}^{-1}$ representing the carbonyl group. Table. 2.3

lists the analogues of the final product compound A shown in Scheme. 2.2 synthesised along with their yields and melting points.



Compound A	Pyridyl	R group	Yield (%)	Melting point (°C)
(23)	2-Pyridyl		87	230.4 – 232.8
(24)	4-Pyridyl		92	177.9 – 179.1
(25)	2-Pyridyl		92	195.6 – 197.1
(26)	4-Pyridyl		74	150.7 – 151.2
(27)	2-Pyridyl		68	149.7 – 150.5
(28)	4-Pyridyl		86	201.7 – 202.7
(29)	2-Pyridyl		69	228.5 – 229.7
(30)	4-Pyridyl		75	218.8 – 220.2
(31)	2-Pyridyl		71	224.3 – 225.4

Compound A	Pyridyl	R group	Yield (%)	Melting point (°C)
(32)	4-Pyridyl		82	148.2 – 149.3
(33)	2-Pyridyl		69	181.5 – 183.1
(34)	4-Pyridyl		71	187.1 – 189.7
(35)	2-Pyridyl		64	167.1 – 168.2
(36)	4-Pyridyl		71	162.8 – 166.7
(37)	2-Pyridyl		77	153.5 – 154.6
(38)	4-Pyridyl		76	149.4 – 151.3
(17)	2-Pyridyl		90	145.2 – 147.5
(39)	4-Pyridyl		95	141.3 – 144.1
(40)	2-Pyridyl		69	224.3 – 225.3
(41)	4-Pyridyl		72	207.1 – 208.5
(42)	2-Pyridyl		59	120.5 – 121.9
(43)	4-Pyridyl		64	206.2 – 207.1
(44)	2-Pyridyl		63	224.7 – 225.8
(45)	4-Pyridyl		69	164.1 – 165.3

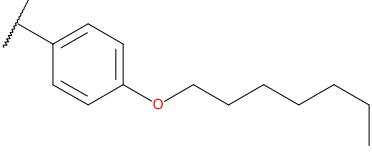
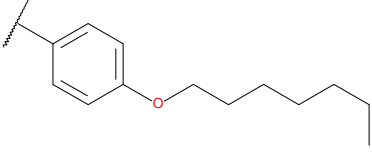
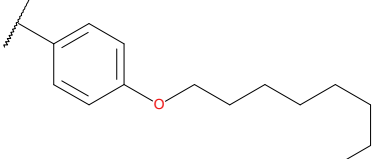
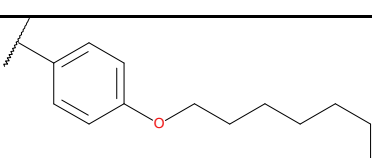
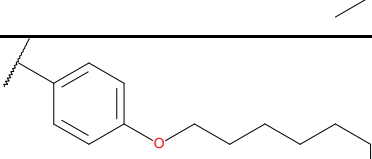
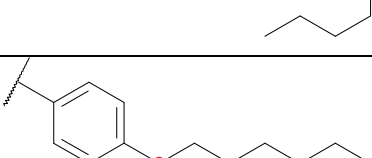
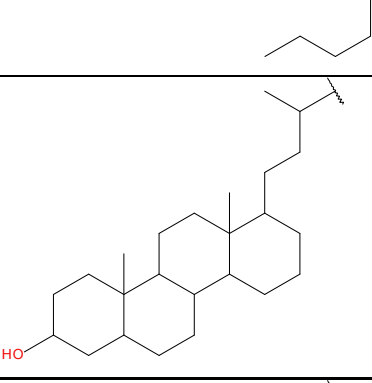
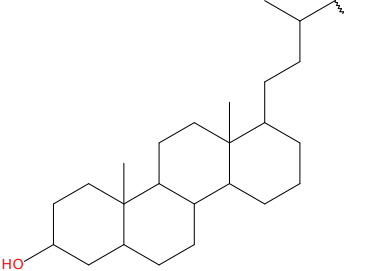
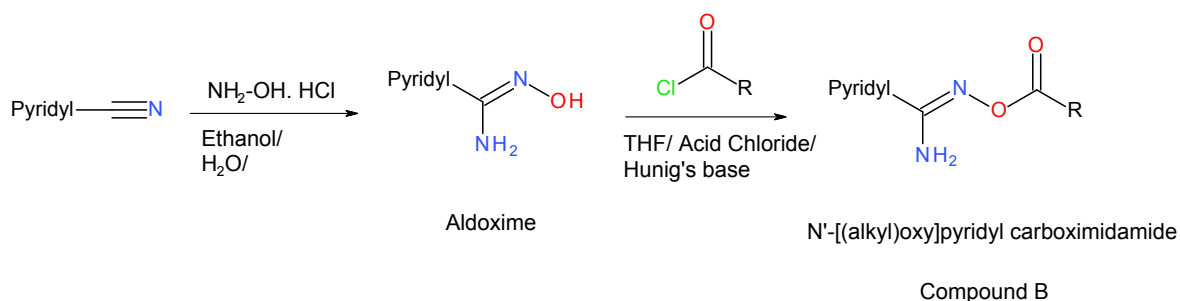
Compound A	Pyridyl	R group	Yield (%)	Melting point (°C)
(46)	2-Pyridyl		57	203.3 – 204.4
(47)	4-Pyridyl		77	177.6 – 178.8
(48)	2-Pyridyl		68	188.6 – 189.7
(49)	4-Pyridyl		66	185.0 – 186.2
(50)	2-Pyridyl		79	165.3 – 166.5
(51)	4-Pyridyl		87	168.9 – 170.1
(21)	2-Pyridyl		78	187.8 – 189.5
(22)	4-Pyridyl		69	187.4 – 189.6

Table 2.3: List of analogues of compound A

2.4.2 COMPOUND B (N^1 -[(alkyl)oxy]pyridyl carboximidamide)

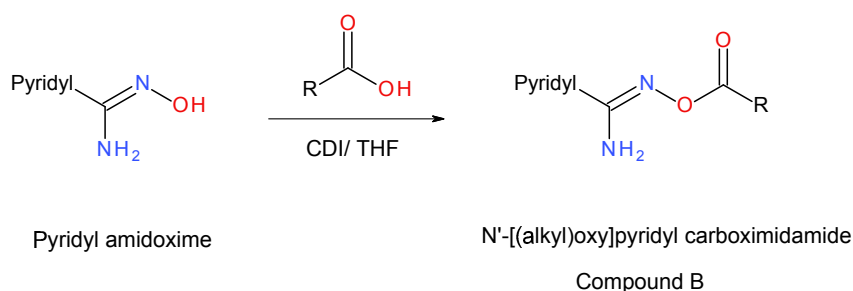
Scheme A for N^1 -[(alkyl)oxy]pyridyl carboximidamide



Scheme 2.4: Synthetic scheme A for Compound B

This was a two step reaction sequence. The first step involved preparation of an amidoxime. The respective cyano pyridine was reacted with hydroxylamine in THF to give the respective amidoxime Hemming (2008). These compounds were then reacted with acid chlorides in the presence of Hünig's base to give the desired N^1 -[(alkyl)oxy]pyridyl carboximidamide.

Scheme B for N^1 -[(alkyl)oxy]pyridyl carboximidamide

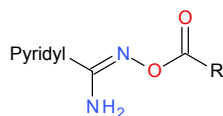


Scheme 2.5: Synthetic scheme B for Compound B

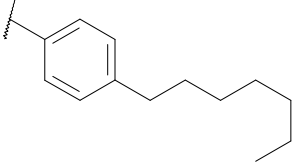
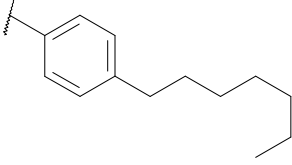
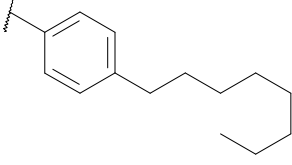
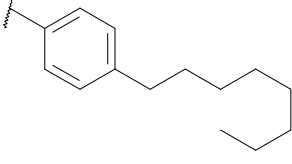
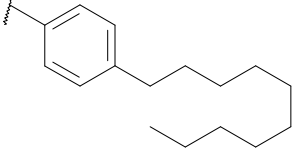
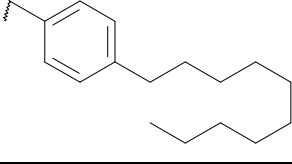
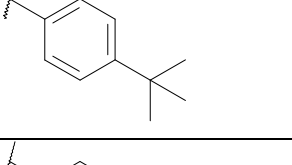
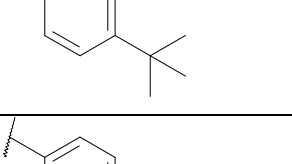
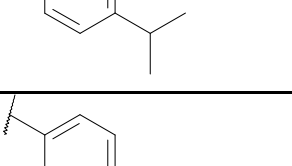
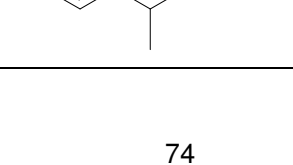
This was also a three step reaction similar to the scheme B for compound A. The only difference is that pyridine amidoxime was used instead of the carboxamidrazone. The CDI was treated with acids to form an intermediate which upon reaction with pyridine amidoxime gave the required N^1 -[(alkyl)oxy]pyridyl carboximidamide product. The crude product was washed with sodium bicarbonate solution and then recrystallized using appropriate solvents to give pure product.

The analytical data (mass spectrum, NMR, and IR) all were found to be consistent with the proposed structure. The IR exhibited strong absorbance in the range of $1665 - 1760 \text{ cm}^{-1}$ typical of the carbonyl

group. The Table. 2.4 lists the analogues of the compound B synthesised along with their yields and melting points.



Compound B	Pyridyl	Aryl group	Yield (%)	Melting point (°C)
(52)	2-Pyridyl		63	180.8 – 181.6
(53)	4-Pyridyl		67	166.8 – 167.5
(54)	2-Pyridyl		59	155.3 – 156.7
(55)	4-Pyridyl		72	134.3 – 135.5
(56)	2-Pyridyl		74	148.2 – 149.3
(57)	4-Pyridyl		65	154.1 – 154.5
(58)	2-Pyridyl		81	146.3 – 147.6
(59)	4-Pyridyl		84	152.1 – 153.6
(60)	2-Pyridyl		69	153.3 – 154.1
(61)	4-Pyridyl		72	120.3 – 121.9
(62)	2-Pyridyl		68	164.2 – 165.8
(63)	4-Pyridyl		75	133.7 – 135.4

Compound B	Pyridyl	Aryl group	Yield (%)	Melting point (°C)
(64)	2-Pyridyl		82	142.2 – 143.4
(65)	4-Pyridyl		74	126.8 – 128.3
(66)	2-Pyridyl		67	138.7 – 139.2
(67)	4-Pyridyl		73	125.0 – 127.2
(68)	2-Pyridyl		67	137.8 – 138.5
(69)	4-Pyridyl		69	132.9 – 134.1
(70)	2-Pyridyl		71	186.4 – 187.8
(71)	4-Pyridyl		74	168.1 – 169.4
(72)	2-Pyridyl		76	178.7 – 179.6
(73)	4-Pyridyl		81	165.4 – 166.3

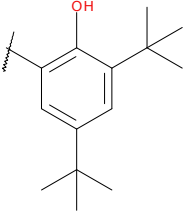
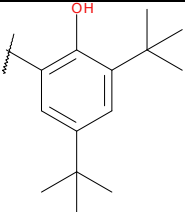
Compound B	Pyridyl	Aryl group	Yield (%)	Melting point (°C)
(74)	2-Pyridyl		64	179.8 – 180.9
(75)	4-Pyridyl		77	176.4 – 177.6

Table 2.4: List of analogues of compound B

2.4.3 COMPOUND C (Bis-amide carboxamidrazone)

At a high temperature the amine (b) (see Fig. 2.15) of the carboxamidrazone becomes reactive, as explained in Chapter 3, where at high temperature a linear carboxamidrazone cyclises. Hence a high temperature reaction was carried out to attack the (b) amino group with an electrophile eg. an acid chloride. However the reaction did not work and instead cyclization of carboxamidrazone took over.

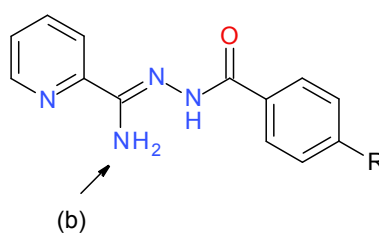
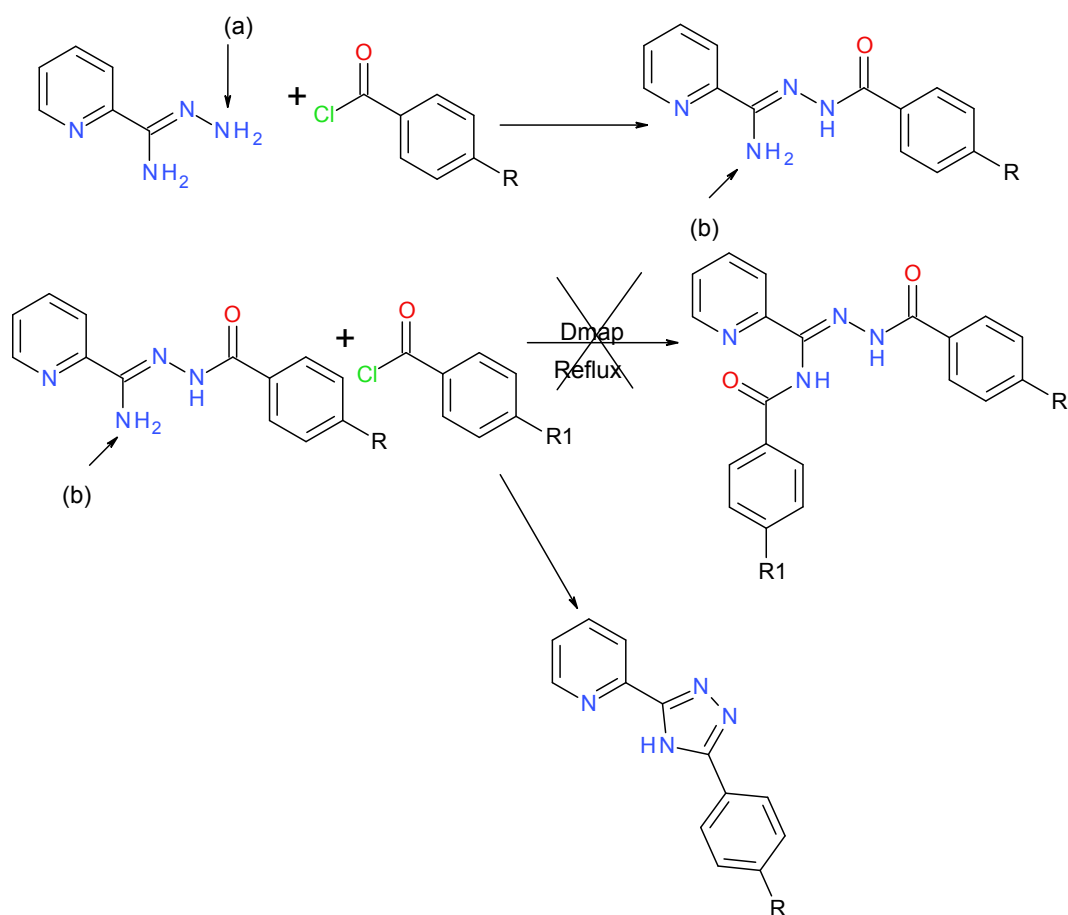


Figure 2.15: General structure of Compound C



Scheme 2.6: Synthetic scheme for Compound C

2.4.4 Purity

The 2-pyridine carboxamidrazone starting material for the preparation of carboxamidrazone amide was clean and did not require further purification and was used as it was. However the 4-pyridine carboxamidrazone (4 PY) compound was purified by recrystallizing it from ethanol. The carboxamidrazone amide products (Compound A) obtained were found to be impure and hence recrystallization was used to purify them.

Both the 2-pyridine amidoxime and 4-pyridine amidoxime compounds obtained from the reaction were pure and in crystalline form. They were used in the crude form for the next reaction as no purification was required. The crude N^1 -[(alkyl)oxy]pyridyl carboximidamide products (Compound B) obtained from reaction were found to contain impurities and hence were purified using recrystallization techniques.

2.4.5 Solubility

It was observed that the yields of 4PY compounds were better than the 2PY compound. This may be because the solubility of 2PY in THF is higher as compared to 4PY and hence large amounts of product was precipitated out.

No such discrepancy was observed in the amidoxime compounds. Both the compounds had similar solubility in THF.

2.4.6 NMR Data

The proton NMR spectra of the carboxamidrazone amides were obtained from d_6 -DMSO and were consistent with the proposed structures. The characteristic amide singlet peak from the carboxamidrazone amide compounds was observed in the range of 10 – 10.5 ppm. In many spectra an extra set of smaller peaks were seen in the range of 10 – 10.5 ppm alongside the amide peak and in the range of 7 – 7.5 alongside the protons from the pyridine ring on the NMR spectrum. Together these small peaks accounted for one proton. At a higher temperature (50°C) the two peaks merge into a single peak. This phenomenon occurs since the rate of interconversion of the two forms of compound are less than the frequency of the NMR machine. At high temperature the rate is increased and an average structure is obtained. Hence at high temperature the two singlets merge into one (see Fig.2.17). Another reason could be the orientation of the pyridine ring.

A similar phenomenon was observed in some of the N^1 -[(alkyl)oxy]pyridyl carboximidamide analogues as well.

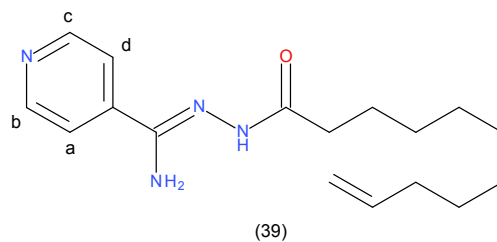


Figure 2.16: Structure of N^1 -(4-(10-Undecenoyl))-pyridine-4-carboxamidrazone

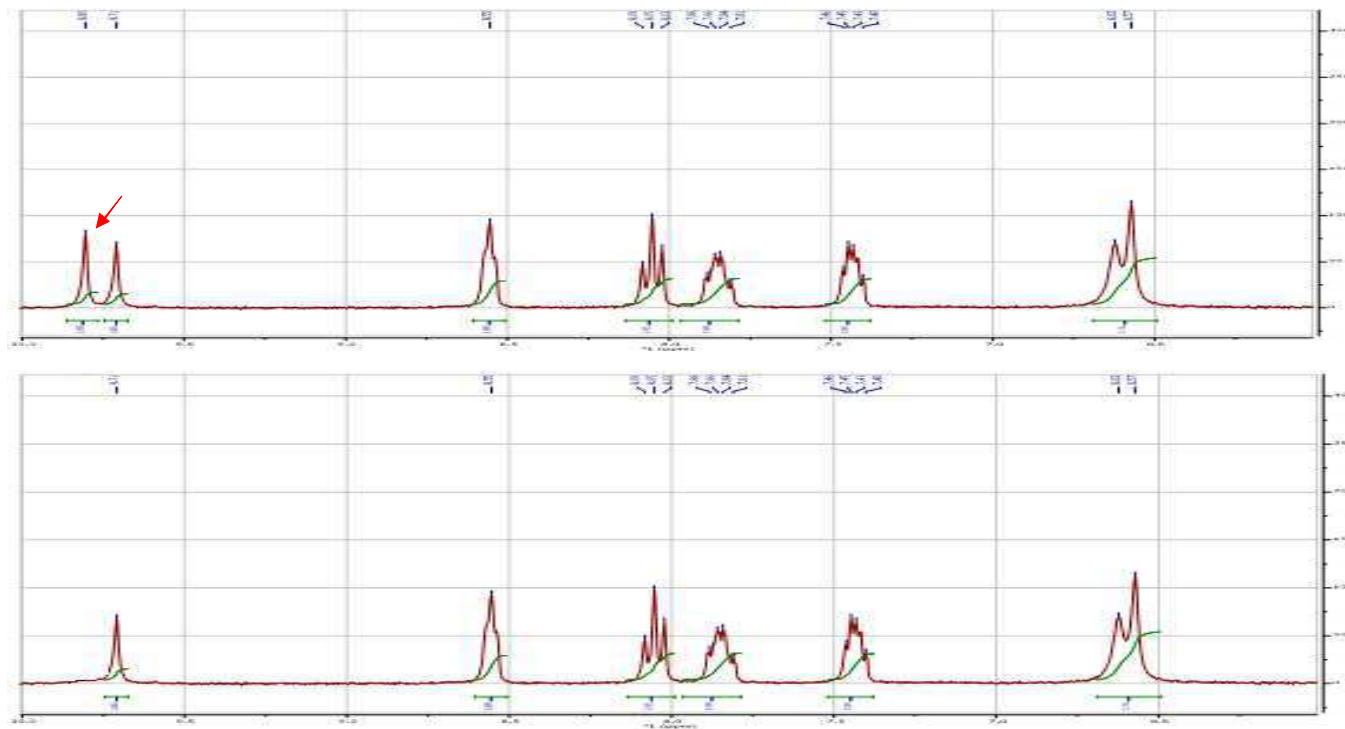


Figure 2.17: The comparison of partial NMR spectra of compound (39) shows the disappearance of the smaller peak in the nmr spectrum taken at 50°C.

2.4.7 Melting point data

The melting points of the compounds showed some anomaly. The anomaly was that the increase in the molecular weight should increase the melting point due to increase in van der Waal's attraction. However it was observed that as the chain length increased the melting point decreased. This phenomenon could be attributed to two factors, the surface area of the molecule and the organisation of the crystal structure of the compound.

It is likely that the preferred conformation for the long alkyl chain is to fold up into a spherical shape as opposed to being a linear structure as shown in the Fig. 2.18. Thus the overall surface area on the carbon chain which was available for the van der Waals effect might be reduced which in turn could have reduced the melting point (Morrison & Boyd (1992)).

The other factor is the energy required to break the rigid and solid structure. The compounds with smaller alkyl chains are packed well in solid phase, forming well organised crystal structures and hence required more energy to break thus increasing their melting points. However the compounds with larger alkyl chains may not be well packed and hence less energy is required to break the loosely packed crystal structure. Thus decreasing the melting points of the compounds (Boese et al. (1999)).

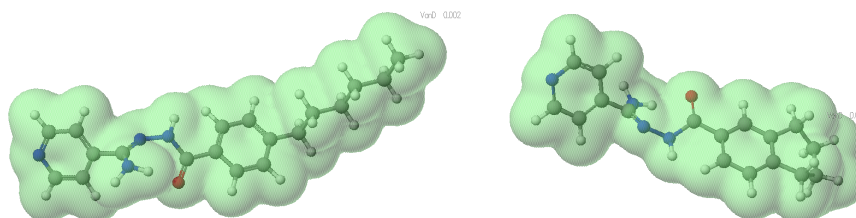


Figure 2.18: The global minimum version of the linear side chain and cyclised side chain carboxamidrazone amide was generated using Cache program and van der Waal's surface was calculated on the compounds

2.4.8 Microbiological results

The entire library of Compound A analogues was sent to the Tuberculosis Antimicrobial Acquisition and Coordinating Facility (TAACF, USA) for screening against *Mycobacterium tuberculosis*. The library of Compound A and Compound B analogues was sent to the National Institute of Allergy and Infectious Diseases (NIAID, USA) for the screening. Both the programs belong to the Southern Research Institute (SRI, USA) and were set-up to assist the scientists to develop new anti tuberculosis drug candidates.

The TAACF, NIAID and SRI have started a new program called high throughput screening (HTS) the resources can be found on their website ¹. This program can screen large compound libraries by the primary *in vitro* assays like MTb or against a specific target. It also supports the design and implementation of *in silico* systems for predicting drug characteristics like solubility, human intestine absorption, bioavailability and potential toxicity.

This screening is designed in two stages: first stage involves a parallel MABA and BTG assay on H37Rv strain to determine the MIC, IC₅₀ and IC₉₀ concentration for the compounds. The compounds which have MIC values of 32.47 μ M or less are further taken to the second stage which involves advanced anti mycobacterial susceptibility profiling. The second stage involves assays for minimal inhibitory concentration (MIC), MBC, LORA, intracellular (macrophage) drug screening, and MTT cell proliferation.

Minimal inhibitory concentration (MIC)

The minimal inhibitory concentration assay is important since it determines the lowest concentration of drug required to visibly inhibit the growth of micro-organisms.

Minimal Bactericidal Concentration (MBC)

The minimal bactericidal concentration assay helps to determine the compound's mechanism of action whether it is bacteriostatic or bactericidal. The bactericidal compound is preferred since it kills the bacteria and it can potentially reduce the standard treatment regime which is a minimum of six months for tuberculosis.

Low Oxygen Recovery Assay (LORA)

The LORA assay is an important assay since it can provide an assessment of drug activity against non-replicating persistent *M. tuberculosis*.

¹<http://www.niaid.nih.gov/pages/default.aspx?wt.ac=tnHome>

Intracellular (macrophage) drug screening

The intracellular (macrophage) drug screening evaluates intracellular drug effectiveness. This is important since *M. tuberculosis* can survive inside a macrophage for many days and hence causing treatment failure and disease relapse. The cytotoxicity control plate assay (MTT proliferation) is performed in parallel with this assay where non infected macrophages are used to confirm that the concentrations used for the assays are non toxic to the macrophages.

Compound name	MIC μM	IC₅₀ μM	IC₉₀ μM
(23)	16.24	14.12	15.33
(25)	32.47	17.11	19.32
(29)	32.47	17.34	19.58
(27)	32.47	26.92	28.02
(40)	32.47	27.54	28.80
(74)	14.94	12.76	14.12
(24)	>32.47	—	—
(26)	>32.47	—	—
(28)	>32.47	—	—
(30)	>32.47	—	—
(31)	>32.47	—	—
(32)	>32.47	—	—
(33)	>32.47	—	—
(34)	>32.47	—	—
(35)	>32.47	—	—
(36)	>32.47	—	—
(37)	>32.47	—	—
(38)	>32.47	—	—
(17)	>32.47	—	—
(39)	>32.47	—	—
(41)	>32.47	—	—
(42)	>32.47	—	—
(43)	>32.47	—	—
(44)	>32.47	—	—

Compound name	MIC μM	IC₅₀ μM	IC₉₀ μM
(45)	>32.47	—	—
(46)	>32.47	—	—
(47)	>32.47	—	—
(48)	>32.47	—	—
(49)	>32.47	—	—
(50)	>32.47	—	—
(51)	>32.47	—	—
(52)	>32.47	—	—
(53)	>32.47	—	—
(54)	>32.47	—	—
(55)	>32.47	—	—
(56)	>32.47	—	—
(57)	>32.47	—	—
(58)	>32.47	—	—
(59)	>32.47	—	—
(60)	>32.47	—	—
(61)	>32.47	—	—
(62)	>32.47	—	—
(63)	>32.47	—	—
(64)	>32.47	—	—
(65)	>32.47	—	—
(66)	>32.47	—	—
(67)	>32.47	—	—
(68)	>32.47	—	—
(69)	>32.47	—	—
(70)	>32.47	—	—
(71)	>32.47	—	—
(72)	>32.47	—	—
(73)	>32.47	—	—
(75)	>32.47	—	—

Table 2.5: The MIC values and IC₅₀ and IC₉₀ values of the most active compounds

The compound (74) was found to be the most active compound of the series and hence it was taken to the second step of screening. The Table. 2.6 presents the data for MIC and MBC values and Table. 2.7 presents data for the macrophage assay.

Compound name	MIC H₃₇Rv μM	% Inhi- bition^a	MBC H₃₇Rv μM	MIC INH- R^b μM	% Inhi- bition	MIC RMP- R^c μM	% Inhi- bition	MIC OFX- R^d μM	% Inhi- bition
(74)	20.29	69	162.35	5.07	60	20.29	83	20.29	68
Rifampin (pos con- trol)	0.16	68	1.27	0.16	64	NA ^d	NA	0.63	66
Isoniazid (pos con- trol)	NA	NA	NA	NA	NA	0.07	74	NA	NA

^a Percent inhibition at the MIC concentration

^b INH-R = Isoniazid Resistance

^c RMP-R = Rifampin Resistance

^d NA = Not Applicable: Compound not used in assay.

Table 2.6: The MIC values and IC₅₀ and IC₉₀ values of the most active compound

Compound name	LORA (μM)	Macrophage log reduc- tion (low conc.)	Macrophage log reduc- tion (mid conc.)	Macrophage log reduc- tion (high conc.)	MTT% via- bility (low conc.)	MTT% via- bility (mid conc.)	MTT% via- bility (high conc.)
(74)	40.59	0.40	0.44	1.30	1	5	1
Rifampin (pos con- trol)	2.54	1.09	1.27	2.11	>100	>100	>100

Table 2.7: The Macrophage assays values and MTT values of the most active compound

2.4.9 Structure activity relationship

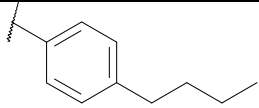
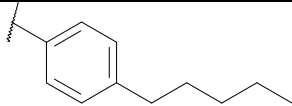
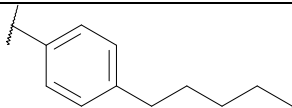
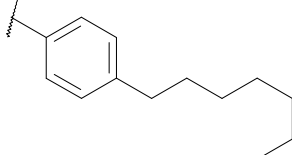
The 2-pyridyl compounds are the more active as compared to the 4-pyridyl compounds. The biological data obtained from the carboxamidrazone compound shows that the compounds containing 2-hydroxy-3, 5-di-tert. butylphenyl substituents have maximum activity (Sikdar (2010)). The carboxamidrazone amides attached to the benzoyl moiety containing an alkyl side chain of 5 to 7 carbons were also found to be active. This increase in the activity could be related to the increase in the logP value, resulting in increased lipophilicity of the molecule and hence an improved permeability of the bacterial cell wall, thus increasing the activity of the molecule.

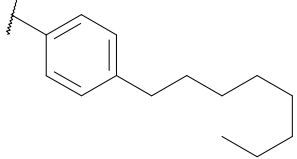
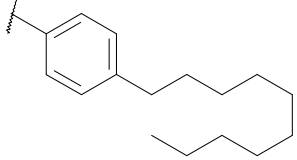
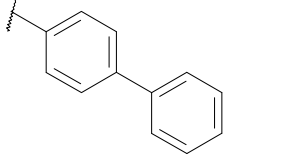
2.5 Summary and Conclusion

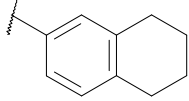
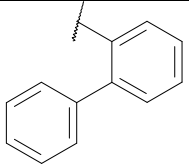
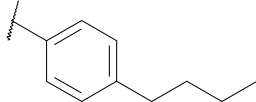
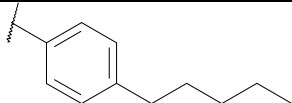
2.5.1 Summary

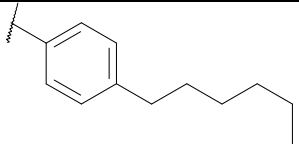
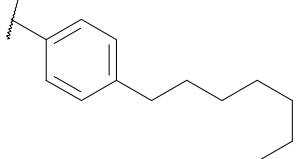
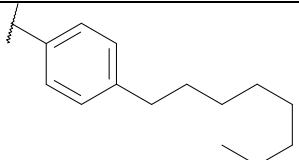
The Table.2.8 and 2.9 summarises the compounds synthesised in the present study and in the previous work at Aston University. The compound class synthesised in Table. 2.8 shows a bell shaped activity curve. The LogP values were calculated using the Accelrys program, which uses ACD/Lab database². In the carboxamidrazone amides, those compounds which has a chain length of 5 or 6 carbons attached to the benzoyl moiety have maximum activity. As the number of carbons in the side chains increases or decreases the activity is further diminished. The microbiological results are reported only for the compounds having MIC values of $\leq 32.47 \mu\text{M}$. Some of the compounds synthesised earlier by Ren (2009) were tested by TAACF, USA which did not test the compounds for MIC values. Hence in the summary table (2.8) the absent values are denoted as hyphen.

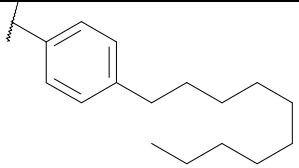
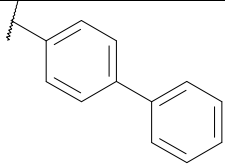
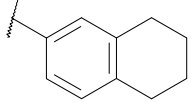
²<http://accelrys.com/>

Compound number	Compound name	Pyridyl group	Aryl group	MIC (μM)	IC ₅₀ (μM)	IC ₉₀ (μM)	Log P	Melting point ($^{\circ}\text{C}$)	Yield (%)	Reference
(23)	<i>N</i> ¹ -(4-Butylbenzoyl)-pyridine-2-carboxamidrazone	2-Pyridyl		16.24	14.12	15.33	3.327	230.4-232.8	87	
(14)	<i>N</i> ¹ -(4-Pentylbenzoyl)-pyridine-2-carboxamidrazone	2-Pyridyl		-	2.88	4.50	3.723	234.1-235.9	45	Ren (2009)
(13)	<i>N</i> ¹ -(4-Hexylbenzoyl)-pyridine-2-carboxamidrazone	2-Pyridyl		-	3.23	4.32	4.119	218.7-220.6	46	Ren (2009)
(15)	<i>N</i> ¹ -(4-Heptylbenzoyl)-pyridine-2-carboxamidrazone	2-Pyridyl		-	4.58	4.96	4.516	215.3-216.1	30	Ren (2009)

Compound number	Compound name	Pyridyl group	Aryl group	MIC (μM)	IC ₅₀ (μM)	IC ₉₀ (μM)	Log P	Melting point ($^{\circ}\text{C}$)	Yield (%)	Reference
(25)	<i>N</i> ¹ -(4-Octylbenzoyl)-pyridine-2-carboxamidrazone	2-Pyridyl		32.47	17.11	19.32	4.912	195.6-197.1	92	
(16)	<i>N</i> ¹ -(4-Decylbenzoyl)-pyridine-2-carboxamidrazone	2-Pyridyl		-	17.75	19.44	5.705	201.2-203.2	32	Ren (2009)
(29)	<i>N</i> ¹ -(4-Phenylbenzoyl)-pyridine-2-carboxamidrazone	2-Pyridyl		32.47	17.34	19.58	3.355	218.8-220.2	75	

Compound number	Compound name	Pyridyl group	Aryl group	MIC (μM)	IC ₅₀ (μM)	IC ₉₀ (μM)	Log P	Melting point ($^{\circ}\text{C}$)	Yield (%)	Reference
(27)	<i>N</i> ¹ -(1,2,3,4-tetrahydronaphthalene)-pyridine-2-carboxamidrazone	2-Pyridyl		32.47	26.92	28.02	2.894	149.7-150.5	68	
(31)	<i>N</i> ¹ -(2-Phenylbenzoyl)-pyridine-2-carboxamidrazone	2-Pyridyl		>32.47	-	-	3.355	224.3 - 225.4	71	
(24)	<i>N</i> ¹ -(4-Butylbenzoyl)-pyridine-4-carboxamidrazone	4-Pyridyl		>32.47	-	-	2.928	177.9 - 179.1	92	
(76)	<i>N</i> ¹ -(4-Pentylbenzoyl)-pyridine-4-carboxamidrazone	4-Pyridyl		-	57.51	80.82	3.324	201.2-201.8	38	Ren (2009)

Compound number	Compound name	Pyridyl group	Aryl group	MIC (μM)	IC ₅₀ (μM)	IC ₉₀ (μM)	Log P	Melting point ($^{\circ}\text{C}$)	Yield (%)	Reference
(77)	<i>N</i> ¹ -(4-Hexylbenzoyl)-pyridine-4-carboxamidrazone	4-Pyridyl		-	38.87	44.88	4.117	187.7-191.0	27	Ren (2009)
(78)	<i>N</i> ¹ -(4-Heptylbenzoyl)-pyridine-4-carboxamidrazone	4-Pyridyl		-	24.53	38.01	3.720	182.2-182.8	23	Ren (2009)
(26)	<i>N</i> ¹ -(4-Octylbenzoyl)-pyridine-4-carboxamidrazone	4-Pyridyl		>32.47	-	-	4.513	150.7-151.2	74	

Compound number	Compound name	Pyridyl group	Aryl group	MIC (μM)	IC ₅₀ (μM)	IC ₉₀ (μM)	Log P	Melting point ($^{\circ}\text{C}$)	Yield (%)	Reference
(79)	<i>N</i> ¹ -(4-Decylbenzoyl)-pyridine-4-carboxamidrazone	4-Pyridyl		-	-	-	5.705	191.5-193.9	57	
(30)	<i>N</i> ¹ -(4-Phenylbenzoyl)-pyridine-4-carboxamidrazone	4-Pyridyl		>32.47	-	-	2.956	218.8-220.2	75	
(28)	<i>N</i> ¹ -(1,2,3,4-tetrahydronaphthalene)-pyridine-4-carboxamidrazone	4-Pyridyl		>32.47	-	-	2.495	20.7-202.7	86	

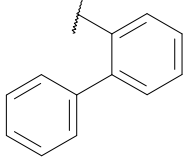

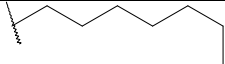
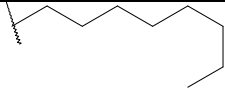
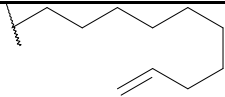
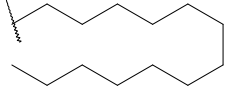
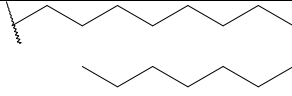
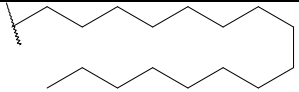
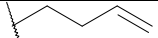
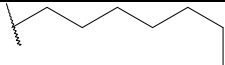
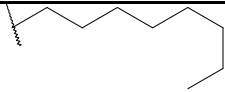
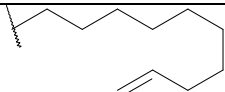
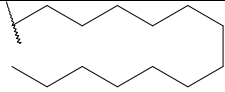
Compound number	Compound name	Pyridyl group	Aryl group	MIC (μM)	IC ₅₀ (μM)	IC ₉₀ (μM)	Log P	Melting point ($^{\circ}\text{C}$)	Yield (%)	Reference
(32)	<i>N</i> ¹ -(2-Phenylbenzoyl)-pyridine-4-carboxamidrazone	4-Pyridyl		>32.47	-	-	2.956	148.2-149.3	82	

Table 2.8: List of the carboxamidrazone amide compounds synthesised at Aston laboratory along with their biological activity.

This class of compound was found to be generally weakly active to inactive. The previous work by Ren (2009) in this class suggested that carboxamidrazone amides attached with an alkyl chain containing more than 10 carbon atoms demonstrated some activity. Hence to investigate this argument a matrix was created where the carboxamidrazone amides were synthesised varying an alkyl chain moiety. The alkyl chains varying between 5 to 15 carbon chain lengths were synthesised. The Table. 2.9 confirms the findings of Ren (2009), that only the carboxamidrazone amides attached to the alkyl chain of 11 carbon atoms, has maximum activity.

Compound number	Compound name	Pyridyl group	Aryl group	MIC (μM)	IC ₅₀ (μM)	IC ₉₀ (μM)	Log P	Melting point ($^{\circ}\text{C}$)	Yield (%)	Reference
(33)	<i>N</i> ¹ -(4-Pentenoyl)-pyridine-2-carboxamidrazone	2-Pyridyl		>32.47	-	-	0.963	191.5-193.9	9	Ren (2009)
(35)	<i>N</i> ¹ -(4-Octenoyl)-pyridine-2-carboxamidrazone	2-Pyridyl		>32.47	-	-	2.367	167.1-168.2	64	
(37)	<i>N</i> ¹ -(4-Nonanoyl)-pyridine-2-carboxamidrazone	2-Pyridyl		>32.47	-	-	2.764	153.5-154.6	77	
(17)	<i>N</i> ¹ -(4-(10-Undecenoyl))-pyridine-2-carboxamidrazone	2-Pyridyl		-	14.37	23.97	3.341	120.9-124.8	9	Ren (2009)
(80)	<i>N</i> ¹ -(4-Myristoyl)-pyridine-2-carboxamidrazone	2-Pyridyl		-	-	-	4.745	123.0-125.3	33	Ren (2009)
(81)	<i>N</i> ¹ -(4-Palmitoyl)-pyridine-2-carboxamidrazone	2-Pyridyl		-	-	-	5.538	75.9-80.4	40	Ren (2009)

Compound number	Compound name	Pyridyl group	Aryl group	MIC (μM)	IC ₅₀ (μM)	IC ₉₀ (μM)	Log P	Melting point ($^{\circ}\text{C}$)	Yield (%)	Reference
(82)	<i>N</i> ¹ -(4-Stearoyl)-pyridine-2-carboxamidrazone	2-Pyridyl		-	137.81	151.80	5.538	118.6-121.4	23	Ren (2009)
(34)	<i>N</i> ¹ -(4-Pentenoyl)-pyridine-4-carboxamidrazone	4-Pyridyl		>32.47	-	-	0.564	187.1-189.7	71	
(36)	<i>N</i> ¹ -(4-Octenoyl)-pyridine-4-carboxamidrazone	4-Pyridyl		>32.47	-	-	1.968	162.8-166.7	71	
(38)	<i>N</i> ¹ -(4-Nonanoyl)-pyridine-4-carboxamidrazone	4-Pyridyl		>32.47	-	-	2.365	149.4-151.3	76	
(39)	<i>N</i> ¹ -(4-(10-Undecenoyl))-pyridine-4-carboxamidrazone	4-Pyridyl		-	81.95	91.80	2.942	113.0-114.2	4.3	Ren (2009)
(83)	<i>N</i> ¹ -(4-Myristoyl)-pyridine-4-carboxamidrazone	4-Pyridyl		-	-	-	4.346	116.8-117.5	40	Ren (2009)

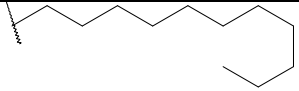
Compound number	Compound name	Pyridyl group	Aryl group	MIC (μM)	IC ₅₀ (μM)	IC ₉₀ (μM)	Log P	Melting point ($^{\circ}\text{C}$)	Yield (%)	Reference
(84)	<i>N</i> ¹ -(Lauroyl)-pyridine-4-carboxamidrazone	4-Pyridyl		-	-	-	3.554	121.2-124.4	31	Ren (2009)

Table 2.9: List of the carboxamidrazone amide compounds synthesised at Aston laboratory along with their biological activity.

2.5.2 Conclusion

Some of the analogues of compound A and B show weak activity, but no significant activity. This class of compound has undergone many modifications to yield a compound with high activity and low toxicity. Further modification can be done to the compound at the benzoyl end and at the centre of the structure.

Chapter. 3 discusses in detail about cyclisation of carboxamidrazone. The introduction of heterocyclic scaffolds in the centre of the carboxamidrazone causes reduction in the overall entropy penalty for the binding of the molecule into an active site and thus might increase the binding affinity of the compound. Another modification involves fluorination of the carboxamidrazone amides as discussed in chapter 4. The most active carboxamidrazone amides were selected and a fluorine atom was introduced in the pyridine ring to investigate the potential change to the compound's metabolism in the organism and/or host.

The synthesis of the analogues of compound C was not possible due to the low reactivity of amine (b). However in future if a low temperature reaction can cause increase in reactivity of the amine (b), the synthesis of compound C can be possible.

Some more carboxamidrazone like imines which are known to possess activity can be reacted with the lithocholic acid and be tested in future for its activity.

2.6 EXPERIMENTAL

2.6.1 Chemicals

All the chemicals and solvents were used as supplied. 2-pyridine cyanide, 4 pyridine cyanide, N, *N*¹-carbonyl di-imidazole, hydrazine, hydroxylamine, Hüinig's base, DMSO, and all the acids and acid chlorides were purchased from Sigma Aldrich. The organic solvents used were purchased from Fisher Chemicals. An aluminium silica gel 60 F254 plates (Merck) were used for thin layer chromatography (TLC).

2.6.2 Instrumentation

Proton NMR spectra were obtained on a Bruker AC 250 instrument operation at 250 MHz as solutions in *d*₆-DMSO or CDCl₃ and referenced from δ DMSO = 2.50 ppm or δ CDCl₃ = 7.27 ppm unless otherwise stated. Infrared spectra were recorded as KBr discs on a Mattson 3000 FTIR spectrophotometer and neat on Nicolet iS5 RT-IR instrument + ID5 ATR Diamond Sampler holder accessory. (APCI-MS) was carried out on a Hewlett-Packard 5989B quadruple instrument connected to an electrospray 59987A unit with an APCI accessory and automatic injecting using a Hewlett-Packard 1100 series autosampler. Accurate MS was carried out on TOF mass spectra (ESI mode) measured on a Waters LCT Premier Mass Spectrometer. Some of the compounds were sent to EPSRC Mass Spectrometry Service Centre at Swansea, the compounds were tested on either of the following machines Thermofisher LTQ Orbitrap XL, Finnigan MAT 95 XP, Applied Biosystems Voyager DE-STR, Waters Micromass ZQ4000, Thermofisher DSQ-II, Agilent 5975 GCMS. Melting points were recorded on a Reichert-Jung Thermo Galen hot stage microscope and were corrected.

2.6.3 Preparation of pyridine-2-carboxamidrazone (85)

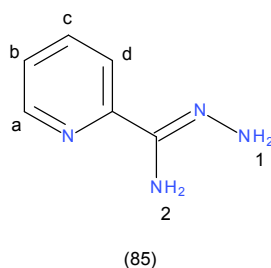


Figure 2.19: Pyridine-2-carboxamidrazone

2-cyano pyridine (29.99 g, 288.4 mmol) was dissolved in ethanol (90 mL) and to it hydrazine monohydrate (60 mL) was added. This reaction mixture was stirred at room temperature for 2 days. The product was collected by removing excess hydrazine under vacuum. The product was collected by filtration. The crude product was then washed 3X with petrol ether 40 – 60°C to give a yellow crystalline compound.

Yield 35.1 g, 89.5%.

R_f value [EtOAc:MeOH (2:1)]: 0.10 (Khan (2008)).

¹H NMR (250 MHz, d₆-DMSO): 8.48 (m, 1H, **a**), 7.91 (m, 1H, **d**), 7.74 (td, 1H, J= 6.92, 1.8 Hz, **b**), 7.31 (td, 1H, J=4.9, 1.2 Hz, **c**), 5.24 (bs, 2H, **NH₂(2)**), 5.71 (bs, 2H, **NH₂(1)**) ppm.

2.6.4 Preparation of pyridine-4-carboxamidrazone (86)

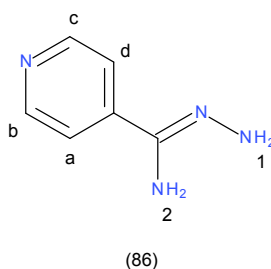


Figure 2.20: Pyridine-4-carboxamidrazone

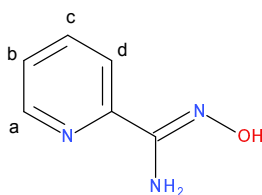
The procedure for the preparation of pyridine-4-carboxamidrazone is same as for pyridine-2-carboxamidrazone. The time required for completion of the reaction is 14 days. The crude product obtained was purified by recrystallization from ethanol.

Yield was 33.5 g, 75%.

R_f value [EtOAc:MeOH (2:1)]: 0.18 (Khan (2008)).

$^1\text{H NMR}$ (250 MHz, $\text{d}_6\text{-DMSO}$): 8.51 (d, 2H, $J=6.3$ Hz, **b and d**), 7.63 (d, 2H, $J=6.3$ Hz, **a and c**), 5.71 (bs, 2H, **NH₂(2)**), 5.33 (bs, 2H, **NH₂(1)**) ppm.

2.6.5 Preparation of pyridine-2-amidoxime (87)



(87)

Figure 2.21: Pyridine-2-amidoxime

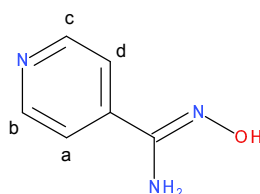
Hydroxyl ammonium chloride (2.1g, 30 mmol) was dissolved in water (10 mL) and anhydrous sodium carbonate (1.6g, 15 mmol) was added to this solution and heated up to 60°C. At this stage 2-cyano pyridine (3g, 29 mmol) was added to the reaction mixture, followed by ethanol (approx. 6 mL) to dissolve the cyano pyridine. The temperature of the reaction mixture was raised and maintained at 85°C for 2 hours. The reaction mixture flask was then cooled to 0°C and some ice cold water was added to the reaction mixture. The resulting crude material was collected by filtration to give a white solid.

Yield was 3.1 g ,91%.

R_f value [EtOAc:MeOH (2:1)]: 0.13.

$^1\text{H NMR}$ (250 MHz, $\text{d}_6\text{-DMSO}$): 9.89 (s, 1H, OH), 8.56 (ddd, 1H, $J = 4.9, 1.7, 1.1$ Hz, **-a**), 8.27 – 7.72 (m, 2H, **-b and d**), 7.53 – 7.33 (m, 1H, **-c**), 5.83 (s, 2H, **NH₂**) ppm.

2.6.6 Preparation of pyridine-4-amidoxime (88)



(88)

Figure 2.22: Pyridine-4-amidoxime

Hydroxyl ammonium chloride (2.1g, 30 mmol) was dissolved in water (10 mL) and anhydrous sodium carbonate (1.6g, 15 mmol) was added to this solution and heated up to 60°C. At this stage 4-cyano pyridine (3g, 29 mmol) was added to the reaction mixture, this is an exothermic reaction and the temperature rises to 75°C and a colourless mass is precipitated out. This reaction mixture is further heated up to 80°C and maintained for 0.5 hours. This reaction flask was then cooled on an ice bath for 15 mins. To this reaction mixture 15 mL of ice cold water was added and a white solid precipitated out which was collected by filtration. The crude product was washed with ice cold water (3x30 mL). The crude product obtained was recrystallised from ethanol to obtain transparent needle like crystals.

Yield was 2.5 g ,84%.

R_f value [EtOAc:MeOH (2:1)]: 0.15.

¹H NMR (250 MHz, d₆-DMSO): 10.03 (s, 1H, OH), 8.57 (dd, J = 4.6, 1.6 Hz, 2H, **a and d**), 7.63 (dd, J = 4.6, 1.6 Hz, 2H, **b and c**), 5.99 (s, 2H, NH₂) ppm.

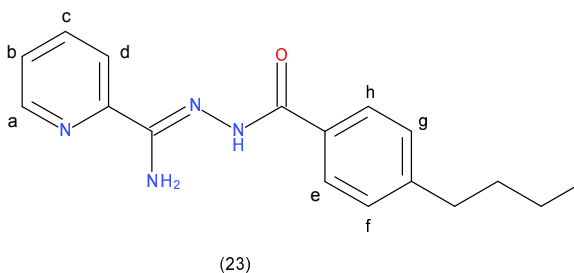
2.6.7 General procedure for carboxamidrazone synthesis from acid chlorides

Heteroaryl carboxamidrazone (1.0 g, 7.35 mmol) was suspended in anhydrous THF (20 mL). To this solution Hünig's base (2 mL) was added, followed by acid chloride (1.1 eq). This reaction mixture was stirred overnight under argon at room temperature. This reaction mixture was added to sat. sodium bicarbonate solution and the product was collected by filtration. The crude product was further purified by recrystallization using appropriate solvent systems (Ethyl acetate: Petroleum ether (40-60°C)).

2.6.8 General procedure for synthesis of carboxamidrazone from acids

N,N'-carbonyl-di-imidazole (1.622 g, 10 mmol) and acid (12 mmol, 1 eq) was dissolved in THF (20 mL). To this reaction mixture appropriate heteroaryl carboxamidrazone (1g, 7.35 mmol) was added and this reaction mixture was stirred under argon at room temperature overnight. This reaction mixture was added to sodium bicarbonate solution and the product was collected by filtration. The crude product was further purified by recrystallization using appropriate solvent systems (Ethyl acetate: Petroleum ether (40-60°C)).

*N*¹-(4-Butylbenzoyl)-pyridine-2-carboxamidrazone (23)



¹H NMR (250 MHz, d₆-DMSO): 10.11 (s, 1H, -NH), 8.61 (d, 2H, J = 4.4 Hz, -b and d), 8.18 (d, 1H, J = 8.1 Hz, -a), 7.99 – 7.74 (overlapping m, 2H, -e and h), 7.50 (m, 1H, -c), 7.31 (d, 2H, J = 8.1 Hz, -f and g), 6.91 (s, 2H, -NH₂), 1.45 (t, 2H, J = 7.5 Hz, -CH₂CH₂CH₂CH₃), 1.33 (dq, 4H, J = 14.3, 7.2 Hz, -CH₂CH₂CH₂CH₃), 0.91 (t, 3H, J = 7.3 Hz, -CH₂CH₂CH₂CH₃) ppm.

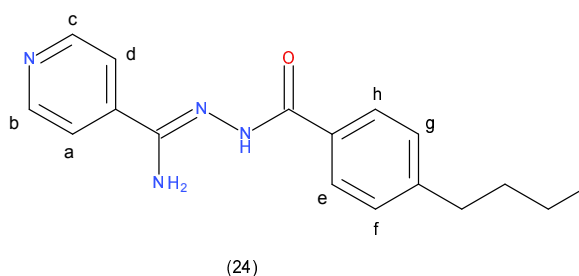
IR (KBr disc) ν : 3341 (N-H), 3340 (N-H), 3303 (N-H), 3120, 3054 (Aromatic C-H), 3022 (Aromatic C-H), 2958 (Alkyl C-H), 2935 (Alkyl C-H), 2849 (Alkyl C-H), 1911, 1665 (C=O), 1634, 1534, 1470, 1443, 1401, 1288 (C-N) cm⁻¹.

Melting point: 230.4 – 232.8 °C.

Mass spectrum (APCI +) m/z: Found 296.1625 (M+H)⁺; calculated for C₁₇H₂₀N₄O 296.1637; 4.1 ppm.

Yield: 1.90 g, 87%.

***N*¹-(4-Butylbenzoyl)-pyridine-4-carboxamidrazone (24)**



¹H NMR (250 MHz, d₆-DMSO): 10.05 (s, 1H, -NH), 8.65 (d, 2H, J = 5.4 Hz, -b and c), 7.79 (d, 4H, J = 7.9 Hz, -h, a, d and e), 7.30 (d, 2H, J = 8.1 Hz, -f and g), 6.88 (s, 2H, -NH₂), 2.65 (t, 2H, J = 7.5 Hz, -CH₂CH₂CH₂CH₃), 1.57 (dd, 2H, J = 15.3, 7.9 Hz, -CH₂CH₂CH₂CH₃), 1.32 (dd, 2H, J = 14.8, 7.2 Hz, -CH₂CH₂CH₂CH₃), 0.91 (t, 3H, J = 7.3 Hz, -CH₂CH₂CH₂CH₃) ppm.

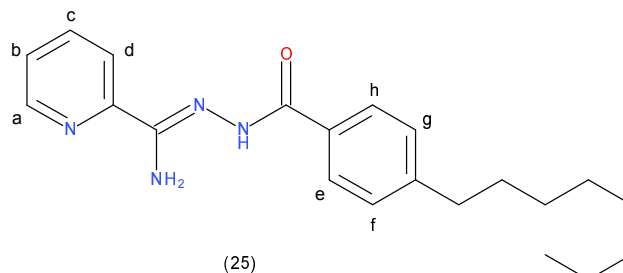
IR (KBr disc) ν : 3398 (N-H), 3367 (N-H), 3302 (N-H), 3150, 3025 (Aromatic C-H), 2946 (Alkyl C-H), 2919 (Alkyl C-H), 2850 (Alkyl C-H), 1696 (C=O), 1587, 1532, 1494, 1400, 1296 (C-N), 1158 cm⁻¹.

Melting point: 177.9 – 179.1 °C.

Mass spectrum (APCI +) m/z: Found 296.1632 (M+H)⁺; calculated for C₁₇H₂₀N₄O 296.1637; 1.6 ppm.

Yield: 2 g, 92%.

***N*¹-(4-Octylbenzoyl)-pyridine-2-carboxamidrazone (25)**



¹H NMR (250 MHz, d₆-DMSO): 10.11 (s, 1H, -NH), 8.60 (d, 2H, J = 4.4 Hz, b and d), 8.17 (d, 1H, J = 7.7 Hz, - a), 7.80 (d, 3H, J = 8.1 Hz, c, e and h), 7.30 (d, 2H, J = 8.1 Hz, f and g), 6.89 (s, 2H, -NH₂),

2.64 (t, 2H, J = 7.6 Hz, $-\text{CH}_2(\text{CH}_2)_6\text{CH}_3$), 1.59 (s, 2H, $-\text{CH}_2\text{CH}_2(\text{CH}_2)_5\text{CH}_3$), 1.27 (overlapping m, 10H, J = 8.9 Hz, $-\text{CH}_2\text{CH}_2(\text{CH}_2)_5\text{CH}_3$), 0.86 (t, 3H, J = 6.5 Hz, $-\text{CH}_2(\text{CH}_2)_6\text{CH}_3$) ppm.

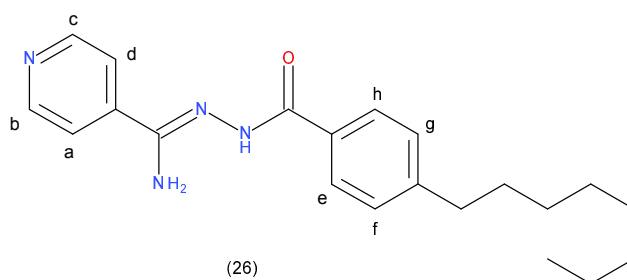
IR (KBr disc) ν : 3413 (N-H), 3344 (N-H), 3307 (N-H), 3211, 3022 (Aromatic C-H), 2948 (Alkyl C-H), 2917 (Alkyl C-H), 2843 (Alkyl C-H), 2357, 2334, 1636 (C=O), 1590, 1539, 1475, 1443, 1337 (C-N), 1149 cm^{-1} .

Melting point: 195.6 – 197.1 °C.

Mass spectrum (APCI +) m/z: Found 352.2258 (M+H)⁺; calculated for $\text{C}_{21}\text{H}_{28}\text{N}_4\text{O}$ 352.2263; 1.4 ppm.

Yield: 2.38 g, 92%.

***N*¹-(4-Octylbenzoyl)-pyridine-4-carboxamidrazone (26)**



¹H NMR (250 MHz, d₆-DMSO): 10.04 (s, 1H, **-NH**), 8.65 (d, 2H, J = 5.7 Hz, **-b and c**), 7.79 (d, 2H, J = 8.0 Hz, **-e and h**), 7.29 (d, 4H, J = 8.1 Hz, **-a, d, f and g**), 6.87 (s, 2H, **-NH₂**), 2.63 (t, 2H, J = 7.5 Hz, $-\text{CH}_2(\text{CH}_2)_6\text{CH}_3$), 1.59 (s, 2H, $-\text{CH}_2\text{CH}_2(\text{CH}_2)_5\text{CH}_3$), 1.59 (s, 2H, $-\text{CH}_2\text{CH}_2\text{CH}_2(\text{CH}_2)_4\text{CH}_3$), 1.27 (d, 8H, J = 8.7 Hz, $-\text{CH}_2\text{CH}_2\text{CH}_2(\text{CH}_2)_4\text{CH}_3$), 0.85 (t, 3H, J = 6.5 Hz, $-\text{CH}_2(\text{CH}_2)_6\text{CH}_3$) ppm.

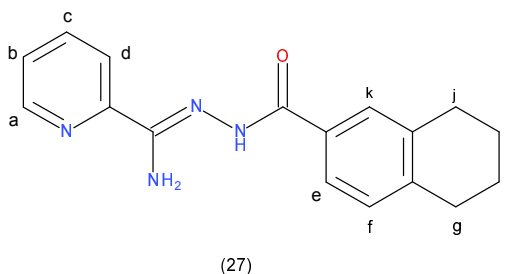
IR (KBr disc) ν : 3356 (N-H), 3320 (N-H), 3252 (N-H), 3207, 3026 (Aromatic C-H), 2957 (Alkyl C-H), 2915 (Alkyl C-H), 2845 (Alkyl C-H), 1672 (C-C in ring), 1634 (C=O), 1583, 1528, 1500, 1463, 1416, 1291 (C-N), 1189 cm^{-1} .

Melting point: 150.7 – 151.2 °C.

Mass spectrum (APCI +) m/z: Found 352.2257 (M+H)⁺; calculated for $\text{C}_{21}\text{H}_{28}\text{N}_4\text{O}$ 352.2263; 1.7 ppm.

Yield: 1.92 g, 74%.

***N*¹-(1,2,3,4-Tetrahydronaphthalene)-pyridine-2-carboxamidrazone (27)**



¹H NMR (250 MHz, d₆-DMSO): 10.05 (s, 1H, **-NH**), 8.60 (d, 1H, J = 4.0 Hz, **-a**), 8.17 (d, 1H, J = 7.9 Hz, **-c**), 7.90 (d, 2H, J = 6.8 Hz, **-b and d**), 7.46 (m, 1H, **-k**), 7.15 (d, 2H, J = 8.4 Hz, **-e and f**), 6.91 (s, 2H, **-NH₂**), 2.78 (d, 6H, J = 4.0 Hz, **-g, h and i**), 1.76 (s, 2H, **-j**) ppm.

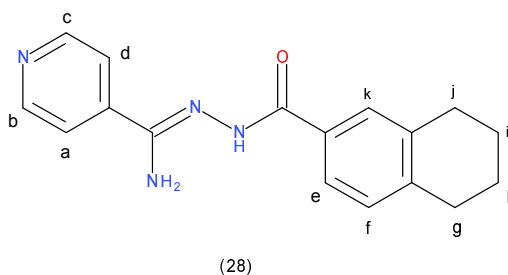
IR (KBr disc) ν : 3457 (N-H), 3349 (N-H), 3278, 3142, 3014 (Aromatic C-H), 2981, 1666, 1635 (C=O), 1572, 1519, 1475, 1386, 1279 (C-N), 1202, 1114 cm⁻¹.

Melting point: 149.7 – 150.5 °C.

Mass spectrum (APCI +) m/z: Found 294.1477 (M+H)⁺; calculated for C₁₇H₁₈N₄O 294.1480; 1.0 ppm.

Yield: 1.47 g, 68%.

***N*¹-(1,2,3,4-Tetrahydronaphthalene)-pyridine-4-carboxamidrazone (28)**



¹H NMR (250 MHz, d₆-DMSO): 10.05 (s, 1H, **-NH**), 8.60 (d, 1H, J = 4.0 Hz, **-b**), 8.17 (d, 1H, J = 7.9 Hz, **-c**), 7.90 (t, 1H, J = 6.8 Hz, **-a**), 7.59 (s, 2H, **-d**), 7.46 (m, 1H, **-k**), 7.15 (d, 1H, J = 8.4 Hz, **-e and f**), 6.91 (s, 2H, **-NH₂**), 2.78 (d, 6H, J = 4.0 Hz, **-g, h, and i**), 1.76 (s, 2H, **-j**) ppm.

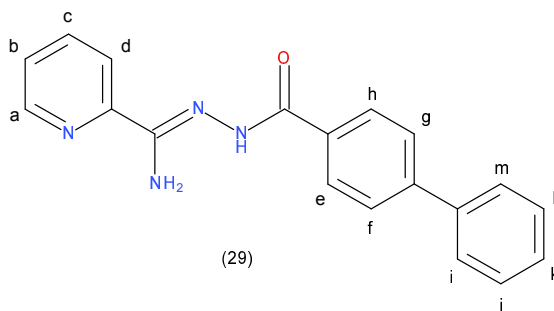
IR (KBr disc) ν : 3467 (N-H), 3357 (N-H), 3204, 3012 (Aromatic C-H), 2931, 2852, 1637 (C=O), 1594, 1545, 1498, 1465, 1407, 1305, 1294, 1265 (C-N), 1191, 1147, 1033 cm⁻¹.

Melting point: 201.7 – 202.7 °C.

Mass spectrum (APCI +) m/z: Found 294.1473 (M+H)⁺; calculated for C₁₇H₁₈N₄O 294.1480; 2.3 ppm.

Yield: 1.86 g, 86%.

***N*¹-(4-Phenylbenzoyl)-pyridine-2-carboxamidrazone (29)**



¹H NMR (250 MHz, d₆-DMSO): 10.23 (s, 1H, **-NH**), 8.61 (d, 1H, J = 4.6 Hz, **-a**), 8.20 (d, 1H, J = 8.0 Hz, **-c**), 8.16 – 7.68 (overlapping m, 7H, **-e, h, f, g, i, k, m**), 7.46 (overlapping m, 4H, **-b, j, l and d**), 6.97 (s, 2H, **-NH₂**) ppm.

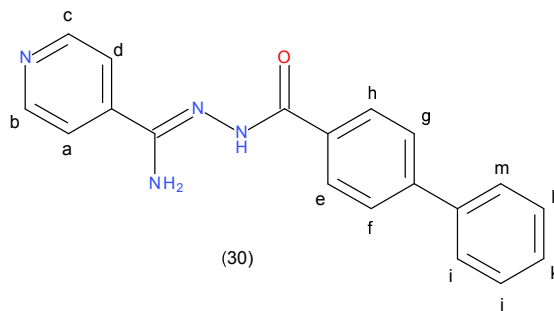
IR (KBr disc) ν : 3386 (N-H), 3300 (N-H), 3186 (N-H), 3054 (Aromatic C-H), 3022 (Aromatic C-H), 1798 (C-C in Aromatic ring), 1752 (C=O), 1634, 1579 (C-C in aromatic ring), 1529, 1461, 1397, 1384, 1293 (C-N), 1156 cm⁻¹.

Melting point: 218.8 – 220.2 °C.

Mass spectrum (APCI +) m/z: Found 316.1320 (M+H)⁺; calculated for C₁₉H₁₆N₄O 316.1324; 1.2 ppm.

Yield: 1.74 g, 75%.

***N*¹-(4-Phenylbenzoyl)-pyridine-4-carboxamidrazone (30)**



¹H NMR (250 MHz, d₆-DMSO): 10.18 (s, 1H, -NH), 8.66 (d, 2H, J = 5.7 Hz, -b and c), 7.99 (d, 2H, J = 8.3 Hz, -f and g), 7.77 (dd, 6H, J = 10.9, 7.7 Hz, -i, m, e, h, a and d), 7.46 (dt, 3H, J = 23.4, 7.1 Hz, -j, k, and l), 6.94 (s, 2H, -NH₂) ppm.

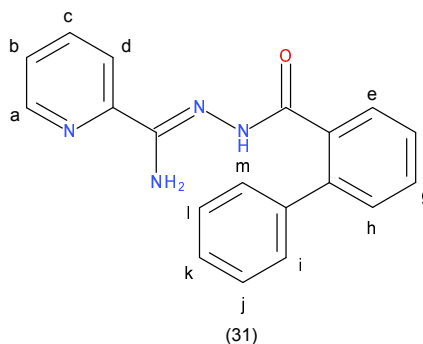
IR (KBr disc) ν : 3449 (N-H), 3367 (N-H), 3312 (N-H), 3179, 3151, 3055 (Aromatic C-H), 3018, 1686, 1645 (C=O), 1590, 1530, 1480, 1397, 1287 (C-N), 1222, 1154 cm⁻¹.

Melting point: 228.5 – 229.7 °C.

Mass spectrum (APCI +) m/z: Found 316.1320 (M+H)⁺; calculated for C₁₉H₁₆N₄O 316.1324; 1.5 ppm.

Yield: 1.6 g, 69%.

***N*¹-(2-Phenylbenzoyl)-pyridine-2-carboxamidrazone (31)**



¹H NMR (250 MHz, d₆-DMSO): 10.13 (s, 1H, **-NH**), 8.52 (dd, 6H, J = 20.2, 4.8 Hz, **-a, c, and g**), 8.08 (d, 4H, J = 8.0 Hz, **-h, and e**), 7.88 (dd, 4H, J = 7.5, 1.7 Hz, **-f, and d**), 7.85 – 7.14 (overlapping m, 4H, **-m, and i**), 6.61 (s, 8H, **-l, k, and j**), 6.48 (s, 2H, **-b**), 6.94 (s, 2H, **-NH₂**) ppm.

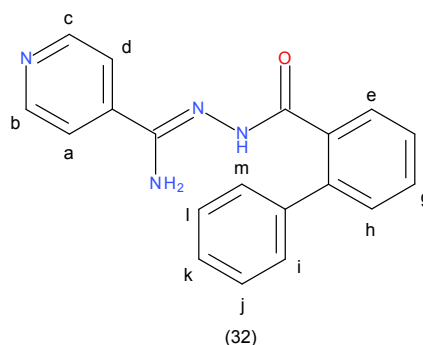
IR (KBr disc) ν : 3426 (N-H), 3312 (N-H), 3271 (N-H), 3197, 3045 (Aromatic C-H), 3013, 2931, 2848, 1636 (C=O), 1581, 1539, 1461, 1434, 1397, 1300 (C-N), 1241, 1158, 1039 cm⁻¹.

Melting point: 224.3 – 225.4 °C.

Mass spectrum (APCI +) m/z: Found 316.1314 (M+H)⁺; calculated for C₁₉H₁₆N₄O 316.1324; 3.1 ppm.

Yield: 1.58 g, 71%.

***N*¹-(2-Phenylbenzoyl)-pyridine-4-carboxamidrazone (32)**



¹H NMR (250 MHz, d₆-DMSO): 10.29 (s, 1H, **-NH**), 9.99 (s, 2H, **-b and c**), 8.64 (d, 2H, J = 5.7 Hz, **-g and h**), 7.80 (s, 1H, **-e**), 7.62 (d, 3H, J = 9.5 Hz, **-a, d and f**), 7.34 – 7.09 (overlapping m, 2H, **-i and m**), 6.86 (s, 2H, **-l and j**), 6.61 (s, 1H, **-k**), 6.94 (s, 2H, **-NH₂**) ppm.

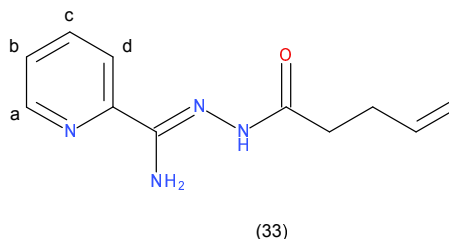
IR (KBr disc) ν : 3401 (N-H), 3374 (N-H), 3301 (N-H), 3275, 3156, 3036 (Aromatic C-H), 2921, 2692, 2600, 2352, 2122, 1939, 1819, 1773, 1677, 1645 (C=O), 1590, 1539, 1438, 1309, 1254 (C-N), 1154, 1062 cm⁻¹.

Melting point: 148.2 – 149.3 °C.

Mass spectrum (APCI +) m/z: Found 316.1315 (M+H)⁺; calculated for C₁₉H₁₆N₄O 316.1324; 2.8 ppm.

Yield: 1.83 g, 82%.

***N*¹-(4-Pentenoyl)-pyridine-2-carboxamidrazone (33)**



¹H NMR (250 MHz, d₆-DMSO): 9.89 (s, 1H, -NH), 9.77 (s, 1H, -a), 8.56 (s, 1H, -c), 8.15 (m, 1H, -d), 7.86 (d, 1H, J = 7.6 Hz, -b), 6.60 (s, 2H, -NH₂), 5.86 (dd, 1H, J = 16.7, 6.5 Hz, -CH₂CH₂CH=CH₂), 5.06 – 4.92 (overlapping m, 2H, -CH₂CH₂CH=CH₂), 3.32 (t, 2H, J = 7.5 Hz, -CH₂CH₂CH=CH₂), 2.72 (q, 2H, J = 7.5 Hz, -CH₂CH₂CH=CH₂) ppm.

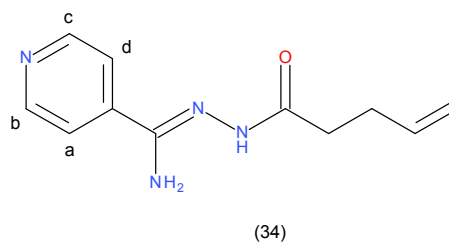
IR (KBr disc) ν : 3409 (N-H), 3340 (N-H), 3277 (N-H), 3227, 3049 (Aromatic C-H), 2995 (Alkyl C-H), 2921 (Alkyl C-H), 2890 (Alkyl C-H), 1652 (C=O) and (C=C), 1607, 1579, 1547, 1475, 1447, 1419, 1338, 1256 (C-N), 1170 cm⁻¹.

Melting point: 181.5 – 183.1 °C.

Mass spectrum (APCI +) m/z: Found 218.1164 (M+H)⁺; calculated for C₁₁H₁₄N₄O 218.1167; 1.3 ppm.

Yield: 1.11 g, 69%.

***N*¹-(4-Pentenoyl)-pyridine-4-carboxamidrazone (34)**



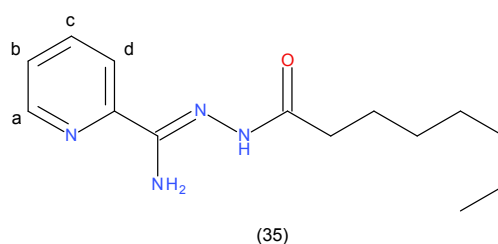
¹H NMR (250 MHz, d₆-DMSO): 9.85 (s, 1H, -NH), 9.72 (d, 2H, J = 6.9 Hz, -b and c), 8.62 (t, 1H, J = 4.9 Hz, -a), 7.72 (d, 1H, J = 4.9 Hz, -d), 6.83 (s, 1H, -CH₂CH₂CH=CH₂), 6.60 (s, 2H, -NH₂), 6.02 – 5.70 (overlapping m, 2H, J = 6.6 Hz, -CH₂CH₂CH=CH₂), 2.70 (t, 2H, J = 7.5 Hz, -CH₂CH₂CH=CH₂), 2.28 (t, 2H, J = 14.3 Hz, -CH₂CH₂CH=CH₂) ppm.

IR (KBr disc) ν : 3422 (N-H), 3381 (N-H), 3206 (N-H), 3068 (Aromatic C-H), 2921 (Alkyl C-H), 2848 (Alkyl C-H), 2471, 2366, 1709, 1645 (C=C) and (C=O), 1594, 1544, 1484, 1438, 1406, 1378, 1310, 1227 (C-N), 1158, 1140 cm⁻¹.

Melting point: 187.1 – 189.7 °C.

Mass spectrum (APCI +) m/z: Found 218.1162 (M+H)⁺; calculated for C₁₁H₁₄N₄O 218.1167; 2.2 ppm. **Yield:** 1.14 g, 71%.

***N*¹-(4-Octenoyl)-pyridine-2-carboxamidrazone (35)**



¹H NMR (250 MHz, d₆-DMSO): 9.83 (s, 1H, -NH), 8.57 (s, 1H, -a), 8.06 (t, 1H, J = 7.3 Hz, -c), 7.87 (dd, 1H, J = 10.5, 4.9 Hz, -d), 7.45 (dt, 1H, J = 7.3, 3.6 Hz, -b), 6.61 (d, 2H, J = 7.2 Hz, -NH₂), 2.61 (t, 2H, J = 7.4 Hz, -CH₂(CH₂)₅CH₃), 2.16 (t, 2H, J = 18.8, 11.3 Hz, -CH₂CH₂(CH₂)₄CH₃), 1.58 (t, 6H, J = 6.7 Hz, -CH₂CH₂(CH₂)₃CH₂CH₃), 1.28 (d, 2H, -CH₂(CH₂)₄CH₂CH₃), 0.86 (t, 3H, J = 4.9 Hz, -CH₂(CH₂)₅CH₃) ppm.

IR (KBr disc) ν : 3399 (N-H), 3345 (N-H), 3284 (N-H), 3206, 3045 (Aromatic C-H), 2940 (Alkyl C-H), 2931 (Alkyl C-H), 2843 (Alkyl C-H), 1645 (C=O), 1604, 1581, 1553, 1480, 1447, 1392, 1323, 1282, 1227 (C-N), 1176 cm⁻¹.

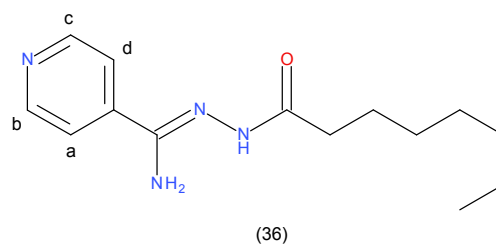
Melting point: 167.1 – 168.2 °C.

Mass spectrum (APCI +) m/z: Found 262.1783 (M+H)⁺; calculated for C₁₄H₂₂N₄O 262.1793; 3.8

ppm.

Yield: 1.23 g, 64%.

***N*¹-(4-Octenyl)-pyridine-4-carboxamidrazone (36)**



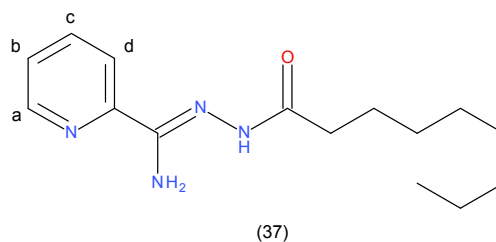
¹H NMR (250 MHz, d₆-DMSO): 9.78 (s, 1H, -NH), 8.61 (d, 2H, J = 4.6 Hz, -b and c), 7.71 (d, 2H, J = 4.6 Hz, -a and d), 6.58 (d, 2H, -NH₂), 2.17 (t, 2H, J = 7.4 Hz, -CH₂CH₂(CH₂)₄CH₃), 1.57 (t, 2H, -CH₂CH₂(CH₂)₄CH₃), 1.26 (t, 8H, J = 5.8 Hz, -CH₂CH₂(CH₂)₄CH₃), 0.86 (t, 3H, J = 5.4 Hz, -CH₂CH₂(CH₂)₄CH₃) ppm.

IR (KBr disc) ν : 3426 (N-H), 3385 (N-H), 3293 (N-H), 3220, 3064 (Aromatic C-H), 2921 (Alkyl C-H), 2848 (Alkyl C-H), 2375, 1705, 1645 (C=O), 1599, 1521, 1461, 1397, 1374, 1204 (C-N), 1117 cm⁻¹.

Melting point: 162.8 – 166.7 °C.

Mass spectrum (APCI +) m/z: Found 262.1788 (M+H)⁺; calculated for C₁₄H₂₂N₄O 262.1793; 1.9 ppm. **Yield:** 1.37 g, 71%.

***N*¹-(4-Nonanoyl)-pyridine-2-carboxamidrazone (37)**



¹H NMR (250 MHz, d₆-DMSO): 9.82 (s, 1H, **-NH**), 9.71 (s, 1H, **-a**), 8.55 (s, 1H, **-c**), 7.97 (s, 1H, **-d**), 7.84 (s, 1H, **-b**), 6.59 (d, 2H, J = 7.7 Hz, **-NH₂**), 3.31 (t, 2H, J = 7.5 Hz, **-CH₂(CH₂)₆CH₃**), 2.76 (s, 2H, **-CH₂CH₂(CH₂)₅CH₃**), 2.60 (d, 2H, J = 7.4 Hz, **-CH₂CH₂CH₂(CH₂)₄CH₃**), 2.15 (dd, 2H, J = 18.5, 11.4 Hz, **-CH₂(CH₂)₃CH₂CH₂CH₂CH₃**), 1.58 (s, 2H, **-CH₂(CH₂)₄CH₂CH₂CH₃**), 1.26 (s, 2H, **-CH₂(CH₂)₅CH₂CH₃**), 0.84 (t, 3H, J = 5.1 Hz, **-CH₂(CH₂)₆CH₃**) ppm.

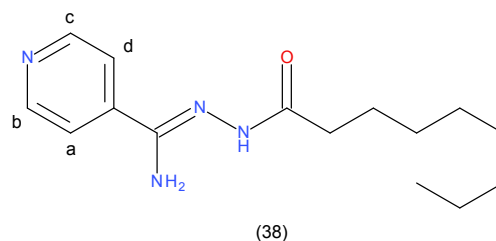
IR (KBr disc) ν : 3408 (N-H), 3344 (N-H), 3321 (N-H), 3301, 3219, 3050 (Aromatic C-H), 2921 (Alkyl C-H), 2852 (Alkyl C-H), 1654 (C=O), 1608, 1581, 1558, 1475, 1443, 1392, 1259, 1222 (C-N), 1172, 1144, 1112 cm⁻¹.

Melting point: 153.5 – 154.6 °C.

Mass spectrum (APCI +) m/z: Found 276.1946 (M+H)⁺; calculated for C₁₅H₂₄N₄O 276.1950; 1.4 ppm.

Yield: 1.56 g, 77%.

***N*¹-(4-Nonanoyl)-pyridine-4-carboxamidrazone (38)**



¹H NMR (250 MHz, d₆-DMSO): 9.78 (t, 1H, **-NH**), 9.63 (d, 2H, J = 10.5 Hz, **-b and c**), 8.60 (d, 1H, J = 3.7 Hz, **-a**), 7.71 (d, 1H, J = 4.6 Hz, **-d**), 6.58 (s, 2H, **-NH₂**), 2.17 (t, 2H, J = 7.4 Hz, **-CH₂(CH₂)₆CH₃**), 1.56 (d, 2H, **-CH₂CH₂(CH₂)₅CH₃**), 1.25 (t, 10H, J = 4.4 Hz, **-CH₂CH₂(CH₂)₅CH₃**), 0.85 (t, 3H, J = 4.9 Hz, **-CH₂(CH₂)₆CH₃**) ppm.

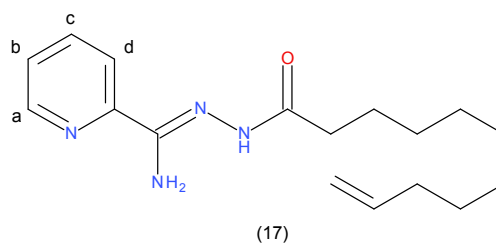
IR (KBr disc) ν : 3463 (N-H), 3394 (N-H), 3357 (N-H), 3275, 3219, 3036 (Aromatic C-H), 2949 (Alkyl C-H), 2917 (Alkyl C-H), 2848 (Alkyl C-H), 1640 (C=O), 1585, 1535, 1489, 1457, 1411, 1388, 1333, 1300, 1268 (C-N), 1222, 1190, 1140 cm⁻¹.

Melting point: 149.4 – 151.3 °C.

Mass spectrum (APCI +) m/z: Found 276.1948 (M+H)⁺; calculated for C₁₅H₂₄N₄O 276.1950; 0.7 ppm.

Yield: 1.54 g, 76%.

***N*¹-(4-(10-Undecenoyl))-pyridine-2-carboxamidrazone (17)**



¹H NMR (250 MHz, d₆-DMSO) 9.77 (s, 1H, -NH), 8.77 – 8.54 (overlapping m, 2H, -a and c), 7.71 (overlapping m, 2H, J = 4.6 Hz, -b and d), 6.56 (s, 2H, -NH₂), 5.77 (ddt, 1H, J = 13.6, 10.3, 5.2 Hz, -CH₂(CH₂)₇CH=CH₂), 4.96 (dd, 2H, J = 14.8 Hz, -CH₂(CH₂)₇CH=CH₂), 3.30 (t, 2H, J = 7.5 Hz, -CH₂(CH₂)₇CH=CH₂), 2.77 (s, 2H, -CH₂(CH₂)₆-CH₂CH=CH₂), 2.73 – 2.43 (overlapping m, 2H, -CH₂CH₂(CH₂)₅-CH₂CH=CH₂), 2.43 – 1.65 (overlapping m, 10H, -CH₂CH₂(CH₂)₅CH₂CH=CH₂) ppm.

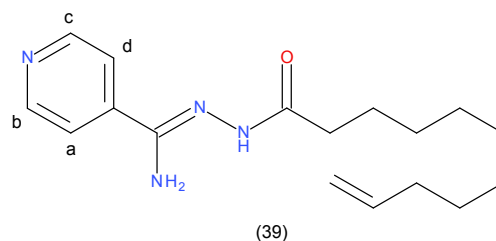
IR (KBr disc) ν: 3418 (N-H), 3341 (N-H), 3286 (N-H), 3222, 3058 (Aromatic C-H), 2913 (Alkyl C-H), 2844 (Alkyl C-H), 2662, 2289, 1647 (C=O), 1584, 1547, 1470, 1438, 1393, 1270 (C-N), 1247, 1170 cm⁻¹.

Melting point: 145.2 – 147.5 °C.

Mass spectrum (APCI +) m/z: Found 302.2103 (M+H)⁺; calculated for C₁₇H₂₆N₄O 302.2106; 0.9 ppm.

Yield: 2 g, 90%.

***N*¹-(4-(10-Undecenoyl))-pyridine-4-carboxamidrazone (39)**



¹H NMR (250 MHz, d₆-DMSO): 9.80 (s, 1H, -NH), 9.71 (s, 2H, -b and c), 8.55 (s, 2H, -a and d), 6.60 (d, 2H, J = 12.5 Hz, -NH₂), 5.78 (ddd, 1H, J = 17.1, 10.4, 4.0 Hz, -CH₂(CH₂)₇CH=CH₂), 4.95 (t, 2H, J = 14.9 Hz, -CH₂(CH₂)₇CH=CH₂), 3.30 (t, 2H, J = 7.5 Hz, -CH₂(CH₂)₇CH=CH₂), 2.77 (s, 2H, -CH₂(CH₂)₆CH₂CH=CH₂), 2.69 – 2.36 (overlapping m, 2H, -CH₂CH₂(CH₂)₅CH₂CH=CH₂), 2.08 – 1.91 (overlapping m, 10H, -CH₂CH₂(CH₂)₅CH₂CH=CH₂) ppm.

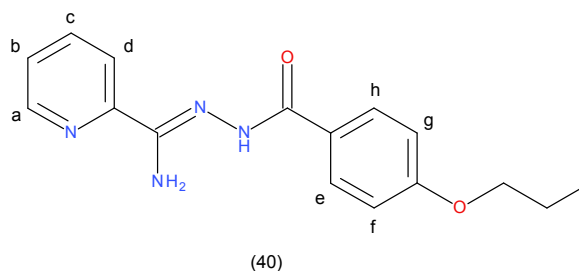
IR (KBr disc) ν : 3400 (N-H), 3331 (N-H), 3275 (N-H), 3112, 3048 (Aromatic C-H), 2876 (Alkyl C-H), 2823 (Alkyl C-H), 2654, 2278, 1645 (C=O), 1581, 1539, 1468, 1435, 1392, 1267 (C-N), 1235, 1167 cm⁻¹.

Melting point: 141.3 – 144.1 °C.

Mass spectrum (APCI +) m/z: Found 302.2102 (M+H)⁺; calculated for C₁₇H₂₆N₄O 302.2106; 1.3 ppm.

Yield: 2.1 g, 95%.

***N*¹-(4-Propoxybenzoyl)-pyridine-2-carboxamidrazone (40)**



¹H NMR (250 MHz, d₆-DMSO): 10.04 (s, 1H, **-NH**), 8.59 (d, 1H, J = 4.7 Hz, **-a**), 8.17 (d, 2H, J = 8.0 Hz, **-e and h**), 7.89 (t, 2H, J = 9.2 Hz, **-c and d**), 7.50 (m, 1H, **-b**), 7.01 (d, 2H, J = 8.8 Hz, **-f and g**), 6.89 (s, 2H, **-NH₂**), 4.00 (t, 2H, J = 6.5 Hz, **-OCH₂CH₂CH₃**), 2.00 – 1.56 (overlapping m, 2H, **-OCH₂CH₂CH₃**), 0.99 (t, 3H, J = 7.4 Hz, **-OCH₂CH₂CH₃**) ppm.

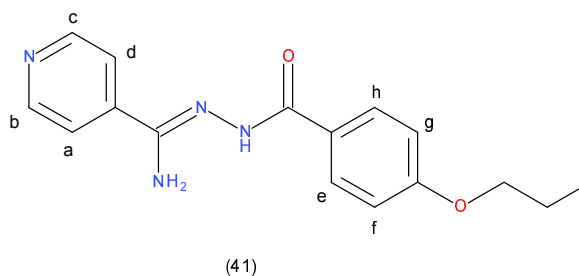
IR (KBr disc) ν : 3413 (N-H), 3330 (N-H), 3298 (N-H), 3206, 3064 (Aromatic C-H), 2958, 2921, 2866, 1668 (C=O), 1631, 1603, 1539, 1502, 1470, 1433, 1396, 1295, 1254 (C-N), 1162, 1112, 1043, 1015 cm⁻¹.

Melting point: 224.3 – 225.3 °C.

Mass spectrum (APCI +) m/z: Found 298.1425 (M+H)⁺; calculated for C₁₆H₁₈N₄O₂ 298.1429; 1.3 ppm.

Yield: 1.51 g, 69%.

***N*¹-(4-Propyloxybenzoyl)-pyridine-4-carboxamidrazone (41)**



¹H NMR (250 MHz, d₆-DMSO): 9.98 (s, 1H, **-NH**), 8.65 (d, 2H, J = 5.9 Hz, **-b and c**), 7.94 – 7.70 (overlapping m, 4H, **-a, d, e and h**), 7.03 (t, 2H, J = 7.8 Hz, **-f and g**), 6.86 (s, 2H, **-NH₂**), 4.01 (t, 2H, J = 6.5 Hz, **-OCH₂CH₂CH₃**), 1.89 – 1.56 (overlapping m, 2H, **-OCH₂CH₂CH₃**), 1.00 (t, 3H, J = 7.4 Hz, **-OCH₂CH₂CH₃**) ppm.

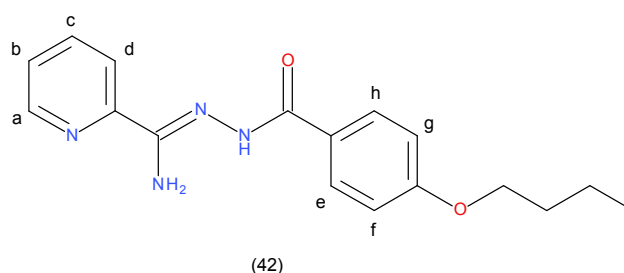
IR (KBr disc) ν : 3459 (N-H), 3348 (N-H), 3284 (N-H), 3183, 2958 (Aromatic C-H), 2880, 1677 (C=O), 1631, 1617, 1539, 1493, 1466, 1406, 1314, 1286 (C-N), 1240, 1163, 1112, 1062 cm⁻¹.

Melting point: 207.1 – 208.5 °C.

Mass spectrum (APCI +) m/z: Found 298.1421 (M+H)⁺; calculated for C₁₆H₁₈N₄O₂ 298.1429; 2.0 ppm.

Yield: 1.58 g, 72%.

***N*¹-(4-Butyloxybenzoyl)-pyridine-2-carboxamidrazone (42)**



¹H NMR (250 MHz, d₆-DMSO): 10.04 (s, 1H, -NH), 8.60 (d, 1H, J = 4.6 Hz, -a), 8.17 (d, 2H, J = 8.0 Hz, -e and f), 7.88 (dd, 4H, J = 11.5, 7.2 Hz, -c and d), 7.45 (m, 1H, -b), 7.01 (d, 2H, J = 8.8 Hz, -f and g), 6.90 (s, 2H, -NH₂), 4.04 (t, 2H, J = 6.5 Hz, -OCH₂(CH₂)₂CH₃), 1.82 – 1.60 (overlapping m, 2H, -OCH₂CH₂CH₂CH₃), 1.59 – 1.31 (overlapping m, 2H, -OCH₂CH₂CH₂CH₃), 0.93 (t, 3H, -OCH₂(CH₂)₂CH₃) ppm.

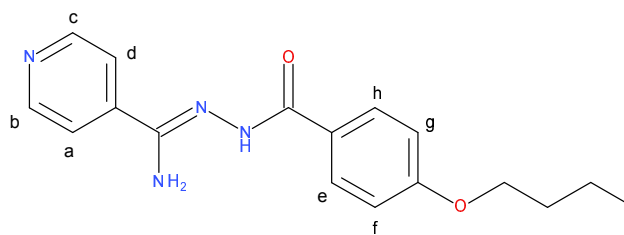
IR (KBr disc) ν : 3409 (N-H), 3331 (N-H), 3302 (N-H), 3213, 3054 (Aromatic C-H), 2949, 2858, 1670 (C=O), 1629, 1538, 1501, 1460, 1388, 1270 (C-N), 1238, 1165, 1042 cm⁻¹.

Melting point: 120.5 – 121.9 °C.

Mass spectrum (APCI +) m/z: Found 312.1576 (M+H)⁺; calculated for C₁₇H₂₀N₄O₂ 312.1586; 3.2 ppm.

Yield: 1.35 g, 59%.

***N*¹-(4-Butyloxybenzoyl)-pyridine-4-carboxamidrazone (43)**



(43)

¹H NMR (250 MHz, d₆-DMSO): 9.98 (s, 1H, -NH), 8.69 (d, 2H, J = 22.0 Hz, -b and c), 8.63 (s, 2H, -e and h), 8.35 (d, 2H, J = 19.9 Hz, -a and d), 7.98 – 7.57 (overlapping m, 2H, -f and g), 7.03 – 6.55 (overlapping m, 2H, -NH₂), 4.04 (t, 2H, J = 6.5 Hz, -OCH₂(CH₂)₂CH₃), 1.86 – 1.60 (overlapping m, 2H, -OCH₂CH₂CH₂CH₃), 1.45 (dq, 2H, J = 14.4, 7.4 Hz, -OCH₂CH₂CH₂CH₃), 0.94 (t, 3H, J = 7.3 Hz, -OCH₂(CH₂)₂CH₃) ppm.

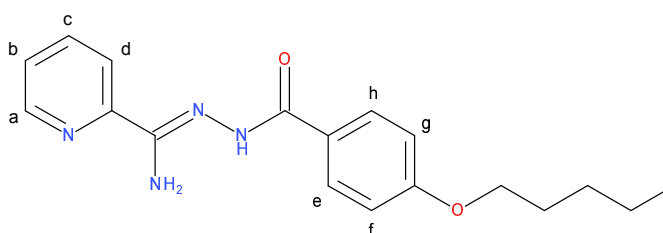
IR (KBr disc) ν : 3363 (N-H), 3351 (N-H), 3296 (N-H), 3189, 3158, 2945 (Aromatic C-H), 2922, 2863, 2699, 2580, 2357, 2330, 1934, 1898, 1757, 1670 (C=O), 1624, 1606, 1538, 1497, 1456, 1402, 1319, 1256 (C-N), 1169, 1119, 1064, 1019 cm⁻¹.

Melting point: 206.2 – 207.1 °C.

Mass spectrum (APCI +) m/z: Found 312.1586 (M+H)⁺; calculated for C₁₇H₂₀N₄O₂ 312.1586; 2.5 ppm.

Yield: 1.47 g, 64%.

***N*¹-(4-Pentyloxybenzoyl)-pyridine-2-carboxamidrazone (44)**



(44)

¹H NMR (250 MHz, d₆-DMSO): 10.03 (s, 1H, -NH), 8.60 (d, 3H, J = 4.5 Hz, -a, e, and h), 8.17 (d, 1H, J = 8.2 Hz, -c,), 7.86 (d, 2H, J = 8.6 Hz, -d, and b), 7.49 (d, 2H, J = 5.1 Hz, -f, and g), 7.09 – 6.60 (overlapping m, 2H, -NH₂), 4.04 (t, 2H, J = 6.5 Hz, -OCH₂(CH₂)₃CH₃), 2.59 – 2.41 (overlapping m, 2H, -OCH₂CH₂(CH₂)₂CH₃), 1.73 (d, J = 7.1 Hz, 2H, -O(CH₂)₂CH₂CH₂CH₃), 1.38 (d, J = 3.6 Hz, 2H, -OCH₂(CH₂)₂CH₂CH₃), 0.90 (t, J = 6.9 Hz, 3H, -OCH₂(CH₂)₃CH₃) ppm.

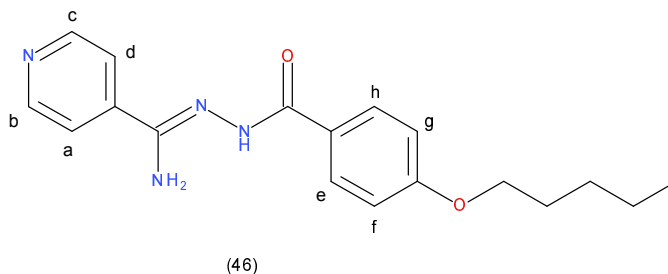
IR (KBr disc) ν : 3417 (N-H), 3330 (N-H), 3302 (N-H), 3215, 3059 (Aromatic C-H), 3027, 2949, 2862, 1897, 1663 (C=O), 1626, 1603, 1535, 1502, 1466, 1434, 1401, 1300, 1254 (C-N), 1167 cm⁻¹.

Melting point: 224.7 – 225.8 °C.

Mass spectrum (APCI +) m/z: Found 326.1736 (M+H)⁺; calculated for C₁₈H₂₂N₄O₂ 326.1742; 1.8 ppm.

Yield: 1.51 g, 63%.

***N*¹-(4-Pentyloxybenzoyl)-pyridine-4-carboxamidrazone (45)**



¹H NMR (250 MHz, d₆-DMSO): 9.97 (s, 3H, -NH), 8.64 (d, 2H, J = 5.9 Hz, -b, and c), 7.98 – 7.63 (overlapping m, 4H, -a, d, e and h), 7.00 (d, 2H, J = 8.8 Hz, -f, and g), 6.84 (s, 1H, -NH₂), 4.04 (t, 2H, J = 6.5 Hz, OCH₂(CH₂)₃CH₃), 1.72 (d, 4H, J = 6.9 Hz, -OCH₂(CH₂)₂CH₂CH₃), 1.38 (d, 2H, J = 3.5 Hz, -OCH₂(CH₂)₂CH₂CH₃), 0.90 (t, 3H, J = 7.1 Hz, OCH₂(CH₂)₃CH₃) ppm.

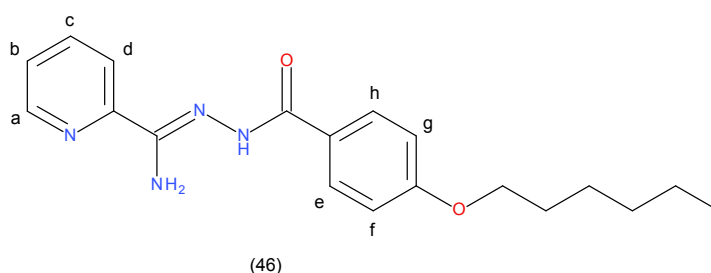
IR (KBr disc) ν : 3429 (N-H), 3375 (N-H), 3330 (N-H), 3151, 2953 (Aromatic C-H), 2926, 2857, 2361, 2333, 1667 (C=O), 1621, 1603, 1539, 1498, 1415, 1319, 1254 (C-N), 1167, 1029 cm⁻¹.

Melting point: 164.1 – 165.3 °C.

Mass spectrum (APCI +) m/z: Found 326.1733 (M+H)⁺; calculated for C₁₈H₂₂N₄O₂ 326.1742; 2.7 ppm.

Yield: 1.66 g, 69%.

***N*¹-(4-Heptyloxybenzoyl)-pyridine-2-carboxamidrazone (46)**



¹H NMR (250 MHz, d₆-DMSO): 10.09 (s, 1H, -NH), 8.62 (d, 1H, J = 4.4 Hz, -a), 8.17 (d, 2H, J = 7.8 Hz, -e and h), 7.87 (d, 2H, J = 8.7 Hz, -c and d), 7.12 (d, 1H, J = 8.9 Hz, -b), 7.00 (d, 2H, J = 8.8 Hz, -f and g), 6.89 (s, 2H, -NH₂), 4.03 (t, 2H, J = 6.5 Hz, -OCH₂(CH₂)₅CH₃), 1.75 – 1.68 (overlapping m, 2H, -OCH₂CH₂(CH₂)₄CH₃), 1.33 (d, 8H, J = 25.3 Hz, -OCH₂CH₂(CH₂)₄CH₃), 0.86 (t, 3H, J = 6.6 Hz, -OCH₂(CH₂)₅CH₃) ppm.

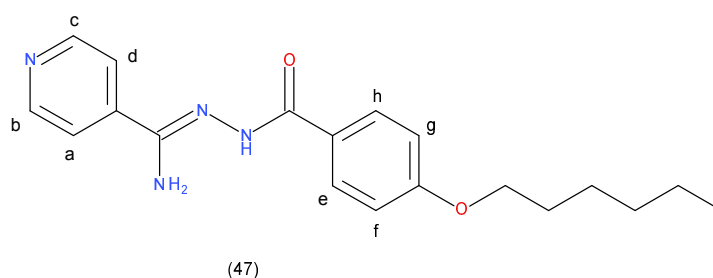
IR (KBr disc) ν : 3399 (N-H), 3339 (N-H), 3302 (N-H), 3220, 3064 (Aromatic C-H), 3031, 2944, 2917, 2871, 2852, 1664 (C=O), 1626, 1594, 1562, 1539, 1502, 1470, 1438, 1401, 1291 (C-N), 1249, 1167, 1112, 1034, 1011 cm⁻¹.

Melting point: 203.3 – 204.4 °C.

Mass spectrum (APCI +) m/z: Found 354.2050 (M+H)⁺; calculated for C₂₀H₂₆N₄O₂ 354.2055; 1.4 ppm.

Yield: 1.49 g, 57%.

***N*¹-(4-Heptyloxybenzoyl)-pyridine-4-carboxamidrazone (47)**



¹H NMR (250 MHz, d₆-DMSO): 10.07 (s, 1H, -NH), 8.64 (d, J = 5.9 Hz, 2H, -b and c), 7.98 – 7.68 (overlapping m, 4H, -a, d, e and h), 7.12 (d, 2H, J = 8.8 Hz, -f and g), 6.99 (d, 2H, J = 8.8 Hz, -NH₂), 4.02 (t, 2H, J = 6.5 Hz, -OCH₂(CH₂)₅CH₃), 1.88 – 1.63 (overlapping m, 2H, -OCH₂CH₂(CH₂)₄CH₃), 1.53 – 1.08 (overlapping m, 8H, -OCH₂CH₂(CH₂)₄CH₃), 0.87 (t, 3H, J = 6.6 Hz, -OCH₂(CH₂)₅CH₃) ppm.

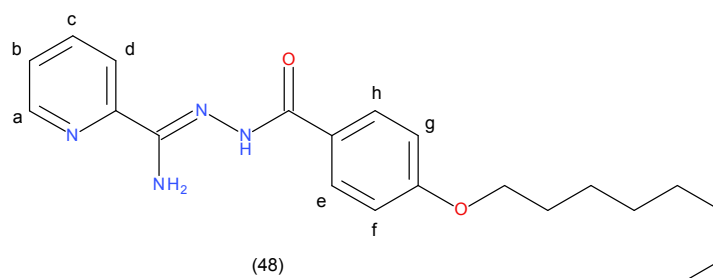
IR (KBr disc) ν : 3471 (N-H), 3349 (N-H), 3322 (N-H), 3172, 3100, 3086 (Aromatic C-H), 3026, 2917, 2853, 1670 (C=O), 1643, 1597, 1538, 1501, 1497, 1472, 1402, 1292, 1246 (C-N), 1179, 1038 cm⁻¹.

Melting point: 177.6 – 178.8 °C.

Mass spectrum (APCI +) m/z: Found 354.2047 (M+H)⁺; calculated for C₂₀H₂₆N₄O₂ 354.2055; 2.2 ppm.

Yield: 2 g, 77%.

***N*¹-(4-Octyloxybenzoyl)-pyridine-2-carboxamidrazone (48)**



¹H NMR (250 MHz, d₆-DMSO): 10.09 (s, 1H, -NH), 8.60 (d, 1H, J = 4.3 Hz, -a), 8.18 (d, 2H, J = 9.9 Hz, -e and h), 8.00 – 7.72 (overlapping m, 2H, -c), 7.63 (m, 1H, -d), 7.46 (m, 1H, -b), 7.33 – 7.09 (overlapping m, 2H, -f and g), 7.09 – 6.71 (overlapping m, 2H, -NH₂), 4.21 (t, 2H, J = 6.5 Hz, -OCH₂(CH₂)₆CH₃), 2.08 (s, 1H, -OCH₂CH₂(CH₂)₅CH₃), 1.86 – 1.58 (overlapping m, 2H, -OCH₂CH₂CH₂(CH₂)₄CH₃), 1.55 – 1.18 (overlapping m, 16H, -OCH₂CH₂CH₂(CH₂)₄CH₃), 0.85 (d, 3H, J = 6.9 Hz, -OCH₂(CH₂)₆CH₃) ppm.

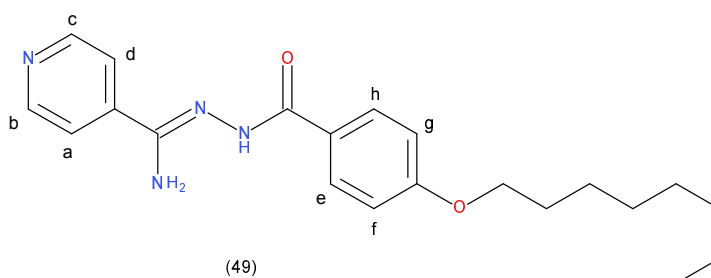
IR (KBr disc) ν : 3416 (N-H), 3342 (N-H), 3330 (N-H), 3202, 3059 (Aromatic C-H), 3040, 2915, 2845, 1672 (C=O), 1620, 1602, 1565, 1541, 1504, 1463, 1435, 1398, 1291, 1249 (C-N), 1161, 1110, 1017 cm⁻¹.

Melting point: 188.6 – 189.7 °C.

Mass spectrum (APCI +) m/z: Found 368.2208 (M+H)⁺; calculated for C₂₁H₂₈N₄O₂ 368.2212; 1.0 ppm.

Yield: 1.84 g, 68%.

N¹-(4-Octyloxybenzoyl)-pyridine-4-carboxamidrazone (49)



¹H NMR (250 MHz, d₆-DMSO): 9.99 (s, 1H, -NH), 8.64 (d, 2H, J = 6.0 Hz, -b and c), 7.95 – 7.72 (overlapping m, 4H, -a, d, e and h), 7.00 (d, 2H, J = 8.8 Hz, -f and g), 6.85 (s, 2H, -NH₂), 4.04 (t, 3H, J = 6.5 Hz, -OCH₂(CH₂)₆CH₃), 1.86 – 1.61 (dq, 2H, J = 14.4, 7.3 Hz, -OCH₂CH₂(CH₂)₅CH₃), 1.45 (overlapping m, 10H, -OCH₂CH₂(CH₂)₅CH₃), 0.94 (t, 3H, J = 7.3 Hz, -OCH₂(CH₂)₆CH₃) ppm.

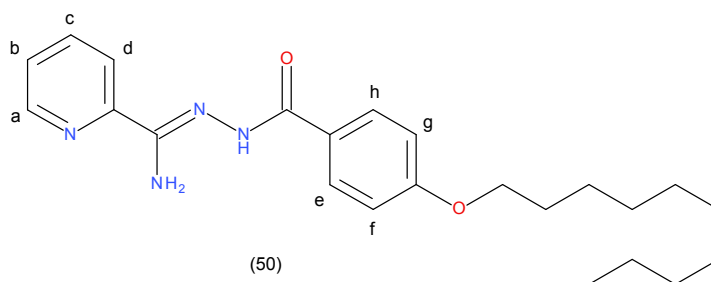
IR (KBr disc) ν : 3468 (N-H), 3348 (N-H), 3301 (N-H), 3215, 3187, 3063 (Aromatic C-H), 3031, 2916, 2847, 1659 (C=O), 1640, 1603, 1539, 1502, 1466, 1397, 1300, 1245 (C-N), 1186, 1107, 1034 cm⁻¹.

Melting point: 185.0 – 186.2 °C.

Mass spectrum (APCI +) m/z: Found 368.2202 (M+H)⁺; calculated for C₂₁H₂₈N₄O₂ 368.2212; 2.7 ppm.

Yield: 1.79 g, 66%.

***N*¹-(4-Decyloxybenzoyl)-pyridine-2-carboxamidrazone (50)**



¹H NMR (250 MHz, d₆-DMSO): 10.05 (s, 1H, -NH), 8.60 (d, 1H, J = 4.4 Hz, -a), 8.18 (d, J = 8.3 Hz, 2H, -e and h), 7.84 (dd, 1H, J = 15.8, 8.7 Hz, -c), 7.47 (m, 1H, -d), 7.13 (d, 1H, J = 9.0 Hz, -b), 7.00 (d, 2H, J = 8.8 Hz, -f and g), 6.90 (s, 2H, -NH₂), 4.42 (t, 2H, J = 6.5 Hz, -OCH₂(CH₂)₉CH₃), 1.75 (dt, 2H, J = 14.8, 5.6 Hz, -OCH₂CH₂(CH₂)₈CH₃), 1.54 – 1.01 (overlapping m, 16H, -OCH₂CH₂(CH₂)₈CH₃), 0.84 (d, 3H, J = 6.8 Hz, -OCH₂(CH₂)₉CH₃) ppm.

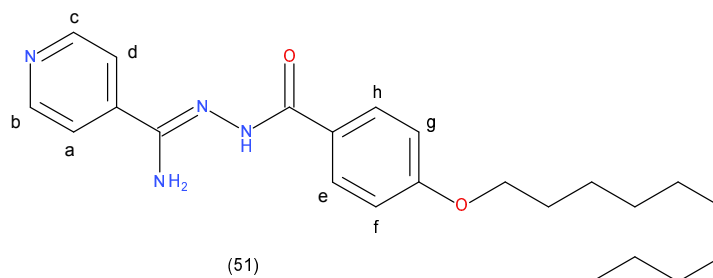
IR (KBr disc) ν: 3426 (N-H), 3325 (N-H), 3298 (N-H), 3270, 3187, 3068 (Aromatic C-H), 2944, 2921, 2843, 1663 (C=O), 1631, 1603, 1580, 1548, 1507, 1461, 1392, 1433, 1304, 1254 (C-N), 1176, 1112, 1015 cm⁻¹.

Melting point: 165.3 – 166.5 °C.

Mass spectrum (APCI +) m/z: Found 396.2520 (M+H)⁺; calculated for C₂₃H₃₂N₄O₂ 396.2525; 1.2 ppm.

Yield: 2.30 g, 79%.

***N*¹-(4-Decyloxybenzoyl)-pyridine-4-carboxamidrazone (51)**



¹H NMR (250 MHz, d₆-DMSO): 10.09 (s, 1H, -NH), 8.65 (d, 4H, J = 5.9 Hz, -b, c, e and h), 8.20 – 7.43 (overlapping m, 4H, -a, d, f and g), 7.38 – 6.45 (overlapping m, 2H, -NH₂), 4.10 (t, 2H, J = 6.5 Hz, -OCH₂(CH₂)₈CH₃), 1.72 (dd, 2H, J = 13.9, 6.5 Hz, -OCH₂CH₂(CH₂)₇CH₃), 1.59 – 1.03 (overlapping m, 14H, -OCH₂CH₂(CH₂)₇CH₃), 0.87 (t, 3H, J = 6.5 Hz, -OCH₂(CH₂)₈CH₃) ppm.

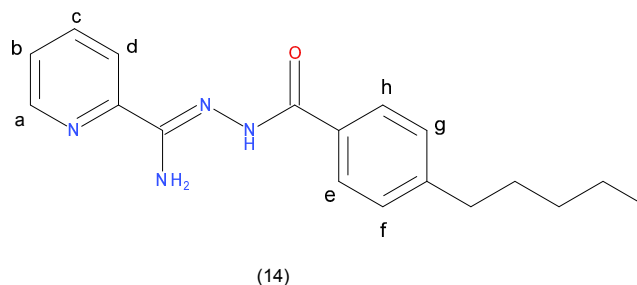
IR (KBr disc) ν : 3445 (N-H), 3300 (N-H), 3181, 3063 (Aromatic C-H), 2926, 2849, 1634 (C=O), 1597, 1533, 1497, 1460, 1393, 1311, 1256 (C-N), 1174, 1115, 1015 cm⁻¹.

Melting point: 168.9 – 170.1 °C.

Mass spectrum (APCI +) m/z: Found 396.2518 (M+H)⁺; calculated for C₂₃H₃₂N₄O₂ 396.2525; 1.7 ppm.

Yield: 2.54 g, 87%.

***N*¹-(4-Pentylbenzoyl)-pyridine-2-carboxamidrazone (14)**



¹H NMR (250 MHz, d₆-DMSO): 10.12 (s, 1H, -NH), 8.61 (d, 2H, J = 4.4 Hz, b and d), 8.17 (d, 1H, J = 7.7 Hz, -a), 7.80 (d, 3H, J = 8.1 Hz, c, e and h), 7.30 (d, 2H, J = 8.1 Hz, f and g), 6.91 (s, 2H, -NH₂),

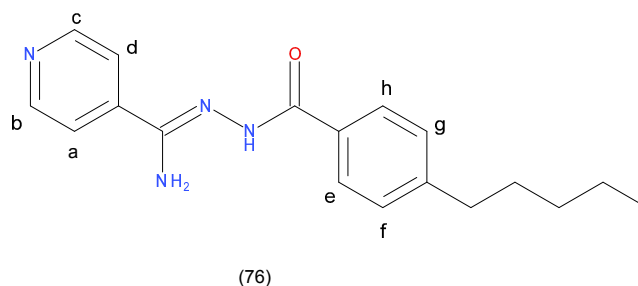
2.64 (t, 2H, J = 7.6 Hz, $-\text{CH}_2 (\text{CH}_2)_3 \text{CH}_3$), 1.59 (s, 2H, $-\text{CH}_2 \text{CH}_2 (\text{CH}_2)_2 \text{CH}_3$), 1.27 (overlapping m, 4H, J = 8.9 Hz, $-\text{CH}_2 \text{CH}_2 (\text{CH}_2)_2 \text{CH}_3$), 0.86 (t, 3H, J = 6.5 Hz, $-(\text{CH}_2)_4 \text{CH}_3$) ppm.

IR (KBr disc) ν : 3411 (N-H), 3216, 3031 (Aromatic C-H), 2995 (Alkyl C-H), 2859 (Alkyl C-H), 1637(C=O), 1559, 1474, 1448, 1403, 1313, 1187(C-N) cm^{-1} .

Melting point: 234.1 – 235.9 °C.

Yield: 1.58 g, 72%.

N^1 -(4-Pentylbenzoyl)-pyridine-4-carboxamidrazone (76)



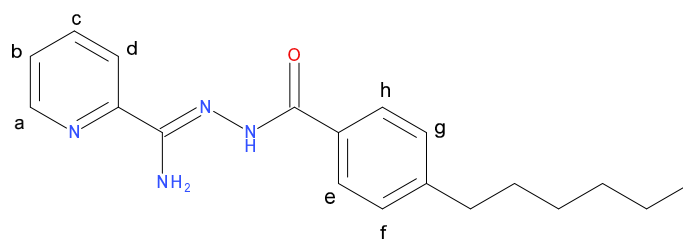
^1H NMR (250 MHz, d_6 -DMSO): 10.06 (s, 1H, $-\text{NH}$), 8.65 (d, 2H, J = 5.7 Hz, **-b and c**), 7.79 (d, 2H, J = 8.0 Hz, **-e and h**), 7.29 (d, 4H, J = 8.1 Hz, **-a, d, f and g**), 6.91 (s, 2H, $-\text{NH}_2$), 2.64 (t, 2H, J = 7.6 Hz, $-\text{CH}_2 (\text{CH}_2)_3 \text{CH}_3$), 1.59 (s, 2H, $-\text{CH}_2 \text{CH}_2 (\text{CH}_2)_2 \text{CH}_3$), 1.27 (overlapping m, 4H, J = 8.9 Hz, $-\text{CH}_2 \text{CH}_2 (\text{CH}_2)_2 \text{CH}_3$), 0.86 (t, 3H, J = 6.5 Hz, $-(\text{CH}_2)_4 \text{CH}_3$) ppm.

IR (KBr disc) ν : 3349 (N-H), 3166, 3040 (Aromatic C-H), 2956 (Alkyl C-H), 2927 (Alkyl C-H), 1625(C=O), 1598, 1544, 1501, 1411, 1291, 1183(C-N) cm^{-1} .

Melting point: 201.2 – 201.8 °C.

Yield: 1.86 g, 76%.

***N*¹-(4-Hexylbenzoyl)-pyridine-2-carboxamidrazone (13)**



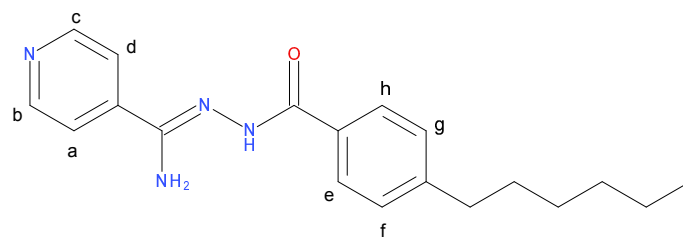
¹H NMR (250 MHz, d₆-DMSO): 10.12 (s, 1H, -NH), 8.61 (d, 2H, J = 4.4 Hz, **b and d**), 8.17 (d, 1H, J = 7.7 Hz, - **a**), 7.80 (d, 3H, J = 8.1 Hz, **c, e and h**), 7.30 (d, 2H, J = 8.1 Hz, **f and g**), 6.91 (s, 2H, -NH₂), 2.64 (t, 2H, J = 7.6 Hz, -CH₂ (CH₂)₄ CH₃), 1.59 (s, 2H, -CH₂ CH₂ (CH₂)₃ CH₃), 1.27 (overlapping m, 6H, J = 8.9 Hz, -CH₂ CH₂ (CH₂)₃ CH₃), 0.86 (t, 3H, J = 6.5 Hz, -(CH₂)₅ CH₃) ppm.

IR (KBr disc) ν : 3407 (N-H), 3214, 3060 (Aromatic C-H), 2925 (Alkyl C-H), 2857 (Alkyl C-H), 1630(C=O), 1548, 1479, 1448, 1397, 1309, 1187(C-N) cm⁻¹.

Melting point: 218.7 – 220.6 °C.

Yield: 2 g, 77%.

***N*¹-(4-Hexylbenzoyl)-pyridine-4-carboxamidrazone (77)**



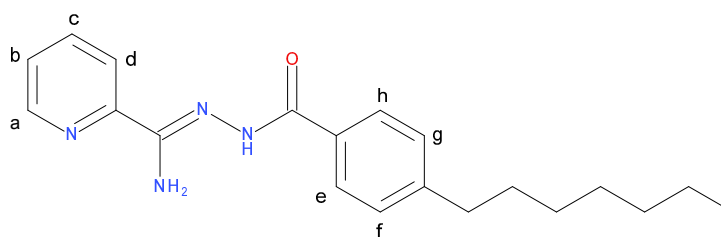
¹H NMR (250 MHz, d₆-DMSO): 10.06 (s, 1H, -NH), 8.65 (d, 2H, J = 5.7 Hz, -**b and c**), 7.79 (d, 2H, J = 8.0 Hz, -**e and h**), 7.29 (d, 4H, J = 8.1 Hz, -**a, d, f and g**), 6.87 (s, 2H, -NH₂), 2.64 (t, 2H, J = 7.6 Hz, -CH₂ (CH₂)₄ CH₃), 1.59 (s, 2H, -CH₂ CH₂ (CH₂)₃ CH₃), 1.27 (overlapping m, 6H, J = 8.9 Hz, -CH₂ CH₂ (CH₂)₃ CH₃), 0.86 (t, 3H, J = 6.5 Hz, -(CH₂)₅ CH₃) ppm.

IR (KBr disc) ν : 3430 (N-H), 3207, 3064 (Aromatic C-H), 2923 (Alkyl C-H), 2856 (Alkyl C-H), 1636 (C=O), 1594, 1552, 1502, 1405, 1301, 1210, 1187 (C-N) cm^{-1} .

Melting point: 187.7 – 191.0 °C.

Yield: 1.86 g, 76%.

***N*¹-(4-Heptylbenzoyl)-pyridine-2-carboxamidrazone (15)**



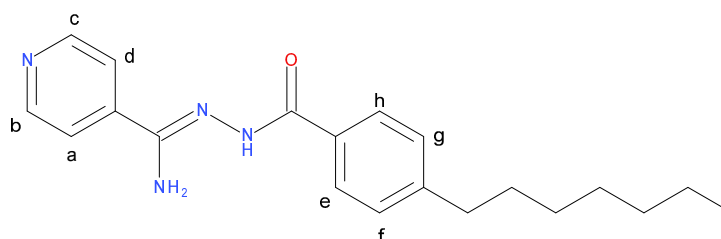
(15)

¹H NMR (250 MHz, d₆-DMSO): 10.12 (s, 1H, -NH), 8.61 (d, 2H, J = 4.4 Hz, **b and d**), 8.17 (d, 1H, J = 7.7 Hz, - **a**), 7.80 (d, 3H, J = 8.1 Hz, **c, e and h**), 7.30 (d, 2H, J = 8.1 Hz, **f and g**), 6.91 (s, 2H, -NH₂), 2.64 (t, 2H, J = 7.6 Hz, -CH₂ (CH₂)₅ CH₃), 1.59 (s, 2H, -CH₂ CH₂ (CH₂)₄ CH₃), 1.27 (overlapping m, 8H, J = 8.9 Hz, -CH₂ CH₂ (CH₂)₄ CH₃), 0.86 (t, 3H, J = 6.5 Hz, -(CH₂)₆ CH₃) ppm.

IR (KBr disc) ν : 3411 (N-H), 3214 (N-H), 3060 (Aromatic C-H), 2927 (Alkyl C-H), 2848 (Alkyl C-H), 1631(C=O), 1548, 1479, 1448, 1397, 1311, 1187(C-N), 1158, 1140 cm^{-1} .

Melting point: 214.9 – 215.8 °C. **Yield:** 1.14 g, 71%.

***N*¹-(4-Heptylbenzoyl)-pyridine-4-carboxamidrazone (81)**



(81)

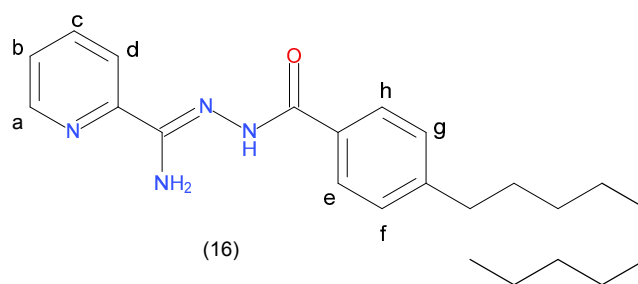
¹H NMR (250 MHz, d₆-DMSO): 10.04 (s, 1H, -NH), 8.65 (d, 2H, J = 5.7 Hz, -b and c), 7.79 (d, 2H, J = 8.0 Hz, -e and h), 7.29 (d, 4H, J = 8.1 Hz, -a, d, f and g), 6.87 (s, 2H, -NH₂), 2.64 (t, 2H, J = 7.6 Hz, -CH₂ (CH₂)₅ CH₃), 1.59 (s, 2H, -CH₂ CH₂ (CH₂)₄ CH₃), 1.27 (overlapping m, 8H, J = 8.9 Hz, -CH₂ CH₂ (CH₂)₄ CH₃), 0.86 (t, 3H, J = 6.5 Hz, -(CH₂)₆ CH₃) ppm.

IR (KBr disc) ν : 3417 (N-H), 3320 (N-H), 3252 (N-H), 3204, 3044 (Aromatic C-H), 2957 (Alkyl C-H), 2915 (Alkyl C-H), 2852 (Alkyl C-H), 1640(C=O), 1582, 1558, 1498, 1411, 1295, 1218, 1183(C-N) cm⁻¹.

Melting point: 182.2 – 182.8 °C.

Yield: 1.72 g, 70%.

***N*¹-(4-Decylbenzoyl)-pyridine-2-carboxamidrazone (16)**



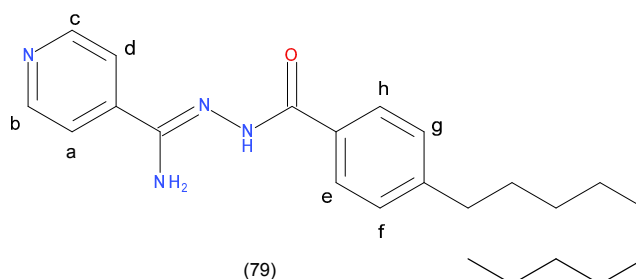
¹H NMR (250 MHz, d₆-DMSO): 10.12 (s, 1H, -NH), 8.61 (d, 2H, J = 4.4 Hz, b and d), 8.17 (d, 1H, J = 7.7 Hz, -a), 7.80 (d, 3H, J = 8.1 Hz, c, e and h), 7.30 (d, 2H, J = 8.1 Hz, f and g), 6.91 (s, 2H, -NH₂), 2.64 (t, 2H, J = 7.6 Hz, -CH₂ (CH₂)₈ CH₃), 1.59 (s, 2H, -CH₂ CH₂ (CH₂)₇ CH₃), 1.27 (overlapping m, 14H, J = 8.9 Hz, -CH₂ CH₂ (CH₂)₇ CH₃), 0.86 (t, 3H, J = 6.5 Hz, -(CH₂)₉ CH₃) ppm.

IR (KBr disc) ν : 3397 (N-H), 3276, 3182, 3056 (Aromatic C-H), 2921 (Alkyl C-H), 2849 (Alkyl C-H), 1629(C=O), 1584, 1540, 1440, 1398, 1295, 1193(C-N) cm⁻¹.

Melting point: 201.2 – 203.2 °C.

Yield: 1.14 g, 71%.

***N*¹-(4-Decylbenzoyl)-pyridine-4-carboxamidrazone (79)**



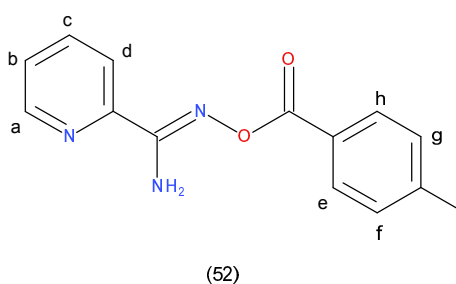
¹H NMR (250 MHz, d₆-DMSO): 10.04 (s, 1H, -NH), 8.65 (d, 2H, J = 5.7 Hz, -b and c), 7.79 (d, 2H, J = 8.0 Hz, -e and h), 7.29 (d, 4H, J = 8.1 Hz, -a, d, f and g), 6.87 (s, 2H, -NH₂), 2.64 (t, 2H, J = 7.6 Hz, -CH₂ (CH₂)₈ CH₃), 1.59 (s, 2H, -CH₂ CH₂ (CH₂)₇ CH₃), 1.27 (overlapping m, 14H, J = 8.9 Hz, -CH₂ CH₂ (CH₂)₇ CH₃), 0.86 (t, 3H, J = 6.5 Hz, -(CH₂)₉ CH₃) ppm.

IR (KBr disc) ν : 3417 (N-H), 3320 (N-H), 3252 (N-H), 3204, 3044 (Aromatic C-H), 2957 (Alkyl C-H), 2915 (Alkyl C-H), 2852 (Alkyl C-H), 1640(C=O), 1582, 1558, 1498, 1411, 1295, 1218, 1183(C-N) cm⁻¹.

Melting point: 191.5 – 193.9 °C.

Yield: 1.49 g, 57%.

***N*-[4-Methylbenzoyl]oxy]-2-pyridinecarboximidamide (52)**



¹H NMR (250 MHz, d₆-DMSO): 8.68 (ddd, 1H, J = 4.8, 1.6, 1.0 Hz, -a), 8.12 (d, 2H, J = 8.2 Hz, -e and h), 8.07 – 7.85 (overlapping m, 2H, -b and d), 7.57 (ddd, 1H, J = 7.3, 4.8, 1.4 Hz, -c), 7.35 (d, 2H, J = 8.0 Hz, -f and g), 7.07 (s, 2H, -NH₂), 2.40 (s, 3H, CH₃) ppm.

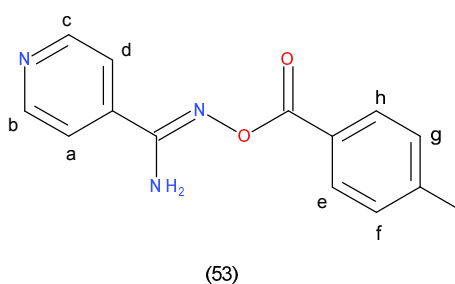
IR (KBr disc) ν : 3472 (N-H), 3357 (N-H), 3068 (Aromatic C-H), 3022, 2962, 2902, 2852, 2324, 2168, 1938, 1713, 1621 (C=O), 1575, 1557, 1407, 1433, 1406, 1392, 1373, 1268, 1171, 1079, 1034, 1011 cm^{-1} .

Melting point: 180.8 – 181.6 °C.

Mass spectrum (APCI +) m/z: Found 255.1003 (M+H)⁺; calculated for C₁₄H₁₃N₃O₂ 255.1007; 1.5 ppm.

Yield: 0.51 g, 63%.

N-[(4-Methylbenzoyl)oxy]-4-pyridinecarboximidamide (53)



¹H NMR (250 MHz, d₆-DMSO): 8.71 (d, 2H, J = 5.0 Hz, -b and c), 8.10 (d, 2H, J = 8.1 Hz, -e and h), 7.75 (d, 2H, J = 6.0 Hz, -a and d), 7.35 (d, 2H, J = 8.0 Hz, -f and g), 7.16 (s, 2H, -NH₂), 2.40 (s, 3H, CH₃) ppm.

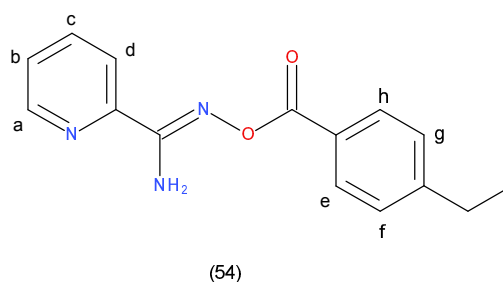
IR (KBr disc) ν : 3458 (N-H), 3357 (N-H), 3206 (Aromatic C-H), 3169, 3045, 2912, 2361, 1713, 1626 (C=O), 1539, 1507, 1410, 1304, 1259, 1181, 1093, 1015 cm^{-1} .

Melting point: 166.8 – 167.5 °C.

Mass spectrum (APCI +) m/z: Found 255.1000 (M+H)⁺; calculated for C₁₄H₁₃N₃O₂ 255.1007; 2.7 ppm.

Yield: 0.55 g, 67%.

***N*-[(4-Ethylbenzoyl)oxy]-2-pyridinecarboximidamide (54)**



¹H NMR (250 MHz, d₆-DMSO): 8.68 (ddd, 1H, J = 4.8, 1.6, 1.0 Hz, **-a**), 8.23 – 8.08 (overlapping m, 2H, **-e and h**), 8.08 – 7.89 (overlapping m, 2H, **-b and d**), 7.57 (ddd, 1H, J = 7.3, 4.8, 1.4 Hz,), 7.38 (d, 2H, J = 8.4 Hz, **-f and g**), 7.06 (s, 2H, **-NH₂**), 2.87 – 2.58 (overlapping m, 2H, **-CH₂CH₃**), 1.30 (t, 3H, J = 6.8 Hz, **-CH₂CH₃**) ppm.

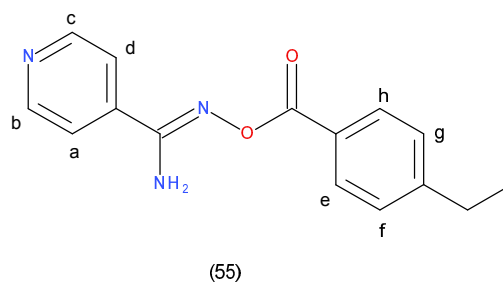
IR (KBr disc) ν : 3466 (N-H), 3355 (N-H), 3049 (Aromatic C-H), 2961, 2924, 2863, 2367, 1931, 1717, 1629 (C=O), 1583, 1555, 1472, 1411, 1388, 1309, 1263, 1165, 1128, 1082, 1045, 1012 cm⁻¹.

Melting point: 155.3 – 156.7 °C.

Mass spectrum (APCI +) m/z: Found 269.1160 (M+H)⁺; calculated for C₁₅H₁₅N₃O₂ 269.1164; 1.4 ppm.

Yield: 0.58 g, 59%.

***N*-[(4-Ethylbenzoyl)oxy]-4-pyridinecarboximidamide (55)**



¹H NMR (250 MHz, d₆-DMSO): 8.70 (d, 2H, J = 5.5 Hz, **-b and c**), 8.09 (d, 2H, J = 8.1 Hz, **-e and h**), 7.75 (d, 3H, J = 5.6 Hz, **-a and d**), 7.38 (d, 2H, J = 8.0 Hz, **-f and g**), 6.99 (s, 2H, **-NH₂**), 2.72 (q, 2H, J

= 7.6 Hz, $-\text{CH}_2\text{CH}_3$), 1.31 (t, 3H, $J = 6.6$ Hz, $-\text{CH}_2\text{CH}_3$) ppm.

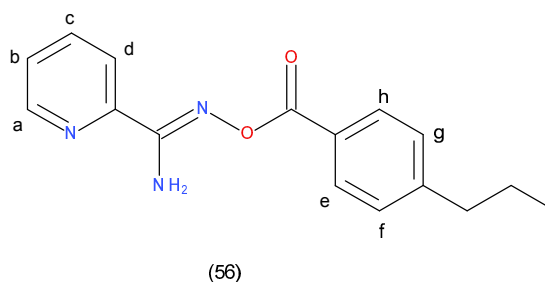
IR (KBr disc) ν : 3392 (N-H), 3309 (N-H), 3183, 3030 (Aromatic C-H), 2956, 2924, 2863, 1727, 1634 (C=O), 1601, 1532, 1499, 1453, 1411, 1258, 1253, 1170, 1073, 1008 cm^{-1} .

Melting point: 134.3 – 135.5 $^\circ\text{C}$.

Mass spectrum (APCI +) m/z : Found 269.1158 ($\text{M}+\text{H}$)⁺; calculated for $\text{C}_{15}\text{H}_{15}\text{N}_3\text{O}_2$ 269.1164; 2.2 ppm.

Yield: 0.72 g, 72%.

***N*-[(4-Propylbenzoyl)oxy]-2-pyridinecarboximidamide (56)**



^1H NMR (250 MHz, d_6 -DMSO): 8.68 (ddd, 1H, $J = 4.8, 1.6, 1.0$ Hz, **-a**), 8.22 – 8.08 (overlapping m, 2H, **-e and h**), 8.08 – 7.86 (overlapping m, 2H, **-b and d**), 7.57 (ddd, 1H, $J = 7.3, 4.8, 1.4$ Hz, **-c**), 7.36 (d, 2H, $J = 8.3$ Hz, **-f and g**), 7.06 (s, 2H, **-NH₂**), 2.72 – 2.58 (t, 2H, $J = 6.5$ Hz, **-CH₂CH₂CH₃**), 1.79 – 1.47 (overlapping m, 2H, **-CH₂CH₂CH₃**), 0.90 (t, 3H, $J = 7.3$ Hz, **-CH₂CH₂CH₃**) ppm.

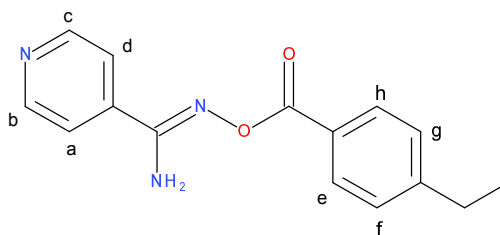
IR (KBr disc) ν : 3425 (N-H), 3333 (N-H), 3211, 3026 (Aromatic C-H), 2943, 2911, 2828, 2351, 1717, 1616 (C=O), 1529, 1511, 1460, 1418, 1317, 1253, 1218, 1161, 1089, 1001 cm^{-1} .

Melting point: 161.2 – 162.5 $^\circ\text{C}$.

Mass spectrum (APCI +) m/z : Found 283.1315 ($\text{M}+\text{H}$)⁺; calculated for $\text{C}_{16}\text{H}_{17}\text{N}_3\text{O}_2$ 283.1320; 1.7 ppm.

Yield: 0.76 g, 74%.

N-[(4-Propylbenzoyl)oxy]-4-pyridinecarboximidamide (57)



(57)

¹H NMR (250 MHz, d₆-DMSO): 8.71 (dd, 2H, J = 4.5, 1.6 Hz, **-b and c**), 8.11 (d, 2H, J = 8.2 Hz, **-e and h**), 7.75 (dd, 2H, J = 4.5, 1.6 Hz, **-a and d**), 7.36 (d, 2H, J = 8.2 Hz, **-f and g**), 7.16 (s, 2H, **-NH₂**), 2.69 – 2.61 (overlapping m, 2H, **-CH₂CH₂CH₃**), 1.79 – 1.46 (overlapping m, 2H, **-CH₂CH₂CH₃**), 0.91 (t, 3H, J = 7.3 Hz, **-CH₂CH₂CH₃**) ppm.

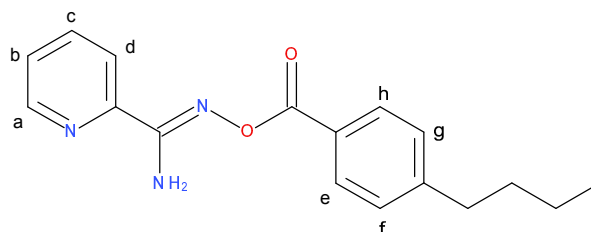
IR (KBr disc) ν : 3449 (N-H), 3348 (N-H), 3215, 3173, 3063 (Aromatic C-H), 3031, 2948, 2921, 2861, 2191, 1906, 1713, 1626 (C=O), 1529, 1456, 1406, 1309, 1272, 1171, 1098, 1020 cm⁻¹.

Melting point: 154.1 – 155.3 °C.

Mass spectrum (APCI +) m/z: Found 283.1311 (M+H)⁺; calculated for C₁₆H₁₇N₃O₂ 283.1320; 3.1 ppm.

Yield: 0.67 g, 65%.

N-[(4-Butylbenzoyl)oxy]-2-pyridinecarboximidamide (58)



(58)

¹H NMR (250 MHz, d₆-DMSO): 8.68 (d, 1H, J = 4.8 Hz, **-a**), 8.13 (d, 2H, J = 8.2 Hz, **-e and h**), 7.97 (ddd, 2H, J = 12.9, 9.4, 4.8 Hz, **-b and d**), 7.57 (ddd, 1H, J = 7.3, 4.9, 1.2 Hz, **-c**), 7.36 (d, 2H, J = 8.2

Hz, **-f and g**), 7.06 (s, 2H, **-NH₂**), 2.67 (t, 2H, J = 7.6 Hz, **-CH₂CH₂CH₂CH₃**), 1.83 – 1.46 (overlapping m, 2H, **-CH₂CH₂CH₂CH₃**), 1.44 – 1.20 (overlapping m, 2H, **-CH₂CH₂CH₂CH₃**), 0.90 (t, 3H, J = 7.3 Hz, **-CH₂CH₂CH₂CH₃**) ppm.

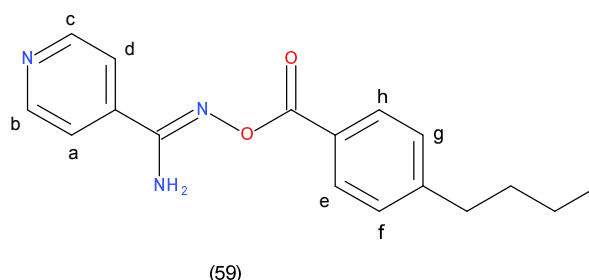
IR (KBr disc) ν : 3463 (N-H), 3348 (N-H), 3045 (Aromatic C-H), 2958, 2916, 2852, 2361, 2333, 1722, 1626 (C=O), 1589, 1557, 1461, 1410, 1392, 1263, 1176, 1084, 1011 cm^{-1} .

Melting point: 146.3 – 147.6 °C.

Mass spectrum (APCI +) m/z: Found 297.1472 (M+H)⁺; calculated for C₁₇H₁₉N₃O₂ 297.1477; 1.6 ppm.

Yield: 0.87 g, 81%.

N-[(4-Butylbenzoyl)oxy]-4-pyridinecarboximidamide (59)



¹H NMR (250 MHz, d₆-DMSO): 8.76 – 8.65 (overlapping m, 2H, **-b and c**), 8.08 (d, 4H, J = 8.3 Hz, **-e and h**), 7.75 (dd, 4H, J = 4.5, 1.6 Hz, **-a and d**), 7.36 (d, 4H, J = 8.3 Hz, **-f and g**), 6.98 (s, 2H, **-NH₂**), 2.77 (t, 2H, J = 6.5 Hz, **-CH₂CH₂CH₂CH₃**), 1.72 – 1.49 (overlapping m, 2H, **-CH₂CH₂CH₂CH₃**), 1.48 – 1.10 (overlapping m, 2H, **-CH₂CH₂CH₂CH₃**), 0.92 (t, 3H, J = 7.3 Hz, **-CH₂CH₂CH₂CH₃**) ppm.

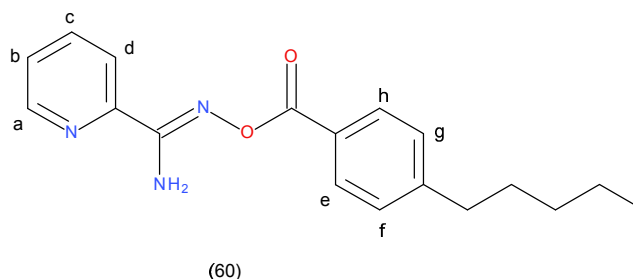
IR (KBr disc) ν : 3444 (N-H), 3394 (N-H), 3348, 3173, 3031 (Aromatic C-H), 2958, 2930, 2852, 1713, 1631 (C=O), 1608, 1539, 1465, 1401, 1373, 1309, 1277, 1176, 1075, 1011 cm^{-1} .

Melting point: 152.1 – 153.6 °C.

Mass spectrum (APCI +) m/z: Found 297.1469 (M+H)⁺; calculated for C₁₇H₁₉N₃O₂ 297.1477; 2.6 ppm.

Yield: 0.90 g, 84%.

***N*-[(4-Pentylbenzoyl)oxy]-2-pyridinecarboximidamide (60)**



¹H NMR (250 MHz, d₆-DMSO): 8.88 (m, 1H, **-a**), 8.13 (d, 2H, J = 8.2 Hz, **-e and h**), 7.97 (ddd, 2H, J = 12.9, 9.6, 4.8 Hz, **-b and d**), 7.57 (ddd, 1H, J = 7.3, 4.9, 1.3 Hz, **-c**), 7.35 (d, 2H, J = 8.3 Hz, **-f and g**), 7.06 (s, 2H, **-NH₂**), 2.81 – 2.58 (t, 2H, J = 6.5 Hz, **-CH₂CH₂(CH₂)₂CH₃**), 1.86 – 1.45 (overlapping m, 2H, **-CH₂CH₂(CH₂)₂CH₃**), 1.39 – 1.18 (overlapping m, 4H, **-CH₂CH₂(CH₂)₂CH₃**), 0.86 (t, 3H, J = 6.8 Hz, **-CH₂CH₂(CH₂)₂CH₃**) ppm.

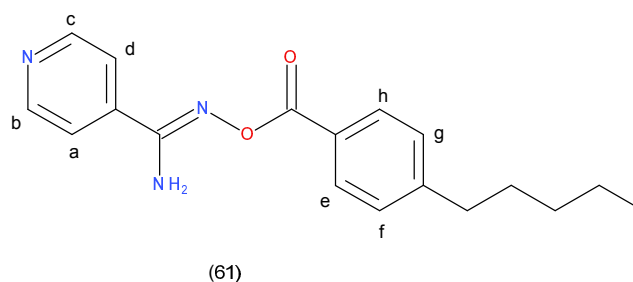
IR (KBr disc) ν : 3462 (N-H), 3337 (N-H), 3054 (Aromatic C-H), 2951, 2919, 2854, 2362, 1810, 1722, 1625 (C=O), 1583, 1555, 1467, 1411, 1379, 1309, 1267, 1179, 1082, 1012 cm⁻¹.

Melting point: 153.3 – 156.7 °C.

Mass spectrum (APCI +) m/z: Found 311.1629 (M+H)⁺; calculated for C₁₈H₂₁N₃O₂ 311.1633; 1.2 ppm.

Yield: 0.77 g, 69%.

N-[(4-Pentylbenzoyl)oxy]-4-pyridinecarboximidamide (61)



¹H NMR (250 MHz, d₆-DMSO): 8.70 (d, 2H, J = 5.4 Hz, **-b and c**), 8.34 – 7.98 (overlapping m, 2H, **-e and h**), 7.75 (dd, 2H, J = 4.5, 1.6 Hz, **-a and d**), 7.36 (d, 2H, J = 8.3 Hz, **-f and g**), 6.98 (s, 2H, **-NH₂**), 2.70 (t, 2H, J = 6.5 Hz, **-CH₂CH₂(CH₂)₂ CH₃**), 1.64 (dt, 1H, J = 14.9, 7.3 Hz, **-CH₂CH₂(CH₂)₂ CH₃**), 1.48 – 1.20 (overlapping m, 4H, **-CH₂CH₂(CH₂)₂ CH₃**), 0.88 (t, 3H, J = 8.3, 5.4 Hz, J = 6.8 Hz, **-CH₂CH₂(CH₂)₂ CH₃**) ppm.

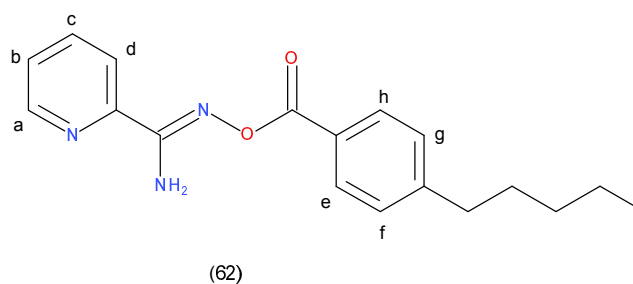
IR (KBr disc) ν : 3448 (N-H), 3346 (N-H), 3030 (Aromatic C-H), 2951, 2928, 2854, 2339, 1722, 1615 (C=O), 1532, 1411, 1309, 1263, 1170, 1110, 1017 cm⁻¹.

Melting point: 120.3 – 121.9 °C.

Mass spectrum (APCI +) m/z: Found 311.1624 (M+H)⁺; calculated for C₁₈H₂₁N₃O₂ 311.1633; 2.8 ppm.

Yield: 0.81 g, 72%.

N-[(4-Hexylbenzoyl)oxy]-2-pyridinecarboximidamide (62)



¹H NMR (250 MHz, d₆-DMSO): 8.68 (ddd, 1H, J = 4.8, 1.7, 1.0 Hz, **-a**), 8.32 – 8.00 (overlapping m, 2H, **-e and h**), 7.99 – 7.86 (overlapping m, 2H, **-b and d**), 7.56 (ddd, 1H, J = 7.4, 4.8, 1.3 Hz, **-c**), 7.36 (d, 2H, J = 8.4 Hz, **-f and g**), 6.89 (s, 2H, **-NH₂**), 2.71 (t, 2H, J = 6.5 Hz, **-CH₂CH₂(CH₂)₃CH₃**), 1.61 (dd, 2H, J = 14.8, 7.2 Hz, **-CH₂CH₂(CH₂)₃CH₃**), 1.33 (d, 6H, J = 10.3 Hz, **-CH₂CH₂(CH₂)₃CH₃**), 1.02 (t, 3H, J = 7.3 Hz, **-CH₂CH₂(CH₂)₃CH₃**) ppm.

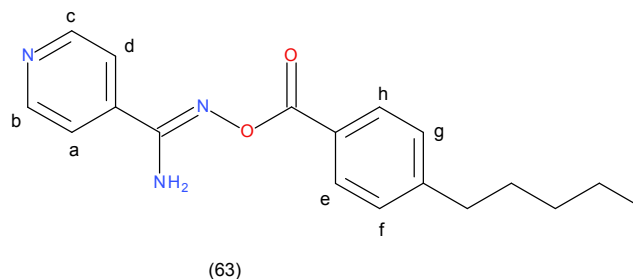
IR (KBr disc) ν : 3463 (N-H), 3348 (N-H), 3049 (Aromatic C-H), 2916, 2953, 2847, 2154, 1929, 1718, 1626 (C=O), 1580, 1548, 1502, 1465, 1415, 1387, 1304, 1259, 1171, 1070, 1038, 1011 cm⁻¹.

Melting point: 164.2 – 165.8 °C.

Mass spectrum (APCI +) m/z: Found 325.1786 (M+H)⁺; calculated for C₁₉H₂₃N₃O₂ 325.1790; 1.2 ppm.

Yield: 0.80 g, 68%.

N-[(4-Hexylbenzoyl)oxy]-4-pyridinecarboximidamide (63)



¹H NMR (250 MHz, d₆-DMSO): 8.70 (d, 2H, J = 5.1 Hz, **-b and c**), 8.10 (d, 2H, J = 8.3 Hz, **-e and h**), 7.75 (dd, 2H, J = 4.6, 1.5 Hz, **-a and d**), 7.35 (d, 2H, J = 8.3 Hz, **-f and g**), 7.16 (s, 2H, **-NH₂**), 2.66 (t, J = 7.6 Hz, 2H, **-CH₂CH₂(CH₂)₃CH₃**), 1.63 (dd, 2H, J = 27.0, 20.5 Hz, **-CH₂CH₂(CH₂)₃CH₃**), 1.29 (dd, J = 11.4 Hz, 6H, **-CH₂CH₂(CH₂)₃CH₃**), 0.84 (t, 3H, J = 6.7 Hz, **-CH₂CH₂(CH₂)₃CH₃**) ppm.

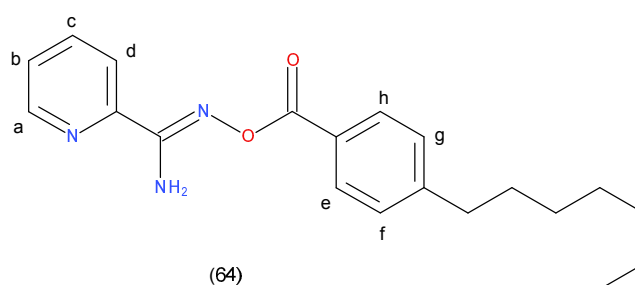
IR (KBr disc) ν : 3443 (N-H), 3346 (N-H), 3207, 3160, 3030 (Aromatic C-H), 2956, 2924, 2849, 1727, 1625 (C=O), 1532, 1499, 1462, 1407, 1305, 1272, 1179, 1110, 1012 cm⁻¹.

Melting point: 133.7 – 135.4 °C.

Mass spectrum (APCI +) m/z: Found 325.1781 (M+H)⁺; calculated for C₁₉H₂₃N₃O₂ 325.1790; 2.7 ppm.

Yield: 0.88 g, 75%.

N-[(4-Heptylbenzoyl)oxy]-2-pyridinecarboximidamide (64)



¹H NMR (250 MHz, d₆-DMSO): 8.68 (ddd, 1H, J = 4.8, 1.6, 1.0 Hz, -a), 8.36 – 8.01 (overlapping m, 2H, -e and h), 7.94 (td, 1H, J = 7.7, 1.7 Hz, -c), 7.56 (ddd, 2H, J = 7.4, 4.8, 1.3 Hz, -b and d), 7.36 (d, 2H, J = 8.3 Hz, -f and g), 6.92 (s, 2H, -NH₂), 2.70 (t, 2H, J = 6.5 Hz, -CH₂CH₂(CH₂)₄CH₃), 1.79 – 1.48 (overlapping m, 2H, -CH₂CH₂(CH₂)₄CH₃), 1.29 (dd, 8H, J = 7.3, 3.4 Hz, -CH₂CH₂(CH₂)₄CH₃), 0.86 (t, 3H, J = 6.8 Hz, -CH₂CH₂(CH₂)₄CH₃) ppm.

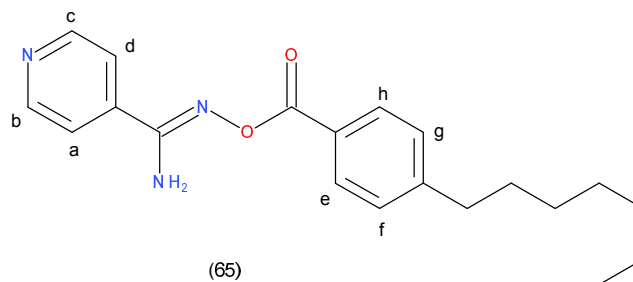
IR (KBr disc) ν : 3472 (N-H), 3366 (N-H), 2958 (Aromatic C-H), 2916, 2856, 2365, 1727, 1631 (C=O), 1580, 1548, 1503, 1461, 1415, 1387, 1309, 1263, 1249, 1181, 1075, 1006 cm⁻¹.

Melting point: 142.2 – 143.4 °C.

Mass spectrum (APCI +) m/z: Found 339.1940 (M+H)⁺; calculated for C₂₀H₂₅N₃O₂ 339.1946; 1.7 ppm.

Yield: 1 g, 82%.

N-[(4-Heptylbenzoyl)oxy]-4-pyridinecarboximidamide (65)



¹H NMR (250 MHz, d₆-DMSO): 8.70 (d, 2H, J = 6.0 Hz, **-b and c**), 8.26 – 8.04 (overlapping m, 2H, **-e and h**), 7.75 (dd, 2H, J = 4.5, 1.6 Hz, **-a and d**), 7.35 (d, 2H, J = 8.3 Hz, **-f and g**), 6.99 (s, 2H, **-NH₂**), 2.70 (t, 2H, J = 6.5 Hz, **-CH₂CH₂(CH₂)₄CH₃**), 1.85 – 1.47 (overlapping m, 2H, **-CH₂CH₂(CH₂)₄CH₃**), 1.30 (dd, 8H, J = 7.3, 3.4 Hz, **-CH₂CH₂(CH₂)₄CH₃**), 0.98 (t, 2H, J = 6.8 Hz, **-CH₂CH₂(CH₂)₄CH₃**) ppm.

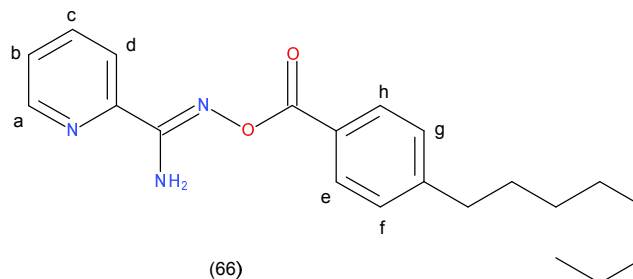
IR (KBr disc) ν : 3435 (N-H), 3343 (N-H), 3201, 3036 (Aromatic C-H), 2953, 2921, 2838, 2361, 1718, 1617 (C=O), 1539, 1502, 1470, 1419, 1318, 1263, 1208, 1171, 1098, 1011 cm⁻¹.

Melting point: 126.8 – 128.3 °C.

Mass spectrum (APCI +) m/z: Found 339.1936 (M+H)⁺; calculated for C₂₀H₂₅N₃O₂ 339.1946; 2.9 ppm.

Yield: 0.90 g, 74%.

N-[(4-Octylbenzoyl)oxy]-2-pyridinecarboximidamide (66)



¹H NMR (250 MHz, d₆-DMSO): 8.68 (ddd, 1H, J = 4.8, 1.6, 1.0 Hz, **-a**), 8.22 – 8.00 (overlapping m, 2H, **-e and h**), 8.00 – 7.86 (overlapping m, 2H, **-b and d**), 7.56 (ddd, 1H, J = 7.4, 4.8, 1.3 Hz, **-c**), 7.35 (d,

2H, J = 8.3 Hz, **-f and g**), 6.90 (s, 2H, **-NH₂**), 2.68 (t, 2H, J = 6.5 Hz, **-CH₂CH₂(CH₂)₅CH₃**), 1.72 – 1.51 (overlapping m, 2H, **-CH₂CH₂(CH₂)₅CH₃**), 1.28 (dd, 10H, J = 8.0, 4.0 Hz, **-CH₂CH₂(CH₂)₅CH₃**), 0.86 (t, 3H, J = 6.7 Hz, **-CH₂CH₂(CH₂)₅CH₃**) ppm.

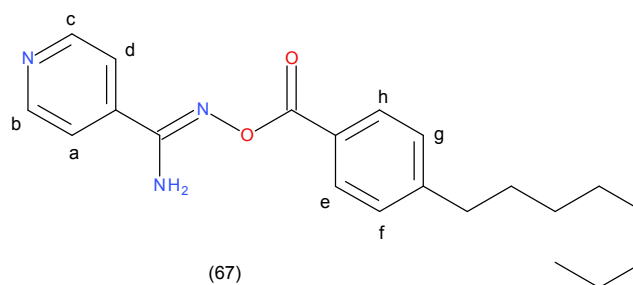
IR (KBr disc) ν : 3476 (N-H), 3371 (N-H), 2962 (Aromatic C-H), 2925, 2843, 1718, 1626 (C=O), 1580, 1562, 1502, 1474, 1406, 1387, 1250, 1181, 1070, 1038 cm^{-1} .

Melting point: 138.7 – 139.2 °C.

Mass spectrum (APCI +) m/z: Found 353.2099 (M+H)⁺; calculated for C₂₁H₂₇N₃O₂ 353.2103; 1.1 ppm.

Yield: 0.85 g, 67%.

N-[(4-Octylbenzoyl)oxy]-4-pyridinecarboximidamide (67)



¹H NMR (250 MHz, d₆-DMSO): 8.95 – 8.51 (overlapping m, 2H, **-b and c**), 8.08 (d, 2H, J = 8.3 Hz, **-e and h**), 7.75 (dd, 2H, J = 4.5, 1.7 Hz, **-a and d**), 7.35 (d, 2H, J = 8.4 Hz, **-f and g**), 6.99 (s, 1H, **-NH₂**), 2.70 (t, 2H, J = 6.5 Hz, **-CH₂CH₂(CH₂)₅CH₃**), 1.85 – 1.48 (overlapping m, 2H, **-CH₂CH₂(CH₂)₅CH₃**), 1.28 (d, 10H, J = 7.3 Hz, **-CH₂CH₂(CH₂)₅CH₃**), 0.87 (t, 3H, J = 6.6 Hz, **-CH₂CH₂(CH₂)₅CH₃**) ppm.

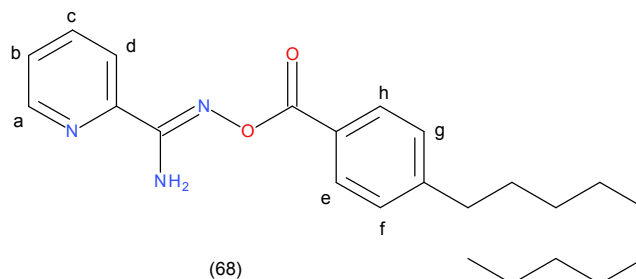
IR (KBr disc) ν : 3444 (N-H), 3339 (N-H), 3045 (Aromatic C-H), 2958, 2921, 2847, 2356, 1718, 1621 (C=O), 1529, 1497, 1461, 1410, 1314, 1263, 1167, 1098, 1006 cm^{-1} .

Melting point: 125.0 – 127.2 °C.

Mass spectrum (APCI +) m/z: Found 353.2093 (M+H)⁺; calculated for C₂₁H₂₇N₃O₂ 353.2103; 2.8 ppm.

Yield: 0.93 g, 73%.

N-[(4-Decylbenzoyl)oxy]-2-pyridinecarboximidamide (68)



¹H NMR (250 MHz, d₆-DMSO): 8.74 – 8.60 (overlapping m, 1H, **-a**), 8.17 – 8.01 (overlapping m, 2H, **-e and h**), 7.99 – 7.86 (overlapping m, 2H, **-b and d**), 7.56 (ddd, 1H, J = 7.4, 4.8, 1.3 Hz, **-c**), 7.35 (d, 2H, J = 8.3 Hz, **-f and g**), 6.89 (s, 2H, **-NH₂**), 2.65 (t, 2H, J = 6.5 Hz, **-CH₂CH₂(CH₂)₇CH₃**), 1.62 (m, 2H, **-CH₂CH₂(CH₂)₇CH₃**), 1.28 (d, 14H, J = 13.0 Hz, **-CH₂CH₂(CH₂)₇CH₃**), 0.86 (t, 3H, J = 6.6 Hz, **-CH₂CH₂(CH₂)₇CH₃**) ppm.

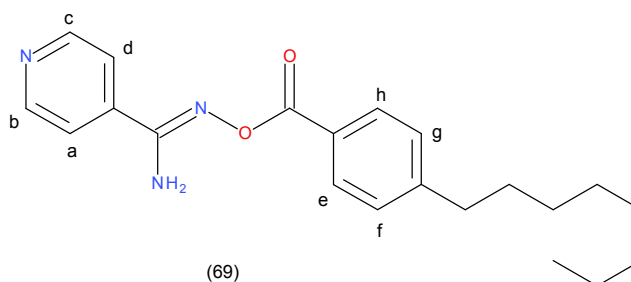
IR (KBr disc) ν : 3467 (N-H), 3371 (N-H), 2953 (Aromatic C-H), 2925, 2847, 1722, 1612 (C=O), 1580, 1562, 1461, 1383, 1268, 1419, 1176, 1089, 1006 cm⁻¹.

Melting point: 137.8 – 138.5 °C.

Mass spectrum (APCI +) m/z: Found 381.2410 (M+H)⁺; calculated for C₂₃H₃₁N₃O₂ 381.2416; 1.5 ppm.

Yield: 0.93 g, 67%.

N-[(4-Decylbenzoyl)oxy]-4-pyridinecarboximidamide (69)



¹H NMR (250 MHz, d₆-DMSO): 8.70 (dd, 2H, J = 4.6, 1.5 Hz, **-b and c**), 8.10 (d, 2H, J = 8.2 Hz, **-e and h**), 7.75 (dd, 2H, J = 4.5, 1.6 Hz, **-a and d**), 7.35 (d, 2H, J = 8.2 Hz, **-f and g**), 7.12 (s, 2H, **-NH₂**), 2.67 (t, 2H, J = 7.6 Hz, **-CH₂CH₂(CH₂)₇CH₃**), 1.60 (overlapping m, 2H, **-CH₂CH₂(CH₂)₇CH₃**), 1.38 – 1.13 (overlapping m, 14H, **-CH₂CH₂(CH₂)₇CH₃**), 0.85 (t, 3H, J = 6.6 Hz, **-CH₂CH₂(CH₂)₇CH₃**) ppm.

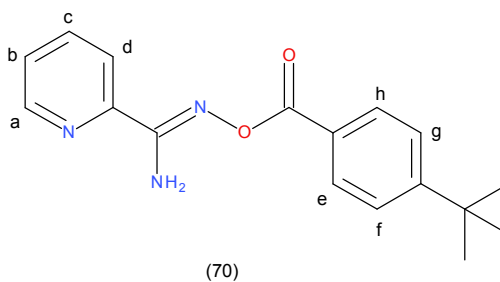
IR (KBr disc) ν : 3442 (N-H), 3338 (N-H), 3115, 3053 (Aromatic C-H), 3021, 2938, 2911, 2851, 1703, 1616 (C=O), 1519, 1446, 1401, 1309, 1262, 1161, 1089, 1010 cm⁻¹.

Melting point: 122.4 – 123.6 °C.

Mass spectrum (APCI +) m/z: Found 381.2407 (M+H)⁺; calculated for C₂₃H₃₁N₃O₂ 381.2416; 2.3 ppm.

Yield: 0.95 g, 69%.

N-[(4-tert-Butylbenzoyl)oxy]-2-pyridinecarboximidamide (70)



¹H NMR (250 MHz, d₆-DMSO): 8.92 – 8.50 (overlapping m, 1H, **-a and c**), 8.31 – 8.08 (overlapping m, 1H, **-b and d**), 8.09 – 7.84 (overlapping m, 2H, **-e and h**), 7.58 (dd, 2H, J = 9.8, 4.9 Hz, **-f and g**), 7.06

(s, 2H, **-NH₂**), 1.41 (s, 9H, **tert. butyl**) ppm.

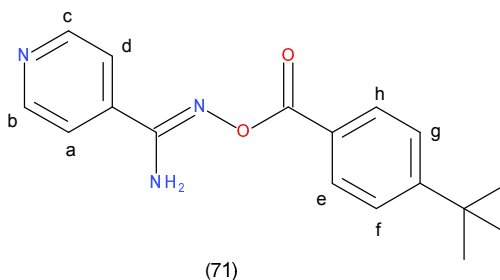
IR (KBr disc) ν : 3448 (N-H), 3328 (N-H), 3044 (Aromatic C-H), 2979, 2891, 2864, 2362, 1718, 1630 (C=O), 1583, 1560, 1472, 1439, 1383, 1356, 1272, 1295, 1184, 1156, 1091, 1026 cm^{-1} .

Melting point: 186.4 – 187.8 °C.

Mass spectrum (APCI +) m/z: Found 297.1471 (M+H)⁺; calculated for C₁₇H₁₉N₃O₂ 297.1477; 2.0 ppm.

Yield: 0.76 g, 71%.

N-[(4-tert-Butylbenzoyl)oxy]-4-pyridinecarboximidamide (71)



¹H NMR (250 MHz, d₆-DMSO): 8.71 (dd, 2H, J = 4.5, 1.6 Hz, **-b and c**), 8.27 – 8.04 (overlapping m, 2H, **-e and h**), 7.75 (dd, 1H, J = 4.5, 1.6 Hz, **-a and d**), 7.56 (d, 1H, J = 8.5 Hz, **-f and g**), 7.15 (s, 2H, **-NH₂**), 1.41 (s, 9H, **tert. butyl**) ppm.

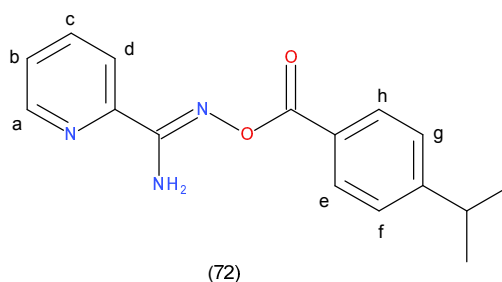
IR (KBr disc) ν : 3500 (N-H), 3454 (N-H), 3302, 3201, 3155, 3036 (Aromatic C-H), 2962, 2893, 2866, 2714, 2365, 1722, 1626 (C=O), 1534, 1451, 1401, 1355, 1272, 1190, 1116, 1089, 1011 cm^{-1} .

Melting point: 168.1 – 169.4 °C.

Mass spectrum (APCI +) m/z: Found 297.1468 (M+H)⁺; calculated for C₁₇H₁₉N₃O₂ 297.1477; 3.0 ppm.

Yield: 0.79 g, 74%.

N-[(4-Isopropylbenzoyl)oxy]-2-pyridinecarboximidamide (72)



¹H NMR (250 MHz, d₆-DMSO): 8.79 (d, 1H, J = 4.7 Hz, **-a**), 8.22 – 7.98 (overlapping m, 2H, **-e and h**), 7.63 (ddd, 3H, J = 7.4, 4.8, 1.1 Hz, **-b, c and d**), 7.55 (d, 2H, J = 8.4 Hz, **-f and g**), 3.01 (dq, 2H, J = 13.7, 6.9 Hz, **-CH₂(CH₃)₂**), 1.25 (d, 6H, J = 6.9 Hz, **-CH₂(CH₃)₂**) ppm.

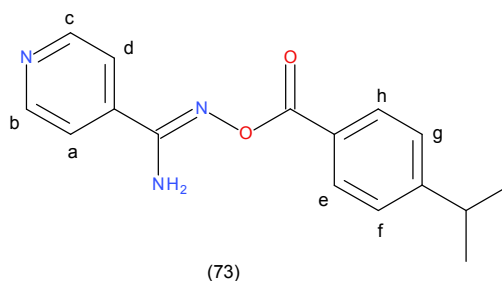
IR (KBr disc) ν : 3480 (N-H), 3382 (N-H), 3317, 3150, 2955 (Aromatic C-H), 2915, 2853, 1500, 1610 (C=O), 1578, 1531, 1462, 1424, 1417, 1373, 1350, 1323, 1225, 1160, 1115, 1001 cm⁻¹.

Melting point: 139.6 – 140.7 °C.

Mass spectrum (APCI +) m/z: Found 283.1314 (M+H)⁺; calculated for C₁₆H₁₇N₃O₂ 283.1320; 2.1 ppm.

Yield: 0.78 g, 76%.

N-[(4-Isopropylbenzoyl)oxy]-4-pyridinecarboximidamide (73)



¹H NMR (250 MHz, d₆-DMSO): 9.22 – 8.65 (overlapping m, 2H, **-b and c**), 8.11 (d, 2H, J = 8.2 Hz, **-e and h**), 7.86 – 7.69 (overlapping m, 2H, **-a and d**), 7.41 (d, 2H, J = 8.2 Hz, **-f and g**), 7.16 (s, 2H, **-NH₂**), 2.99 (dt, 1H, J = 13.6, 6.7 Hz, **-CH₂(CH₃)₂**), 1.23 (d, 6H, J = 6.9 Hz, **-CH₂(CH₃)₂**) ppm.

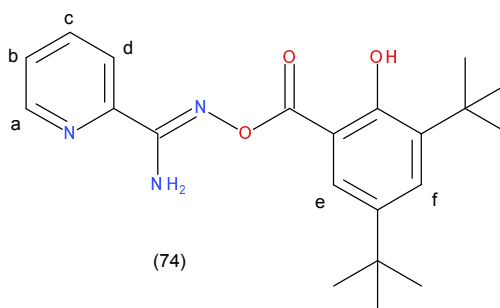
IR (KBr disc) ν : 3438 (N-H), 3317 (N-H), 3034 (Aromatic C-H), 2969, 2881, 2853, 2352, 1716, 1619 (C=O), 1573, 1550, 1462, 1429, 1373, 1346, 1285, 1262, 1174, 1146, 1081, 1016 cm^{-1} .

Melting point: 135.4 – 136.3 $^{\circ}\text{C}$.

Mass spectrum (APCI +) m/z: Found 283.1309 (M+H)⁺; calculated for C₁₆H₁₇N₃O₂ 283.1320; 3.8 ppm.

Yield: 0.83 g, 81%.

***N*-[(3, 5-ditert-butyl-2-hydroxy-phenyl)oxy]-2-pyridinecarboximidamide (74)**



¹H NMR (250 MHz, d₆-DMSO): 11.55 (s, 1H, –OH), 8.71 (d, 1H, J = 4.0 Hz, -a), 8.23 – 7.86 (overlapping m, 2H, -e and f), 7.58 (ddd, 3H, J = 11.5, 7.5, 1.9 Hz, -b, c and d), 7.16 (s, 2H, -NH₂), 1.43 (s, 9H, *tert. butyl*), 1.27 (s, 9H, *tert. butyl*) ppm.

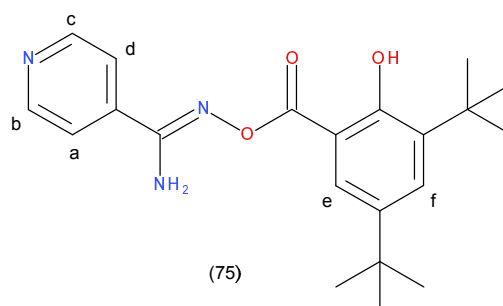
IR (KBr disc) ν : 3480 (OH), 3382 (N-H), 3317 (N-H), 3150, 2955 (Aliphatic C-H), 2915, 2856, 1680, 1610 (C=O), 1578, 1531, 1462, 1424, 1417, 1373, 1350, 1323, 1262, 1225, 1160, 1127, 1115, 1107 cm^{-1} .

Melting point: 166.4 – 177.8 $^{\circ}\text{C}$.

Mass spectrum (APCI +) m/z: Found 369.2046 (M+H)⁺; calculated for C₂₁H₂₇N₃O₂ 369.2052; 1.6 ppm.

Yield: 0.86 g, 64%.

***N*-[(3, 5-ditert-butyl-2-hydroxy-phenyl)oxy]-4-pyridinecarboximidamide (75)**



¹H NMR (250 MHz, d₆-DMSO): 11.51 (s, 1H, –OH), 8.85 (d, 2H, J = 5.9 Hz, **-b and c**), 8.14 (d, 2H, J = 6.0 Hz, **-e and f**), 7.58 (ddd, 2H, J = 11.5, 7.5, 1.9 Hz, **-a and d**), 7.33 (s, 2H, **-NH₂**), 1.43 (s, 9H, **tert. butyl**), 1.27 (s, 9H, **tert. butyl**) ppm.

IR (KBr disc) ν : 3490 (OH), 3392 (N-H), 3327 (N-H), 3160, 2965 (Aromatic C-H), 2905, 2863, 2719, 2367, 1690, 1620 (C=O), 1588, 1541, 1472, 1434, 1407, 1383, 1360, 1332, 1272, 1235, 1170, 1137, 1105 cm⁻¹.

Melting point: 176.4 – 177.6 °C.

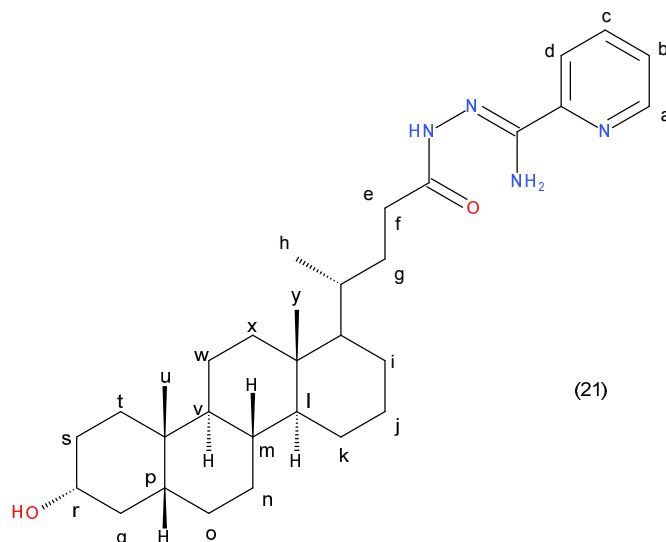
Mass spectrum (APCI +) m/z: Found 369.2040 (M+H)⁺; calculated for C₂₁H₂₇N₃O₂ 369.2052; 3.2 ppm.

Yield: 1.03 g, 77%.

2.6.9 General method for preparation of Lithocholic acid derivatives

To a stirred solution of Lithocholic acid (0.5g, 1.35 mmol) in 20mL THF, under argon, *N*-methyl-morpholine (0.15 g, 1.35 mmol) was added and the reaction was cooled over the ice bath for 10 mins. To this reaction mixture ethylchloro carbonate (0.15 g, 1.35 mmol) was added over a period of 10 mins, followed by amine (0.181 g, 1.35 mmol). This reaction mixture was stirred at 30 °C for 3 hours. The reaction mixture is then poured in NaHCO₃ sat. solution. The product precipitates out and was collected by filtration and washed with water (3×10mL).

***N*-[(*Z*)-[amino(2-pyridyl)methylene]amino]-4-(8-hydroxy-10a,12a-dimethyl-1,2,3,4,4a,4b,5,6,6a,7,8,9,10,10b,11,12-hexadecahydrochrysen-1-yl)-2-methyl-butanamide (21)**



¹H NMR (250 MHz, d₆-DMSO): 10.05 (s, 1H, -NH), 9.81 (s, 1H, -a), 8.56 (d, 1H, J = 4.5 Hz, -c), 8.06 (m, 1H, -d), 7.85 (t, 1H, J = 7.7 Hz, -b), 7.55 – 7.32 (overlapping m, 2H, -NH₂), 6.87 (s, 1H, -OH), 6.63 (d, 5H, J = 17.5 Hz, -e and q), 4.47 (s, 4H, -s and u), 4.08 (q, 5H, J = 7.0 Hz, -r, g and h), 2.36 – 2.04 (overlapping m, 3H, -y), 2.04 – -0.26 (overlapping m, 20H, -i, j, k, l, m, n, o, p, t, v, w and x) ppm.

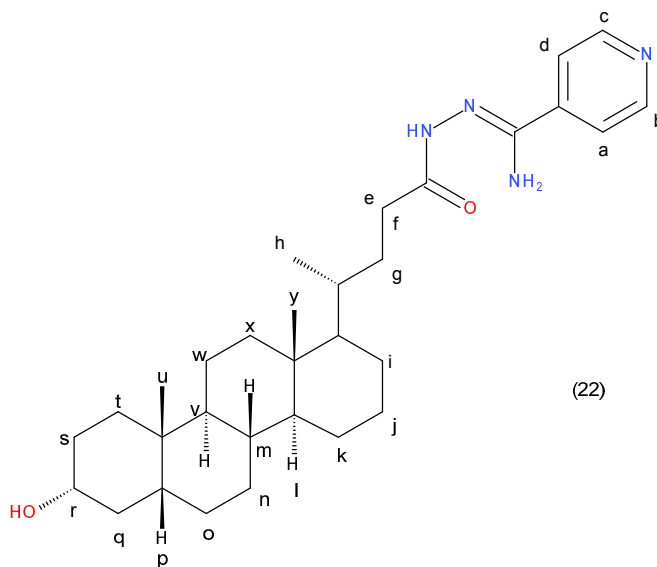
IR (KBr disc) ν : 3421 (OH), 3392 (N-H), 3377, 3327 (N-H), 3310, 3140, 2927, 2955 (Aromatic C-H), 2901, 2861, 2837, 2715, 2347, 1690, 1623 (C=O), 1588, 1541, 1463, 1414, 1407, 1371, 1350, 1332, 1272, 1235, 1170, 1137, 1105 cm⁻¹.

Melting point: 187.8 – 189.5 °C.

Mass spectrum (APCI +) m/z: Found 508.3778 (M+H)⁺; calculated for C₃₁H₄₈N₄O₂ 508.3777; 0.1 ppm.

Yield: 0.54 g, 78%.

***N*-[(*Z*)-[amino(4-pyridyl)methylene]amino]-4-(8-hydroxy-10a,12a-dimethyl-1,2,3,4,4a,4b,5,6,6a,7,8,9,10,10b,11,12-hexadecahydrochrysen-1-yl)-2-methyl-butanamide (22)**



¹H NMR (250 MHz, d₆-DMSO): 9.74 (s, 1H, -NH), 8.60 (d, 2H, J = 4.9 Hz, -b and c), 7.71 (d, 2H, J = 5.5 Hz, -a and d), 6.87 (s, 2H, -NH₂), 6.58 (d, 1H, J = 9.7 Hz, -f), 4.42 (s, 1H, -OH), 4.06 (dd, 6H, J = 12.0, 7.0 Hz, -r, l, g and h), 2.18 (s, 2H, -s), 1.93 (s, 2H, -m and n), 1.72 (d, 2H, J = 35.8 Hz, -i and j), 1.35 (s, 2H, -o), 1.28 – 1.04 (overlapping m, 4H, -k and p), 1.05 (s, 1H, -x), 0.98 – 0.76 (overlapping m, 5H, -t, v and w), 0.61 (s, 3H, -y) ppm.

IR (KBr disc) ν : 3490 (OH), 3365 (N-H), 3346, 3327 (N-H), 3270, 3160, 3079, 2929, 2965 (Aromatic C-H), 2905, 2863, 2851, 2719, 2401, 2367, 1641, 1610 (C=O), 1556, 1541, 1472, 1414, 1387, 1353, 1332, 1272, 1235, 1160, 1127, 1102 cm⁻¹.

Melting point: 187.4 – 189.6 °C.

Mass spectrum (APCI +) m/z: Found 508.3768 (M+H)⁺; calculated for C₃₁H₄₈N₄O₂ 508.3777; 1.7 ppm.

Yield: 0.47 g, 69%.

Chapter 3

Cyclisation of carboxamidrazone amides

3.1 Introduction

The compounds that subsume a heterocyclic scaffold continue to gather a special interest due to their wide spectrum of biological activity. This chapter reviews the literature concerning five membered ring systems like 1,2,4-triazoles and 1,2,4-oxadiazoles.

Bladin (1885) first named a five membered carbon and nitrogen ring as triazole. His work depends heavily on Fischer (1878)'s findings, that reaction of phenylhydrazine with cyanogen results in formation of dicyanophenylhydrazine. Although the structures reported by Bladin (1885) were slightly incorrect, it formed the basis of the triazole chemistry (Pellizzari 1911). Andreocci (1893) suggested an alternative name for the ring system as pyrrodiazole, as it is an analogue of the parent structure pyrrole (Levy & Andreocci (1888)). It was suggested that the numbering of pyrrodiazole should be similar to that of the pyrrole, but later this was changed and the name triazole was universally accepted (see Fig. 3.1). There was no significant research carried out in this field between 1925 to 1946.

The 1,2,4-triazoles developed a renewed interest when it was found that they possess agricultural, industrial and biological activities (Rabea et al. (2006), Labanauskas et al. (2004)), including antibacterial (Bayrak et al. (2009), Holla et al. (2000), Shafiee et al. (2002), Sharma et al. (2008), Gülerman et al. (2001), Papakonstantinou-Garoufalias et al. (2002), Turan-Zitouni et al. (2001)), anti-fungal (Sharma et al. (2008), Gülerman et al. (2001), Papakonstantinou-Garoufalias et al. (2002), Turan-Zitouni et al. (2005), Jalilian et al. (2000)), anti-tubercular (Küçükgüzel et al. (2001), Zahajska et al.

(2004), Foroumadi et al. (2003)), analgesic (Turan-Zitouni et al. (2001), Tozkoparan et al. (2007)), anti-inflammatory (Tozkoparan et al. (2007), Rabea et al. (2006), Labanauskas et al. (2004)), anticancer (Shivarama Holla et al. (2003), Duran et al. (2002)), anti-convulsant (Almasirad et al. (2004), Küçükgülzel et al. (2004)), antiviral (Kritsanida et al. (2002), Abdel-Aal et al. (2008)), insecticidal (Chai et al. (2003)), and antidepressant (Varvaresou et al. (1998)) properties. The simple and fused ring triazoles emerged as an important alternative to prepare photographic emulsions, this made it possible to avoid fogging and also found its use in chemical herbicides. The triazole rings do not occur in nature and are prepared synthetically.

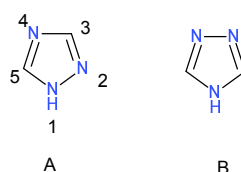


Figure 3.1: Two structures for 1,2,4-triazole. A: the widely accepted structure of triazole. B: the structure of the pyrrodiazole.

Another related and important five membered ring is 1,2,4-oxadiazole. The cyclisation of aldoxime yields oxadiazole. Tiemann & Krüger (1884) first synthesised 1,2,4-oxadiazoles and named it as 'oxozimes'. The early French scientists considered the oxadiazole ring as a furan ring with nitrogen substituting two carbon atoms in the furan nucleus. They assigned the name furodiazole or furadiazole and the position of nitrogen was determined by the symbols α and β' , while the early German literature (1800s) considered the carbon atoms in the nucleus as a part of the substituents. Table. 3.1 Compares the three nomenclature systems.

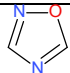
Nomenclature	
German	Dimethenylazoxim
French	α, β' -furadiazole
IUPAC	1,2,4-oxadiazole

Table 3.1: Comparison of three nomenclature systems.

Most of the oxadiazole analogues were synthesised by Tiemann and group. However their work involved synthesis of 3,5 substituted aromatic compounds. It was Barrans in 1959 who first synthesised oxadiazoles with aliphatic substituents (Lenaers et al. (1962)). The 1,2,4-oxadiazole on its own and other mono-substituted oxadiazoles were synthesised in early 1960s (Lenaers et al. (1962), Hellmann

et al. (1961), Moussebois et al. (1962), Eloy et al. (1961)). The 1,2,4-oxadiazole is also well known for its biological activity such as anti asthmatics, anti diabetic, anti inflammatory, anti microbial, anti tumoral and anti mycobacterial.

The following section discusses synthesis of libraries of 1,2,4-triazole and 1,2,4-oxadiazole analogues by attaching the substituents which are known to possess biological activity.

3.2 Lead optimisation

This study is a continuation of the linear and flexible carboxamidrazone compounds synthesised at Aston university as discussed in chapter 2. The structure in Fig. 3.2 shows the modifications made in the original lead compound (see 2.10).

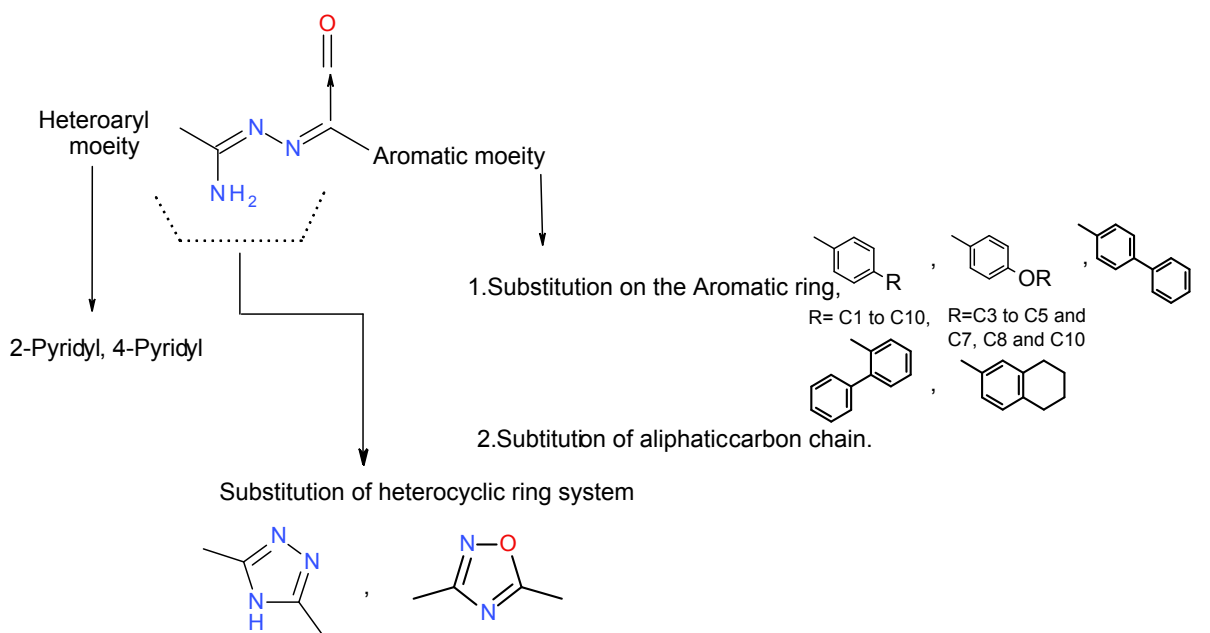


Figure 3.2: Summary of the changes made in this study to the original lead compound.

A series of biologically active carboxamidrazone compounds were synthesised at Aston university, which are linear and flexible. Based on this knowledge some newer carboxamidrazone compounds that are structurally similar were synthesised by building a heterocyclic scaffold in the centre of the active compound's structure. To study this effect a small experiment was carried out using the molecular modelling software 'Cache'. The linear carboxamidrazone amide and a 1,2,4-triazole (cyclised) were modelled using Cache and optimised using MOPAC PM3. The linear and cyclised compounds were superimposed in the Cache to study the effect of different scaffold ring sizes on the relative orientations of the

substituents on the scaffold in comparison to the original linear carboxamidrazones. The computational data revealed that upon cyclisation the structure becomes rigid and all the rings are in the same plane as opposed to the original carboxamidrazone, which has a benzoyl moiety forming an obtuse angle with the pyridine ring. This gave an advantage over the linear structure as the structure became rigid (see Fig. 3.3) and the overall entropy penalty of the compound was decreased, potentially increasing its binding affinity providing the size and shape constraints imposed by the receptor are met.

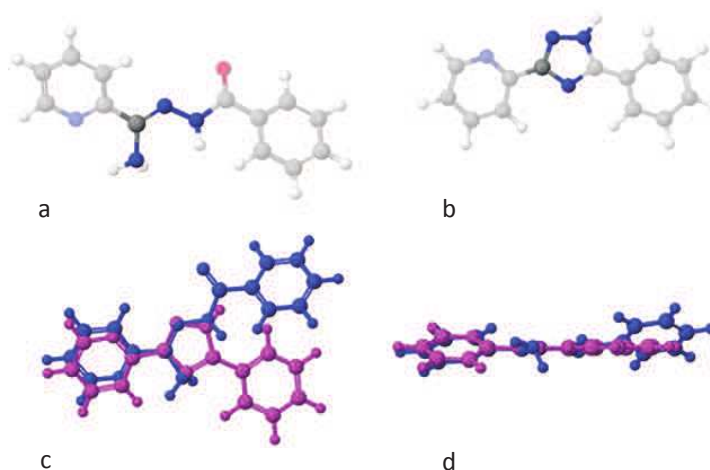


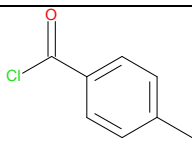
Figure 3.3: Superimposed structures of the linear and cyclised compounds; (a) carboxamidrazone amide; (b) cyclised carboxamidrazone amide; The highlighted atoms were the super-impositioning sites; (c) superimposed; (d) superimposed side view.

3.2.1 Synthesis of the intended triazoles and oxadiazoles

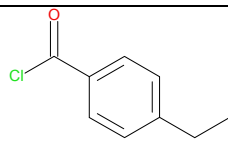
Choosing the Aryl building block

To synthesise a library of 1,2,4-triazole and 1,2,4-oxadiazole compounds, the aryl groups were selected based on the knowledge of the previous research carried out at Aston university.

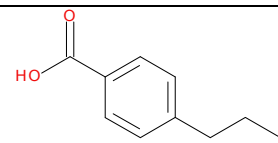
Ren (2009) has shown that the five or six carbon alkyl chain attached at para position of the benzoyl ring is optimum for the activity. Hence the compounds with chain length of one to eight carbons and ten carbons were chosen to complete this matrix. Table. 3.2 lists all the acids and acid chlorides used for synthesis of compound D. Some of the acyclic aliphatic substituents are also used. The past research suggests that 2,4-ditert-butyl-phenol substituent has biological activity. Hence for this study the 2,4-ditert-butyl-phenol and its compounds with similar side chains were used. For this study alkoxy substituted benzoyl groups were also considered, as they are structurally similar to the alkyl substituted benzoyl group.



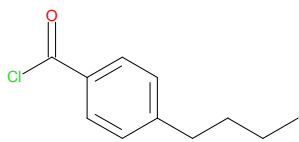
aa



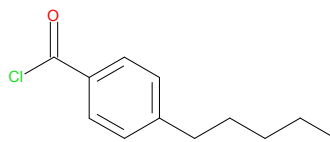
ab



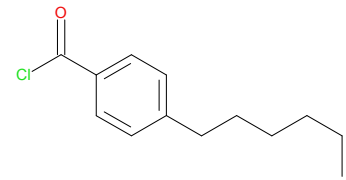
ac



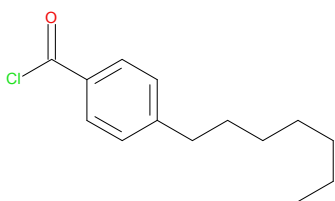
ad



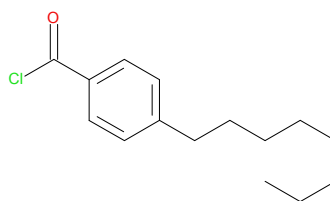
ae



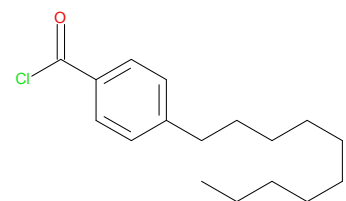
af



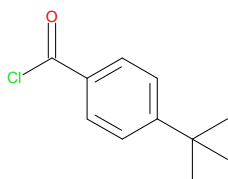
ag



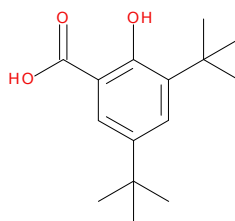
ah



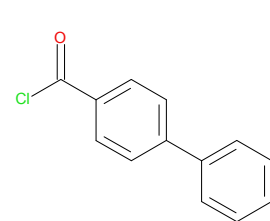
ai



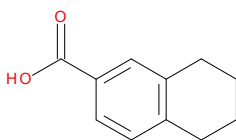
aj



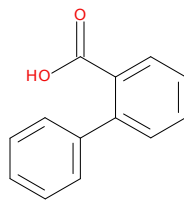
ak



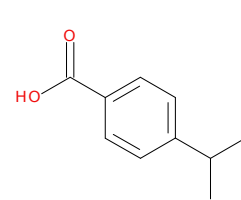
al



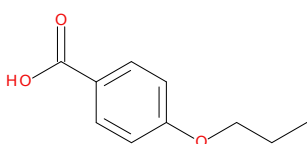
am



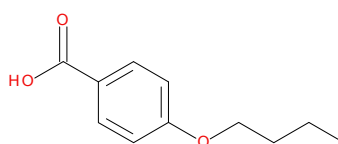
an



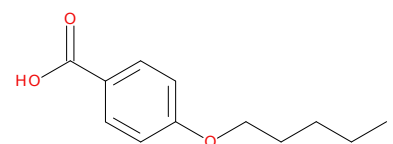
ao



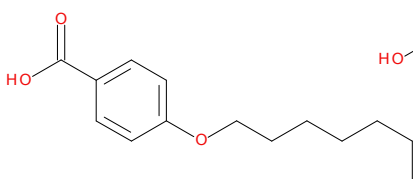
ba



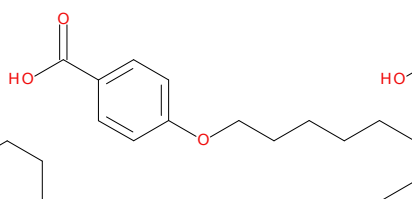
bb



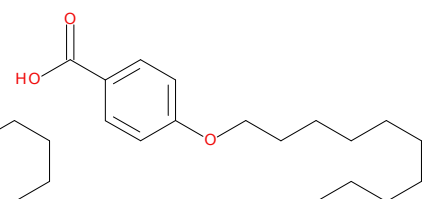
bc



bd



be



bf

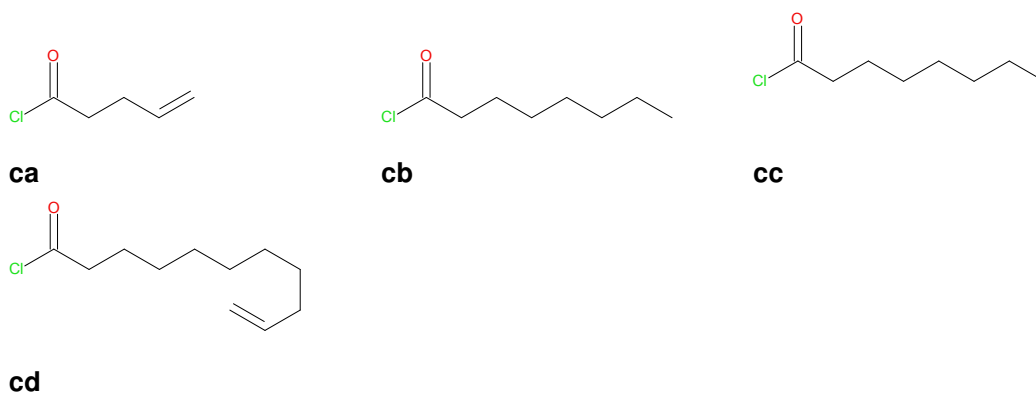


Table 3.2: Acid chlorides and acids used in synthesis of cyclised compounds

Pyridyl building block

Tanaka et al. (1994) and Rathbone et al. (2006) have synthesised various pyridine carboxamidrazones by reacting cyanopyridines with hydrazine and have tested them against *Mycobacterium tuberculosis*. Some of the compounds exhibited antimycobacterial activity. The previous research carried out in Aston university by Tims (2002), Ren (2009), and Sikdar (2010) has shown that 2- and 4- substituted pyridyl carboxamidrazones are the most active and stable pyridyl carboxamidrazones (see chapter 2.3.1). Hence for this study these two pyridyl carboxamidrazones were predominantly used. However other pyridyl groups used were pyridine-*N*-oxides. In the following are the lead compounds of this study:

3.2.2 COMPOUND D (1,2,4-triazole compounds)

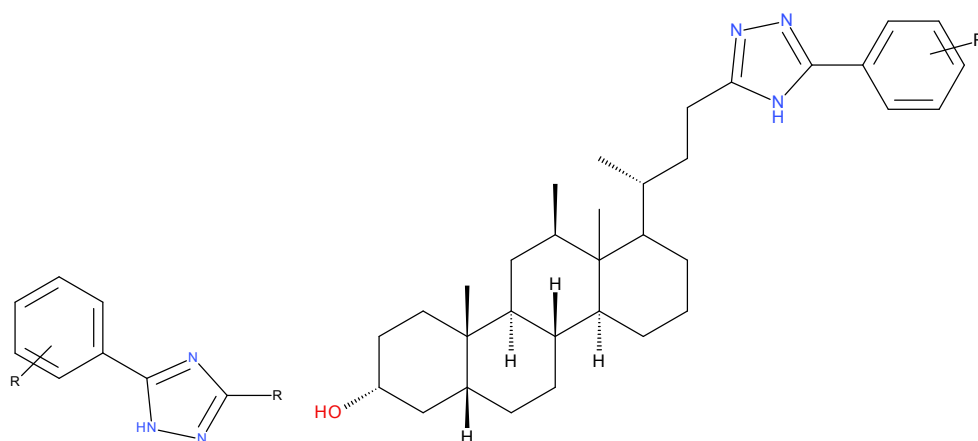


Figure 3.4: General structure of 1,2,4-triazole compounds

This class of compound was synthesised with a view to combine different fragments of known activity like 2 and 4 substituted pyridyl moieties and a benzoyl moiety with an alkyl or fused ring substitution along with the 1,2,4-triazole ring system.

The synthesis of the bile acid related compounds discussed in this chapter is a continuation of the work carried out in chapter 2. This phase two reaction involves cyclisation of the carboxamidrazone amide fragment attached to a bile acid to the 1,2,4-triazole ring.

3.2.3 COMPOUND E (1,2,4-oxadiazole compounds)

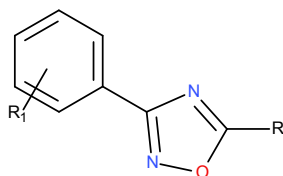


Figure 3.5: General structure of Compound B

The 1,2,4-oxadiazole class of compound was selected as it is known to possess antimycobacterial activity (Kumar et al. (2011)). A library of compounds was synthesised and tested against *Mycobacterium tuberculosis*.

3.2.4 Cyclisation of urea compounds

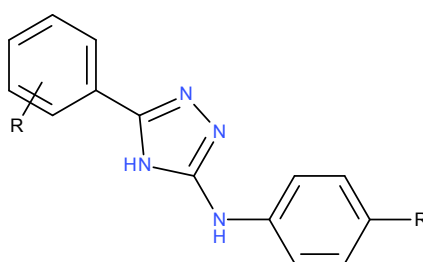


Figure 3.6: General structure of Compound C

This reaction involved cyclisation of the urea carboxamidrazone at high temperature. The linear chain urea carboxamidrazone compounds were found to be generally inactive as mentioned in chapter 2. In an attempt to increase the activity, cyclisation was carried out.

3.2.5 Cyclisation of *N*-oxide compounds

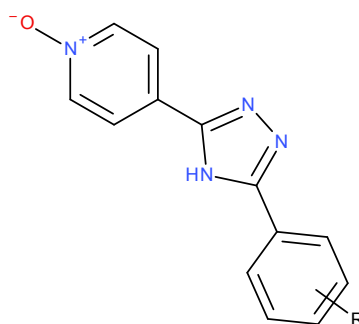


Figure 3.7: General structure of Compound D

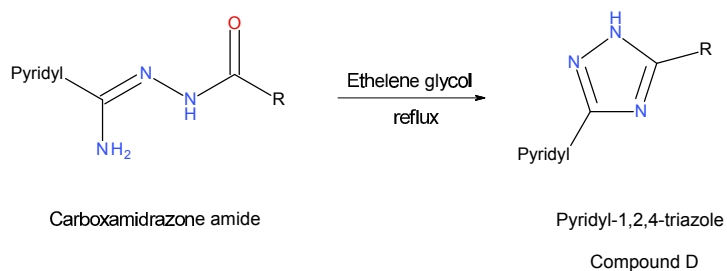
This class of compound was synthesised to study the effect *N*-oxide has on cyclisation chemistry.

3.3 Results and Discussion

3.3.1 COMPOUND D (1,2,4-triazole compounds)

The carboxamidrazone amides were synthesised according to the synthetic pathway depicted in the Scheme. 2.4.1, in accordance with previously reported procedures. Synthesis of the target compounds required a single step reaction where the aryl carboxamidrazone amide was heated at reflux in ethylene glycol for 10-12 hours, as a result carboxamidrazone amide condensed to give 1,2,4, -triazole products (see Scheme. 3.1).

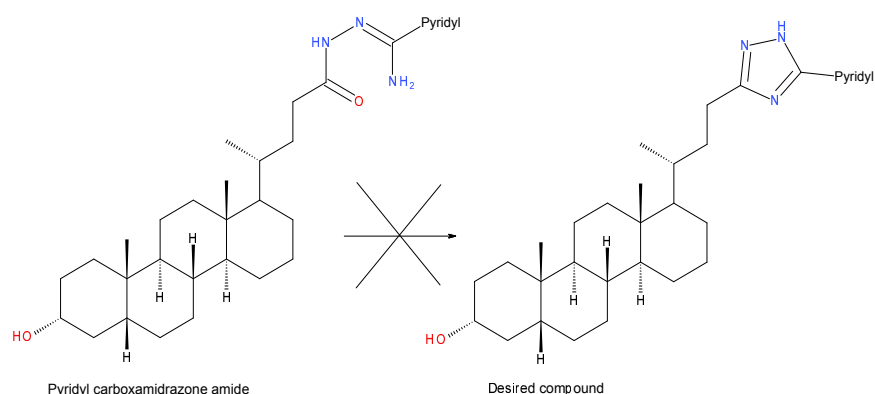
Some of the analogues of carboxamidrazone amides where acid chlorides were unavailable were prepared from acids as discussed in Scheme. 2.4.1 in chapter 2.



Scheme 3.1: Scheme for the synthesis of 1,2,4-triazole compound from condensation of carboxamidrazone amide.

The pyridyl carboxamidrazone 3 α -hydroxy-5 β -cholan-24-oic acid compound was synthesised as dis-

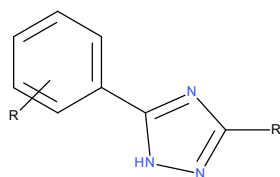
cussed in the Scheme. 2.4.1 in chapter 2. These carboxamidrazone amides on heating at reflux in ethylene glycol for 8 hours' charred. Therefore the reaction time was reduced from 8 to 4 hours with hourly TLC performed to monitor the progress of the reaction. The compound decomposed at the end of 4 hours and a sticky mass was obtained which did not dissolve in either polar or non-polar solvents. The compounds also did not separate into different spots on TLC thus ruling out column chromatography as a method of isolation. The NMR spectrum of the partially soluble portion of the compound in DMSO showed a number of complex peaks, but no significant structure could be elucidated.



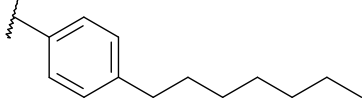
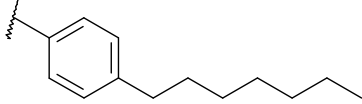
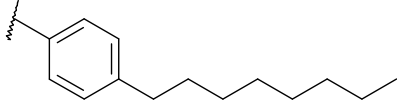
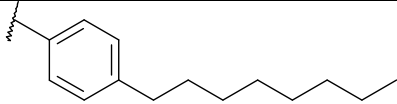
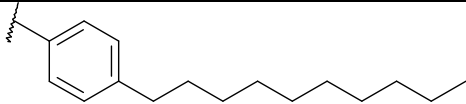
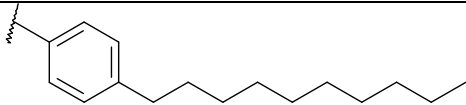
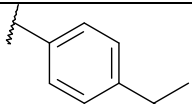
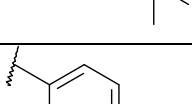
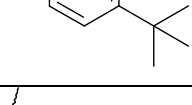
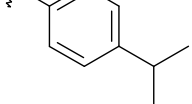
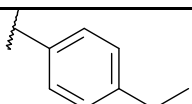
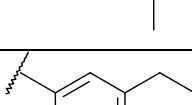
Scheme 3.2: Scheme for the attempted synthesis of 1,2,4-triazole compound from condensation of bile acid related carboxamidrazone amide.

All the compounds were characterised by their melting points and spectral data (^1H NMR, IR and MS). The IR spectrum shows a characteristic peak of 1,2,4, -triazole compound (C=N) at $1640 - 1560\text{ cm}^{-1}$ (Curtis & Jennings (2008)). The absence of the NH bond in NMR spectrum in the region of 9 to 10 ppm as seen in the parent carboxamidrazone amide NMR spectrum and the absence of the broad carbonyl peak in IR spectrum in the range of $1665 - 1760\text{ cm}^{-1}$ suggests the complete conversion of the carboxamidrazone amide to carboxamidrazone 1,2,4-triazole compound. According to Curtis & Jennings (2008), the 1,2,4-triazole shows an additional N=N peak at $1570 - 1550\text{ cm}^{-1}$, however it was observed that the IR spectrum had many smaller insignificant peaks which made it difficult to identify the compound structure. To confirm whether the structure has an exchangeable hydrogen bond attached to one of the nitrogens in the ring or to the triazole carbon, an experiment was conducted. A D_2O shake NMR was obtained to see if the peak observed in the range of 5 to 6 ppm disappears. The absence of the peak confirmed that it was an exchangeable hydrogen bond attached to nitrogen. These results were in agreement with the results obtained by Nagahara & Takada (1982).

Table. 3.3 lists the analogues of the final product compound D shown in Fig. 3.1 synthesised along with their yields and melting points.



Compound number	Pyridyl	Aryl group	Yield (%)	Melting point (°C)
(89)	2-Pyridyl		72.3	143.0 – 144.2
(90)	4-Pyridyl		71.2	229.1 – 231.3
(91)	2-Pyridyl		64.4	176.9 – 178.9
(92)	4-Pyridyl		69.2	219.5 – 221.2
(93)	2-Pyridyl		24.4	–
(94)	4-Pyridyl		64	202.2 – 203.9
(95)	2-Pyridyl		67.1	148.7 – 150.3
(96)	4-Pyridyl		61.3	183.5 – 185.2
(97)	2-Pyridyl		73.2	130.4 – 131.6
(98)	4-Pyridyl		58.2	171.8 – 172.7
(99)	2-Pyridyl		47.2	128.4 – 129.5
(100)	4-Pyridyl		49.3	156.1 – 157.0

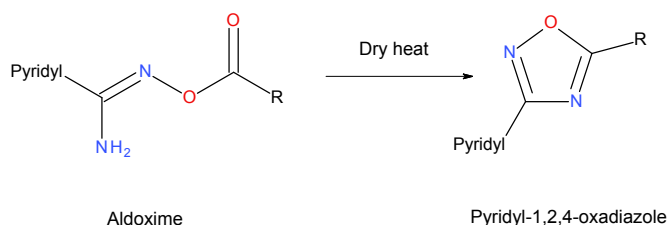
Compound number	Pyridyl	Aryl group	Yield (%)	Melting point (°C)
(101)	2-Pyridyl		57.1	113.0 – 114.9
(102)	4-Pyridyl		71	142.8 – 144.2
(103)	2-Pyridyl		71.4	121.8 – 123.9
(104)	4-Pyridyl		65.2	143.1 – 144.6
(105)	2-Pyridyl		75.3	104.8 – 105.9
(106)	4-Pyridyl		78.3	154.4 – 155.7
(107)	2-Pyridyl		67.2	178.3 – 180.7
(108)	4-Pyridyl		64.4	253.9 – 255.2
(109)	2-Pyridyl		23.1	–
(110)	4-Pyridyl		65.2	218.2 – 219.6
(111)	2-Pyridyl		32	212.5 – 213.3
(112)	4-Pyridyl		47.2	277.6 – 278.8

Compound number	Pyridyl	Aryl group	Yield (%)	Melting point (°C)
(113)	2-Pyridyl		28.1	—
(114)	4-Pyridyl		37.4	288.1 – 292.3
(115)	2-Pyridyl		74.2	217.5 – 219.5
(116)	4-Pyridyl		82.3	287.1 – 291.3
(117)	2-Pyridyl		61	157.9 – 161.0
(118)	4-Pyridyl		58.3	192.4 – 193.1
(119)	2-Pyridyl		67.2	151.2 – 152.6
(120)	4-Pyridyl		78.4	177.3 – 179.2
(121)	2-Pyridyl		63	124.3 – 125.9
(122)	2-Pyridyl		68	163.3 – 164.5
(123)	4-Pyridyl		46	154.3 – 155.1

Compound number	Pyridyl	Aryl group	Yield (%)	Melting point (°C)
(124)	4-Pyridyl		75.4	167.8 – 168.5
(125)	2-Pyridyl		62.1	181.8 – 182.6
(126)	4-Pyridyl		57.1	143.2 – 144.4
(127)	2-Pyridyl		20.3	—
(128)	2-Pyridyl		33.1	49.1 – 50.7
(129)	4-Pyridyl		62.4	104.2 – 106.8
(130)	2-Pyridyl		69	65.9 – 67.1
(131)	4-Pyridyl		73.3	101.2 – 103.3
(132)	2-Pyridyl		27.2	—
(133)	4-Pyridyl		46.4	87.3 – 88.4

Table 3.3: List of analogues of compound D

3.3.2 COMPOUND E (1,2,4-oxadiazole compounds)



Scheme 3.3: Scheme for the synthesis of 1,2,4-oxadiazole compound from condensation of aldoxime.

The dehydration of the acyl derivatives of the aldoximes facilitates the easy formation of 1,2,4-oxadiazole. Eloy et al. (1961) suggested various methods for dehydration of the aldoximes which involves heating the compounds in water, dilute NaOH, glacial acetic acid, acetic anhydride, H₂SO₄ or in a dry state. The authors observed that if acylation of aldoxime is carried out at 100 °C or above, cyclisation occurs (Eloy

et al. (1961)).

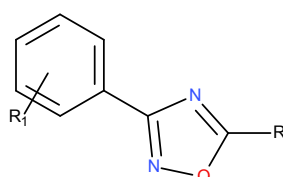
The N'-[(alkyl)oxy]pyridyl carboximidamide (compound B) were synthesised from aldoximes as discussed in Scheme. 2.4 in chapter 2. The compound B was heated in water at reflux for 4 hours to allow the dehydration. However the reaction did not go to the completion, although a hint of the product was observed by TLC. This reaction was optimised by increasing the reaction time to 12 hours and to the 10 mL solution of aldoxime in water, 5 mL of acetonitrile was added to completely dissolve the sample, yet the cyclisation was not completed. Similarly, on heating the aldoximes in DMSO at reflux, the reaction did not go to completion.

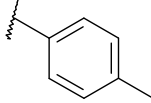
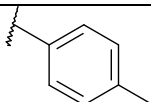
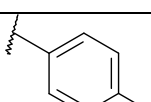
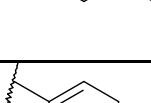
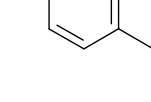
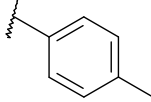
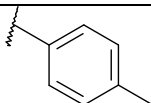
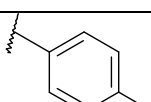
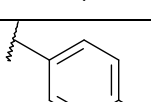
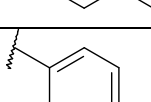
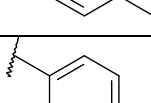
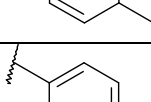
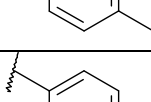
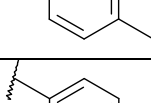
The compound B was then subjected to the ethylene glycol reaction as discussed in the Scheme. 3.1. Ethylene glycol boils at 197.3 °C which is much higher than the required temperature to induce cyclisation in aldoximes and their derivatives. The compound B when heated at reflux in ethylene glycol for 4 hours causes the compound to decompose and char.

The next reaction involved dry heating of the compound B in a borosilicate glass vessel at 150°C, for 30 mins. The dry powder melted and upon slow cooling to room temperature the desired 1,2,4, -oxadiazole product precipitated out which was be isolated by recrystallisation techniques (see Scheme. 3.3).

Some analogues of compound B where acid chlorides were unavailable were prepared from acids as discussed in Scheme. 2.5 in chapter 2.

The analytical data, namely, mass spectrum, NMR, and IR were found to be consistent with the proposed structure. The IR spectrum shows the characteristic peaks of 1,2,4, oxadiazole compound at (C=N) at 1598 – 1592 cm^{-1} , (C-O) at 1218 – 1119 cm^{-1} and (N-O) at 913 – 904 cm^{-1} as observed by Hemming (2008). The absence of the broad carbonyl peak in IR spectrum in the range of 1665 – 1760 cm^{-1} suggests the complete conversion of the aldoxime to 1,2,4-oxadiazole compound. The data obtained from NMR spectrum suggests that the NH_2 peak present in the parent compound was found to be absent in the product. Table 3.4 lists the analogues of the final product compound E shown in Fig. 3.3 synthesised along with their yields and melting points.



Compound number	Pyridyl	Aryl group	Yield (%)	Melting point (°C)
(134)	2-Pyridyl		75.1	167.8 – 168.5
(135)	4-Pyridyl		68.1	181.8 – 182.6
(136)	2-Pyridyl		71.3	143.2 – 144.4
(137)	4-Pyridyl		47.2	127.8 – 129.3
(138)	2-Pyridyl		46.3	154.3 – 155.1
(139)	4-Pyridyl		81.8	121.3 – 122.9
(140)	2-Pyridyl		63.1	156.3 – 157.7
(141)	4-Pyridyl		78	147.3 – 148.6
(142)	2-Pyridyl		75.3	165.2 – 166.8
(143)	4-Pyridyl		61.7	139.7 – 140.2
(144)	2-Pyridyl		57.6	138.8 – 139.5
(145)	4-Pyridyl		71.4	135.4 – 136.9
(146)	2-Pyridyl		64.2	135.3 – 136.5
(147)	4-Pyridyl		68.5	151.6 – 152.9

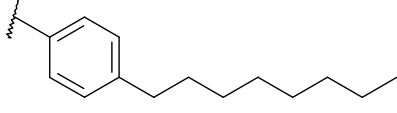
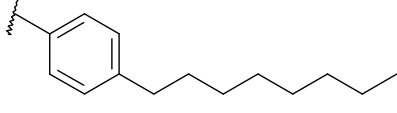
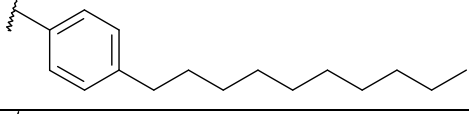
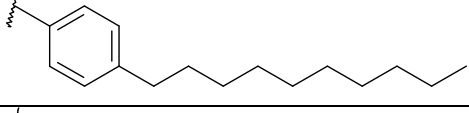
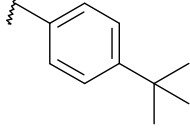
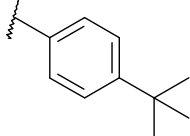
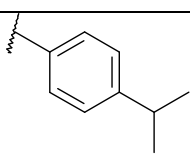
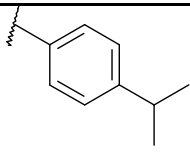
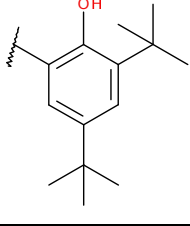
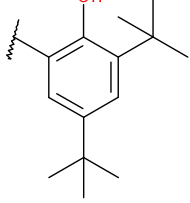
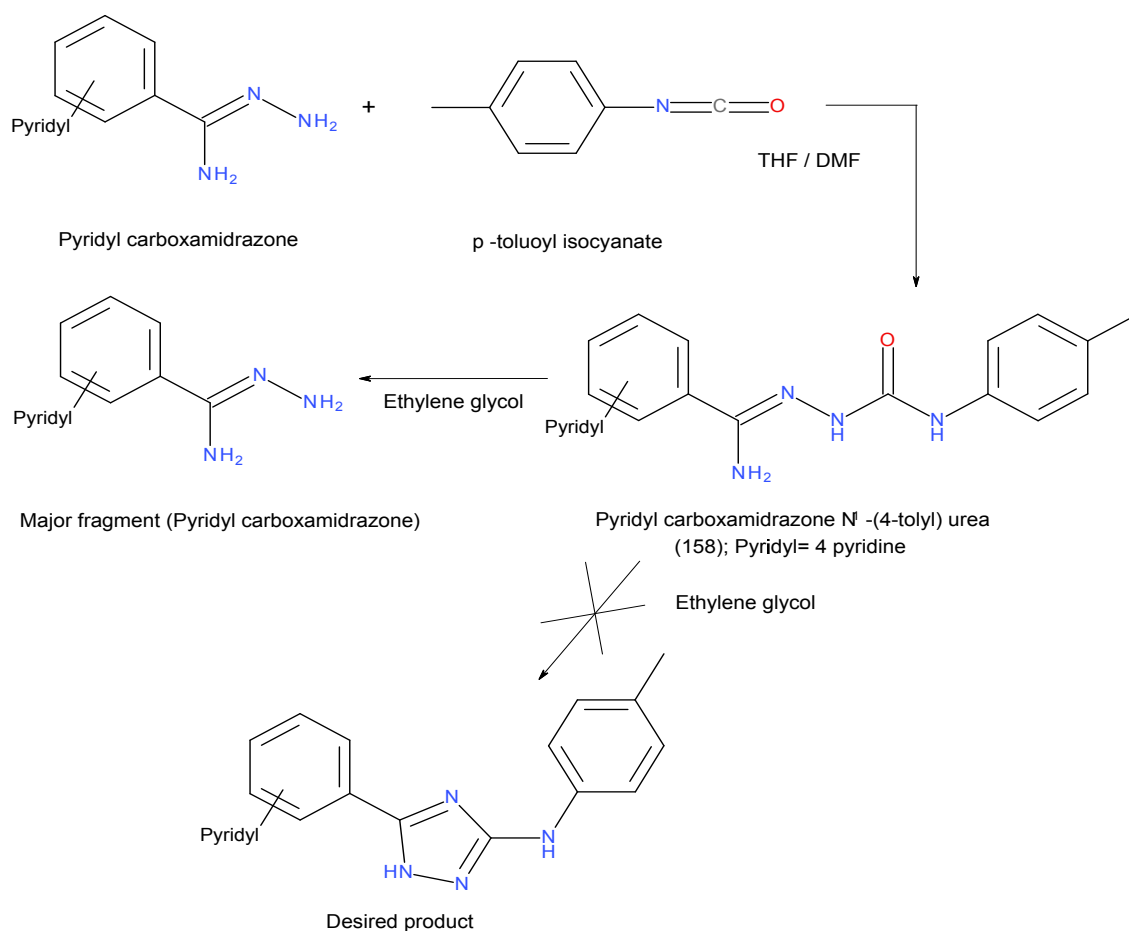
Compound number	Pyridyl	Aryl group	Yield (%)	Melting point (°C)
(148)	2-Pyridyl		58	135.4 – 137.3
(149)	4-Pyridyl		49.4	129.4 – 130.8
(150)	2-Pyridyl		64.3	156.7 – 159.1
(151)	4-Pyridyl		65	156.9 – 157.9
(152)	2-Pyridyl		56.2	187.4 – 188.8
(153)	4-Pyridyl		65.2	168.1 – 169.4
(154)	2-Pyridyl		68.4	154.5 – 155.8
(155)	4-Pyridyl		63.4	153.8 – 155.2
(156)	2-Pyridyl		59.4	166.8 – 170.2
(157)	4-Pyridyl		61.3	176.8 – 177.9

Table 3.4: List of analogues of compound E

3.3.3 Attempted cyclisation of carboxamidrazone urea compounds



Scheme 3.4: Scheme for the cyclisation of urea derivative of carboxamidrazone amides.

The carboxamidrazone urea compounds were generally found to be inactive, hence an attempt was made to cyclise these compounds in order to increase their activity. Pyridine-4-carboxamidrazone N¹-(4-tolyl)urea was synthesised by reacting 4-pyridyl carboxamidrazone with *p*-toluoyl isocyanate in DMF and THF. The crude product was purified by recrystallisation using ethanol. The pure product obtained was then heated at reflux in ethylene glycol for 8 hours. The product obtained was charred. Hence the reaction time was reduced from 8 to 3 hours with an hourly TLC check performed to monitor the completion of the reaction. However at the end of 3 hours the compound disintegrated into fragments, major fragment identified was the starting material 4-pyridyl carboxamidrazone. At the high temperature of the attempted cyclisation reactions, the carboxamidrazone urea fragmented to regenerate the carboxamidrazone.

Another reaction was carried out with fluorine substituted isocyanate to study the effect an electron withdrawing group has on the cyclisation reaction. However the compound disintegrated and similar

fragments of starting material were observed as in the previous reaction.

3.3.4 Cyclisation of *N*-oxide compounds

The *N*-oxide carboxamidrazone amide was obtained from the Aston university laboratory which was synthesised by Khan (2008). In an attempt to cyclise, the compound was heated at reflux in ethylene glycol. The crude product obtained contained hints of possibly the desired product along with starting material, which was observed by two separate but closely placed spots on TLC that could not be separated using column techniques. Recrystallisation techniques also failed to isolate a single product.

In order to ascertain if the positive charge on the pyridyl nitrogen was the potential reason for the failure of the carboxamidrazone *N*-oxide to cyclise, another experiment was conducted in parallel to this experiment as a control where 4-pyridyl substituted aldoxime compound synthesised was treated with methyl iodide in DCM. The product obtained was then taken for the next step of cyclisation. As expected the compound did not cyclise and the starting material was recovered. It was also observed that 2-pyridyl substituted aldoxime did not react with methyl iodide.

3.3.5 Purity

The 2 and 4 substituted pyridine carboxamidrazones, both the starting materials for the preparation of linear carboxamidrazone amide were clean and did not require further purification. The crude linear carboxamidrazone amides were found to possess impurities and the pure compound was isolated by recrystallisation techniques. Most of the 1,2,4-triazole compounds obtained by cyclisation of these linear carboxamidrazones were found to be clean, however some compounds were isolated by recrystallisation.

Both the 2 and 4 substituted pyridyl aldoxime starting materials for *N*'-[(alkyl)oxy]pyridyl carboximidamide were found to be clean and in crystalline form. The aldoxime derivatives were generally pure, however some of the compounds required purification. The 1,2,4-oxadiazole compounds obtained from cyclisation of the linear *N*'-[(alkyl)oxy]pyridyl carboximidamide were contaminated with some impurities and were cleaned up using recrystallisation techniques.

3.3.6 Solubility

The 2-pyridyl and 4-pyridyl carboxamidrazone amides were readily soluble in hot ethylene glycol.

3.3.7 NMR Data

The proton NMR spectra of the 1,2,4-triazole compounds were obtained from d_6 -DMSO and were consistent with the proposed structures. The characteristic amide singlet peak from the carboxamidrazone amide compounds which was observed in the range of 10 – 10.5 ppm, was absent indicating completion of the reaction. In many of the triazole compounds, an extra set of smaller peaks were seen in the range of 5 – 6 ppm alongside the triazole -NH peak on the NMR spectrum. This is observed since the compound exists in two forms (see Fig. 3.8). At a higher temperature (50°C) the two peaks merge into a single peak. This phenomenon occurs since the rate of interconversion of the two forms of compound are less than the frequency of the NMR machine. At high temperature the rate is increased and an average structure is obtained. Hence at high temperature the two singlets merge into one (see Fig. 3.10).

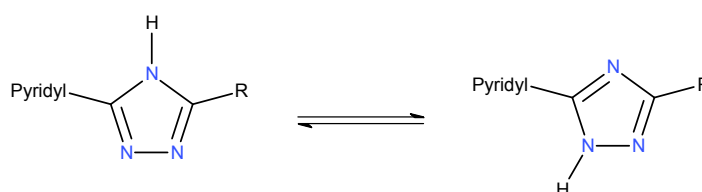


Figure 3.8: The two form of 1,2,4-triazole compound



Figure 3.9: Structure of 2-[5-(4-butoxyphenyl)-1H-1,2,4-triazol-3-yl]pyridine

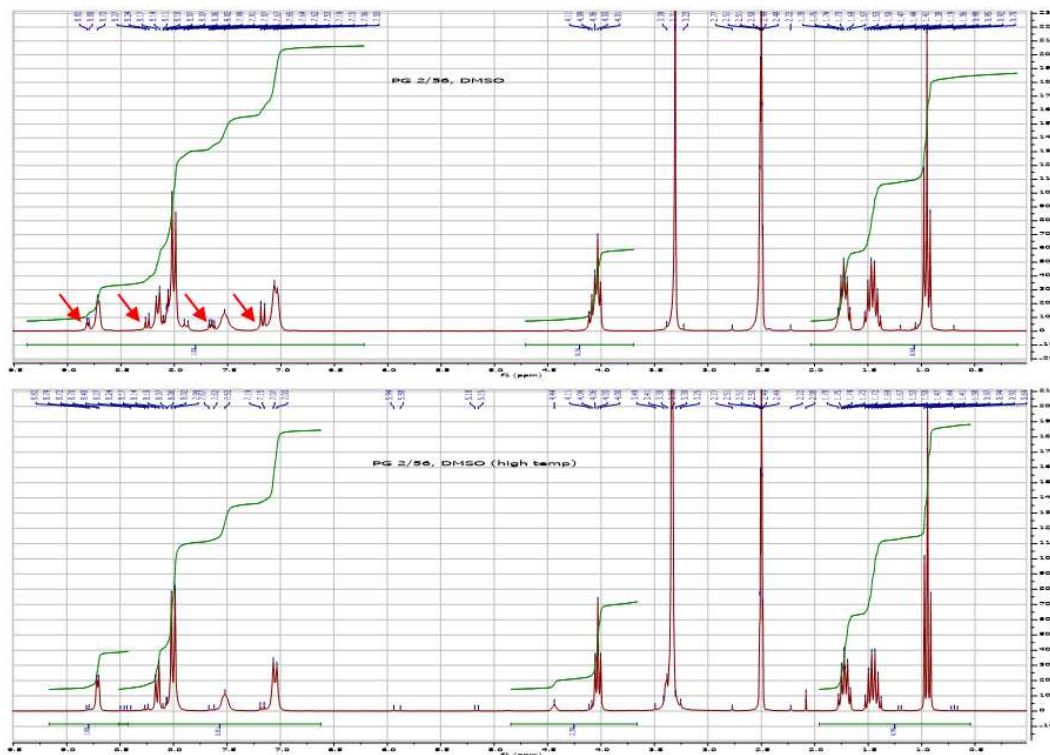


Figure 3.10: A comparison of NMR spectra representing two forms of 2-[5-(4-butoxyphenyl)-1H-1,2,4-triazol-3-yl]pyridine.

3.3.8 Melting point data

The melting points of the compounds show a similar pattern as observed in section 2.4.7 in chapter 2. As the chain length of the benzoyl substituent increases, the melting point increases due to the organisation of the crystal structure of the molecule and the surface area.

However there are exceptions to this rule, as in the case of (155) which has a higher mp than the (151) where more rigid tert-butyl group present in the compound (155) may pack better in the crystal than compound (151) with the longer and more flexible chain.

3.3.9 Microbiological results

The analogues of both the triazoles and oxadiazoles were sent to the National Institute of Allergy and Infectious Diseases (NIAID, US) for screening against *Mycobacterium tuberculosis*. As discussed in 2.4.8 in chapter 2 these compound libraries were subjected to high throughput screening (HTS) process. This process involves two stages: in the first stage, MABA and BTG assay are carried out in parallel on H37Rv strain to determine the MIC, IC₅₀ and IC₉₀ concentration for the compounds. The compounds which have MIC values of 32.47 μM or less are further taken to the second stage which involves advanced anti mycobacterial susceptibility profiling (see 2.4.8) in chapter 2. The table gives the results obtained from NIAID.

Compound number	Activity	MIC (μM)	IC ₅₀ (μM)	IC ₉₀ (μM)
(111)	Active	16.24	14.71	15.68
(95)	Active	32.47	19.38	22.14
(120)	Weakly active	32.47	15.81	17.47
(117)	Weakly active	32.47	27.08	28.83
(124)	Weakly active	32.47	17.27	19.38
(89)	Inactive	>32.47	—	—
(90)	Inactive	>32.47	—	—
(91)	Inactive	>32.47	—	—
(92)	Inactive	>32.47	—	—
(93)	Inactive	>32.47	—	—
(94)	Inactive	>32.47	—	—

Compound number	Activity	MIC (μM)	IC₅₀ (μM)	IC₉₀ (μM)
(96)	Inactive	>32.47	—	—
(97)	Inactive	>32.47	—	—
(98)	Inactive	>32.47	—	—
(99)	Inactive	>32.47	—	—
(100)	Inactive	>32.47	—	—
(101)	Inactive	>32.47	—	—
(102)	Inactive	>32.47	—	—
(103)	Inactive	>32.47	—	—
(104)	Inactive	>32.47	—	—
(105)	Inactive	>32.47	—	—
(106)	Inactive	>32.47	—	—
(107)	Inactive	>32.47	—	—
(108)	Inactive	>32.47	—	—
(109)	Inactive	>32.47	—	—
(110)	Inactive	>32.47	—	—
(112)	Inactive	>32.47	—	—
(113)	Inactive	>32.47	—	—
(114)	Inactive	>32.47	—	—
(115)	Inactive	>32.47	—	—
(116)	Inactive	>32.47	—	—
(118)	Inactive	>32.47	—	—
(119)	Inactive	>32.47	—	—
(121)	Inactive	>32.47	—	—
(122)	Inactive	>32.47	—	—
(123)	Inactive	>32.47	—	—
(125)	Inactive	>32.47	—	—
(126)	Inactive	>32.47	—	—
(127)	Inactive	>32.47	—	—
(128)	Inactive	>32.47	—	—
(129)	Inactive	>32.47	—	—

Compound number	Activity	MIC (μM)	IC ₅₀ (μM)	IC ₉₀ (μM)
(130)	Inactive	>32.47	—	—
(131)	Inactive	>32.47	—	—
(132)	Inactive	>32.47	—	—
(133)	Inactive	>32.47	—	—

Table 3.5: The IC₅₀ and IC₉₀ values of the triazole compounds when tested against *Mycobacterium tuberculosis* at the NIAID

The NIAID calculated the IC₅₀ and IC₉₀ values of the compounds having the MIC value less than or equal to 32.47 μM .

The table 3.6 gives the microbiological results of oxadiazole compounds obtained from NIAID, US.

Compound number	Activity	MIC (μM)	IC ₅₀ (μM)	IC ₉₀ (μM)
(153)	Active	50.00	38.55	45.62
(146)	Active	50.00	26.38	47.99
(144)	Weakly active	100.00	47.22	59.75
(142)	Weakly active	100.00	49.70	72.33
(136)	Weakly active	100.00	65.57	93.99
(137)	Weakly active	100.00	67.18	89.18
(140)	Inactive	NA	70.50	>100.00
(150)	Inactive	NA	23.39	>100.00
(148)	Inactive	NA	23.38	>100.00
(138)	Inactive	NA	90.83	>100.00
(134)	Inactive	NA	>100.00	>100.00
(135)	Inactive	NA	>100.00	>100.00
(139)	Inactive	NA	>100.00	>100.00
(141)	Inactive	NA	>100.00	>100.00
(143)	Inactive	NA	>100.00	>100.00
(145)	Inactive	NA	>100.00	>100.00
(147)	Inactive	NA	>100.00	>100.00
(149)	Inactive	NA	>100.00	>100.00

Compound number	Activity	MIC (μM)	IC ₅₀ (μM)	IC ₉₀ (μM)
(151)	Inactive	NA	>100.00	>100.00
(152)	Inactive	NA	>100.00	>100.00
(154)	Inactive	NA	>100.00	>100.00
(155)	Inactive	NA	>100.00	>100.00
(156)	Inactive	NA	>100.00	>100.00
(157)	Inactive	NA	>100.00	>100.00

Table 3.6: The MIC, IC₅₀ and IC₉₀ values of the oxadiazole compounds when tested against *Mycobacterium tuberculosis* at the NIAID

3.3.10 Structure activity relationship

The 2-pyridyl compounds were generally more active than the 4-pyridyl compounds. Upon cyclisation of these carboxamidrazones to 1,2,4-triazoles and 1,2,4-oxadiazoles, a small number of the compounds retained their activity while in most of the remaining compounds the activity was diminished. This might be attributed to the significant increase in logP value caused by cyclisation of these linear carboxamidrazones amides, resulting in high lipophilicity and decreased cell permeability. Another reason might be that the rigidity conferred upon the compound due to cyclisation, results in failure of the compound to fit into the active site of the putative target enzyme. A direct correlation between the logP values and activity could be made based on the concept of 'sweet spot' as defined in the molecular mass-logP space (Hann & Keserü (2012)) (see Fig. 3.11).

The results obtained are in agreement with the Lipinski's rule of five. The compounds in general passed the first three rules: molecular weight (MW) < 500, number of hydrogen bond donors (HBD) < 5 and number of hydrogen bond acceptors (HBA) < 10. But many compounds failed the last octanol-water partition coefficient (ALOGP) criterion. The compounds which have the least activity have higher logP values.

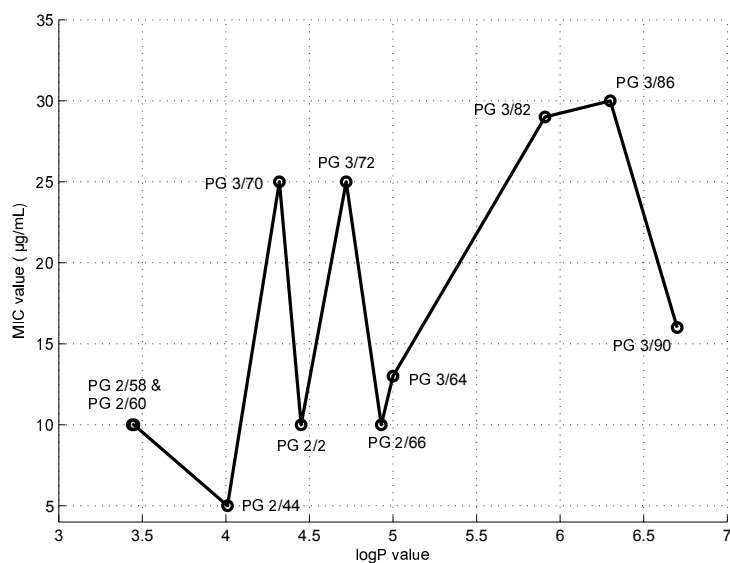


Figure 3.11: MIC value as a function of logP

3.4 Summary and Conclusion

The incorporation of 1,2,4 substituted triazole and oxadiazole rings has not resulted in the desired improvement in the activity. For the future work other 5 and 6 membered cyclic structures can be synthesised like 2-aminothiazoles, oxadiazolythio, thiazolythio and triazolythio. Some compounds which are structurally similar to cyclised carboxamidrazones, with the above mentioned rings have been shown to possess activity against *M. tuberculosis* H37Rv strain (Ananthan et al. (2009)).

3.5 EXPERIMENTAL

3.5.1 Chemicals

All the chemicals and solvents were used as supplied. 2-pyridine cyanide, 4-pyridine cyanide, N, N'-carbonyl di-imidazole, hydrazine, hydroxylamine, Hüinig's base, DMSO, and all the acids and acid chlorides were purchased from Sigma Aldrich. The organic solvents used were purchased from Fisher Chemicals. An aluminium silica gel 60 F254 plates (Merck) were used for thin layer chromatography (TLC).

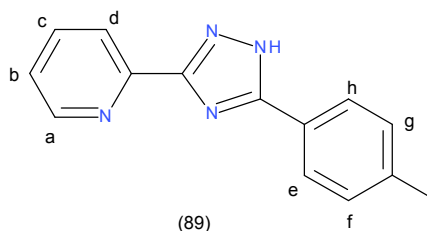
3.5.2 Instrumentation

Proton NMR spectra were obtained on a Bruker AC 250 instrument operation at 250MHz as solutions in d_6 -DMSO or $CDCl_3$ and referenced from δ DMSO=2.50ppm or δ CDCl₃=7.27ppm unless otherwise stated. Infrared spectra were recorded as KBr discs on a Mattson 3000 FTIR spectrophotometer and neat on Nicolet iS5 RT-IR instrument + ID5 ATR Diamond Sampler holder accessory. (APCI-MS) was carried out on a Hewlett-Packard 5989B quadruple instrument connected to an electrospray 59987A unit with an APCI accessory and automatic injecting using a Hewlett-Packard 1100 series autosampler. Accurate MS was carried out on TOF mass spectra (ESI mode) measured on a Waters LCT Premier Mass Spectrometer. Some of the compounds were sent to EPSRC Mass Spectrometry Service Centre at Swansea, the compounds were tested on either of the following machines Thermofisher LTQ Orbitrap XL, Finnigan MAT 95 XP, Applied Biosystems Voyager DE-STR, Waters Micromass ZQ4000, Thermofisher DSQ-II, Agilent 5975 GCMS. Melting points were recorded on a Reichert-Jung Thermo Galen hot stage microscope and were corrected.

3.5.3 General procedure for synthesis of 1,2,4-triazole from carboxamidrazone amide

The carboxamidrazone amide (0.5 g) was heated in ethylene glycol (4 mL) at reflux for 10-12 hours. This reaction mixture was then added to ice cold water and crude product was precipitated. The crude product was further purified by recrystallisation using appropriate solvent systems (water to methanol).

2-[5-(p-Tolyl)-1H-1,2,4-triazol-3-yl]pyridine (89)



$^1\text{H NMR}$ ($\text{d}_6\text{-DMSO}$): 8.71 (d, 1H, $J = 4.7$ Hz, **-a**), 8.16 (d, 2H, $J = 7.9$ Hz, **-e and h**), 7.99 (d, 2H, $J = 8.1$ Hz, **-b and d**), 7.89 (d, $J = 8.2$ Hz, 3H, **-c, f and g**), 4.27 (s, 1H, **triazole -NH**), 2.38 (s, 3H, **CH₃**) ppm.

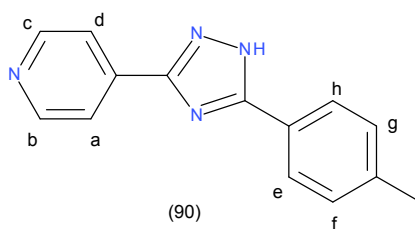
IR (neat) ν : 3035 (Aromatic C-H), 2919, 2841 (Alkyl C-H), 1713, 1599, 1570 (C=N), 1563 (N=N), 1458, 1411, 1372, 1273, 1178, 1149, 1112, 1021, 1008 cm^{-1} .

Melting point: 143.0 – 144.2 °C.

Mass spectrum (APCI +) m/z: Found 236.1053 ($\text{M}+\text{H}$)⁺; calculated for $\text{C}_{14}\text{H}_{12}\text{N}_4$ 236.1061; 3.3 ppm.

Yield: 0.37 g, 72.3%.

4-[5-(p-Tolyl)-1H-1,2,4-triazol-3-yl]pyridine (90)



$^1\text{H NMR}$ ($\text{d}_6\text{-DMSO}$): 8.71 (dd, 2H, $J = 4.5, 1.6$ Hz, **-b and c**), 8.02 – 7.93 (overlapping m, 4H, **-a, d, e and h**), 7.37 (d, 2H, $J = 7.9$ Hz, **-f and g**), 4.28 (s, 1H, **triazole -NH**), 2.39 (s, 3H, **CH₃**) ppm.

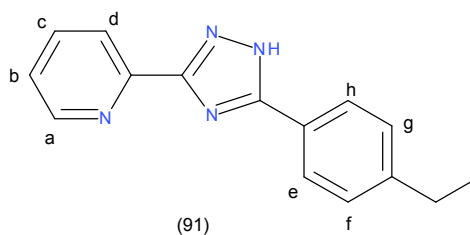
IR (neat) ν : 3104, 3046 (Aromatic C-H), 2936 (Alkyl C-H), 2877 (Alkyl C-H), 2792, 1643, 1609 (C=N), 1572, 1547 (N=N), 1507, 1456, 1423, 1386, 1334, 1297, 1218, 1190, 1177, 1144, 1085, 1068, 1038, 1019, 1002 cm^{-1} .

Melting point: 229.1 – 231.3 °C.

Mass spectrum(APCI +) m/z: Found 236.1100 (M+H)⁺; calculated for C₁₄H₁₂N₄ 236.1061; 16.5 ppm.

Yield: 0.4 g, 71.2%.

2-[5-(4-Ethylphenyl)-1H-1,2,4-triazol-3-yl]pyridine (91)



¹H NMR (d₆-DMSO): 8.60 (d, 1H, J = 4.7 Hz, **-a**), 8.27 (d, 2H, J = 7.9 Hz, **-e and h**), 8.05 (d, 2H, J = 8.1 Hz, **-b and d**), 7.84 (d, J = 8.2 Hz, 3H, **-c, f and g**), 4.46 (s, 1H, **triazole -NH**), 2.64 (q, 2H, J = 7.6 Hz, **-CH₂CH₃**), 1.22 (t, 3H, J = 6.5 Hz, **-CH₂CH₃**)ppm.

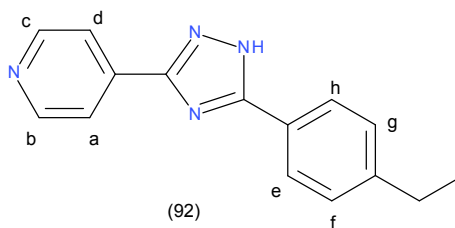
IR (neat) ν : 3028 (Aromatic C-H), 2958 (Alkyl C-H), 1651, 1599 (C=N), 1571, 1554 (N=N), 1478, 1460, 1416, 1372, 1311, 1290, 1180, 1147, 1110, 1062, 1009 cm⁻¹.

Melting point: 176.9 – 178.9 °C.

Mass spectrum(APCI +) m/z: Found 250.1198 (M+H)⁺; calculated for C₁₅H₁₄N₄ 250.1218; 7.9 ppm.

Yield: 0.33 g, 64.4%.

4-[5-(4-Ethylphenyl)-1H-1,2,4-triazol-3-yl]pyridine (92)



¹H NMR (d₆-DMSO): 8.71 (dd, 2H, J = 4.5, 1.6 Hz, **-b and c**), 8.04 – 7.95 (overlapping m, 4H, **-a, d, e and h**), 7.40 (d, 2H, J = 8.4 Hz, **-f and g**), 4.25 (s, 1H, **triazole -NH**), 2.70 (q, 2H, J = 7.6 Hz, **-CH₂CH₃**), 1.24 (t, 3H, J = 6.5 Hz, **-CH₂CH₃**) ppm.

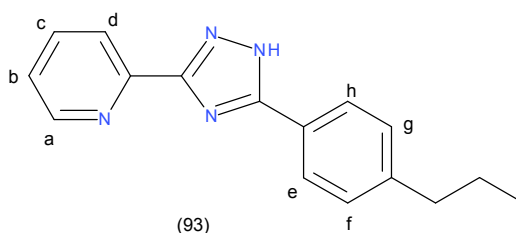
IR (neat) ν : 3105, 3042 (Aromatic C-H), 2961, 2871 (Alkyl C-H), 2759, 1715, 1611 (C=N), 1547 (N=N), 1509, 1446, 1422, 1413, 1385, 1213, 1175, 1139, 1062, 1021, 1003 cm⁻¹.

Melting point: 219.5 – 221.2 °C.

Mass spectrum(APCI +) m/z: Found 250.1301 (M+H)⁺; calculated for C₁₅H₁₄N₄ 250.1218; 6.7 ppm.

Yield: 0.34 g, 69.2%.

2-[5-(4-Propylphenyl)-1H-1,2,4-triazol-3-yl]pyridine (93)



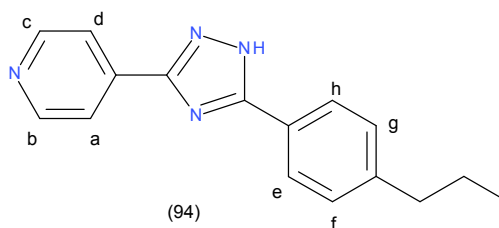
¹H NMR (d₆-DMSO): 8.76 (d, 1H, J = 4.7 Hz, **-a**), 8.42 (d, 2H, J = 7.9 Hz, **-e and h**), 7.98 (d, 2H, J = 8.1 Hz, **-b and d**), 7.75 (d, J = 8.2 Hz, 3H, **-c, f and g**), 4.63 (s, 2H, **triazole -NH**), 2.64 (t, 2H, J = 6.5 Hz, **-CH₂CH₂CH₃**), 1.86 (q, 2H, J = 7.6 Hz, **-CH₂CH₂CH₃**), 1.21 (t, 3H, J = 6.5 Hz, **-(CH₂)₂CH₃**) ppm.

IR (neat) ν : 3043 (Aromatic C-H), 2952, 2862 (Alkyl C-H), 1712, 1597 (C=H), 1571, 1539 (N=N), 1483, 1462, 1415, 1374, 1273, 1179, 1144, 1083, 1021, 1007 cm⁻¹.

Mass spectrum(APCI +) m/z: Found 264.1369 (M+H)⁺; calculated for C₁₆H₁₆N₄ 264.1374; 1.8 ppm.

Yield: 0.09 g, 24.4%.

4-[5-(4-Propylphenyl)-1H-1,2,4-triazol-3-yl]pyridine (94)



$^1\text{H NMR}$ (d_6 -DMSO): 8.71 (dd, 2H, $J = 4.5, 1.6$ Hz, **-b and c**), 8.02 – 7.94 (overlapping m, 4H, **-a, d, e and h**), 7.38 (d, 2H, $J = 8.2$ Hz, **-f and g**), 4.27 (s, 1H, **triazole -NH**), 2.65 (t, 2H, $J = 6.5$ Hz, **-CH₂CH₂CH₃**), 1.65 (dq, 2H, $J = 14.7, 7.3$ Hz, **-CH₂CH₂CH₃**), 0.93 (dd, 3H, $J = 9.3, 5.4$ Hz, **-(CH₂)₂CH₃**) ppm.

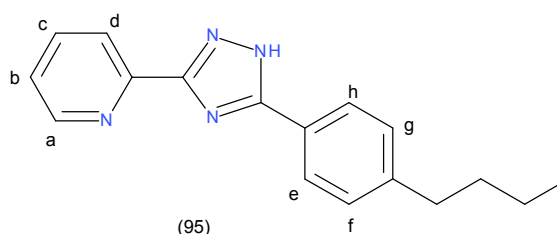
IR (neat) ν : 3109, 3072, 3030 (Aromatic C-H), 2956, 2929 (Alkyl C-H), 2869 (Alkyl C-H), 2753, 1682, 1645, 1613 (C=N), 1578, 1560 (N=N), 1504, 1487, 1443, 1421, 1391, 1381, 1345, 1305, 1279, 1232, 1174, 1150, 1117, 1086, 1036, 1006 cm^{-1} .

Melting point: 202.2 – 203.9 °C.

Mass spectrum (APCI +) m/z : Found 264.1364 ($M+H$)⁺; calculated for $C_{16}H_{16}N_4$ 264.1374; 3.7 ppm.

Yield: 0.3 g, 64%.

2-[5-(4-Butylphenyl)-1H-1,2,4-triazol-3-yl]pyridine (95)



$^1\text{H NMR}$ (d_6 -DMSO): 8.71 (d, 1H, $J = 4.1$ Hz, **-a**), 8.16 (d, 1H, $J = 7.9$ Hz, **-e**), 8.05 – 7.96 (overlapping m, 3H, **-h, b, and d**), 7.51 (m, 1H, **-c**), 7.33 (d, 2H, $J = 8.2$ Hz, **-f and g**), 5.73 (s, 1H, **triazole -NH**), 2.64

(t, 2H, J = 6.5 Hz, **-CH₂CH₂CH₂CH₃**), 1.62 (m, 2H, **-CH₂CH₂CH₂CH₃**), 1.35 (dq, 2H, J = 14.0, 7.2 Hz, **-CH₂CH₂CH₂CH₃**), 0.93 (t, 3H, J = 7.3 Hz, **-CH₂CH₂CH₂CH₃**) ppm.

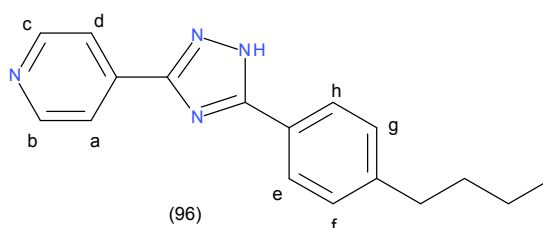
IR (neat) ν : 3123, 3068 (Aromatic C-H), 3028 (Aromatic C-H), 2928 (Alkyl C-H), 2854 (Alkyl C-H), 2781, 1600 (C=N), 1571 (N=N), 1555, 1497, 1478, 1461, 1442, 1427, 1416, 1374, 1307, 1288, 1247, 1177, 1150, 1099, 1043, 1021, 1009 cm^{-1} .

Melting point: 148.7 – 150.3 °C.

Mass spectrum (APCI +) m/z: Found 278.1525 (M+H)⁺; calculated for C₁₇H₁₈N₄ 278.1531; 2.1 ppm.

Yield: 0.29 g, 67.1%.

4-[5-(4-Butylphenyl)-1H-1,2,4-triazol-3-yl]pyridine (96)



¹H NMR (d₆-DMSO): 8.71 (d, 2H, J = 4.6 Hz, **-b and c**), 8.07 – 7.95 (overlapping m, 4H, **-e, h, a and d**), 7.38 (d, 2H, J = 8.2 Hz, **-f and g**), 5.73 (s, 1H, **triazole -NH**), 2.67 (t, 2H, J = 7.6 Hz, **-CH₂CH₂CH₂CH₃**), 1.60 (dd, 2H, J = 15.2, 7.7 Hz, **-CH₂CH₂CH₂CH₃**), 1.35 (dq, 2H, J = 14.2, 7.2 Hz, **-CH₂CH₂CH₂CH₃**), 0.92 (t, 3H, J = 7.3 Hz, **-CH₂CH₂CH₂CH₃**) ppm.

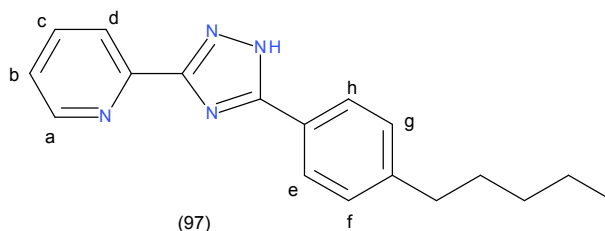
IR (neat) ν : 3044 (Aromatic C-H), 2959 (Aromatic C-H), 2927 (Alkyl C-H), 2855 (Alkyl C-H), 2541, 1668, 1611 (C=N), 1572 (N=N), 1505, 1446, 1422, 1411, 1384, 1328, 1284, 1214, 1175, 1139, 1098, 1081, 1064, 1022, 1003 cm^{-1} .

Melting point: 183.5 – 185.2 °C.

Mass spectrum (APCI +) m/z: Found 278.1520 (M+H)⁺; calculated for C₁₇H₁₈N₄ 278.1531; 3.9 ppm.

Yield: 0.32 g, 61.3%.

2-[5-(4-Pentylphenyl)-1H-1,2,4-triazol-3-yl]pyridine (97)



¹H NMR (d₆-DMSO): 9.06 (d, 1H, J = 4.4 Hz, **-a**), 8.76 (d, 1H, J = 8.1 Hz, **-e**), 8.46 – 8.11 (overlapping m, 3H, **-h, b, and d**), 7.61 (m, 1H, **-c**), 7.12 (d, 2H, J = 8.1 Hz, **-f and g**), 6.51 (s, 1H, **triazole -NH**), 1.55 (t, 2H, J = 6.5 Hz, **-CH₂(CH₂)₃CH₃**), 1.33 (dq, 6H, J = 14.3, 7.2 Hz, **-CH₂(CH₂)₃CH₃**), 0.91 (t, 3H, J = 7.3 Hz, **-CH₂(CH₂)₃CH₃**) ppm.

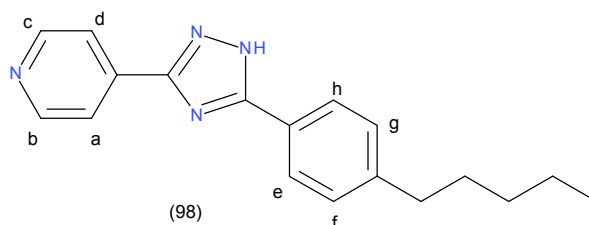
IR (neat) ν : 3119 (Aromatic C-H), 3031 (Aromatic C-H), 2956 (Aromatic C-H), 2930 (Alkyl C-H), 2850 (Alkyl C-H), 1611 (C=N), 1595, 1567 (N=N), 1475, 1457, 1445, 1429, 1410, 1389, 1358, 1335, 1317, 1283, 1258, 1218, 1202, 1189, 1165, 1115, 1055, 1042, 1028, 1007 cm⁻¹.

Melting point: 130.4 – 131.6 °C.

Mass spectrum(APCI +) m/z: Found 292.1682 (M+H)⁺; calculated for C₁₈H₂₀N₄ 292.1687; 1.7 ppm.

Yield: 0.33 g, 63%.

4-[5-(4-Pentylphenyl)-1H-1,2,4-triazol-3-yl]pyridine (98)



¹H NMR (d₆-DMSO): 8.71 (dd, 2H, J = 4.5, 1.6 Hz, **-b and c**), 8.06 – 7.91 (overlapping m, 4H, **-a, d, e and h**), 7.37 (d, 2H, J = 8.2 Hz, **-f and g**), 4.27 (s, 1H, **triazole -NH**), 2.65 (t, 2H, J = 6.5 Hz,

$-\text{CH}_2(\text{CH}_2)_3\text{CH}_3$), 2.05 – 1.54 (overlapping m, 2H, $-\text{CH}_2(\text{CH}_2)_2\text{CH}_2\text{CH}_3$), 1.32 (dd, $J = 7.1, 3.8$ Hz, 4H, $-\text{CH}_2(\text{CH}_2)_2\text{CH}_2\text{CH}_3$), 0.88 (t, 3H, $J = 6.8$ Hz, $-\text{CH}_2(\text{CH}_2)_3\text{CH}_3$) ppm.

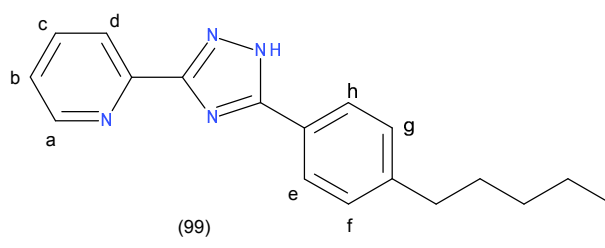
IR (neat) ν : 3106, 3059 (Aromatic C-H), 2952, 2925 (Alkyl C-H), 2849, 1715, 1611 (C=N), 1569 (N=N), 1509, 1474, 1449, 1422, 1409, 1386, 1328, 1290, 1213, 1185, 1139, 1062, 1040, 1023, 1003 cm^{-1} .

Melting point: 171.8 – 172.7 °C.

Mass spectrum(APCI +) m/z: Found 292.1689 (M+H)⁺; calculated for $\text{C}_{18}\text{H}_{20}\text{N}_4$ 292.1687; 0.6 ppm.

Yield: 0.29 g, 58%.

2-[5-(4-Hexylphenyl)-1H-1,2,4-triazol-3-yl]pyridine (99)



¹H NMR (d₆-DMSO): 8.71 (d, 1H, $J = 4.4$ Hz, **-a**), 8.16 (d, 1H, $J = 7.8$ Hz, **-e**), 8.00 (d, 3H, $J = 8.2$ Hz, **-h, b, and d**), 7.57 – 7.47 (m, 1H, **-c**), 7.32 (d, 2H, $J = 8.1$ Hz, **-f and g**), 4.27 (dd, 1H, $J = 6.4, 3.8$ Hz, **triazole -NH**), 2.65 (t, 2H, $J = 6.5$ Hz, $-\text{CH}_2(\text{CH}_2)_4\text{CH}_3$), 1.61 (dd, 2H, $J = 15.0, 7.1$ Hz, $-\text{CH}_2\text{CH}_2(\text{CH}_2)_3\text{CH}_3$), 1.39 – 1.24 (overlapping m, 6H, $-\text{CH}_2\text{CH}_2(\text{CH}_2)_3\text{CH}_3$), 0.86 (dd, 3H, $J = 8.5, 5.5$ Hz, $-\text{CH}_2(\text{CH}_2)_4\text{CH}_3$) ppm.

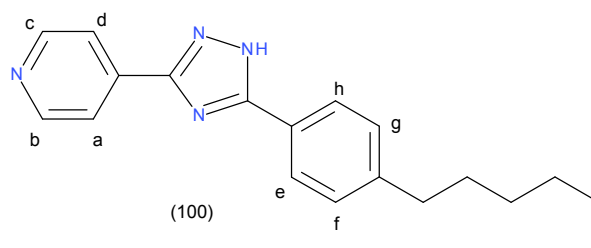
IR (neat) ν : 3029 (Aromatic C-H), 2926, 2849 (Alkyl C-H), 2849, 1715, 1601 (C=N), 1562 (N=N), 1551, 1531, 1478, 1461, 1416, 1374, 1150, 1070, 1009 cm^{-1} .

Melting point: 128.4 – 129.5 °C.

Mass spectrum(APCI +) m/z: Found 306.1837 (M+H)⁺; calculated for $\text{C}_{19}\text{H}_{22}\text{N}_4$ 306.1844; 2.2 ppm.

Yield: 0.22 g, 47.2%.

4-[5-(4-Hexylphenyl)-1H-1,2,4-triazol-3-yl]pyridine (100)



$^1\text{H NMR}$ (d_6 -DMSO): 8.71 (dd, 2H, $J = 4.5, 1.6$ Hz, **-b and c**), 8.02 – 7.95 (overlapping m, 4H, **-a, d, e and h**), 7.38 (d, 2H, $J = 8.3$ Hz, **-f and g**), 4.27 (s, 1H, **triazole -NH**), 2.65 (t, 2H, $J = 6.5$ Hz, **$-\text{CH}_2(\text{CH}_2)_4\text{CH}_3$**), 1.61 (d, 2H, $J = 7.4$ Hz, **$-\text{CH}_2\text{CH}_2(\text{CH}_2)_3\text{CH}_3$**), 1.31 (overlapping m, 6H, **$-\text{CH}_2\text{CH}_2(\text{CH}_2)_3\text{CH}_3$**), 0.92 – 0.83 (t, 3H, $J = 6.8$ Hz, **$-\text{CH}_2(\text{CH}_2)_4\text{CH}_3$**) ppm.

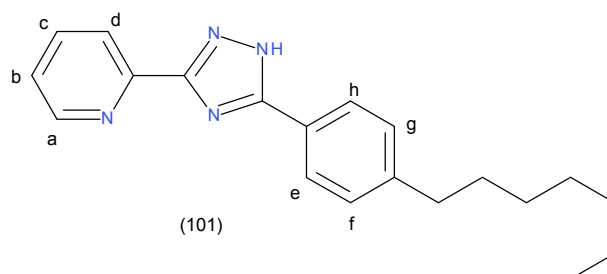
IR (neat) ν : 3174, 3150, 3108, 3062 (Aromatic C-H), 2949 (Alkyl C-H), 2927 (Alkyl C-H), 2850 (Alkyl C-H), 1715, 1644, 1609 (C=N), 1568, 1548 (N=N), 1506, 1448, 1420, 1386, 1328, 1272, 1214, 1186, 1174, 1138, 1062, 1036, cm^{-1} .

Melting point: 156.1 – 157.0 °C.

Mass spectrum (APCI +) m/z : Found 306.1833 ($\text{M}+\text{H}$) $^+$; calculated for $\text{C}_{19}\text{H}_{22}\text{N}_4$ 306.1844; 3.5 ppm.

Yield: 0.21 g, 49.3%.

2-[5-(4-Heptylphenyl)-1H-1,2,4-triazol-3-yl]pyridine (101)



$^1\text{H NMR}$ (d_6 -DMSO): 8.71 (d, 1H, $J = 4.1$ Hz, **-a**), 8.16 (d, 1H, $J = 7.9$ Hz, **-e**), 7.99 (t, 3H, $J = 6.7$ Hz, **-h, b, and d**), 7.52 (m, 1H, **-c**), 7.32 (d, 2H, $J = 8.1$ Hz, **-f and g**), 4.27 (s, 1H, **triazole -NH**), 2.65 (t, 2H,

J = 6.5 Hz, **-CH₂(CH₂)₅CH₃**), 1.69 – 1.54 (overlapping m, 2H, **-CH₂CH₂(CH₂)₄CH₃**), 1.30 (dd, 8H, J = 7.8, 4.1 Hz, **-CH₂CH₂(CH₂)₄CH₃**), 0.87 (t, 3H, J = 6.8 Hz, **-CH₂(CH₂)₅CH₃**) ppm.

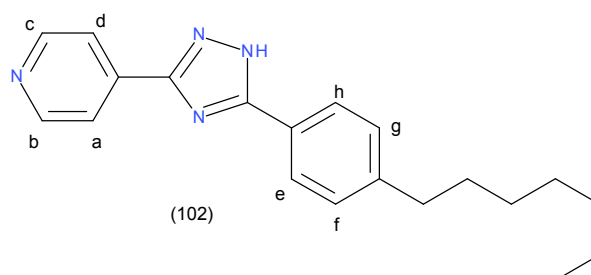
IR (neat) ν : 3167, 2921 (Aromatic C-H), 2929 (Alkyl C-H), 2869 (Alkyl C-H), 2850 (Alkyl C-H), 1715, 1644, 1615, 1598 (C=N), 1571, 1554 (N=N), 1482, 1462, 1425, 1373, 1272, 1178, 1143, 1115, 1097, 1049, 1020, 1008 cm^{-1} .

Melting point: 113.0 – 114.9 °C.

Mass spectrum(APCI +) m/z: Found 320.2020 (M+H)⁺; calculated for C₂₀H₂₄N₄ 320.2000; 6.2 ppm.

Yield: 0.29 g, 57.1%.

4-[5-(4-Heptylphenyl)-1H-1,2,4-triazol-3-yl]pyridine (102)



¹H NMR (d₆-DMSO): 8.71 (dd, 2H, J = 4.5, 1.6 Hz, **-b and c**), 8.01 – 7.96 (overlapping m, 4H, **-a, d, e and h**), 7.37 (d, 2H, J = 8.3 Hz, **-f and g**), 4.28 (m, 1H, **triazole -NH**), 2.65 (t, 2H, J = 6.5 Hz, **-CH₂(CH₂)₅CH₃**), 1.78 – 1.52 (overlapping m, 2H, **-CH₂CH₂(CH₂)₄CH₃**), 1.35 – 1.22 (overlapping m, 8H, **-CH₂CH₂(CH₂)₄CH₃**), 0.86 (t, 3H, J = 6.8 Hz, **-CH₂(CH₂)₅CH₃**) ppm.

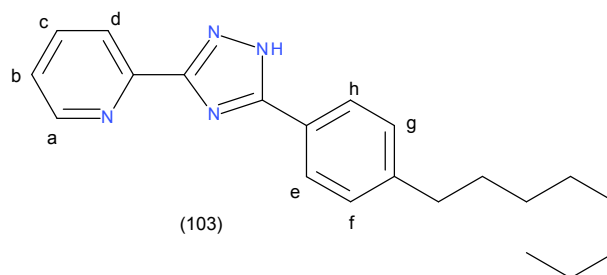
IR (neat) ν : 3108, 3062 (Aromatic C-H), 2951, 2925 (Alkyl C-H), 2853 (Alkyl C-H), 1609 (C=N), 1568, 1507 (N=N), 1467, 1448, 1420, 1387, 1328, 1280, 1213, 1186, 1173, 1138, 1123, 1062, 1036, 1024, 1001 cm^{-1} .

Melting point: 142.8 – 144.2 °C.

Mass spectrum(APCI +) m/z: Found 320.2015 (M+H)⁺; calculated for C₂₀H₂₄N₄ 320.2000; 4.6 ppm.

Yield: 0.41 g, 71%.

2-[5-(4-Octylphenyl)-1H-1,2,4-triazol-3-yl]pyridine (103)



¹H NMR (d₆-DMSO): 8.71 (d, 1H, J = 4.3 Hz, **-a**), 8.16 (d, J = 7.9 Hz, 1H, **-e**), 8.00 (d, 3H, J = 8.1 Hz, **-h, b, and d**), 7.51 (m, 1H, **-c**), 7.32 (d, 2H, J = 8.0 Hz, **-f and g**), 5.75 (s, 1H, **triazole -NH**), 2.64 (t, 2H, J = 6.5 Hz, **-CH₂ (CH₂)₆ CH₂**), 1.61 (d, 2H, J = 7.1 Hz, **-CH₂ CH₂ (CH₂)₅ CH₃**), 1.39 – 1.19 (overlapping m, 10H, **-CH₂ CH₂ (CH₂)₅ CH₃**), 0.90 – 0.82 (t, 3H, J = 7.3 Hz, **-CH₂ (CH₂)₆ CH₃**) ppm.

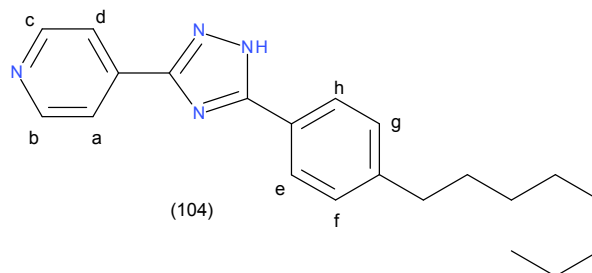
IR (neat) ν : 3129, 3071 (Aromatic C-H), 3030 (Aromatic C-H), 2947 (Alkyl C-H), 2918 (Alkyl C-H), 2848 (Alkyl C-H), 2774, 2625, 2531, 2155, 2027, 1900, 1715, 1619, 1600 (C=N), 1571 (N=N), 1555, 1478, 1462, 1428, 1416, 1374, 1313, 1289, 1267, 1178, 1152, 1112, 1099, 1074, 1044, 1010 cm⁻¹.

Melting point: 121.8 – 123.9 °C.

Mass spectrum (APCI +) m/z: Found 334.2151 (M+H)⁺; calculated for C₂₁H₂₆N₄ 334.2157; 1.7 ppm.

Yield: 0.38 g, 71.4%.

4-[5-(4-Octylphenyl)-1H-1,2,4-triazol-3-yl]pyridine (104)



¹H NMR (d₆-DMSO): 8.71 (d, 2H, J = 5.1 Hz, **-b and c**), 8.02 – 7.96 (overlapping m, 4H, **-e, h, a and d**), 7.37 (d, 2H, J = 7.9 Hz, **-f and g**), 5.75 (s, 1H, **triazole -NH**), 2.68 (t, 2H, J = 6.5 Hz, **-CH₂ (CH₂)₆**)

CH₂), 1.68 – 1.56 (overlapping m, 2H, -CH₂ **CH**₂ (CH₂)₅ CH₃), 1.38 – 1.19 (overlapping m, 10H, -CH₂ CH₂ (**CH**₂)₅ CH₃), 0.90 – 0.82 (t, 3H, J = 7.3 Hz, -CH₂ (CH₂)₆ **CH**₃) ppm.

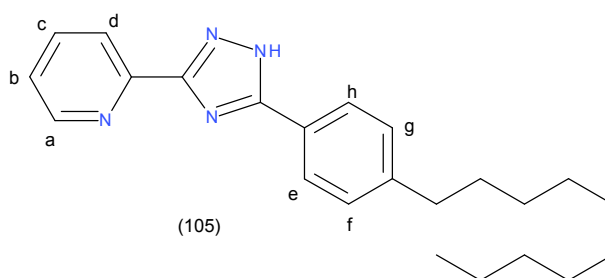
IR (neat) ν : 3047 (Aromatic C-H), 2955 (Aromatic C-H), 2918 (Alkyl C-H), 2848 (Alkyl C-H), 2774, 2637, 2534. 2155, 1795, 1612 (C=N), 1571 (N=N), 1510, 1463, 1447, 1421, 1387, 1329, 1277, 1213, 1183, 1173, 1141, 1099, 1064, 1021, 1004 cm⁻¹.

Melting point: 143.1 – 144.6 °C.

Mass spectrum(APCI +) m/z: Found 334.2148 (M+H)⁺; calculated for C₂₁H₂₆N₄ 334.2157; 2.6 ppm.

Yield: 0.31 g, 65.2%.

2-[5-(4-Decylphenyl)-1H-1,2,4-triazol-3-yl]pyridine (105)



¹H NMR (d₆-DMSO): 8.60 (d, 1H, J = 4.4 Hz, **-a**), 8.15 (s, 1H, **-e**), 7.93 – 7.77 (overlapping m, 3H, **-h, b, and d**), 7.47 (m, 1H, **-c**), 7.29 (d, 2H, J = 8.2 Hz, **-f and g**), 6.79 (s, 1H, **triazole -NH**), 2.68 (t, 2H, J = 6.5 Hz, **-CH₂(CH₂)₈CH₃**), 1.70 – 1.56 (overlapping m, 2H, **-CH₂CH₂(CH₂)₇CH₃**), 1.31 (dd, 14H, J = 15.9, 12.4 Hz, **-CH₂CH₂(CH₂)₇CH₃**), 0.86 (t, 3H, J = 6.6 Hz, **-CH₂(CH₂)₈CH₃**) ppm.

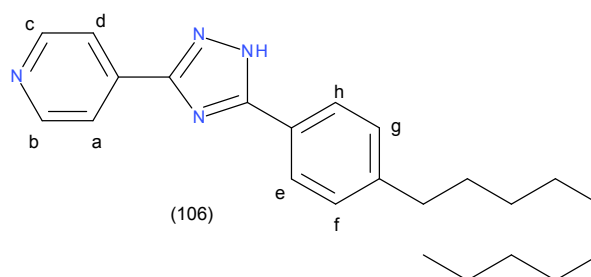
IR (neat) ν : 3129, 3068, 3030 (Aromatic C-H), 2917 (Alkyl C-H), 2847, 1646, 1615, 1601 (C=N), 1572, 1556 (N=N), 1479, 1462, 1416, 1374, 1269, 1178, 1151, 1113, 1098, 1044, 1010 cm⁻¹.

Melting point: 104.8 – 105.9 °C.

Mass spectrum(APCI +) m/z: Found 362.2466 (M+H)⁺; calculated for C₂₃H₃₀N₄ 362.2470; 1.1 ppm.

Yield: 0.4 g, 75.3%.

4-[5-(4-Decylphenyl)-1H-1,2,4-triazol-3-yl]pyridine (106)



$^1\text{H NMR}$ ($\text{d}_6\text{-DMSO}$): 8.65 (dd, 2H, $J = 4.5, 1.6$ Hz, **-b and c**), 8.09 – 7.96 (overlapping m, 4H, **-a, d, e and h**), 7.27 (d, 2H, $J = 8.3$ Hz, **-f and g**), 4.32 (m, 1H, **triazole -NH**), 2.58 (t, 2H, $J = 6.5$ Hz, **-CH₂(CH₂)₈CH₃**), 1.65 – 1.51 (overlapping m, 2H, **-CH₂CH₂(CH₂)₇CH₃**), 1.26 (dd, 14H, $J = 15.9, 12.4$ Hz, **-CH₂CH₂(CH₂)₇CH₃**), 0.94 (t, 3H, $J = 6.6$ Hz, **-CH₂(CH₂)₈CH₃**) ppm.

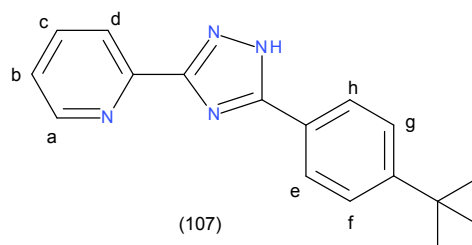
IR (neat) ν : 3058 (Aromatic C-H), 2953, 2918 (Alkyl C-H), 2848, 1719, 1647, 1611 (C=N), 1568 (N=N), 1552, 1537, 1488, 1467, 1451, 1413, 1387, 1369, 1324, 1273, 1180, 1138, 1110, 1078, 1065, 1047, 1021, 1005 cm^{-1} .

Melting point: 154.4 – 155.7 °C.

Mass spectrum (APCI +) m/z: Found 362.2463 ($\text{M}+\text{H}^+$); calculated for $\text{C}_{23}\text{H}_{30}\text{N}_4$ 362.2470; 1.9 ppm.

Yield: 0.42 g, 78.3%.

2-[5-(4-tert-Butylphenyl)-1H-1,2,4-triazol-3-yl]pyridine (107)



$^1\text{H NMR}$ ($\text{d}_6\text{-DMSO}$): 8.72 (d, 1H, $J = 4.3$ Hz, **-a**), 8.62 (d, 1H, $J = 8.1$ Hz, **-e**), 8.46 – 8.11 (overlapping m, 3H, **-h, b, and d**), 7.61 (m, 1H, **-c**), 7.12 (d, 2H, $J = 8.1$ Hz, **-f and g**), 6.51 (s, 2H, **triazole -NH**), 1.34

(s, 9H, **tert. butyl** -(CH₃)₃) ppm.

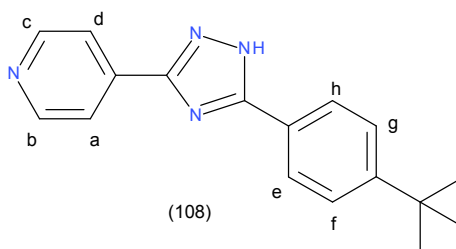
IR (neat) ν : 3167, 3092, 3062 (Aromatic C-H), 2955, 2907 (Alkyl C-H), 2865 (Alkyl C-H), 1718, 1597 (C=N), 1568 (N=N), 1551, 1480, 1460, 1422, 1369, 1315, 1301, 1267, 1192, 1170, 1138, 1113, 1095, 1050, 1018, 1007 cm⁻¹.

Melting point: 178.3 – 180.7 °C.

Mass spectrum(APCI +) m/z: Found 278.1526 (M+H)⁺; calculated for C₁₇H₁₈N₄ 278.1531; 1.7 ppm.

Yield: 0.3 g, 67.2%.

4-[5-(4-**tert**-Butylphenyl)-1H-1,2,4-triazol-3-yl]pyridine (108)



¹H NMR (d₆-DMSO): 8.90 (d, 2H, J = 5.9 Hz, **-b and c**), 8.58 (d, 4H, J = 8.3 Hz, **-a, d, e and h**) 8.30 – 7.63 (overlapping m, 2H, **-f and g**), 6.51 (m, 1H, **triazole -NH**), 1.34 (s, 9H, **tert. butyl** -(CH₃)₃) ppm.

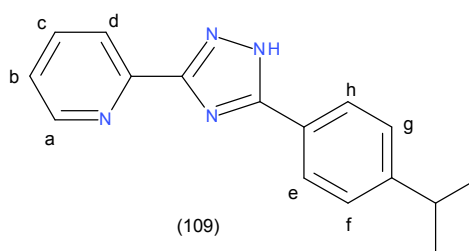
IR (neat) ν : 3059 (Aromatic C-H), 2965, 2945 (Alkyl C-H), 2878 (Alkyl C-H), 1715, 1611 (C=N), 1585, 1571, 1552 (N=N), 1510, 1472, 1449, 1419, 1385, 1361, 1313, 1292, 1265, 1243, 1212, 1198, 1169, 1142, 1109, 1062, 1044, 1024, 1003 cm⁻¹.

Melting point: 253.9 – 255.2 °C.

Mass spectrum(APCI +) m/z: Found 278.1522 (M+H)⁺; calculated for C₁₇H₁₈N₄ 278.1531; 3.2 ppm.

Yield: 0.27 g, 64.4%.

2-[5-(4-Isopropylphenyl)-1H-1,2,4-triazol-3-yl]pyridine (109)



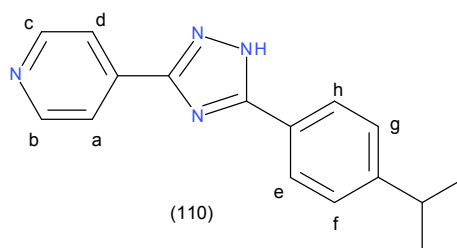
¹H NMR (d₆-DMSO): 8.96 – 8.49 (d, 1H, J = 4.4 Hz, **-a**), 8.45 (d, 1H, J = 8.1 Hz, **-e**), 8.31 – 8.10 (overlapping m, 3H, **-h, b, and d**), 7.54 (m, 1H, **-c**), 7.09 (d, 2H, J = 8.1 Hz, **-f and g**) 4.82 (d, 1H, J = 23.9 Hz, **triazole -NH**), 2.97 (dt, 1H, J = 13.7, 6.8, 3.7 Hz, **Isopropyl -(CH₂)**), 1.61 (s, 6H, **Isopropyl -(CH₃)₂**) ppm.

IR (neat) ν : 3052 (Aromatic C-H), 2954, 2868 (Alkyl C-H), 1715, 1610 (C=N), 1591, 1572, 1551 (N=N), 1505, 1462, 1416, 1394, 1336, 1310, 1274, 1249, 1182, 1153, 1085, 1038, 1007 cm⁻¹.

Mass spectrum(APCI +) m/z: Found 264.1361 (M+H)⁺; calculated for C₁₆H₁₆N₄ 264.1374; 4.9 ppm.

Yield: 0.08 g, 23.1%.

4-[5-(4-Isopropylphenyl)-1H-1,2,4-triazol-3-yl]pyridine (110)



¹H NMR (d₆-DMSO): 9.03 (d, 2H, J = 5.9 Hz, **-b and c**), 8.69 (d, 4H, J = 8.3 Hz, **-a, d, e and h**) 8.46 – 7.78 (overlapping m, 2H, **-f and g**), 4.82 (d, 1H, J = 23.9 Hz, **triazole -NH**), 2.94 (dt, 1H, J = 13.7, 6.8, 3.7 Hz, **Isopropyl -(CH₂)**), 1.41 (s, 6H, **Isopropyl -(CH₃)₂**) ppm.

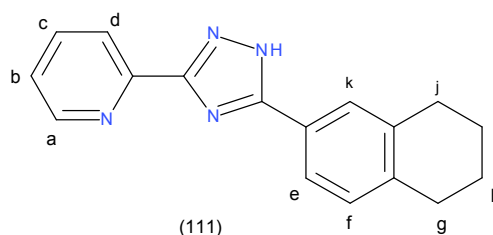
IR (neat) ν : 3043 (Aromatic C-H), 2957, 2870 (Alkyl C-H), 1714, 1610 (C=N), 1569 (N=N), 1505, 1446, 1413, 1384, 1362, 1328, 1274, 1212, 1172, 1138, 1084, 1054, 1019, 1003 cm⁻¹.

Melting point: 218.2 – 219.6 °C.

Mass spectrum(APCI +) m/z: Found 264.1358 (M+H)⁺; calculated for C₁₆H₁₆N₄ 264.1374; 6.0 ppm.

Yield: 0.31 g, 65.2%.

2-(5-Tetralin-6-yl-1H-1,2,4-triazol-3-yl)pyridine (111)



¹H NMR (d₆-DMSO): 8.71 (m, 1H, **-a**), 7.99 (m, 1H, **-c**), 7.78 (d, 2H, J = 6.9 Hz, **-b and d**), 7.22 (d, 1H, J = 8.5 Hz, **triazole -NH**), 3.20 (s, 5H, **-k, e, f and g**), 2.86 – 2.76 (overlapping m, 2H, **-h**), 2.50 (d, 2H, J = 1.9 Hz, **-i**), 1.79 (t, 2H, J = 3.1 Hz, **-j**) ppm.

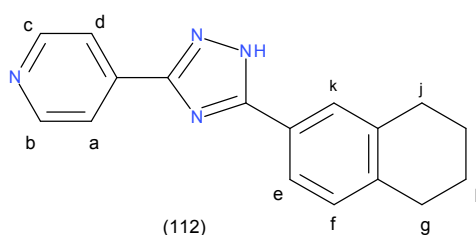
IR (neat) ν : 3175 (Aromatic C-H), 3002 (Aromatic C-H), 2924 (Alkyl C-H), 2854 (Alkyl C-H), 1615, 1597 (C=N), 1581, 1571, 1551 (N=N), 1488, 1468, 1416, 1382, 1336, 1310, 1282, 1247, 1184, 1151, 1127, 1086, 1105, 1044, 1007 cm⁻¹.

Melting point: 212.5 – 213.3 °C.

Mass spectrum(APCI +) m/z: Found 276.1369 (M+H)⁺; calculated for C₁₇H₁₆N₄ 276.1374; 1.8 ppm.

Yield: 0.16 g, 32%.

4-(5-Tetralin-6-yl-1H-1,2,4-triazol-3-yl)pyridine (112)



¹H NMR (d₆-DMSO): 8.71 (d, 2H, J = 4.3 Hz, **-b and c**), 8.38 – 7.72 (overlapping m, 2H, **-a and d**), 6.69 (s, 1H, **triazole -NH**), 4.28 (s, 3H, **-e, f and k**), 3.42 (s, 4H, **g and h**), 2.95 – 2.62 (overlapping m, 2H, **i**), 1.78 (d, 2H, J = 3.5 Hz, **-j**) ppm.

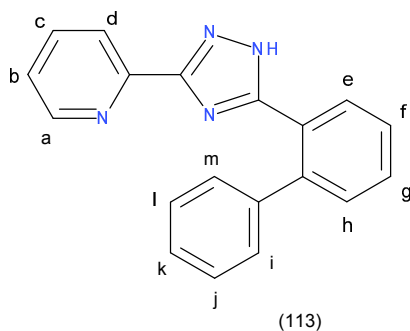
IR (neat) ν : 3165,3092 (Aromatic C-H), 3041 (Aromatic C-H), 3017, 2989, 2925 (Alkyl C-H), 2865 (Alkyl C-H), 2828, 1659 (C=N), 1569 (N=N), 1499, 1457, 1451, 1422, 1396, 1351, 1317, 1281, 1247, 1208, 1190, 1175, 1120, 1007 cm⁻¹.

Melting point: 277.6 – 278.8 °C.

Mass spectrum(APCI +) m/z: Found 276.1358 (M+H)⁺; calculated for C₁₇H₁₆N₄ 276.1374; 5.7 ppm.

Yield: 0.19 g, 47.2%.

2-[5-(2-Phenylphenyl)-1H-1,2,4-triazol-3-yl]pyridine (113)



¹H NMR (d₆-DMSO): 8.74 (m, 1H, **-a**), 8.66 (d, 2H, J = 4.7 Hz, **-c and d**), 8.01 (td, 1H, J = 7.4, 1.4 Hz, **-h**), 7.94 (dd, 3H, J = 6.7, 2.7 Hz, **-m, e, and g**), 7.86 – 7.69 (overlapping m, 5H, **-b, i, k, l and j**), 7.53 (m, 1H, **-f**), 7.13 (m, 1H, **triazole -NH**) ppm.

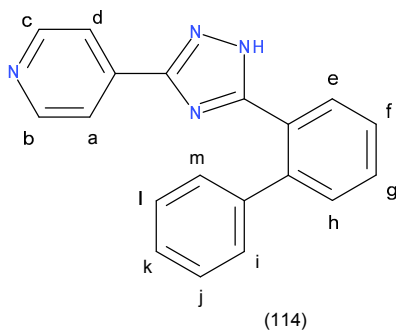
IR (neat) ν : 3169, 3132 (Aromatic C-H), 3089 (Aromatic C-H), 3046, 2947 (Alkyl C-H), 2895 (Alkyl C-H), 2837, 1659, 1596 (C=N), 1570 (N=N), 1547, 1485, 1442, 1419, 1366, 1304, 1277, 1244, 1171, 1140, 1119, 1091, 1070, 1045, 1010 cm⁻¹.

Melting point: – °C.

Mass spectrum(APCI +) m/z: Found 298.1210 (M+H)⁺; calculated for C₁₉H₁₄N₄ 298.1218; 2.6 ppm.

Yield: 0.08 g, 28.1%.

4-[5-(2-Phenylphenyl)-1H-1,2,4-triazol-3-yl]pyridine (114)



¹H NMR (d₆-DMSO): 8.68 (ddd, J = 12.0, 4.4, 1.6 Hz, 2H, **-b and c**), 7.96 (td, 2H, J = 7.4, 1.4 Hz, **-a and d**), 7.82 (dd, 3H, J = 6.7, 2.7 Hz, **-e, m and h**), 7.76 – 7.69 (overlapping m, 5H, **-f, i, g, k and l**), 7.51 (m, 1H, **-j**), 6.26 (m, 1H, **triazole -NH**) ppm.

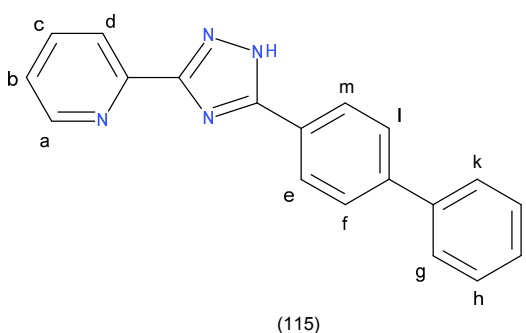
IR (neat) ν : 3169, 3130 (Aromatic C-H), 3079 (Aromatic C-H), 3046, 2951 (Alkyl C-H), 2885 (Alkyl C-H), 2832, 1660, 1576 (C=N), 1575 (N=N), 1550, 1475, 1445, 1421, 1364, 1303, 1267, 1242, 1176, 1138, 1129, 1095, 1060, 1025, 1007 cm⁻¹.

Melting point: 288.1 – 292.3 °C.

Mass spectrum (APCI +) m/z: Found 298.1207 (M+H)⁺; calculated for C₁₉H₁₄N₄ 298.1218; 3.6 ppm.

Yield: 0.26 g, 37.4%.

2-[5-(4-Phenylphenyl)-1H-1,2,4-triazol-3-yl]pyridine (115)



¹H NMR (d₆-DMSO): 8.74 (m, 1H, **-a**), 8.25 – 8.16 (overlapping m, 4H, **-c, e, h and f**), 8.02 (m, 1H, **-g**), 7.82 (d, 2H, J = 8.4 Hz, **-i and k**), 7.77 – 7.71 (overlapping m, 2H, **-m and b**), 7.52 (dt, 3H, J = 6.9, 3.2 Hz, **-j, l and d**), 7.49 – 7.22 (overlapping m, 1H, **triazole -NH**) ppm.

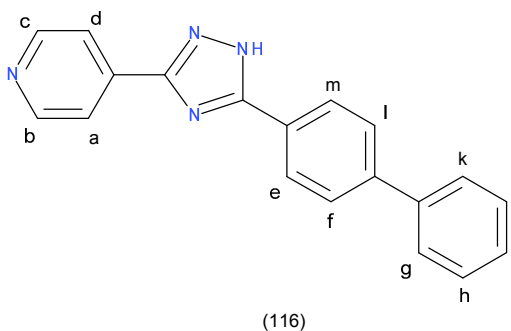
IR (neat) ν : 3129 (Aromatic C-H), 3065 (Aromatic C-H), 3029 (Aromatic C-H), 2958, 2892 (Alkyl C-H), 2844 (Alkyl C-H), 1682, 1598 (C=N), 1569 (N=N), 1552, 1479, 1462, 1447, 1427, 1410, 1373, 1332, 1314, 1298, 1248, 1183, 1145, 1109, 1075, 1048, 1011 cm⁻¹.

Melting point: 217.5 – 219.5 °C.

Mass spectrum(APCI +) m/z: Found 298.1201 (M+H)⁺; calculated for C₁₉H₁₄N₄ 298.1218; 5.7 ppm.

Yield: 0.43 g, 74.2%.

4-[5-(4-Phenylphenyl)-1H-1,2,4-triazol-3-yl]pyridine (116)



¹H NMR (d₆-DMSO): 8.73 (dd, 2H, J = 4.5, 1.5 Hz, **-b and c**), 8.21 – 8.14 (overlapping m, 2H, **-f and g**), 8.02 (dd, 2H, J = 4.5, 1.6 Hz, **-i and m**), 7.87 (d, 2H, J = 8.5 Hz, **-e and h**), 7.77 (dd, 1H, J = 5.2, 3.2 Hz, **-a**), 7.58 (m, 1H, **-d**), 7.50 (d, 1H, J = 6.0 Hz, **-j and k**), 7.44 (t, J = 1.3 Hz, 1H, **-l**), 7.39 (m, 1H, **triazole -NH**) ppm.

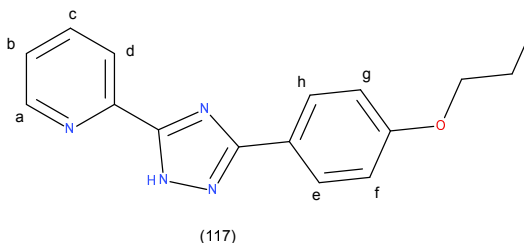
IR (neat) ν : 3031 (Aromatic C-H), 2927 (Alkyl C-H), 2855 (Alkyl C-H), 1652 (C=N), 1611, 1559 (N=N), 1515, 1487, 1438, 1421, 1384, 1213, 1175, 1145, 1709, 1062, 1023, 1006 cm⁻¹.

Melting point: 287.1 – 291.3 °C.

Mass spectrum(APCI +) m/z: Found 298.1206 (M+H)⁺; calculated for C₁₉H₁₄N₄ 298.1218; 4.0 ppm.

Yield: 0.44 g, 82.3%.

2-[3-(4-Propoxyphenyl)-1H-1,2,4-triazol-5-yl]pyridine (117)



¹H NMR (d₆-DMSO): 8.71 (d, 1H, J = 4.7 Hz, -a), 8.46 (d, 2H, J = 8.0 Hz, -c and d), 7.71 (t, 2H, J = 9.2 Hz, -e and h), 7.61 – 7.35 (m, 1H, -b), 7.07 (d, 2H, J = 8.8 Hz, -f and g), 6.77 (s, 1H, triazole -NH), 4.01 (t, 2H, J = 6.5 Hz, -OCH₂CH₂CH₃), 2.00 – 1.58 (overlapping m, 2H, -OCH₂CH₂CH₃), 0.76 (t, 3H, J = 7.4 Hz, -OCH₂CH₂CH₃) ppm.

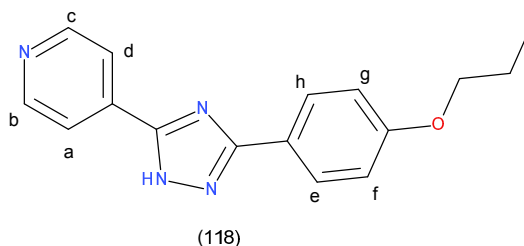
IR (neat) ν : 3053 (Aromatic C-H), 2967, 2941 (Alkyl C-H), 2838, 1731, 1617, 1600, 1584 (C=N), 1571, 1553 (N=N), 1533, 1461, 1427, 1417, 1389, 1372, 1312, 1300, 1291, 1244, 1169, 1149, 1112, 1100, 1069, 1046, 1008 cm⁻¹.

Melting point: 157.9 – 161.0 °C.

Mass spectrum (APCI +) m/z: Found 280.1319 (M+H)⁺; calculated for C₁₆H₁₆N₄O 280.1324; 1.7 ppm.

Yield: 0.3 g, 61%.

4-[3-(4-Propoxyphenyl)-1H-1,2,4-triazol-5-yl]pyridine (118)



¹H NMR (d₆-DMSO): 8.78 (d, 2H, J = 5.9 Hz, **-b and c**), 8.47 (s, 2H, **-a and d**), 8.36 – 7.70 (overlapping m, 2H, **-e and h**), 7.34 (t, 2H, J = 7.8 Hz, **-f and g**), 6.89 (s, 1H, **triazole -NH**), 3.57 (t, 2H, J = 6.5 Hz, **-OCH₂CH₂CH₃**), 1.95 – 1.56 (overlapping m, 2H, **-OCH₂CH₂CH₃**), 0.80 (t, 3H, J = 7.4 Hz, **-OCH₂CH₂CH₃**) ppm.

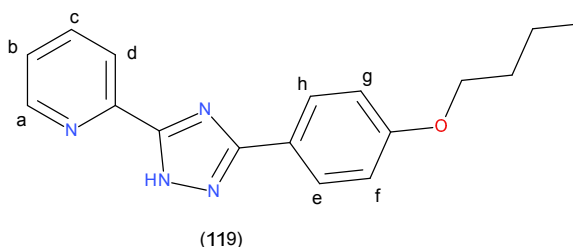
IR (neat) ν : 3102 (Aromatic C-H), 3062 (Aromatic C-H), 3040 (Aromatic C-H), 2962, 2937 (Alkyl C-H), 2878 (Alkyl C-H), 2825, 1712, 1678, 1643 (C=N), 1610, 1557 (N=N), 1507, 1451, 1419, 1392, 1281, 1256, 1245, 1212, 1175, 1139, 1115, 1063, 1035, 1012, 1003 cm⁻¹.

Melting point: 192.4 – 193.1 °C.

Mass spectrum(APCI +) m/z: Found 280.1316 (M+H)⁺; calculated for C₁₆H₁₆N₄O 280.1324; 2.8 ppm.

Yield: 0.28 g, 58.3%.

2-[3-(4-Butoxyphenyl)-1H-1,2,4-triazol-5-yl]pyridine (119)



¹H NMR (d₆-DMSO): 8.90 (d, 1H, J = 4.6 Hz, **-a**), 8.76 (d, 2H, J = 8.0 Hz, **-c and d**), 7.88 (dd, 1H, J = 11.5, 7.2 Hz, **-b**), 7.53 – 7.37 (overlapping m, 2H, **-f and g**), 7.01 (d, 2H, J = 8.8 Hz, **-e and h**), 6.90 (s, 1H, **triazole -NH**), 4.04 (t, 2H, J = 6.5 Hz, **-OCH₂(CH₂)₂CH₃**), 1.82 – 1.60 (overlapping m, 2H, **-OCH₂CH₂CH₂CH₃**), 1.59 – 1.31 (overlapping m, 2H, **-OCH₂CH₂CH₂CH₃**), 0.90 (t, 3H, **-OCH₂(CH₂)₂CH₃**) ppm.

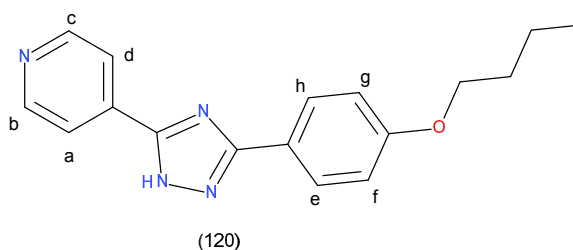
IR (neat) ν : 3172, 3101 (Aromatic C-H), 2955 (Alkyl C-H), 2869 (Alkyl C-H), 1682, 1612, 1598 (C=N), 1582, 1573, 1554 (N=N), 1532, 1482, 1460, 1438, 1428, 1396, 1372, 1314, 1268, 1242, 1172, 1143, 1127, 1108, 1098, 1037, 1007 cm⁻¹.

Melting point: 151.2 – 152.6 °C.

Mass spectrum(APCI +) m/z: Found 294.1477 (M+H)⁺; calculated for C₁₇H₁₈N₄O 294.1480; 1.0 ppm.

Yield: 0.33 g, 67.2%.

4-[3-(4-Butoxyphenyl)-1H-1,2,4-triazol-5-yl]pyridine (120)



¹H NMR (d₆-DMSO): 8.58 (d, 2H, J = 22.0 Hz, **-b and c**), 8.48 (s, 2H, **-a and d**), 8.39 (d, 2H, J = 19.9 Hz, **-e and h**), 7.89 – 7.53 (overlapping m, 2H, **-f and g**), 6.55 (m, 1H, **triazole -NH**), 4.02 (t, 2H, J = 6.5 Hz, **-OCH₂(CH₂)₂CH₃**), 1.76 – 1.57 (overlapping m, 2H, **-OCH₂CH₂CH₂CH₃**), 1.41 (dq, 2H, J = 14.4, 7.4 Hz, **-OCH₂CH₂CH₂CH₃**), 0.93 (t, 3H, J = 7.3 Hz, **-OCH₂(CH₂)₂CH₃**) ppm.

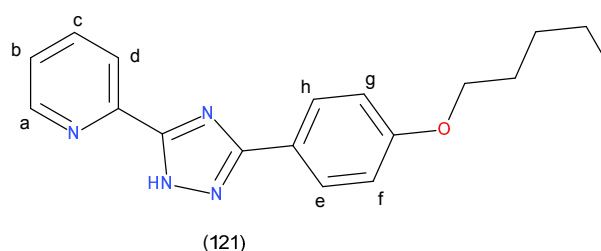
IR (neat) ν : 3326, 3165, 3108 (Aromatic C-H), 3068 (Aromatic C-H), 3035, 2953 (Alkyl C-H), 2925 (Alkyl C-H), 2868 (Alkyl C-H), 1612, 1575 (C=N), 1565 (N=N), 1506, 1469, 1451, 1417, 1378, 1302, 1244, 1181, 1141, 1108, 1065, 1040, 1002 cm⁻¹.

Melting point: 177.3 – 179.2 °C.

Mass spectrum(APCI +) m/z: Found 294.1472 (M+H)⁺; calculated for C₁₇H₁₈N₄O 294.1480; 2.7 ppm.

Yield: 0.41 g, 78.4%.

2-[3-(4-Pentoxyphenyl)-1H-1,2,4-triazol-5-yl]pyridine (121)



$^1\text{H NMR}$ (d_6 -DMSO): 8.71 (d, 1H, $J = 4.1$ Hz, -a), 8.15 (d, 2H, $J = 7.8$ Hz, -e and h), 8.10 – 7.85 (overlapping m, 2H, -b and d), 7.73 – 7.32 (overlapping m, 3H, -c, f and g), 7.05 (d, 1H, $J = 8.8$ Hz, triazole -NH), 4.04 (t, 2H, $J = 6.5$ Hz, $-\text{OCH}_2(\text{CH}_2)_3\text{CH}_3$), 2.59 – 2.41 (overlapping m, 2H, $-\text{OCH}_2\text{CH}_2(\text{CH}_2)_2\text{CH}_3$), 1.74 (dd, 2H, $J = 13.7, 6.7$ Hz, $-\text{O}(\text{CH}_2)_2\text{CH}_2\text{CH}_2\text{CH}_3$), 1.59 – 1.23 (overlapping m, 2H, $-\text{OCH}_2(\text{CH}_2)_2\text{CH}_2\text{CH}_3$), 1.23 – 0.74 (t, 3H, $J = 6.9$ Hz, $-\text{OCH}_2(\text{CH}_2)_3\text{CH}_3$) ppm.

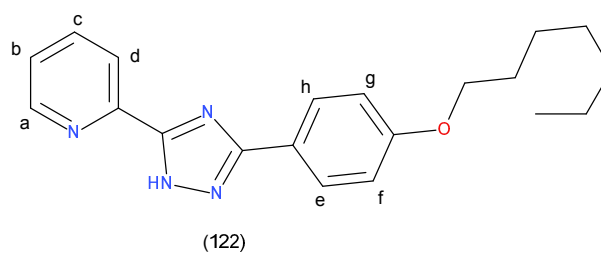
IR (neat) ν : 3032 (Aromatic C-H), 2932, 2854 (Alkyl C-H), 1600, 1572 (C=N), 1567 (N=N), 1532, 1459, 1418, 1378, 1313, 1299, 1236, 1177, 1153, 1115, 1060, 1010 cm^{-1} .

Melting point: 124.3 – 125.9 $^\circ\text{C}$.

Mass spectrum(APCI +) m/z : Found 308.1632 ($\text{M}+\text{H}$) $^+$; calculated for $\text{C}_{18}\text{H}_{20}\text{N}_4\text{O}$ 308.1637; 1.6 ppm.

Yield: 0.31 g, 63%.

2-[3-(4-Heptoxyphenyl)-1H-1,2,4-triazol-5-yl]pyridine (122)



$^1\text{H NMR}$ (d_6 -DMSO): 8.80 (d, 1H, $J = 4.4$ Hz, -a), 8.35 (s, 1H, -e), 7.89 – 7.67 (overlapping m, 3H, -h, b, and d), 7.38 (m, 1H, -c), 7.10 (d, 2H, $J = 8.2$ Hz, -f and g), 6.12 (d, 2H, $J = 8.8$ Hz, triazole -NH), 4.47

(t, 2H, J = 6.5 Hz, $-\text{OCH}_2(\text{CH}_2)_5\text{CH}_3$), 1.89 – 1.69 (overlapping m, 2H, $-\text{OCH}_2\text{CH}_2(\text{CH}_2)_4\text{CH}_3$), 1.49 – 1.11 (overlapping m, 8H, $-\text{OCH}_2\text{CH}_2(\text{CH}_2)_4\text{CH}_3$), 0.89 (t, 3H, J = 6.6 Hz, $-\text{OCH}_2(\text{CH}_2)_5\text{CH}_3$) ppm.

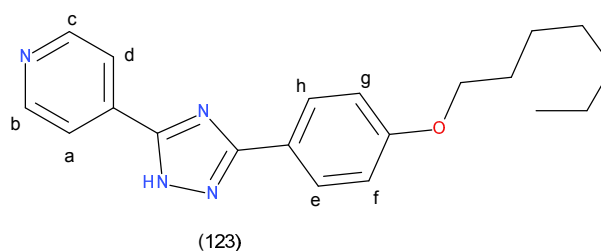
IR (neat) ν : cm^{-1} .

Melting point: 163.3 – 164.5 °C.

Mass spectrum (APCI +) m/z: Found 336.1938 ($\text{M}+\text{H}^+$); calculated for $\text{C}_{20}\text{H}_{24}\text{N}_4\text{O}$ 336.1950; 3.5 ppm.

Yield: 0.33 g, 68%.

4-[3-(4-Heptoxyphenyl)-1H-1,2,4-triazol-5-yl]pyridine (123)



^1H NMR ($\text{d}_6\text{-DMSO}$): 8.61 (d, J = 5.9 Hz, 2H, **-b and c**), 8.34 – 7.38 (overlapping m, 4H, **-a, d, e and h**), 7.35 (d, 2H, J = 8.8 Hz, **-f and g**), 6.06 (d, 1H, J = 8.8 Hz, **triazole -NH**), 4.58 (t, 2H, J = 6.5 Hz, $-\text{OCH}_2(\text{CH}_2)_5\text{CH}_3$), 1.99 – 1.74 (overlapping m, 2H, $-\text{OCH}_2\text{CH}_2(\text{CH}_2)_4\text{CH}_3$), 1.51 – 1.13 (overlapping m, 8H, $-\text{OCH}_2\text{CH}_2(\text{CH}_2)_4\text{CH}_3$), 0.94 (t, 3H, J = 6.6 Hz, $-\text{OCH}_2(\text{CH}_2)_5\text{CH}_3$) ppm.

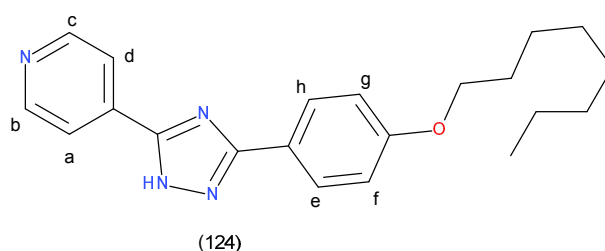
IR (neat) ν : 3162, 3033 (Aromatic C-H), 2942, 2852 (Alkyl C-H), 1689, 1609 (C=N), 1545 (N=N), 1506, 1455, 420, 1392, 1282, 1251, 1176, 1136, 1074, 1038, 1012 cm^{-1} .

Melting point: 97.3 – 98.2 °C.

Mass spectrum (APCI +) m/z: Found 336.1943 ($\text{M}+\text{H}^+$); calculated for $\text{C}_{20}\text{H}_{24}\text{N}_4\text{O}$ 336.1950; 2.0 ppm.

Yield: 0.39 g, 73.2%.

4-[3-(4-Octoxyphenyl)-1H-1,2,4-triazol-5-yl]pyridine (124)



$^1\text{H NMR}$ (d_6 -DMSO): 9.04 (d, 2H, $J = 6.0$ Hz, **-b and c**), 8.34 (s, 2H, **-a and d**), 7.85 – 7.70 (overlapping m, 4H, **-e and h**), 7.09 (d, 2H, $J = 8.8$ Hz, **-f and g**), 6.42 (s, 1H, **triazole -NH**), 4.12 (t, 3H, $J = 6.5$ Hz, **-OCH₂(CH₂)₆CH₃**), 1.96 – 1.71 (dq, 2H, $J = 14.4, 7.3$ Hz, **-OCH₂CH₂(CH₂)₅CH₃**), 1.38 (overlapping m, 10H, **-OCH₂CH₂(CH₂)₅CH₃**), 0.91 (t, 3H, $J = 7.3$ Hz, **-OCH₂(CH₂)₆CH₃**) ppm.

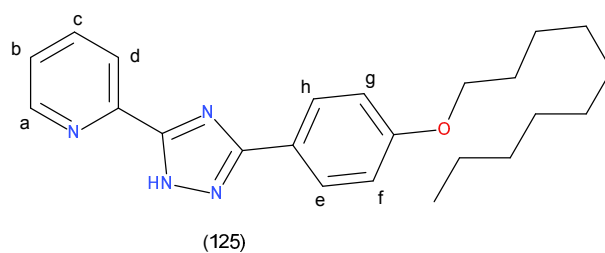
IR (neat) ν : 3106 (Aromatic C-H), 3057 (Aromatic C-H), 2930, 2854 (Alkyl C-H), 1712, 1608, 1575 (C=N), 1565 (N=N), 1505, 1473, 1453, 1419, 1406, 1391, 1329, 1300, 1280, 1249, 1171, 1136, 1063, 1043, 1016, 1000 cm^{-1} .

Melting point: 141.9 – 143.1 $^{\circ}\text{C}$.

Mass spectrum (APCI +) m/z : Found 350.2099 ($\text{M}+\text{H}$) $^{+}$; calculated for $\text{C}_{21}\text{H}_{26}\text{N}_4\text{O}$ 350.2106; 1.9 ppm.

Yield: 0.42 g, 75.4%.

2-[3-(4-Decoxyphenyl)-1H-1,2,4-triazol-5-yl]pyridine (125)



$^1\text{H NMR}$ (d_6 -DMSO): 8.75 (dd, 1H, $J = 25.1, 4.7$ Hz, **-a**), 8.49 (d, 2H, $J = 8.3$ Hz, **-c and d**), 7.82 (dd, 1H, $J = 15.8, 8.7$ Hz, **-b**), 7.39 (m, 1H, **-e**), 7.12 (d, 1H, $J = 9.0$ Hz, **-h**), 7.08 (d, 2H, $J = 8.8$ Hz, **-f and g**), 4.12 (t, 3H, $J = 6.5$ Hz, **-OCH₂(CH₂)₉CH₃**), 1.96 – 1.71 (dq, 2H, $J = 14.4, 7.3$ Hz, **-OCH₂CH₂(CH₂)₈CH₃**), 1.38 (overlapping m, 10H, **-OCH₂CH₂(CH₂)₈CH₃**), 0.91 (t, 3H, $J = 7.3$ Hz, **-OCH₂(CH₂)₉CH₃**) ppm.

g), 6.46 (s, 1H, **triazole -NH**), 4.04 (t, 2H, J = 6.5 Hz, $-\text{OCH}_2(\text{CH}_2)_9\text{CH}_3$), 1.68 (dt, 2H, J = 14.8, 5.6 Hz, $-\text{OCH}_2\text{CH}_2(\text{CH}_2)_8\text{CH}_3$), 1.34 – 1.01 (overlapping m, 16H, $-\text{OCH}_2\text{CH}_2(\text{CH}_2)_8\text{CH}_3$), 0.83 (d, 3H, J = 6.8 Hz, $-\text{OCH}_2(\text{CH}_2)_9\text{CH}_3$) ppm.

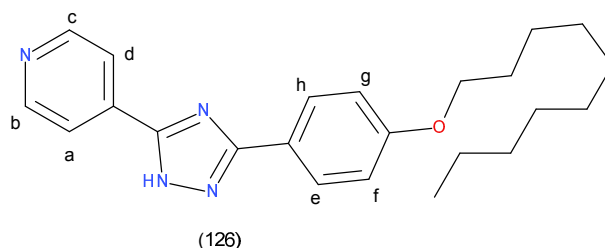
IR (neat) ν : 3175, 3086 (Aromatic C-H), 3047 (Aromatic C-H), 2921 (Alkyl C-H), 2850 (Alkyl C-H), 1711, 1661, 1606 (C=N), 1582 (N=N), 1552, 1532, 1510, 1494, 1462, 1440, 1426, 1392, 1369, 132, 1248, 1166, 1140, 1106, 1074, 1047, 1028, 1007 cm^{-1} .

Melting point: 108.3 – 109.4 °C.

Mass spectrum (APCI +) m/z: Found 378.2412 (M+H)⁺; calculated for $\text{C}_{23}\text{H}_{30}\text{N}_4\text{O}$ 378.2419; 1.8 ppm.

Yield: 0.31 g, 62.1%.

4-[3-(4-Decoxyphenyl)-1H-1,2,4-triazol-5-yl]pyridine (126)



$^1\text{H NMR}$ ($\text{d}_6\text{-DMSO}$): 8.70 (d, 2H, J = 5.9 Hz, **-b and c**), 8.38 (d, 2H, J = 8.3 Hz, **-a and d**) 8.20 – 7.43 (overlapping m, 4H, **-e, h, f and g**), 6.74 (m, 1H, **triazole -NH**), 4.43 – 4.04 (t, 2H, J = 6.4 Hz, $-\text{OCH}_2(\text{CH}_2)_8\text{CH}_3$), 2.18 (dd, 2H, J = 13.9, 6.5 Hz, $-\text{OCH}_2\text{CH}_2(\text{CH}_2)_7\text{CH}_3$), 1.57 – 1.03 (overlapping m, 14H, $-\text{OCH}_2\text{CH}_2(\text{CH}_2)_7\text{CH}_3$), 0.89 (t, 3H, J = 6.5 Hz, $-\text{OCH}_2(\text{CH}_2)_8\text{CH}_3$) ppm.

IR (neat) ν : 3106, 3070 (Aromatic C-H), 3041 (Aromatic C-H), 2944 (Alkyl C-H), 2919 (Alkyl C-H), 2845, 2789, 1614 (C=N), 1574, 1525 (N=N), 1505, 1453, 1422, 1406, 1394, 1298, 1285, 1252, 1211, 1174, 1138, 1114, 1053, 1033, 1021, 1003 cm^{-1} .

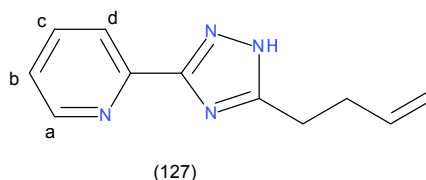
Melting point: 125.1 – 125.9 °C.

Mass spectrum (APCI +) m/z: Found 378.2407 (M+H)⁺; calculated for $\text{C}_{23}\text{H}_{30}\text{N}_4\text{O}$ 378.2419; 3.1

ppm.

Yield: 0.26 g, 57.1%.

2-(5-But-3-enyl-1H-1,2,4-triazol-3-yl)pyridine (127)



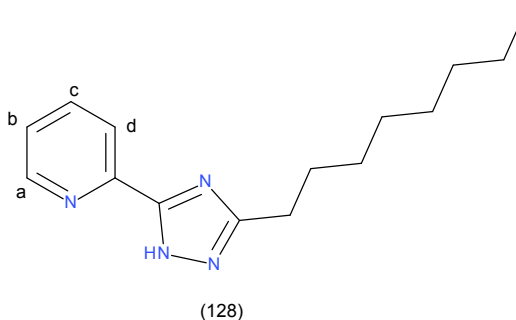
¹H NMR (d₆-DMSO): 8.65 (d, 1H, J = 4.1 Hz, **-a**), 8.04 (d, 1H, J = 7.9 Hz, **-c**), 7.92 (s, 1H, **-b**), 7.44 (s, 1H, **-d**), 5.89 (ddt, 1H, J = 16.8, 10.2, 6.4 Hz, **-CH₂CH₂CH=CH₂**), 5.21 – 4.87 (overlapping m, 2H, **-CH₂CH₂CH=CH₂**), 4.28 (s, 1H, **triazole -NH**), 2.82 (t, 2H, J = 6.5 Hz, **-CH₂CH₂CH=CH₂**), 2.59 – 2.38 (overlapping m, 2H, **-CH₂CH₂CH=CH₂**) ppm.

IR (neat) ν : 3055 (Aromatic C-H), 2975 (Aromatic C-H), 2943 (Alkyl C-H), 2897 (Alkyl C-H), 2791 (Alkyl C-H), 1778, 1638 (C=N), 1593, 1570 (N=N), 1542, 1518, 1459, 1416, 1374, 1340, 1319, 1294, 1278, 1245, 1207, 1174, 1149, 1127, 1119, 1089, 1052, 1016 cm⁻¹.

Mass spectrum(APCI +) m/z: Found 200.1056 (M+H)⁺; calculated for C₁₁H₁₂N₄ 200.1061; 2.4 ppm.

Yield: 0.08 g, 20.3%.

2-(3-Heptyl-1H-1,2,4-triazol-5-yl)pyridine (128)



¹H NMR (d₆-DMSO): 8.65 (d, 1H, J = 3.4 Hz, **-a**), 8.03 (d, 1H, J = 7.7 Hz, **-c**), 7.92 (s, 1H, **-b**), 7.45 (s, 1H, **-d**), 4.43 (s, 1H, **triazole -NH**), 2.70 (t, 2H, J = 6.5 Hz, **-CH₂CH₂(CH₂)₄CH₃**), 1.89 – 1.55 (overlapping m, 2H, **-CH₂CH₂(CH₂)₄CH₃**), 1.28 (dd, 8H, J = 9.1, 4.4 Hz, **-CH₂CH₂(CH₂)₄CH₃**), 0.85 (t, 3H, J = 6.7 Hz, **-CH₂CH₂(CH₂)₄CH₃**) ppm.

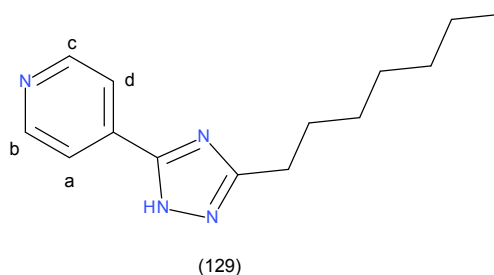
IR (neat) ν : 3148 (Aromatic C-H), 3107 (Aromatic C-H), 2948 (Alkyl C-H), 2923 (Alkyl C-H), 2847 (Alkyl C-H), 1665, 1597, 1573, 1556 (N=N), 1448, 1462, 1446, 1427, 1377, 1320, 1293, 1272, 1247, 1207, 1150, 1128, 1092, 1055, 1011 cm⁻¹.

Melting point: 49.1 – 50.7 °C.

Mass spectrum(APCI +) m/z: Found 244.1681 (M+H)⁺; calculated for C₁₄H₂₀N₄ 244.1687; 2.4 ppm.

Yield: 0.22 g, 33.1%.

4-(3-Heptyl-1H-1,2,4-triazol-5-yl)pyridine (129)



¹H NMR (d₆-DMSO): 8.65 (d, 2H, J = 4.5 Hz, **-b and c**), 8.12 – 7.73 (overlapping m, 2H, **-a and d**), 4.43 (s, 1H, **triazole -NH**), 2.80 (t, 2H, J = 6.5 Hz, **-CH₂CH₂(CH₂)₄CH₃**), 1.73 (s, 2H, **-CH₂CH₂(CH₂)₄CH₃**), 1.30 (s, 8H, **-CH₂CH₂(CH₂)₄CH₃**), 0.85 (s, 3H, **-CH₂CH₂(CH₂)₄CH₃**) ppm.

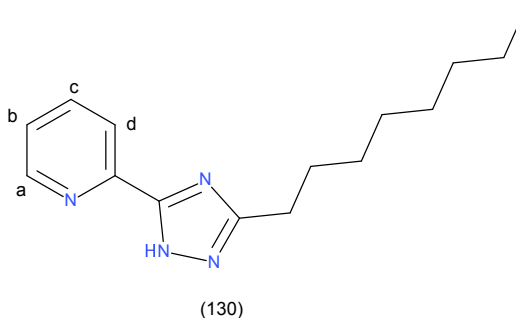
IR (neat) ν : 3219 (Aromatic C-H), 3044 (Aromatic C-H), 2952 (Aromatic C-H), 2923 (Alkyl C-H), 2850 (Alkyl C-H), 1611, 1595 (C=N), 1547 (N=N), 1485, 1467, 1455, 1438, 1416, 1388, 1348, 1325, 1307, 1284, 1258, 1238, 1212, 1193, 1170, 1111, 1061, 1044, 1026, 1000 cm⁻¹.

Melting point: 104.2 – 106.8 °C.

Mass spectrum(APCI +) m/z: Found 244.1673 (M+H)⁺; calculated for C₁₄H₂₀N₄ 244.1687; 5.7 ppm.

Yield: 0.31 g, 62.4%.

2-(3-Octyl-1H-1,2,4-triazol-5-yl)pyridine (130)



¹H NMR (d₆-DMSO): 8.65 (d, 1H, J = 4.4 Hz, **-a**), 8.03 (d, 1H, J = 7.8 Hz, **-c**), 7.91 (s, 1H, **-b**), 7.44 (s, 1H, **-d**), 4.27 (s, 1H, **triazole -NH**), 2.71 (t, 2H, J = 6.5 Hz, **-CH₂(CH₂)₆CH₃**), 1.70 (dd, 2H, J = 14.4, 7.2 Hz, **-CH₂CH₂(CH₂)₅CH₃**), 1.39 – 1.20 (overlapping m, 10H, **-CH₂CH₂(CH₂)₅CH₃**), 0.86 (dd, 3H, J = 9.2, 4.3 Hz, **-CH₂(CH₂)₆CH₃**) ppm.

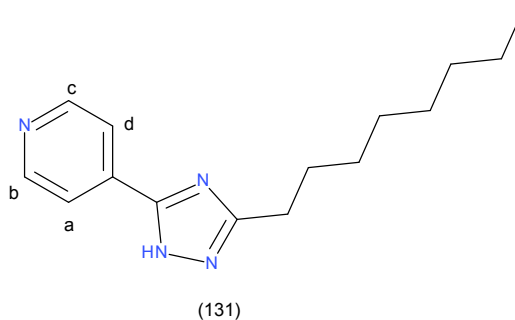
IR (neat) ν : 3180 (Aromatic C-H), 3106 (Aromatic C-H), 3048 (Aromatic C-H), 2948 (Alkyl C-H), 2919 (Alkyl C-H), 2867 (Alkyl C-H), 2846 (Alkyl C-H), 1667, 1598 (C=N), 1572 (N=N), 1555, 1493, 1480, 1463, 1440, 1423, 1375, 1350, 1314, 1291, 1259, 1244, 1221, 1146, 1131, 1092, 1047, 1019, 1010 cm⁻¹.

Melting point: 65.9 – 67.1 °C.

Mass spectrum (APCI +) m/z: Found 258.1852 (M+H)⁺; calculated for C₁₅H₂₂N₄ 258.1844; 3.0 ppm.

Yield: 0.33 g, 69%.

4-(3-Octyl-1H-1,2,4-triazol-5-yl)pyridine (131)



$^1\text{H NMR}$ ($\text{d}_6\text{-DMSO}$): 8.64 (d, 2H, $J = 5.1$ Hz, **-b and c**), 7.89 (dd, 2H, $J = 4.5, 1.6$ Hz, **-a and d**), 4.76 (s, 1H, **triazole -NH**), 1.71 (t, 2H, $J = 6.5$ Hz, **$-\text{CH}_2(\text{CH}_2)_6\text{CH}_3$**), 1.51 (s, 2H, **$-\text{CH}_2\text{CH}_2(\text{CH}_2)_5\text{CH}_3$**), 1.28 (d, 10H, $J = 11.2$ Hz, **$-\text{CH}_2\text{CH}_2(\text{CH}_2)_5\text{CH}_3$**), 0.91 – 0.79 (overlapping m, 3H, **$-\text{CH}_2(\text{CH}_2)_6\text{CH}_3$**) ppm.

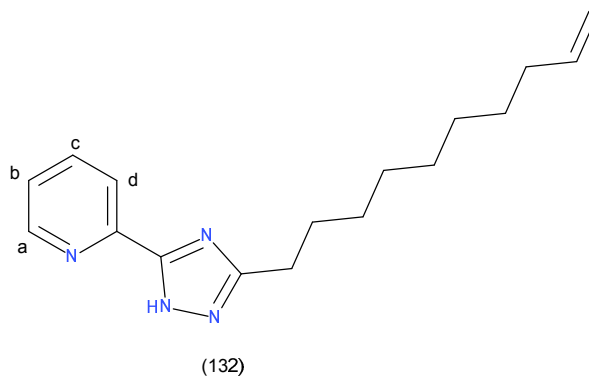
IR (neat) ν : 3217 (Aromatic C-H), 3045 (Aromatic C-H), 2956 (Aromatic C-H), 2919 (Alkyl C-H), 2848 (Alkyl C-H), 1595 (C=N), 1559 (N=N), 1496, 1479, 1462, 1412, 1390, 1283, 1262, 1223, 1189, 1111, 1058, 1034, 1002 cm^{-1} .

Melting point: 101.2 – 103.3 $^\circ\text{C}$.

Mass spectrum (APCI +) m/z : Found 258.1838 ($\text{M}+\text{H}^+$); calculated for $\text{C}_{15}\text{H}_{22}\text{N}_4$ 258.1844; 2.3 ppm.

Yield: 0.42 g, 73.2%.

2-(3-Dec-9-enyl-1H-1,2,4-triazol-5-yl)pyridine (132)



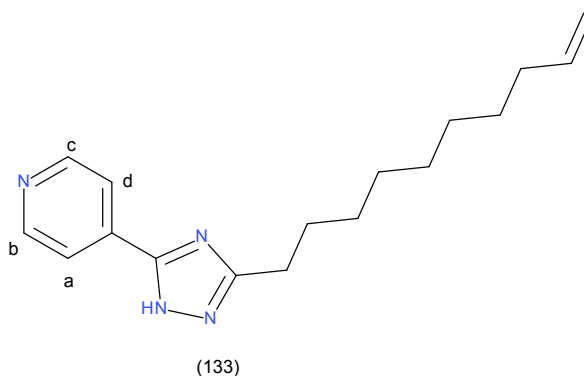
¹H NMR (d₆-DMSO): 8.65 (m, 1H, **-a**), 8.04 (d, 1H, J = 7.9 Hz, **-c**), 7.89 (dd, 1H, J = 11.6, 3.8 Hz, **-b**), 7.44 (m, 1H, **-d**), 5.77 (ddt, 1H, J = 16.9, 10.1, 6.6 Hz, **triazole -NH**), 4.96 (m, 1H, -CH₂(CH₂)₇**CH=CH₂**), 4.36 (dd, 2H, J = 16.7, 11.7 Hz, -CH₂(CH₂)₇**CH=CH₂**), 2.71 (t, 2H, J = 7.5 Hz, **-CH₂-(CH₂)₇CH=CH₂**), 1.98 (t, 2H, J = 6.4 Hz, -CH₂(CH₂)₆-**CH₂CH=CH₂**), 1.79 – 1.68 (overlapping m, 2H, -CH₂**CH₂**(CH₂)₅-CH₂CH=CH₂), 1.41 – 0.99 (overlapping m, 10H, -CH₂CH₂(**CH₂**)₅CH₂CH=CH₂) ppm.

IR (neat) ν : 3175 (Aromatic C-H), 3073 (Aromatic C-H), 2924 (Alkyl C-H), 2853 (Alkyl C-H), 2322, 1976, 1737, 1639 (C=N), 1595, 1573 (N=N), 1556, 1514, 1464, 1417, 1387, 1324, 1279, 1246, 1177, 1148, 1088, 1043, 1002 cm⁻¹.

Mass spectrum(APCI +) m/z: Found 284.2019 (M+H)⁺; calculated for C₁₇H₂₄N₄ 284.2000; 6.6 ppm.

Yield: 0.13 g, 27.2%.

4-(3-Dec-9-enyl-1H-1,2,4-triazol-5-yl)pyridine (133)



¹H NMR (d₆-DMSO): 8.64 (dd, 2H, J = 4.5, 1.6 Hz, **-b and c**), 7.89 (dd, 2H, J = 4.5, 1.6 Hz, **-a and d**), 5.80 (m, 1H, **triazole -NH**), 5.08 (m, 1H, -CH₂(CH₂)₇**CH=CH₂**), 4.85 (dd, 2H, J = 16.7, 11.7 Hz, -CH₂(CH₂)₇**CH=CH₂**), 2.76 (t, 2H, J = 7.5 Hz, **-CH₂-(CH₂)₇CH=CH₂**), 2.08 – 1.93 (overlapping m, 2H, -CH₂(CH₂)₆-**CH₂CH=CH₂**), 1.71 (dd, 2H, J = 14.4, 7.2 Hz, -CH₂**CH₂**(CH₂)₅-CH₂CH=CH₂), 1.29 (d, 10H, J = 1.9 Hz, -CH₂CH₂(**CH₂**)₅CH₂CH=CH₂) ppm.

IR (neat) ν : 3222 (Aromatic C-H), 3047 (Aromatic C-H), 2922 (Alkyl C-H), 2849 (Alkyl C-H), 2555, 1640 (C=N), 1612, 1597, 1580, 1549 (N=N), 1488, 1459, 1488, 1459, 1446, 1427, 1389, 1324, 1283, 1267, 1212, 1172, 1112, 1057, 1037, 1020, 1001 cm⁻¹.

Melting point: 87.3 – 88.4 °C.

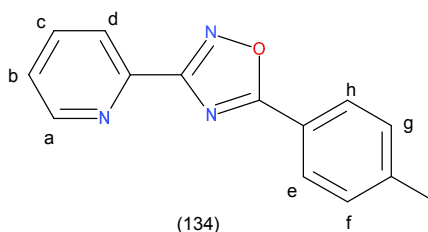
Mass spectrum(APCI +) m/z: Found 284.2029 (M+H)⁺; calculated for C₁₇H₂₄N₄ 284.2000; 10.2 ppm.

Yield: 0.24 g, 46.4%.

3.5.4 General procedure for synthesis of 1,2,4-oxadiazole from aldoxime

The dry powder of aldoxime (0.2 g) was heated in a borosilicate vial at 150°C for 30 mins. The dry powder melted and upon slow cooling to room temperature the crude compound precipitated out. The crude product was further purified by recrystallisation using water to methanol solvent system.

5-(p-Tolyl)-3-(2-pyridyl)-1,2,4-oxadiazole (134)



¹H NMR (d₆-DMSO): 8.79 (ddd, 1H, J = 4.8, 1.7, 0.9 Hz, **-a**), 8.21 – 8.02 (overlapping m, 3H, **-b, d and h**), 7.78 (ddd, 1H, J = 7.6, 4.8, 1.3 Hz, **-e**), 7.60 (d, 2H, J = 8.0 Hz, **-f and g**), 7.52 (m, 1H, **-c**), 2.44 (s, 3H, **-CH₃**) ppm.

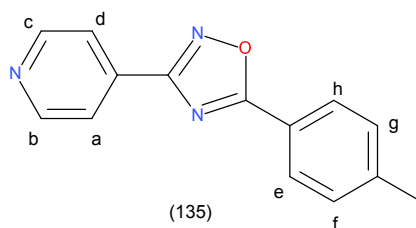
IR (neat) ν : 3070, 3032 (Aromatic C-H), 2918 (Alkyl C-H), 2851 (Alkyl C-H), 1625, 1608, 1598 (C=N), 1584, 1561, 1520, 1496, 1470, 1438, 1408, 1391, 1359, 1312, 1265, 1209 (C-O), 1180, 1153, 1124, 1083, 1045, 1019, 989, 958, 926, 910 (N-O), 865, 809, 753 cm⁻¹.

Melting point: 167.8 – 168.5 °C.

Mass spectrum(APCI +) m/z: Found 237.0897 (M+H)⁺; calculated for C₁₄H₁₁N₃O 237.0902; 2.1 ppm.

Yield: 0.14 g, 75.1%.

5-(p-Tolyl)-3-(4-pyridyl)-1,2,4-oxadiazole (135)



$^1\text{H NMR}$ (d_6 -DMSO): 9.09 – 8.61 (overlapping m, 2H, **-b and c**), 8.10 (d, 2H, $J = 8.2$ Hz, **-a and d**), 8.01 (dd, 2H, $J = 4.5, 1.5$ Hz, **-e and h**), 7.49 (d, 2H, $J = 8.2$ Hz, **-f and g**), 2.44 (s, 3H, **-CH₃**) ppm.

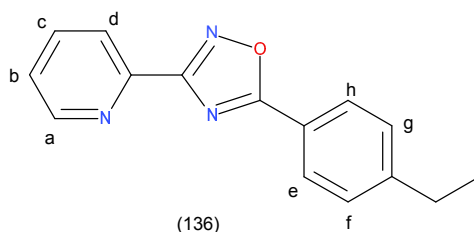
IR (neat) ν : 3068, 3024 (Aromatic C-H), 2924 (Alkyl C-H), 1704, 1611, 1598 (C=N), 1581, 1561, 1517, 1500, 1458, 1412, 1365, 1300, 1297, 1288, 1271, 1244, 1180, 1136 (C-O), 1109, 1071, 1060, 1032, 1015, 989, 961, 929, 910 (N-O), 872, 835, 826, 749 cm^{-1} .

Melting point: 181.8 – 182.6 $^{\circ}\text{C}$.

Mass spectrum(APCI +) **m/z**: Found 237.0908 ($\text{M}+\text{H}$) $^{+}$; calculated for $\text{C}_{14}\text{H}_{11}\text{N}_3\text{O}$ 237.0902; 2.5 ppm.

Yield: 0.09 g, 68.1%.

5-(4-Ethylphenyl)-3-(4-pyridyl)-1,2,4-oxadiazole (136)



$^1\text{H NMR}$ (d_6 -DMSO): 8.79 (ddd, 1H, $J = 4.7, 1.6, 0.9$ Hz, **-a**), 8.40 – 8.23 (overlapping m, 3H, **-b, d and h**), 7.80 (m, 1H, **-e**), 7.61 (d, 2H, $J = 8.3$ Hz, **-f and g**), 7.52 (m, 1H, **-c**), 2.72 (dt, 2H, $J = 10.9, 5.5$ Hz, **-CH₂CH₃**), 1.25 (t, 3H, $J = 7.5$ Hz, **-CH₂CH₃**) ppm.

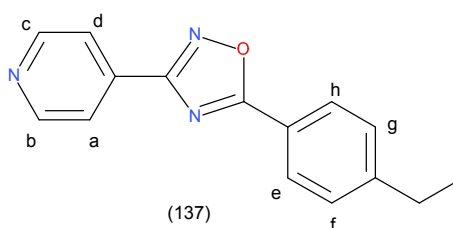
IR (neat) ν : 3049 (Aromatic C-H), 2968, 2878 (Alkyl C-H), 1675, 1611, 1598 (C=N), 1582, 1556, 1513, 1488, 1466, 1420, 1375, 1300, 1275, 1245, 1185 (C-O), 1159, 1125, 1087, 1049, 1012, 986, 965, 931, 910 (N-O), 888, 856, 810, 762 cm^{-1} .

Melting point: 143.2 – 144.4 $^{\circ}\text{C}$.

Mass spectrum(APCI +) m/z: Found 251.1047 ($\text{M}+\text{H}^+$); calculated for $\text{C}_{15}\text{H}_{13}\text{N}_3\text{O}$ 251.1058; 4.3 ppm.

Yield: 0.1 g, 71.3%.

5-(4-Ethylphenyl)-3-(4-pyridyl)-1,2,4-oxadiazole (137)



^1H NMR ($\text{d}_6\text{-DMSO}$): 9.00 – 8.78 (overlapping m, 2H, **-b and c**), 8.15 (t, 2H, $J = 6.4$ Hz, **-a and d**), 8.07 – 7.97 (overlapping m, 2H, **-e and h**), 7.53 (d, 2H, $J = 8.3$ Hz, **-f and g**), 2.74 (q, 2H, $J = 7.6$ Hz, **$-\text{CH}_2\text{CH}_3$**), 1.24 (t, 3H, $J = 7.6$ Hz, **$-\text{CH}_2\text{CH}_3$**) ppm.

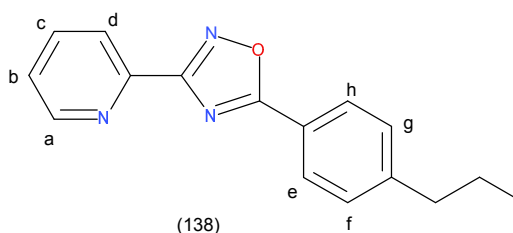
IR (neat) ν : 3041 (Aromatic C-H), 2973, 2929 (Alkyl C-H), 2889 (Alkyl C-H), 1716, 1611, 1598 (C=N), 1588, 1566, 1553, 1520, 1500, 1466, 1423, 1414, 1367, 1277, 1216, 1180 (C-O), 1141, 1123, 1080, 1064, 1056, 1020, 988, 976, 968, 910 (N-O), 844, 833, 779 cm^{-1} .

Melting point: 127.8 – 129.3 $^{\circ}\text{C}$.

Mass spectrum(APCI +) m/z: Found 251.1045 ($\text{M}+\text{H}^+$); calculated for $\text{C}_{15}\text{H}_{13}\text{N}_3\text{O}$ 251.1058; 5.1 ppm.

Yield: 0.08 g, 47.2%.

5-(4-Propylphenyl)-3-(2-pyridyl)-1,2,4-oxadiazole (138)



$^1\text{H NMR}$ ($\text{d}_6\text{-DMSO}$): 8.80 (ddd, 1H, $J = 4.8, 1.7, 0.9$ Hz, **-a**), 8.38 – 7.92 (overlapping m, 4H, **-b, d, e and h**), 7.64 (ddd, 2H, $J = 7.6, 4.8, 1.3$ Hz, **-f and g**), 7.50 (d, 1H, $J = 8.3$ Hz, **-c**), 2.68 (t, 2H, $J = 7.5$ Hz, **-CH₂CH₂CH₃**), 1.77 – 1.50 (overlapping m, 2H, **-CH₂CH₂CH₃**), 0.92 (t, 3H, $J = 7.3$ Hz, **-CH₂CH₂CH₃**) ppm.

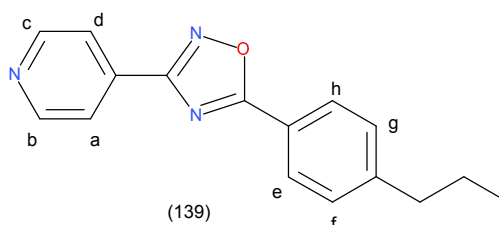
IR (neat) ν : 3422, 3065, 3032 (Aromatic C-H), 2956, 2921 (Alkyl C-H), 2865 (Alkyl C-H), 1675, 1611, 1598 (C=N), 1578, 1558, 1517, 1493, 1467, 1461, 1414 1362, 1288, 1271, 1186, 1159, 1118 (C-O), 1092, 1048, 1019, 998, 962, 929, 910 (N-O), 867, 849, 808, 761 cm^{-1} .

Melting point: 154.3 – 155.1 °C.

Mass spectrum (APCI +) m/z : Found 265.1220 ($\text{M}+\text{H}$)⁺; calculated for $\text{C}_{16}\text{H}_{15}\text{N}_3\text{O}$ 265.1215; 1.8 ppm.

Yield: 0.07 g, 46.3%.

5-(4-Propylphenyl)-3-(4-pyridyl)-1,2,4-oxadiazole (139)



$^1\text{H NMR}$ ($\text{d}_6\text{-DMSO}$): 8.80 (ddd, 1H, $J = 4.8, 1.7, 0.9$ Hz, **-b and c**), 8.38 – 7.92 (overlapping m, 2H, **-a and d**), 7.64 (ddd, 2H, $J = 7.6, 4.8, 1.3$ Hz, **-e and h**), 7.50 (d, 2H, $J = 8.3$ Hz, **-f and g**), 2.68 (t,

2H, J = 7.5 Hz, **-CH₂CH₂CH₃**), 1.77 – 1.50 (overlapping m, 2H, **-CH₂CH₂CH₃**), 0.92 (t, 3H, J = 7.3 Hz, **-CH₂CH₂CH₃**) ppm.

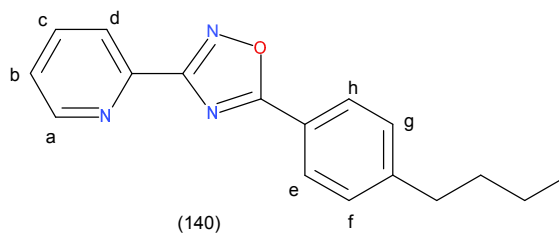
IR (neat) ν : 3041 (Aromatic C-H), 2956, 2930 (Alkyl C-H), 2868 (Alkyl C-H), 1713, 1611, 1598 (C=N), 1584, 1555, 1523, 1501, 1467, 1416, 1368, 1321, 1303, 1271, 1221, 1180 (C-O), 1136, 987, 966, 946, 910 (N-O), 878, 829, 815, 796 cm^{-1} .

Melting point: 121.3 – 122.9 °C.

Mass spectrum(APCI +) m/z: Found 265.1228 (M+H)⁺; calculated for C₁₆H₁₅N₃O 265.1215; 4.9 ppm.

Yield: 0.14 g, 81.8%.

5-(4-Butylphenyl)-3-(2-pyridyl)-1,2,4-oxadiazole (140)



¹H NMR (d₆-DMSO): 8.80 (m, 1H, **-a**), 8.46 – 7.87 (overlapping m, 4H, **-b, d, e and h**), 7.63 (ddd, 1H, J = 7.5, 4.8, 1.2 Hz, **-c**), 7.50 (d, 2H, J = 8.1 Hz, **-f and g**), 2.71 (t, 2H, J = 7.5 Hz, **-CH₂(CH₂)₂CH₃**), 1.60 (dt, 2H, J = 15.4, 7.6 Hz, **-CH₂CH₂CH₂CH₃**), 1.32 (dq, 2H, J = 14.7, 7.3 Hz, **-(CH₂)₂CH₂CH₃**), 0.91 (t, 3H, J = 7.3 Hz, **-(CH₂)₃CH₃**) ppm.

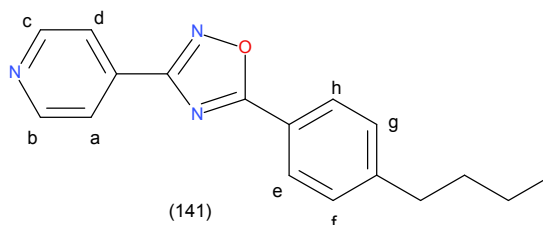
IR (neat) ν : 3428, 3044 (Aromatic C-H), 2959, 2930 (Alkyl C-H), 2856 (Alkyl C-H), 1675, 1611, 1598 (C=N), 1581, 1555, 1514, 1493, 1456, 1414, 1367, 1277, 1247, 1186 (C-O), 1156, 1124, 1098, 1048, 1019, 995, 955, 933, 910 (N-O), 865, 839, 803, 761 cm^{-1} .

Melting point: 156.3 – 157.7 °C.

Mass spectrum(APCI +) m/z: Found 279.1368 (M+H)⁺; calculated for C₁₇H₁₇N₃O 279.1371; 1.0 ppm.

Yield: 0.1 g, 63.1%.

5-(4-Butylphenyl)-3-(4-pyridyl)-1,2,4-oxadiazole (141)



¹H NMR (d₆-DMSO): 8.84 (dd, 2H, J = 4.4, 1.6 Hz, **-b and c**), 8.12 (d, 2H, J = 8.3 Hz, **-a and d**), 8.02 (dd, 2H, J = 4.4, 1.6 Hz, **-e and h**), 7.50 (d, 2H, J = 8.3 Hz, **-f and g**), 2.70 (t, 2H, J = 7.5 Hz, **-CH₂(CH₂)₂CH₃**), 1.60 (dt, 2H, J = 12.7, 7.4 Hz, **-CH₂CH₂CH₂CH₃**), 1.33 (dq, 2H, J = 14.2, 7.2 Hz, **-(CH₂)₂CH₂CH₃**), 1.01 – 0.78 (t, 3H, J = 7.3 Hz, **-(CH₂)₃CH₃**) ppm.

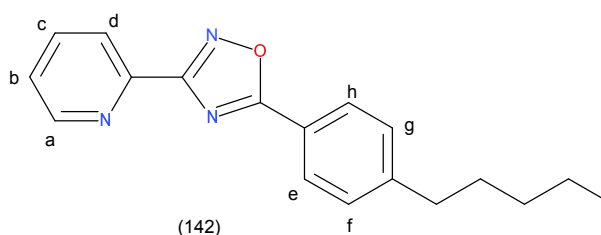
IR (neat) ν : 3050 (Aromatic C-H), 2950 (Alkyl C-H), 2930 (Alkyl C-H), 2865 (Alkyl C-H), 2854 (Alkyl C-H), 1681, 1611, 1598 (C=N), 1587, 1567, 1552, 1523, 1499, 1488, 1464, 1432, 1367, 1318, 1300, 1262, 1218, 1177, 1139, 1118 (C-O), 1104, 1065, 1022, 986, 965, 931, 910 (N-O), 888, 856, 810, 762 cm^{-1} .

Melting point: 147.3 – 148.6 °C.

Mass spectrum (APCI +) m/z: Found 279.1358 (M+H)⁺; calculated for C₁₇H₁₇N₃O 279.1371; 4.6 ppm.

Yield: 0.13 g, 78%.

5-(4-Pentylphenyl)-3-(2-pyridyl)-1,2,4-oxadiazole (142)



¹H NMR (d₆-DMSO): 8.80 (d, 1H, J = 3.9 Hz, **-a**), 8.11 (ddd, 4H, J = 17.7, 10.9, 7.0 Hz, **-b, d, e and h**), 7.64 (dd, 1H, J = 7.5, 4.8 Hz, **-c**), 7.50 (d, 2H, J = 8.1 Hz, **-f and g**), 2.70 (t, 2H, J = 7.5 Hz, **-CH₂(CH₂)₃CH₃**), 1.64 (d, 2H, J = 7.1 Hz, **-CH₂CH₂(CH₂)₂CH₃**), 1.31 (d, 4H, J = 3.3 Hz, **-(CH₂)₂(CH₂)₂CH₃**), 0.87 (t, 3H, J = 6.6 Hz, **-(CH₂)₄CH₃**) ppm.

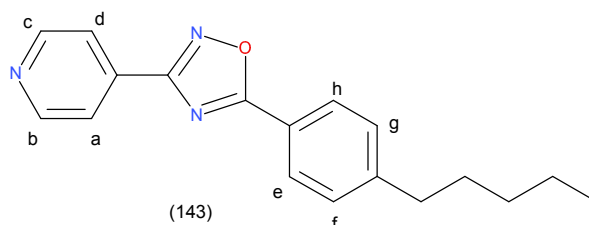
IR (neat) ν : 3109, 3059 (Aromatic C-H), 2941 (Alkyl C-H), 2924 (Alkyl C-H), 2900 (Alkyl C-H), 2865 (Alkyl C-H), 1690, 1611, 1598 (C=N), 1587, 1558, 1514, 1496, 1467, 1452, 1438, 1420, 1356, 1311, 1280, 1271, 1247, 1177, 1153, 1142, 1121 (C-O), 1095, 1071, 1045, 1027, 989, 971, 931, 910 (N-O), 872, 854, 811, 763 cm⁻¹.

Melting point: 165.2 – 166.8 °C.

Mass spectrum (APCI +) m/z: Found 293.1523 (M+H)⁺; calculated for C₁₈H₁₉N₃O 293.1528; 1.7 ppm.

Yield: 0.12 g, 75.3%.

5-(4-Pentylphenyl)-3-(4-pyridyl)-1,2,4-oxadiazole (143)



¹H NMR (d₆-DMSO): 8.84 (d, 2H, J = 6.0 Hz, **-b and c**), 8.12 (d, 1H, J = 8.2 Hz, **-a and d**), 8.02 (dd, 2H, J = 4.5, 1.6 Hz, **-e and h**), 7.51 (d, 2H, J = 8.2 Hz, **-f and g**), 2.69 (t, 2H, J = 7.5 Hz, **-CH₂(CH₂)₃CH₃**), 1.84 – 1.48 (overlapping m, 2H, **-CH₂CH₂(CH₂)₂CH₃**), 1.53 – 1.09 (overlapping m, 4H, **-(CH₂)₂(CH₂)₂CH₃**), 0.86 (t, 3H, J = 8.8, 4.7 Hz, **-(CH₂)₄CH₃**) ppm.

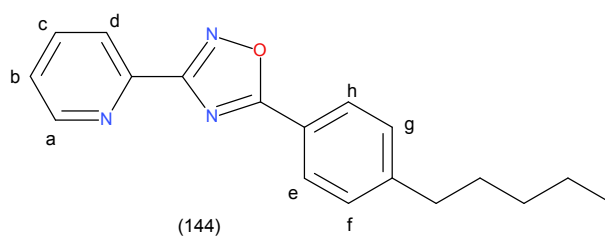
IR (neat) ν : 3047 (Aromatic C-H), 3024, 2953, 2921 (Alkyl C-H), 2854 (Alkyl C-H), 1716, 1675, 1611, 1598 (C=N), 1567, 1555, 1523, 1502, 1464, 1417, 1369, 1318, 1300, 1271, 1215, 1174, 1142, 1118 (C-O), 1104, 1063, 1039, 1019, 995, 963, 932, 910 (N-O), 845, 811, 755 cm⁻¹.

Melting point: 139.7 – 140.2 °C.

Mass spectrum(APCI +) m/z: Found 293.1531 (M+H)⁺; calculated for C₁₈H₁₉N₃O 293.1528; 1.0 ppm.

Yield: 0.12 g, 61.7%.

5-(4-Hexylphenyl)-3-(2-pyridyl)-1,2,4-oxadiazole (144)



¹H NMR (d₆-DMSO): 8.80 (d, 1H, J = 4.7 Hz, **-a**), 8.30 – 7.98 (overlapping m, 4H, **-b, d, e and h**), 7.64 (ddd, 1H, J = 7.5, 4.8, 1.2 Hz, **-c**), 7.50 (d, 2H, J = 8.2 Hz, **-f and g**), 2.70 (t, 2H, J = 7.6 Hz, **-CH₂(CH₂)₄CH₃**), 1.60 (d, 2H, J = 7.3 Hz, **-CH₂CH₂(CH₂)₃CH₃**), 1.41 – 1.17 (overlapping m, 6H, **-(CH₂)₂(CH₂)₃CH₃**), 0.87 (t, 3H, J = 6.9 Hz, **-(CH₂)₅CH₃**) ppm.

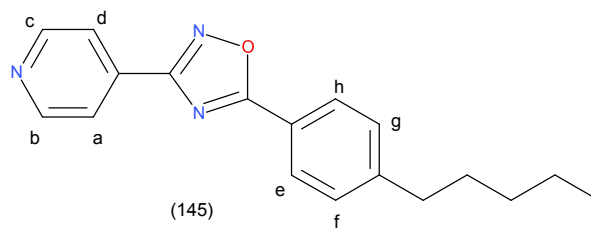
IR (neat) ν : 3050 (Aromatic C-H), 2953, 2921 (Alkyl C-H), 2854 (Alkyl C-H), 1672, 1611, 1598 (C=N), 1584, 1558, 1520, 1499, 1461, 1414, 1364, 1279, 1253, 1186, 1148, 1121 (C-O), 1089, 1042, 1016, 989, 963, 931, 910 (N-O), 872, 845, 812, 761 cm⁻¹.

Melting point: 138.8 – 139.5 °C.

Mass spectrum(APCI +) m/z: Found 307.1677 (M+H)⁺; calculated for C₁₉H₂₁N₃O 307.1684; 2.2 ppm.

Yield: 0.09 g, 57.6%.

5-(4-Hexylphenyl)-3-(4-pyridyl)-1,2,4-oxadiazole (145)



$^1\text{H NMR}$ ($\text{d}_6\text{-DMSO}$): 8.84 (dd, 2H, $J = 4.4, 1.6$ Hz, **-b and c**), 8.12 (d, 2H, $J = 8.3$ Hz, **-a and d**), 8.02 (dd, 2H, $J = 4.4, 1.6$ Hz, **-e and h**), 7.50 (d, 2H, $J = 8.3$ Hz, **-f and g**), 2.70 (t, 2H, $J = 7.6$ Hz, **$-\text{CH}_2(\text{CH}_2)_4\text{CH}_3$**), 1.75 – 1.48 (overlapping m, 2H, **$-\text{CH}_2\text{CH}_2(\text{CH}_2)_3\text{CH}_3$**), 1.43 – 1.09 (overlapping m, 6H, **$-(\text{CH}_2)_2(\text{CH}_2)_3\text{CH}_3$**), 0.85 (t, 3H, $J = 6.9$ Hz, **$-(\text{CH}_2)_5\text{CH}_3$**) ppm.

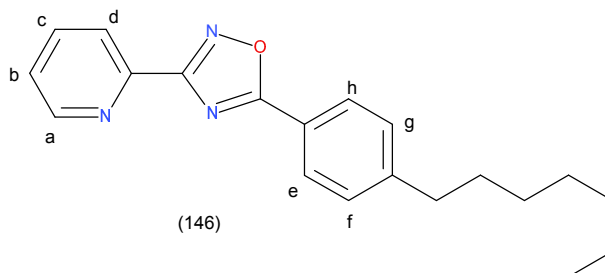
IR (neat) ν : 3167, 3041 (Aromatic C-H), 3024, 2959, 2918 (Alkyl C-H), 2868 (Alkyl C-H), 2848, 2689, 1713, 1611, 1598 (C=N), 1584, 1567, 1555, 1520, 1488, 1464, 1452, 1432, 1414, 1364, 1315, 1303, 1268, 1215, 1177, 1136, 1115 (C-O), 1068, 1060, 1039, 1022, 991, 973, 926, 910 (N-O), 868, 843, 823, 774 cm^{-1} .

Melting point: 135.4 – 136.9 $^\circ\text{C}$.

Mass spectrum (APCI +) m/z : Found 307.1692 ($\text{M}+\text{H}$) $^+$; calculated for $\text{C}_{19}\text{H}_{21}\text{N}_3\text{O}$ 307.1684; 2.6 ppm.

Yield: 0.12 g, 71.4%.

5-(4-Heptylphenyl)-3-(2-pyridyl)-1,2,4-oxadiazole (146)



¹H NMR (d₆-DMSO): 8.80 (d, 1H, J = 4.7 Hz, **-a**), 8.09 (ddd, 4H, J = 11.1, 9.5, 4.8 Hz, **-b, d, e and h**), 7.68 (m, 1H, **-c**), 7.50 (d, 2H, J = 8.2 Hz, **-f and g**), 2.70 (t, 2H, J = 7.5 Hz, **-CH₂(CH₂)₅CH₃**), 1.62 (t, 2H, J = 7.0 Hz, **-CH₂CH₂(CH₂)₄CH₃**), 1.27 (d, 8H, J = 11.5 Hz, **-(CH₂)₂(CH₂)₄CH₃**), 0.85 (t, 3H, J = 6.3 Hz, **-(CH₂)₆CH₃**) ppm.

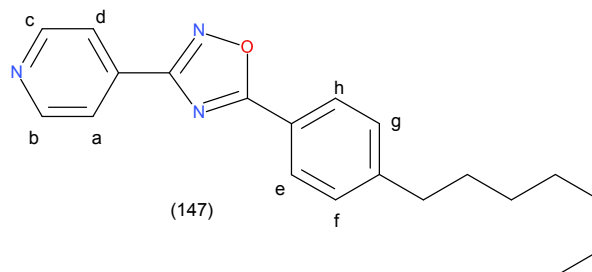
IR (neat) ν : 3053 (Aromatic C-H), 2953 (Alkyl C-H), 2925 (Alkyl C-H), 2850 (Alkyl C-H), 1681, 1613, 1598 (C=N), 1588, 1553, 1518, 1497, 1463, 1439, 1420, 1365, 1321, 1311, 1299, 1272, 1241, 1178 (C-O), 1145, 1120, 1087, 1041, 1009, 999, 984, 967, 945, 910 (N-O), 888, 856, 809, 766 cm⁻¹.

Melting point: 135.3 – 136.5 °C.

Mass spectrum(APCI +) m/z: Found 321.1835 (M+H)⁺; calculated for C₂₀H₂₃N₃O 321.1841; 1.8 ppm.

Yield: 0.13 g, 64.2%.

5-(4-Heptylphenyl)-3-(4-pyridyl)-1,2,4-oxadiazole (147)



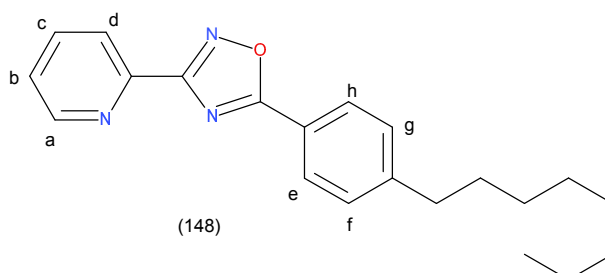
¹H NMR (d₆-DMSO): 8.84 (d, 2H, J = 5.0 Hz, **-b and c**), 8.12 (d, 2H, J = 8.2 Hz, **-a and d**), 8.02 (d, 2H, J = 5.9 Hz, **-e and h**), 7.50 (d, 2H, J = 8.3 Hz, **-f and g**), 2.70 (t, 2H, J = 7.5 Hz, **-CH₂(CH₂)₅CH₃**), 1.62 (s, 2H, **-CH₂CH₂(CH₂)₄CH₃**), 1.28 (dd, 8H, J = 7.7, 4.0 Hz, **-(CH₂)₂(CH₂)₄CH₃**), 0.85 (t, 3H, J = 6.7 Hz, **-(CH₂)₆CH₃**) ppm.

IR (neat) ν : 3044 (Aromatic C-H), 2956 (Alkyl C-H), 2921 (Alkyl C-H), 2848, 1611, 1598 (C=N), 1584, 1567, 1555, 1517, 1499, 1464, 1426, 1388, 1374, 1362, 1321, 1309, 1271, 1259, 1224, 1180 (C-O), 1136, 1124, 1101, 1074, 1063, 1041, 1025, 993, 968, 933, 910 (N-O), 893, 855, 807, 762 cm⁻¹.

Melting point: 151.6 – 152.9 °C.

Mass spectrum(APCI +) m/z: Found 321.1849 (M+H)⁺; calculated for C₂₀H₂₃N₃O 321.1841; 2.4 ppm.

5-(4-Octylphenyl)-3-(2-pyridyl)-1,2,4-oxadiazole (148)



¹H NMR (d₆-DMSO): 8.80 (d, 1H, J = 4.0 Hz, -a), 8.39 – 7.93 (overlapping m, 4H, -b, d, e and h), 7.64 (dd, 1H, J = 6.9, 5.4 Hz, -c), 7.50 (d, 2H, J = 8.2 Hz, -f and g), 2.70 (t, 2H, J = 7.6 Hz, -CH₂(CH₂)₆CH₃), 1.62 (s, 2H, -CH₂CH₂(CH₂)₅CH₃), 1.41 – 1.09 (overlapping m, 10H, -(CH₂)₂(CH₂)₅CH₃), 0.85 (t, 3H, J = 6.5 Hz, -(CH₂)₇CH₃) ppm.

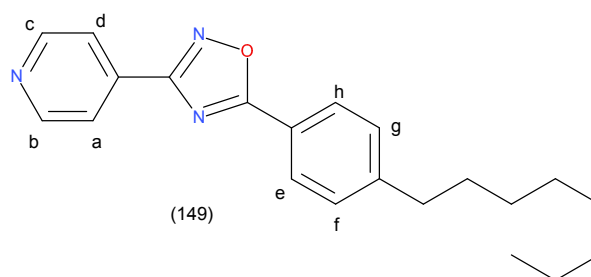
IR (neat) ν : 3053 (Aromatic C-H), 2950 (Alkyl C-H), 2921 (Alkyl C-H), 2848, 1611, 1598 (C=N), 1584, 1558, 1514, 1499, 1473, 1452, 1414, 1378, 1326, 1277, 1244, 1183 (C-O), 1156, 1121, 1095, 1039, 1022, 992, 971, 932, 910 (N-O), 872, 856, 811, 766 cm⁻¹.

Melting point: 135.4 – 137.3 °C.

Mass spectrum(APCI +) m/z: Found 335.1990 (M+H)⁺; calculated for C₂₁H₂₅N₃O 335.1997; 2.0 ppm.

Yield: 0.11 g, 58%.

5-(4-Octylphenyl)-3-(4-pyridyl)-1,2,4-oxadiazole (149)



$^1\text{H NMR}$ (d_6 -DMSO): 8.84 (d, 2H, $J = 5.8$ Hz, **-b and c**), 8.12 (d, 2H, $J = 8.1$ Hz, **-a and d**), 8.02 (d, 2H, $J = 6.0$ Hz, **-e and h**), 7.50 (d, 2H, $J = 8.1$ Hz, **-f and g**), 2.70 (t, 2H, $J = 7.6$ Hz, **-CH₂(CH₂)₆CH₃**), 1.88 – 1.50 (overlapping m, 2H, **-CH₂CH₂(CH₂)₅CH₃**), 1.48 – 1.04 (overlapping m, 10H, $J = 12.0$ Hz, **-(CH₂)₂(CH₂)₅CH₃**), 0.83 (t, 3H, $J = 6.4$ Hz, **-(CH₂)₇CH₃**) ppm.

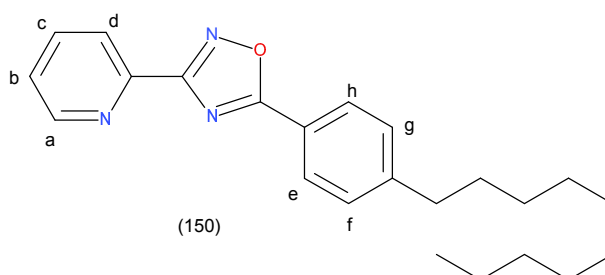
IR (neat) ν : 3035 (Aromatic C-H), 3024, 2944 (Alkyl C-H), 2927 (Alkyl C-H), 2845, 1713, 1669, 1611, 1598 (C=N), 1584, 1564, 1552, 1517, 1499, 1464, 1388, 1364, 1306, 1274, 1224, 1177 (C-O), 1139, 1124, 1112, 1077, 1063, 1016, 989, 967, 942, 910 (N-O), 875, 827, 812, 793 cm^{-1} .

Melting point: 129.4 – 130.8 °C.

Mass spectrum (APCI +) m/z : Found 335.1205 ($M+H$)⁺; calculated for $C_{21}H_{25}N_3O$ 335.1997; 3.8 ppm.

Yield: 0.09 g, 49.4%.

5-(4-Decylphenyl)-3-(2-pyridyl)-1,2,4-oxadiazole (150)



¹H NMR (d₆-DMSO): 8.80 (d, 1H, J = 4.1 Hz, **-a**), 8.38 – 7.93 (overlapping m, 4H, **-b, d, e and h**), 7.69 (m, 1H, **-c**), 7.50 (d, 2H, J = 8.3 Hz, **-f and g**), 2.70 (t, 2H, J = 7.6 Hz, **-CH₂(CH₂)₈CH₃**), 1.78 – 1.44 (overlapping m, 2H, **-CH₂CH₂(CH₂)₇CH₃**), 1.42 – 1.13 (overlapping m, 14H, J = 15.3 Hz, **-(CH₂)₂(CH₂)₇CH₃**), 0.84 (t, 3H, J = 6.5 Hz, **-(CH₂)₉CH₃**) ppm.

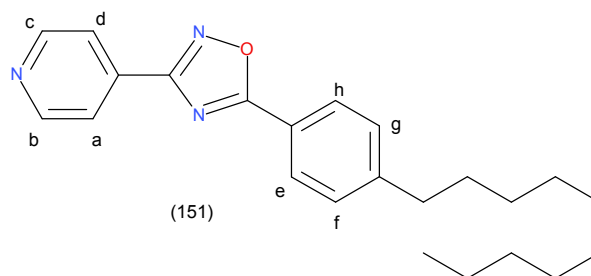
IR (neat) ν : 3050 (Aromatic C-H), 2953 (Alkyl C-H), 2918 (Alkyl C-H), 2868 (Alkyl C-H), 2845, 1611, 1598 (C=N), 1581, 1555, 1520, 1499, 1461, 1452, 1441, 1423, 1367, 1417, 1312, 1297, 1288, 1271, 1244, 1183, 1156, 1145, 1115 (C-O), 1098, 1074, 1045, 1016, 992, 967, 939, 910 (N-O), 888, 835, 807, 786 cm⁻¹.

Melting point: 156.7 – 159.1 °C.

Mass spectrum(APCI +) m/z: Found 363.2323 (M+H)⁺; calculated for C₂₃H₂₉N₃O 363.2310; 3.5 ppm.

Yield: 0.13 g, 64%.

5-(4-Decylphenyl)-3-(4-pyridyl)-1,2,4-oxadiazole (151)



¹H NMR (d₆-DMSO): 8.84 (t, 2H, J = 6.0 Hz, **-b and c**), 8.12 (d, 2H, J = 8.2 Hz, **-a and d**), 8.02 (d, 2H, J = 6.1 Hz, **-e and h**), 7.50 (d, 2H, J = 8.1 Hz, **-f and g**), 2.70 (t, 2H, J = 7.6 Hz, **-CH₂(CH₂)₈CH₃**), 1.82 – 1.50 (overlapping m, 2H, **-CH₂CH₂(CH₂)₇CH₃**), 1.47 – 1.07 (overlapping m, 14H, J = 14.8 Hz, **-(CH₂)₂(CH₂)₇CH₃**), 0.83 (t, 3H, J = 6.5 Hz, **-(CH₂)₉CH₃**) ppm.

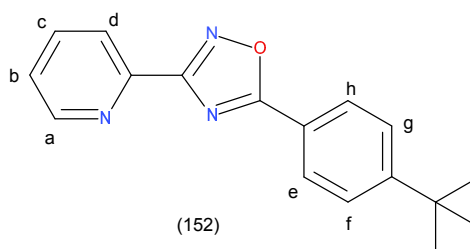
IR (neat) ν : 3396, 3030 (Aromatic C-H), 2953 (Alkyl C-H), 2878 (Alkyl C-H), 2848 (Alkyl C-H), 1611, 1598 (C=N), 1587, 1567, 1555, 1502, 1489, 1461, 1421, 1342, 1309, 1277, 1224, 1183 (C-O), 1136, 1121, 1077, 1060, 1019, 992, 954, 904 (N-O), 873, 851, 813, 789 cm⁻¹.

Melting point: 156.9 – 157.9 °C.

Mass spectrum(APCI +) m/z: Found 363.2329 (M+H)⁺; calculated for C₂₃H₂₉N₃O 363.2310; 5.2 ppm.

Yield: 0.13 g, 65%.

5-(4-tert-Butylphenyl)-3-(2-pyridyl)-1,2,4-oxadiazole (152)



¹H NMR (d₆-DMSO): 8.80 (ddd, 1H, J = 4.8, 1.7, 0.9 Hz, **-a**), 8.28 – 8.09 (overlapping m, 3H, **-b, d and h**), 8.03 (dd, 1H, J = 7.8, 1.8 Hz, **-e**), 7.84 – 7.65 (overlapping m, 2H, **-f and g**), 7.59 (m, 1H, **-c**), 1.36 (s, 9H, **tert. butyl -(CH₃)₃**) ppm.

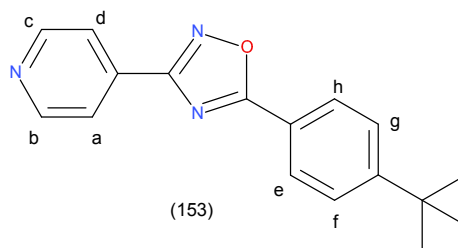
IR (neat) ν: 3050 (Aromatic C-H), 2953, 2921 (Alkyl C-H), 2865 (Alkyl C-H), 1675, 1611, 1598 (C=N), 1578, 1558, 1514, 1499, 1473, 1452, 1408, 1388, 1326, 1309, 1294, 1265, 1364, 1315, 1303, 1268, 1215 (C-O), 1177, 1136, 1083, 1042, 1030, 992, 972, 906 (N-O), 893, 855, 807, 762 cm⁻¹.

Melting point: 187.4 – 188.8 °C.

Mass spectrum(APCI +) m/z: Found 279.1379 (M+H)⁺; calculated for C₁₇H₁₇N₃O 279.1371; 2.8 ppm.

Yield: 0.09 g, 56.2%.

5-(4-tert-Butylphenyl)-3-(4-pyridyl)-1,2,4-oxadiazole (153)



$^1\text{H NMR}$ ($\text{d}_6\text{-DMSO}$): 8.99 – 8.74 (overlapping m, 2H, **-b and c**), 8.14 (d, 2H, $J = 8.4$ Hz, **-a and d**), 8.03 (m, 1H, **-e and h**), 7.71 (d, $J = 8.4$ Hz, 2H, **-f and g**), 1.34 (s, 9H, **tert. butyl $-(\text{CH}_3)_3$**) ppm.

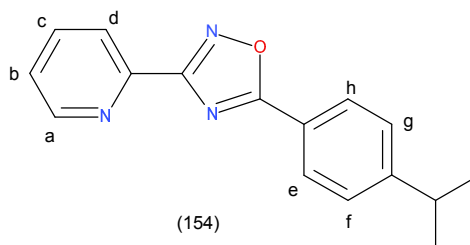
IR (neat) ν : 3044 (Aromatic C-H), 2982, 2956, 2900 (Alkyl C-H), 2865 (Alkyl C-H), 1699, 1678, 1611, 1598 (C=N), 1584, 1549, 1517, 1473, 1458, 1408, 1388, 1326, 1309, 1294, 1265, 1224, 1194, 1145, 1115 (C-O), 1063, 1016, 986, 966, 945, 910 (N-O), 872, 823, 805, 786 cm^{-1} .

Melting point: 168.1 – 169.4 $^\circ\text{C}$.

Mass spectrum (APCI +) m/z : Found 279.1383 ($\text{M}+\text{H}$) $^+$; calculated for $\text{C}_{17}\text{H}_{17}\text{N}_3\text{O}$ 279.1371; 4.2 ppm.

Yield: 0.12 g, 65.2%.

5-(4-Isopropylphenyl)-3-(2-pyridyl)-1,2,4-oxadiazole (154)



$^1\text{H NMR}$ ($\text{d}_6\text{-DMSO}$): 8.85 (d, 1H, $J = 4.1$ Hz, **-a**), 8.46 – 7.99 (overlapping m, 4H, **-b, d, e and h**), 7.68 (m, 1H, **-c**), 7.47 (d, 2H, $J = 8.3$ Hz, **-f and g**), 2.87 (dtt, 1H, $J = 13.7, 6.8, 3.7$ Hz, **Isopropyl $-(\text{CH}_2)$**), 1.51 (s, 6H, **Isopropyl $-(\text{CH}_3)_2$**) ppm.

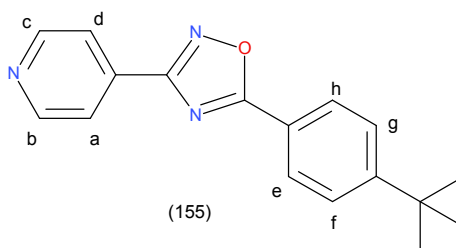
IR (neat) ν : 3157, 3066 (Aromatic C-H), 2955 (Alkyl C-H), 2882 (Alkyl C-H), 2725, 2631, 2517, 2423, 1906, 1823, 1714, 1675, 1625, 1608, 1598 (C=N), 1541, 1429, 1354, 1245, 1163 (C-O), 1073, 1032, 1027, 972, 932, 910 (N-O), 883, 861, 812, 758 cm^{-1} .

Melting point: 154.5 – 155.8 $^{\circ}\text{C}$.

Mass spectrum(APCI +) m/z: Found 265.1209 ($\text{M}+\text{H}$)⁺; calculated for $\text{C}_{16}\text{H}_{15}\text{N}_3\text{O}$ 265.1215; 2.2 ppm.

Yield: 0.14 g, 68.4%.

5-(4-Isopropylphenyl)-3-(4-pyridyl)-1,2,4-oxadiazole (155)



^1H NMR ($\text{d}_6\text{-DMSO}$): 8.80 (t, 2H, $J = 6.0$ Hz, **-b and c**), 8.35 (d, 2H, $J = 8.2$ Hz, **-a and d**), 8.09 (d, 2H, $J = 6.1$ Hz, **-e and h**), 7.60 (d, 2H, $J = 8.1$ Hz, **-f and g**), 2.89 (dt, 1H, $J = 13.7, 6.8, 3.7$ Hz, **Isopropyl $-\text{CH}_2$**), 1.57 (s, 6H, **Isopropyl $-(\text{CH}_3)_2$**) ppm.

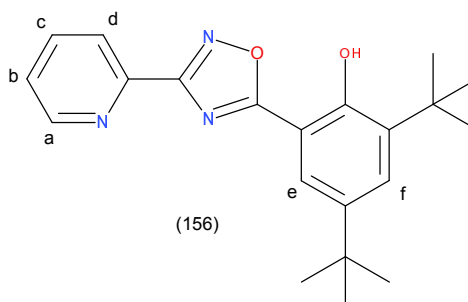
IR (neat) ν : 3167, 3076 (Aromatic C-H), 2965 (Alkyl C-H), 2892 (Alkyl C-H), 2745, 2631, 2537, 2443, 1916, 1833, 1725, 1690, 1640, 1611, 1598 (C=N), 1546, 1447, 1379, 1265, 1177 (C-O), 1083, 1042, 1030, 992, 972, 906 (N-O), 893, 862, 802, 778 cm^{-1} .

Melting point: 153.8 – 155.2 $^{\circ}\text{C}$.

Mass spectrum(APCI +) m/z: Found 265.1223 ($\text{M}+\text{H}$)⁺; calculated for $\text{C}_{16}\text{H}_{15}\text{N}_3\text{O}$ 265.1215; 3.0 ppm.

Yield: 0.11 g, 63.4%.

2,4-Ditert-butyl-6-[3-(2-pyridyl)-1,2,4-oxadiazol-5-yl]phenol (156)



¹H NMR (d₆-DMSO): 10.94 (s, 1H, -OH), 8.89 (m, 1H, -a), 8.30 (d, 1H, J = 7.8 Hz, -e), 8.07 (td, 1H, J = 7.8, 1.7 Hz, -d), 7.83 (s, 1H, -c), 7.65 (ddd, 2H, J = 17.5, 8.8, 1.7 Hz, -b and f), 1.45 (overlapping m, 18H, tert. butyl -(CH₃)₉) ppm.

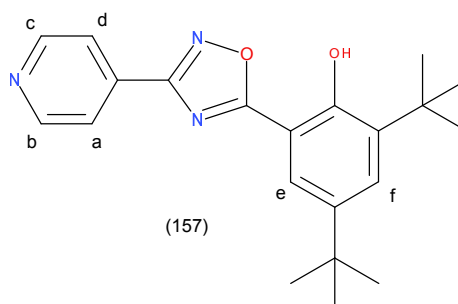
IR (neat) ν : 3233, 3215, 3156, 3033 (Aromatic C-H), 2966, 2912 (Alkyl C-H), 2875 (Alkyl C-H), 1601, 1598 (C=N), 1565, 1523, 1508, 1477, 1413, 1365, 1333, 1268, 1239, 1224, 1213 (C-O), 1120, 1100, 1062, 1014, 1009, 996, 972, 943, 910 (N-O), 889, 841, 810, 784 cm⁻¹.

Melting point: 166.8 – 170.2 °C.

Mass spectrum(APCI +) m/z: Found 351.1939 (M+H)⁺; calculated for C₂₁H₂₅N₃O₂ 351.1946; 1.9 ppm.

Yield: 0.1 g, 59.4%.

2,4-Ditert-butyl-6-[3-(4-pyridyl)-1,2,4-oxadiazol-5-yl]phenol (157)



¹H NMR (d₆-DMSO): 10.65 (s, 1H, **-OH**), 8.85 (d, 2H, J = 5.7 Hz, **-b and c**), 8.28 – 8.08 (overlapping m, 2H, **-a and d**), 7.81 (d, 1H, J = 2.3 Hz, **-e**), 7.61 (d, 1H, J = 2.3 Hz, **-f**), 1.39 (d, 18H, J = 31.1 Hz, **tert. butyl -(CH₃)₉**) ppm.

IR (neat) ν : 3235, 3205, 3155, 3038 (Aromatic C-H), 2956, 2909 (Alkyl C-H), 2865 (Alkyl C-H), 1609, 1598 (C=N), 1570, 1543, 1517, 1473, 1423, 1375, 1335, 1268, 1247, 1221, 1203 (C-O), 1130, 1101, 1063, 1024, 1001, 928, 909 (N-O), 876, 851, 810, 776 cm⁻¹.

Melting point: 176.8 – 177.9 °C.

Mass spectrum(APCI +) m/z: Found 351.1938 (M+H)⁺; calculated for C₂₁H₂₅N₃O₂ 351.1946; 2.2 ppm.

Yield: 0.12 g, 61.3%.

Chapter 4

Fluorinated Carboxamidrazone Derivatives

4.1 Introduction

The element fluorine has been prominent and has interested the scientific community because of its very particular properties (small size, strong electronegativity, low polarisability) ever since it was discovered and isolated by Henri Moissan in 1886. The addition of one or more fluorine atoms in an organic compound can cause significant change in the properties and reactivity of the compound without causing many changes in the steric conformation. This is because the C-F bond length is almost the same as the length between C-H bond (1.39 and 1.09 respectively). The study of fluorinated organic compounds has seen a significant increase during the last 10-15 decades due to the unique properties of the fluorine atom and its resulting applications and potential. Today, the use of compounds with at least one fluorine atom is found to be common in many fields like agrochemicals (Theodoridis (2006)), electronics (Babudri et al. (2007)) and in separation process of ^{235}U from ^{238}U in nuclear power stations (Gurs (1976)). However, its the medicinal chemistry field that has seen a major expansion of fluorinated compounds. Before 1957 there were no fluorinated drugs, the first fluorinated drug synthesised was 5-fluorouracil, an anti-tumour drug (Montgomery & Hewson (1957)). This changed the entire scenario in the medicinal world. As of today, there are over 150 fluorinated drugs in the market representing $\sim 20\%$ of all pharmaceuticals. Some fluorinated drugs are among the best sellers, such as the anti-depressant fluoxetine (Prozac), the anti-cholesterol atorvastatin (Lipitor) and the anti-bacterial ciprofloxacin (Ciprobay). Of the

total 39 new molecular entities approved by the US FDA in 2012 eight compounds contained a fluorine atom, and so far till August 2013 US FDA had approved 16 compounds of which six are fluorinated compounds.

The inclusion of fluorine atoms in the drugs has some useful advantages such as metabolic stability, improved bioavailability, increased binding affinity (Bühm et al. (2004)). The metabolic stability is the most important factor determining the bioavailability of the compound. The liver enzymes, especially the P450 cytochromes, often cause rapid oxidative metabolism of the drug, thus limiting its bioavailability. This problem is addressed by introducing a C-F group in place of an oxidisable C-H group. Thus increasing the metabolic stability. A classic example of this is Ezetimibe, a cholesterol-absorption inhibitor. The molecules contain two labile sites (the phenyl rings), which are blocked by the fluorine atom. Thus preventing the oxidation of the phenyl ring to phenol and dealkylation of the methoxy group (see Fig. 4.1) (Clader (2004), Bühm et al. (2004)). The fluorine atom being an electro negative atom has a strong effect on the nearby atom. Thus substitution of fluorine atom can alter the acidic or basic properties of the molecule, resulting in change in pKa, another important factor affecting the bioavailability.

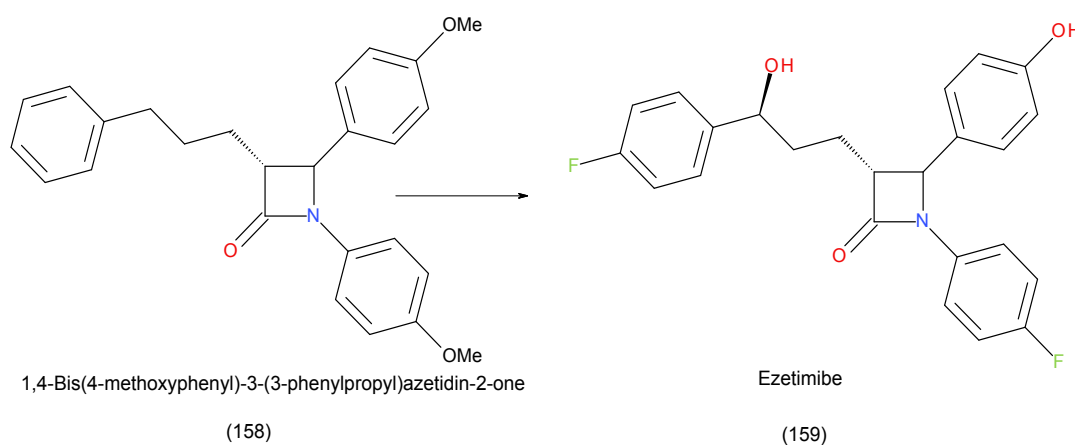


Figure 4.1: Ezetimibe: an example representing the significant contribution of fluorine substitution on metabolic stability.

The substitution of a fluorine atom in a molecule can cause change in the preferred molecular conformation. This effect can be explained by the example of a drug fluoxetine. The mechanism of action of fluoxetine involves selective inhibition of the reuptake of serotonin, thus allowing the neurotransmitter to activate its specific receptor. The SAR studies shows that the substitution of a trifluoromethyl group in the para position of the phenolic ring increased the potency for inhibiting 5-HT uptake by 6-fold, compared to the non-fluorinated parent compound. This could be attributed to the fact that the trifluoromethane molecule is roughly twice the size of methyl group as shown by the van der Waal's radius of 1.47 Å for

fluorine thus the steric bulk of the trifluoromethyl group at the para position allows the phenoxy ring to adopt a conformation which favours binding to the serotonin transporter.

In the following section the fluorination of the carboxamidrazone compounds which are known to possess biological activity is discussed (see table 2.5).

4.2 Lead optimisation

This study is a subset of the larger project carboxamidrazone amides discussed in chapter 2.

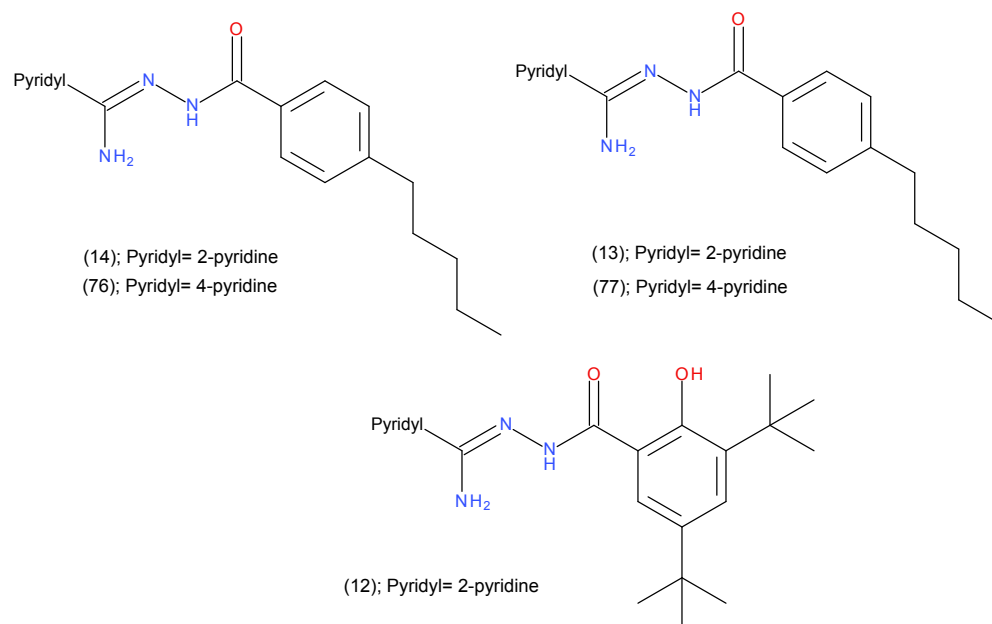


Figure 4.2: Active compounds for CF_3

Based on the findings in chapter 2, the most active carboxamidrazone amides (Fig. 4.2) were selected for further optimisation. These candidates were then subjected to various radical based fluorine chemistry reactions in an attempt to incorporate the fluorine atom(s) on to the pyridyl ring of the compound and study its effect on the carboxamidrazone amides (see Fig. 4.3).

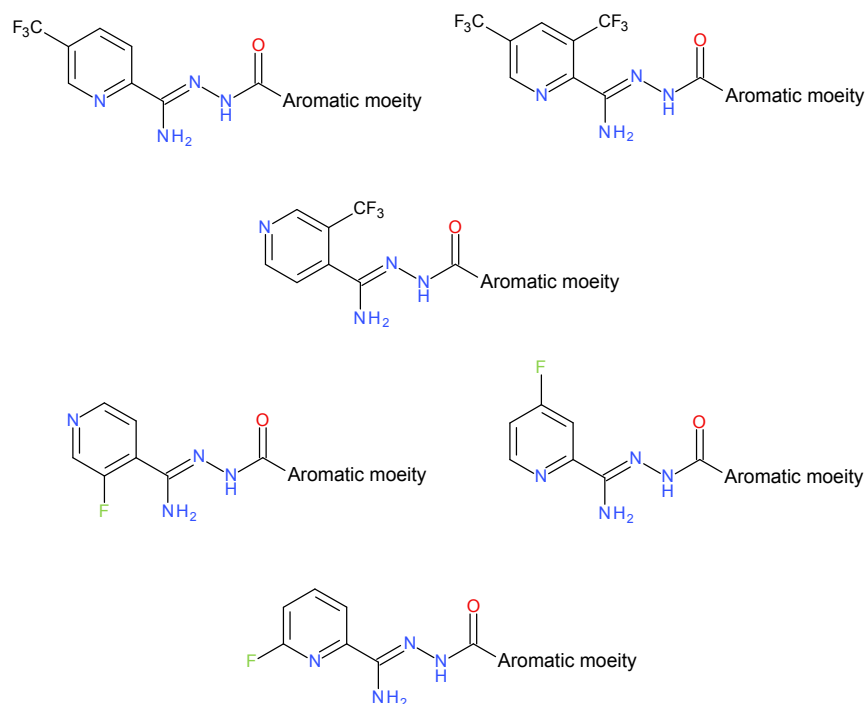
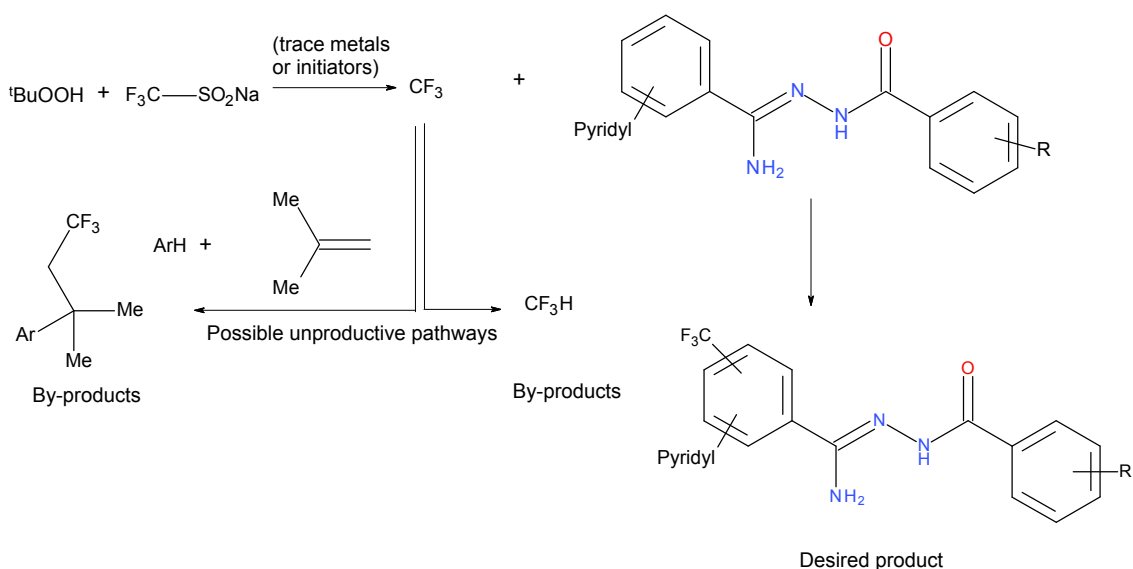


Figure 4.3: Structure of the proposed fluorine containing compounds

4.3 Results and Discussion

4.3.1 Trifluoromethylation of heteroaryl amidrazone compounds using Langlois reagent

The Langlois reagent, i.e. sodium salt of trifluoromethanesulfinic acid, in presence of catalytic metal is known to initiate a free radical reaction to introduce a trifluoromethyl group onto the electron rich aromatic compounds (Langlois et al. (1991)). Based on the recent findings of Ji et al. (2011) the trifluoromethylation reactions can be carried out in milder conditions by avoiding the use of a metal catalyst, although it is still debated if the traces of metal elements present in the compound are responsible for reaction initiation. The authors also demonstrated that the trifluoromethyl group can be introduced in the electron deficient compounds such as pyridines using excess of reagents. Hence a trifluoromethylation of heteroaryl amidrazone compounds was attempted using Langlois reagent (see Scheme. 4.1).



Scheme 4.1: Scheme for the trifluoromethylation of the heteroaryl amidrazone compounds using Langois reagent. Adapted from Ji et al. (2011)

Following the procedure of (Ji et al. (2011)), 2-pyridyl-4-butylbenzoyl carboxamidrazone was dissolved in a solution of DMSO and water along with 3 equivalents of sodium trifluoromethanesulfonate at 0°C, followed by dropwise addition of 5 equivalent of *tert*-butylhydroperoxide with vigorous stirring. This reaction mixture was allowed to warm up to room temperature and the progress of the reaction was monitored with an hourly TLC check. However by the end of 4 hours the reaction did not progress and the starting material was recovered.

The reaction conditions were varied, where all the steps were followed as mentioned earlier with only changing the temperature. The reaction mixture instead of warming to room temperature was heated up to 30°C and stirred for 4 hours with an hourly TLC check. However the reaction did not progress and the starting material was recovered. In the next reaction all the steps were followed along with heating up to 30°C for 4 hours with hourly TLC check, with the only change being degassing of the system and argon back fill, as is done generally in the radical reaction experiments. Again the reaction did not progress and the starting material was recovered. The next reaction was performed with the same quantities of chemicals with degassing of the system and argon back fill, the reaction mixture was heated up to 30°C and was stirred for a longer duration of 8 hours with hourly TLC checks. The reaction did not progress and the starting material was recovered.

In the next set of experiments an excess of reagents were used i.e. two times addition of three equivalent of Sodium trifluoromethanesulfonate and 5 equivalents of *tert*-butylhydroperoxide at the intervals of

4 hours. This reaction mixture was stirred overnight at 60°C. The system was degassed and argon back fill was performed before the start of the experiment. The reaction did not go to completion with large amount of starting material recovered with some impurity which was identified as the by product mentioned in the literature (see Scheme. 4.1, Ji et al. (2011)). The next reaction performed was with the same parameters as in the previous reaction with use of excess of reagents and was stirred for a longer duration of 5 days. The reaction was stopped since it did not go to completion and the starting material was recovered with some impurities.

Further optimisation was carried out for this reaction where the reaction mixture was stirred at room temperature between 20-24°C for 8 days. The reaction system was degassed followed by the argon back fill at the start of the experiment and the excess of reagent was added (2 times addition of 3 equivalent Sodium trifluoromethanesulfinate and 5 equivalent of *tert*-butylhydroperoxide) at the intervals of 24 hours. The reaction was halted after 8 days with the starting material being recovered.

A parallel set of reactions was carried out with the 4-pyridyl-4-butylbenzoyl. Similar results were obtained.

In an attempt to validate the reaction, a controlled experiment was carried out with 4-cyanopyridine. The reaction system was degassed followed by the argon back fill, excess of reagent was added (two times addition of 3 equivalents Sodium trifluoromethanesulfinate and 5 equivalents of *tert*-butylhydroperoxide) at the intervals of 24 hours and stirred at room temperature (20-24°C) for 2 days. The completion of reaction was monitored with TLC. At the end of two days, the reaction went to 80 % completion. The product obtained contained the desired compound (10 %), with some starting material and by product (see Scheme. 4.1).

Since the yield obtained was low no further optimisation was carried out to this reaction.

4.3.2 Trifluoromethylation of heteroaryl amidrazone compounds by photoredox catalysis method

Nagib & MacMillan (2011) have recently published a mechanism for direct trifluoromethylation of unactivated arenes and heteroarenes which requires milder experimental conditions like household light and commercially available photo-catalysts. The proposed mechanism by Nagib & MacMillan (2011) suggests that the photoredox catalytic cycle is initiated by the excitation of the photo-catalyst in the

presence of a household bulb. This excited state catalyst acts as a reductant and via single electron transfer reduces the triflyl chloride to a high energy species, which spontaneously collapses to form CF_3 radical. This CF_3 radical then selectively attaches with the most electron-rich position of any arene or heteroarene resulting in the trifluoromethylation of the compound. In the process the catalyst is promoted to the next level where it acts as an oxidant on the trifluoromethylated aromatic system to provide a cation and thereby completing the catalytic cycle. This cation on subsequent deprotonation gives the required trifluoromethylated aromatic system (see Fig. 4.4). Using this principle a trifluoromethylation of the heteroaryl amidrazone compounds was attempted. The authors (Nagib & MacMillan (2011)) suggested that for the electron deficient species a photo catalyst with longer excited state should be used along with excess of CF_3 source i.e. triflyl chloride).



Figure 4.4: Proposed mechanism for direct trifluoromethylation of arenes by photoredox catalysis. Assembled from Nagib & MacMillan (2011)

A borosilicate tube was equipped with a small stirrer bar, 0.02 equivalent of iridium photocatalyst (Tris[2-(2,4-difluorophenyl)pyridine]iridium(III), $\text{Ir}(\text{Fppy})_3$) and 3 equivalent of phosphate buffer (K_2HPO_4) and sealed with a rubber cork. This system was then degassed with alternate vacuum suction and argon backfill (three times) before injecting the solvent anhydrous acetonitrile and 1 equivalent of 4-pyridyl-4-octylbenzoyl carboxamidrazone. The resulting reaction mixture was again degassed with alternate vacuum suction and argon backfill (three times). To this triflyl chloride 4 equivalent was injected and the tube was placed approximately 2 cm apart from the normal household light (compact fluorescent light bulb, 600 lumens output) with very slow stirring (< 4000 rpm), to allow more light penetration through the solution, for 24 hours. The reaction did not yield desired product. The proton and fluorine NMR data

suggested a mixture of starting material and some compounds with CF_3 substituted in multiple positions as impurities. Isolation of these compounds was difficult as they did not separate on TLC. Based on the results, the experiment was repeated with the same quantities and the entire reaction system was kept dry. The reaction did not go to completion and starting material was recovered with impurities.

It was thought that during the work up, the iridium catalyst present in the system carried on the reaction and multiple substitutions occurred. To address this problem the next experiment was set up under similar conditions with the same chemical quantities, however the work up was done rapidly and in the dark. The catalyst was removed by column chromatography and resulting product obtained was impure. To further optimise this reaction, a new experiment was set up with half the quantities of the photo-catalyst iridium (0.01 eq) and CF_3 source triflyl chloride (2 eq). To check the completion of the reaction an hourly TLC check was performed. The reaction did not go to completion and after 24 hours the reaction was stopped and the starting material was recovered along with some impurities after the work up.

The reaction conditions were also probed using a simpler compound, 4-cyano pyridine, which if fluorinated could be used as precursor to the carboxamidrazone compound. In this experiment the 0.02 eq. of iridium was added to 3 eq. of phosphate buffer and after the degassing and argon backfill (three times) anhydrous acetonitrile solvent was added along with 1 eq. of 4-cyano pyridine. To this 4 eq. of triflyl chloride was added after another round of alternate degassing and argon backfill (three times) and placed approximately 2 cm from light source. After monitoring the experiment with TLC it was observed that the reaction did not go to completion after 24 hours and hence the reaction was stopped. After the column chromatography to remove the catalyst, starting material was recovered with impurities. Another experiment was set with further halving the quantities of the catalyst iridium (0.01 eq) and triflyl chloride (2 eq), while the quantities of remaining chemicals remained unchanged. The reaction did not yield the desired product and starting material along with impurities was obtained.

The previous sets of reactions have seen lowered concentrations of the photo-catalyst and CF_3 source in order to prevent the reaction from undergoing multiple CF_3 substitutions. Another attempt was made by changing the photo-catalyst. In the next experiment, ruthenium catalyst (Dichlorotris(1,10-phenanthroline)ruthenium(II) hydrate) was used as it has lower lived excited state as compared to iridium. All the chemicals were used in the same quantities 0.01 eq ruthenium, 3 eq phosphate buffer, 1 eq 4-cyano pyridine and 2 eq triflyl chloride along with anhydrous acetonitrile as solvent. The reaction conditions were same as in the previous experiment. The reaction did not progress after 24 hours and

the starting material was obtained with some impurities. To make the conditions milder, the quantity of CF₃ source triflyl chloride was further lowered to (1 eq). The reaction did not progress and starting material was obtained.

As the reaction failed to go to the completion, in the next set of reactions a large amount of the iridium catalyst (0.04 eq) and triflyl chloride (8 eq) was added. The quantities of phosphate buffer and 4-cyano pyridine remained constant. The reaction progressed but did not go to the completion. Hence another reaction was set up with the excess of catalyst (0.04 eq) and triflyl chloride (8 eq) for a longer duration (3 days). The reaction did not go to completion and starting material was obtained.

It was observed that normal household light (energy saving soft white) has a colour temperature of 2700 to 3000 K and lumen output up to 600 lumens. The literature suggests the use of any fluorescent light. Hence a white light which has the colour temperature of 6500 K and up to 1900 lumens output was selected for the next set of experiments due to its intense luminosity (Nagib & MacMillan (2011)). The chemicals used were 0.02 eq iridium catalyst, 3 eq phosphate buffer, 1 eq 4-cyano pyridine and 4 eq triflyl chloride along with anhydrous acetonitrile as solvent. The reaction mixture was stirred for 72 hours. Upon work up the crude product was found to be a mixture of starting material and desired product with some impurities as evidenced by ¹⁹F NMR shifts (see Fig. 4.5).

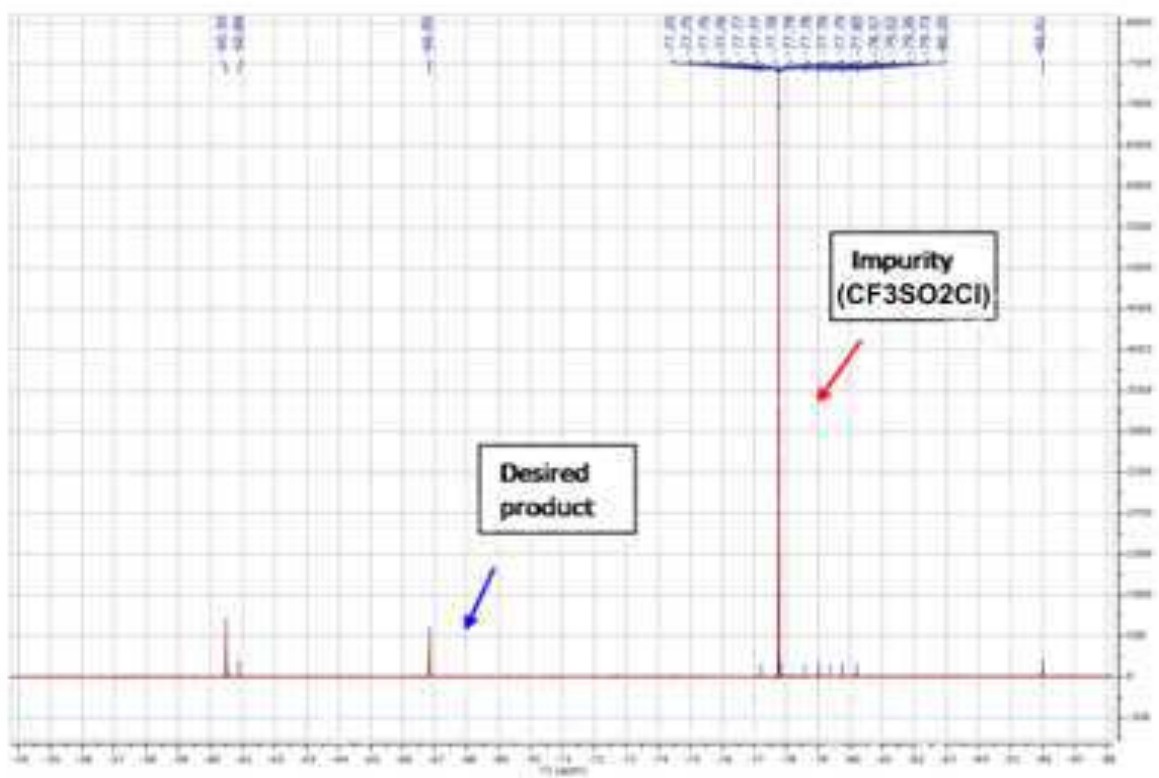


Figure 4.5: Fluorine NMR showing the ratio of desired product to impurities.

For the next set two experiments were set up in parallel with the same quantities of chemicals one with 4-cyano pyridine and another with 4-pyridyl-4-octylbenzoyl carboxamidrazone and were allowed to stir for longer period of time (7 days) and were monitored with ^{19}F NMR. In the first experiment with 4-cyano pyridine the reaction did not go to the completion and the crude product obtained contained a mixture of the starting material and the desired product with some impurities. The ratio of the desired product to the starting material was increased (see Fig. 4.6). In the second experiment, it was observed that the crude product obtained was mixture of the starting material, desired product and cyclised version of the 4-pyridyl-4-octylbenzoyl carboxamidrazone. The last experiment in this set was set up with 4-cyano pyridine, all the chemicals were used in the same quantities, the only change in parameters was longer time (14 days). The reaction did not progress and was stopped. The crude product contained starting material as a major product.

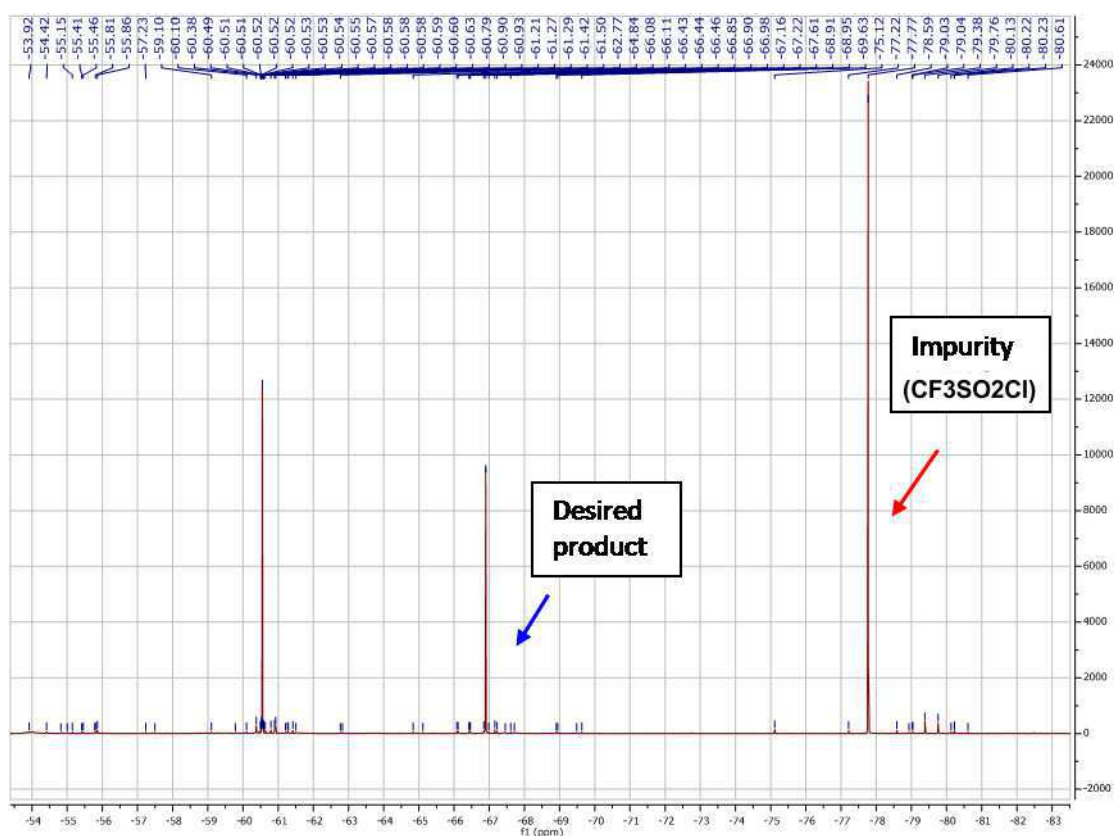


Figure 4.6: Fluorine NMR showing increase in the desired product.

The next set of reactions was carried out in a UV chamber as it has higher lumen intensity (4200 lumens) as compared to the household light and white light. The chemical quantities remained same. The reaction mixture ejected out of the reaction vessel after 24 hours. Hence for next experiment, the reaction vessel was sealed with paraffin film and reaction was monitored by ^{19}F NMR. After 7 days the reaction was stopped as it did not progress and starting material was obtained after work up.

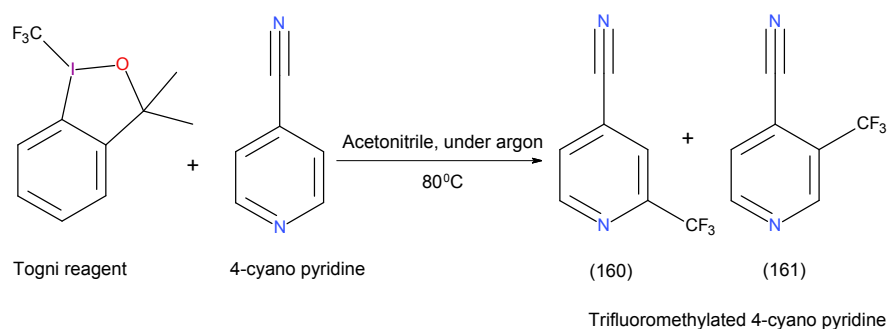
In a separate strand the cyclisation of 4-pyridyl-4-octylbenzoyl carboxamidrazone was very interesting as it offered a possibility of cyclisation of carboxamidrazone compound at lower temperature, which is in contrast to the methods requiring harsh temperature conditions as discussed in chapter 3. To find the exact conditions that caused cyclisation, a series of experiments were set up (see Table. 4.1). It was observed that the cyclisation occurred in the presence of acetonitrile, daylight bulb, catalyst and triflyl chloride, i.e entry number 14, the presence of the buffer did not affect the reaction. The column chromatography was performed to isolate the cyclised product, however the yield of the cyclised compound was much lower ($\sim 15\%$) as compared to the conventional high temperature reaction.

Entry	30°C	Carbox-amidrazone	Trifluoromethyl source	Acetonitrile	K ₂ HPO ₄	Daylight bulb	Catalyst (Iridium, Ir(Fppy) ₃)
1	✓	✓		✓			
2	✓	✓		✓	✓		
3		✓		✓		✓	
4		✓		✓	✓	✓	
5	✓	✓		✓			✓
6	✓		✓	✓	✓		
7		✓		✓		✓	✓
8		✓		✓	✓	✓	✓
9	✓	✓	✓	✓			
10	✓	✓	✓	✓	✓		
11		✓	✓	✓		✓	
12		✓	✓	✓	✓	✓	
13	✓	✓	✓	✓	✓		✓
14		✓	✓	✓	✓	✓	✓

Table 4.1: Table of experiments for cyclisation

4.3.3 Trifluoromethylation of heteroaryl amidrazone compounds using the Togni reagent

The direct trifluoromethylation usually requires harsh experimental conditions, and hence cannot be used for the compounds which have sensitive functionalities in the molecules. The Rupert-Prakash reagent (Me₃SiCF₃) has large applications in nucleophilic trifluoromethylation, however the electrophilic trifluoromethylation methods are considerably less developed. In an attempt to solve this problem Antonio Togni and co-workers have recently developed a new hypervalent iodine based reagent, 3,3-dimethyl-1-(trifluoromethyl)-1,2-benziodoxole, which facilitates direct addition of CF₃ group on to the heteroaryl systems. This reagent is known to be tolerant towards short exposure of moisture without causing significant alterations to the compound. Although this reagent is shown to react readily with the electron rich compound, it requires an elevated temperature for the less reactive system. Hence a trifluoromethylation of 4-cyano pyridine was attempted using Togni reagent at an elevated temperature

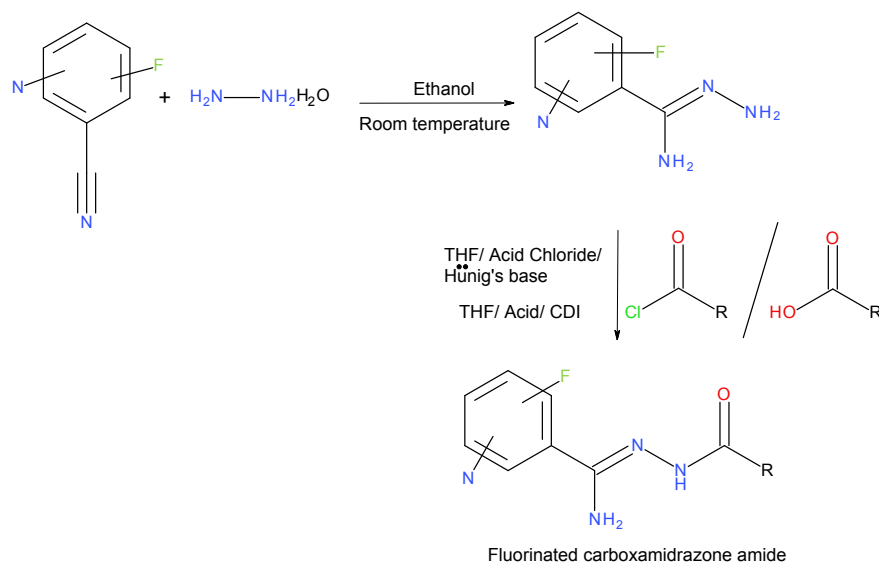


Scheme 4.2: Scheme for the trifluoromethylation of the heteroaryl amidrazone compounds using Togni reagent

(see Scheme. 4.2).

4-cyano pyridine (0.3 mmol) was dissolved in anhydrous acetonitrile along with (0.6 mmol) of Togni reagent. The entire system was degassed by alternate vacuum suction and argon backfill (three times). This reaction mixture was stirred at 80°C for 96 hours under argon. The reaction was monitored by ^{19}F NMR. The subsequent work up showed a mixture of two products, one with CF_3 substitution at 2nd position on the pyridine ring and other with CF_3 substitution at the 3rd position. The mixture could not be isolated and the yield of the target compound in the mixture was low (9%). Since the yield was low and isolation of the compounds was not possible, also as discussed in chapter3 at a high temperature the possibility of cyclisation of the carboxamidrazone increases, this reaction was not taken any further.

4.3.4 Synthesis of fluorinated carboxamidrazone amides



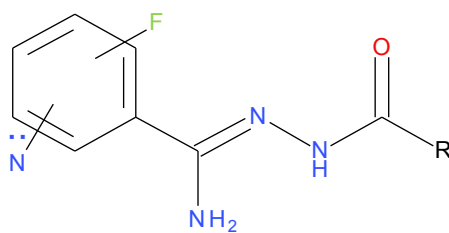
Scheme 4.3: Scheme for the synthesis of fluorinated caxboxamidrazone amide.

The direct trifluoromethylation techniques did not yield the desired product, hence another attempt was made to synthesise fluorinated carboxamidrazone amides. This reaction was carried out in two steps. The first step involved preparation of carboxamidrazone. 4-Cyano-2-fluoro pyridine was bought commercially. This compound was then suspended in ethanol and was treated with hydrazine monohydrate and stirred at room temperature for 14 days. The crude product obtained was recrystallised from ethanol to obtain the subsequent carboxamidrazone compound. This fluorinated carboxamidrazone was then reacted with the acid chloride to yield the desired carboxamidrazone amide. Using the similar process two more cyano pyridines which were bought commercially, namely 2-cyano-5-fluoro pyridine and 2-cyano-3-fluoro pyridine, were converted to carboxamidrazones and treated with acid chlorides and acid to yield fluorinated carboxamidrazone amides (see Scheme. 4.3).

Based on the microbiological results of the most active carboxamidrazone amides discussed in chapter 2 the acid chloride and acid substrates used were 4-pentylbenzoyl chloride, 4-hexylbenzoyl chloride and 3,5-ditert-butyl-2-hydroxy benzoic acid.

The 4-cyano-2-fluoro pyridine carboxamidrazone when reacted with the acid chlorides and acid in 1: 1.1 equivalent yielded the desired fluorinated carboxamidrazone. However the reactions with 2-cyano-5-fluoro pyridine carboxamidrazone and 2-cyano-3-fluoro pyridine carboxamidrazone with the acid chlorides and acid in 1: 1.1 equivalent did not go to completion. Hence the 4-pentyl benzoyl chloride was selected for the next set of reactions. Excess of reagent was used (2.5 equivalent of acid chloride to 1 equivalent of carboxamidrazone) to facilitate the reaction to go to completion and the desired fluorinated 2-pyridyl carboxamidrazone amide was obtained. The fluorinated carboxamidrazone amide compounds are sent for anti tuberculosis screening at NIAID, US. The microbiology results are still pending.

The analytical data, namely, NMR spectra, IR spectra were found to be consistent with the proposed structures. The NH bond was observed in the proton NMR spectrum in the region of 9 to 10 ppm indicating the formation of an amide. The IR showed a broad peak in the range of 1665 – 1760 cm^{-1} representing the carbonyl group. The single peak in the region of -115 to -130 ppm on ^{19}F NMR confirmed the presence of fluorine atom. These compounds were characterised with melting points. Table. 4.2 lists the fluorinated carboxamidrazone compounds synthesised along with its % yields and melting points.



Compound number	Pyridyl	R group	Yield (%)	Melting point (°C)
(162)	2-fluoro-4-pyridyl		83	210 – 213.5
(163)	2-fluoro-4-pyridyl		86	199.1 – 200.6
(164)	2-fluoro-4-pyridyl		72	200.1 – 203.5
(165)	3-fluoro-2-pyridyl		79	207.2 – 208.8
(166)	5-fluoro-2-pyridyl		76	209.1 – 211

Table 4.2: List of analogues of fluorinated carboxamidrazones.

4.3.5 Purity

The fluorine substituted pyridine carboxamidrazones synthesised were clean and were used as it is for next step. The crude linear carboxamidrazone amides synthesised were found to possess impurities and the pure compound was isolated by recrystallisation.

4.3.6 Solubility

The fluorinated carboxamidrazone amides were readily soluble in most of the common polar and non-polar solvents.

4.3.7 Microbiological results

The analogues of both the fluorinated carboxamidrazones and α -keto, β -hydroxy esters were sent to the Infectious Disease Research Institute (IDRI, US) for screening against *Mycobacterium tuberculosis* H37Rv strain. These compound libraries were subjected to MIC under aerobic conditions assay. The assay was carried out on H37Rv strain to determine the MIC, IC₅₀ and IC₉₀ concentration for the compounds. As discussed in 2.4.8 in chapter 2 the fluorinated carboxamidrazone analogues were subjected to high throughput screening (HTS) process. This process involves two stages: in the first stage, assays are carried out on H37Rv strain to determine the MIC, IC₅₀ and IC₉₀ concentration for the compounds. The compounds which have MIC values of 32.47 μ M or less are further taken to the second stage which involves advanced anti mycobacterial susceptibility profiling (see 2.4.8) in chapter 2. The Table. 4.3 presents the first stage microbiological results obtained from IDRI. While the Table. 4.4 represents the values of the control drug used in the testing.

Test Compounds			
Compound number	MIC (μ M)	IC ₅₀ (μ M)	IC ₉₀ (μ M)
(162)	2.6	1.2	4.0
(163)	>200	>200	>200
(164)	>200	190	>200

Table 4.3: The first stage microbiological data summary of the fluorinated carboxamidrazone amides.

Controlled Compound			
Compound number	MIC (μM)	IC ₅₀ (μM)	IC ₉₀ (μM)
Rifampicin	0.007	0.006	0.013

Table 4.4: Microbiological data for the Control drug used in the first stage analysis.

The compounds (162) and (164) were found to be active and hence they were taken to the second stage of screening. The Table. 4.5 presents the data for MIC assays performed in aerobic conditions and under low oxygen conditions. Both the compounds were found to have activity against *Mycobacterium tuberculosis* H37Rv strain under aerobic and low oxygen condition.

Assays	MIC under aerobic conditions		MIC under low oxygen	
	(162)	(164)	(162)	(164)
Compound numbers	(162)	(164)	(162)	(164)
MIC (μM)	12	>200	3.4	11
IC ₅₀ (μM)	2	62	6.5	13
IC ₉₀ (μM)	12	>200	13	15

Table 4.5: The second stage MIC data summary of the fluorinated carboxamidrazone amides.

Both the compounds showed the bactericidal activity in the MBC assay. The minimum bactericidal concentrations were found to be: 13 μM for compound (162) and 100 μM for compound (164). The bactericidal action was found to be time dependent but not concentration dependent. The compound (164) was found to be cytotoxic with the IC₅₀ value of 83 μM , while both the compounds exhibited intracellular activity against *M. tuberculosis*. The compounds (162) and (164) also showed activity against *M. tuberculosis* resistant isolates RIF-R1 strain with the MIC values of 6.1 μM and 26 μM respectively.

4.4 Summary and Conclusion

This study has explored the various possible ways for incorporation of fluorine and trifluoromethyl groups on to the carboxamidrazone in an attempt to alter the penetration, and the subsequent metabolism of the compound. Some activity was observed in two of the fluorinated compounds (162) and (164). The com-

pound (162) i.e. *N*-[(*Z*)-[amino-(2-fluoro-4-pyridyl)methylene]amino]-4-pentyl-benzamide exhibited very significant activity. The related non fluorinated carboxamidrazone amide (*N*¹-(4-Pentylbenzoyl)-pyridine-4-carboxamidrazone) synthesised by Ren (2009) was noted to have a weak activity with the IC₅₀ value of 57.51 μM and the IC₉₀ value of 80.82 μM. A significant improvement in the activity was observed post fluorination. The IC₅₀ value of 1.2 μM, IC₉₀ value of 4.0 μM and the MIC of 2.6 μM was observed. The possible improvement in the activity could be result of the increased cell permeability caused by the fluorine. The microbiological data for the fluorine substituted 2-pyridyl carboxamidrazone amides i.e. compounds (165) and (166) is in process. It would be very interesting to observe the data for these compounds as they were the most active compounds of the Ren (2009) series.

The future work could possibly involve synthesis of analogues of fluorinated carboxamidrazone amide. Also if an appropriate method is found, a direct trifluoromethylation can be performed on these compounds to compare the activity of the compounds.

4.5 Experimental

The chemicals and instrumentations used are the same as discussed in 3.5.

4.5.1 Preparation of pyridine(2-fluoro)-4-carboxamidrazone (167)

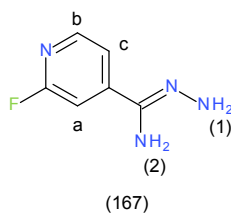


Figure 4.7: Pyridine(2-fluoro)-4-carboxamidrazone

4-cyano-2-fluoro pyridine (4.5 g, 36.88 mmol) was suspended in ethanol (13.5 mL) and to it hydrazine monohydrate (9 mL) was added. This reaction mixture was stirred at room temperature for 14 days. The excess of hydrazine was removed by rotary evaporation under reduced pressure at 50°C and the product was collected by filtration. The crude product was then washed three times with petrol ether 40 60°C to give a yellowish compound. The crude product obtained was then recrystallised using ethanol.

Yield: 4.34 g, 86.5%.

R_f value [EtOAc:MeOH (2:1)]: 0.15.

¹H NMR (250 MHz, d₆-DMSO): 8.53 (d, 2H, J=6.3 Hz, **a and b**), 7.52 (d, 1H, J=6.3 Hz, **c**), 5.51 (bs, 2H, NH₂(2)), 4.23 (bs, 2H, NH₂(1)) ppm.

¹⁹F NMR: -67.58 (s, **F**) ppm.

4.5.2 Preparation of pyridine(5-fluoro)-2-carboxamidrazone (168)

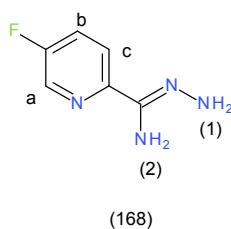


Figure 4.8: Pyridine(5-fluoro)-2-carboxamidrazone

The procedure for the preparation of Pyridine(5-fluoro)-2-carboxamidrazone is same as for Pyridine(2-fluoro)-4-carboxamidrazone.

Yield: 3.98 g, 79.3 %.

R_f value [EtOAc:MeOH (2:1)]: 0.15.

¹H NMR (250 MHz, d₆-DMSO): 8.47 (m, 1H, **a**), 7.93 (m, 1H, **b**), 7.71 (td, 1H, J= 6.92, 1.8 Hz, **c**), 5.33 (bs, 2H, **NH₂(2)**), 5.71 (bs, 2H, **NH₂(1)**) ppm.

¹⁹F NMR: -129.13 (s, **F**) ppm

4.5.3 Preparation of pyridine(3-fluoro)-2-carboxamidrazone (169)

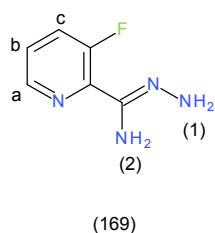


Figure 4.9: Pyridine(3-fluoro)-2-carboxamidrazone

The procedure for the preparation of Pyridine(3-fluoro)-2-carboxamidrazone is same as for Pyridine(2-fluoro)-4-carboxamidrazone.

Yield: 4.16 g, 82.9 %.

R_f value [EtOAc:MeOH (2:1)]: 0.15.

¹H NMR (250 MHz, d₆-DMSO): 8.53 (m, 1H, **a**), 8.33 (td, 1H, J= 6.92, 1.8 Hz, **c**), 7.68 (td, 1H, J=4.9, 1.2 Hz, **b**), 7.21 (s, 2H, **NH₂(2)**), 5.37 (s, 2H, **NH₂(1)**) ppm.

¹⁹F NMR: -117.03 (s, **F**) ppm.

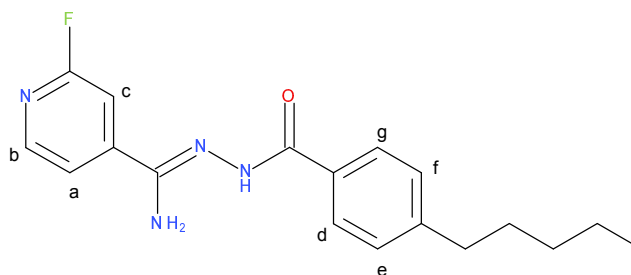
4.5.4 General procedure for fluorinated carboxamidrazone amide synthesis from acid chlorides

Heteroaryl fluorinated carboxamidrazone (1.0 g, 6.49 mmol) was suspended in an anhydrous THF (20 mL). To this solution Hünig's base (2 mL) was added, followed by acid chloride (1.1 eq). This reaction mixture was stirred overnight under argon at room temperature. This reaction mixture was added to sodium bicarbonate solution (20 mL) and the product was collected by filtration. The crude product obtained was then washed with water and dried under vacuum. The product obtained was pure and hence used as it is.

4.5.5 General procedure for synthesis of fluorinated carboxamidrazone amide from acids

N,N'-carbonyl-di-imidazole (1.05 g, 6.49 mmol) and acid (6.49 mmol, 1 eq) was dissolved in THF (20 mL). To this reaction mixture appropriate fluorinated heteroaryl carboxamidrazone (1 g, 6.49 mmol) was added and this reaction mixture was stirred under argon at room temperature for overnight. This reaction mixture was added to sodium bicarbonate solution (20 mL) and the product was collected by filtration. The crude product obtained was then washed with water and dried under vacuum. The product obtained was pure and hence used as it is.

***N*-[(*Z*)-[amino-(2-fluoro-4-pyridyl)methylene]amino]-4-pentyl-benzamide (162)**



(162)

¹H NMR (250 MHz, d₆-DMSO): 10.82 (s, 1H, -NH), 8.53 (d, 2H, J = 5.4 Hz, -b and c), 8.34–7.98 (overlapping m, 2H, -d and g), 7.87 (dd, 1H, J = 4.5, 1.6 Hz, -a), 7.34 (d, 2H, J = 8.3 Hz, -e and

f), 6.74 (s, 2H, **-NH₂**), 2.63 (t, 2H, J = 7.5 Hz, **-CH₂CH₂(CH₂)₂CH₃**), 1.60 (dt, 1H, J = 14.9, 7.3 Hz, **-CH₂CH₂(CH₂)₂CH₃**), 1.35 – 1.27 (overlapping m, 4H, **-CH₂CH₂(CH₂)₂CH₃**), 0.84 (t, 3H, J = 8.3, 5.4 Hz, J = 6.8 Hz, **-CH₂CH₂(CH₂)₂CH₃**) ppm.

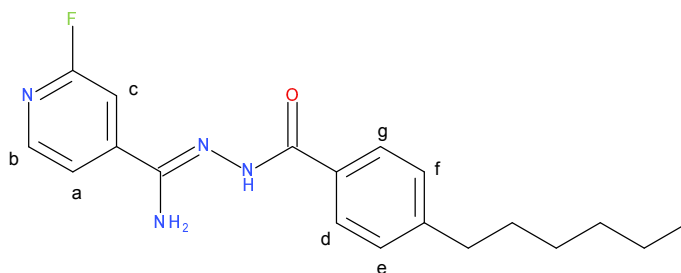
¹⁹F NMR: -67.58 (s, **F**) ppm.

IR (neat) ν : 3885, 3851, 3730, 3648, 3587 (N-H), 3026 (Aromatic C-H), 2965 (Alkyl C-H), 2929 (Alkyl C-H), 2555, 2361, 2213, 2021, 1973, 1772, 1748, 1710, 1681 (C-C in ring), 1654, 1627 (C=O), 1618, 1578, 1557, 1539, 1502, 1490, 1475, 1454, 1390, 1357, 1342, 1257, 1099 cm⁻¹.

Melting point: 210 – 213.5°C

Yield: 2.00 g, 83 %

***N*-[*Z*]-[amino-(2-fluoro-4-pyridyl)methylene]amino]-4-hexyl-benzamide (163)**



(163)

¹H NMR (250 MHz, d₆-DMSO): 10.80 (s, 1H, **-NH**), 8.55 (d, 1H, J = 5.4 Hz, **-c**), 8.41 – 8.02 (overlapping m, 2H, **-a and b**), 7.89 (dd, 2H, J = 4.5, 1.6 Hz, **-d and g**), 7.31 (d, 2H, J = 8.3 Hz, **-e and f**), 6.65 (s, 2H, **-NH₂**), 2.70 (t, 2H, J = 7.5 Hz, **-CH₂CH₂(CH₂)₃CH₃**), 1.64 (dd, 2H, J = 27.0, 20.5 Hz, **-CH₂CH₂(CH₂)₃CH₃**), 1.33 (dd, J = 11.4 Hz, 6H, **-CH₂CH₂(CH₂)₃CH₃**), 0.84 (t, 3H, J = 6.7 Hz, **-CH₂CH₂(CH₂)₃CH₃**) ppm.

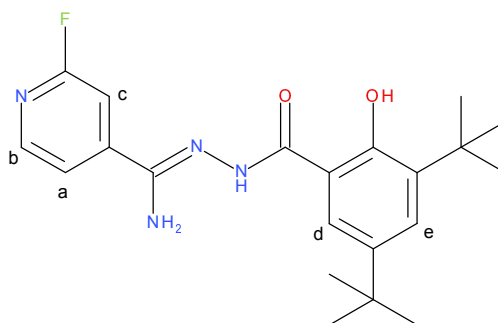
¹⁹F NMR: -67.58 (s, **F**) ppm.

IR (neat) ν : 3356 (N-H), 3320 (N-H), 3150, 3025 (Aromatic C-H), 2948 (Alkyl C-H), 2917 (Alkyl C-H), 1705, 1645 (C=O), 1599, 1521, 1461, 1397, 1388, 1333, 1300, 1268 (C-N), 1222, 1190, 1140 cm⁻¹.

Melting point: 199.1 – 200.6°C

Yield: 2.16 g, 86 %

***N*-[*Z*]-[amino-(2-fluoro-4-pyridyl)methylene]amino]-3,5-ditert-butyl-2-hydroxy-benzamide (164)**



(164)

¹H NMR (250 MHz, d₆-DMSO): 11.51 (s, 1H, –OH), 10.03 (s, 1H, –NH), 8.41 (d, 2H, J = 5.4 Hz, **-b and c**), 8.31 (complex m, 1H, **d**), 7.81 (dd, 1H, J = 4.5, 1.6 Hz, **-a**), 7.32 (d, 1H, J = 8.3 Hz, **-e**), 6.63 (s, 2H, –NH₂), 1.42 (s, 9H, **tert. butyl**), 1.26 (s, 9H, **tert. butyl**) ppm.

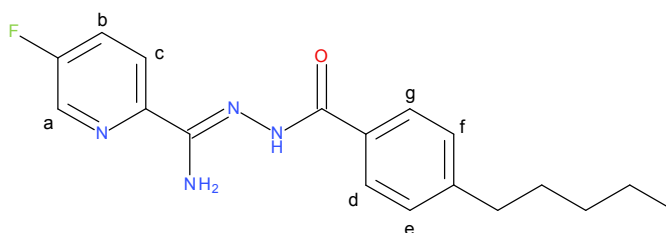
¹⁹F NMR: -67.58 (s, **F**) ppm.

IR (neat) ν : 3441, 3333 (N-H), 3277 (N-H), 3035 (Aromatic C-H), 2919 (Alkyl C-H), 2853 (Alkyl C-H), 1636 (C=O), 1606, 1551, 1515, 1496, 1481, 1433, 1351, 1305, 1275 (C-N), 1244, 1175, 1102, 1068, 1020 cm⁻¹.

Melting point: 200.1 – 203.5°C

Yield: 2.04 g, 72 %

***N*-[*Z*]-[amino-(5-fluoro-2-pyridyl)methylene]amino]-4-pentyl-benzamide (165)**



(165)

¹H NMR (250 MHz, d₆-DMSO): 10.41 (s, 1H, **-NH**), 8.63 (complex m, 1H, **-a**), 8.04 (d, 1H, J = 8.2 Hz, **-b**), 7.74 (ddd, 2H, J = 12.9, 9.6, 4.8 Hz, **-d and g**), 7.39 (ddd, 1H, J = 7.3, 4.9, 1.3 Hz, **-c**), 7.11 (d, 2H, J = 8.3 Hz, **-e and f**), 6.64 (s, 2H, **-NH₂**), 2.68 (t, 2H, J = 7.5 Hz, **-CH₂CH₂(CH₂)₂ CH₃**), 1.82 1.54 (overlapping m, 2H, **-CH₂CH₂(CH₂)₂ CH₃**), 1.36 1.20 (overlapping m, 4H, **-CH₂CH₂(CH₂)₂ CH₃**), 0.83 (t, 3H, J = 6.8 Hz, **-CH₂CH₂(CH₂)₂ CH₃**) ppm.

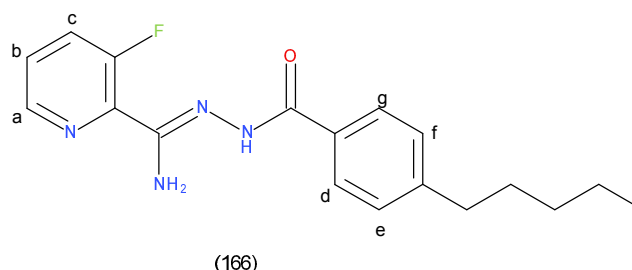
¹⁹F NMR: -129.13 (s, **F**) ppm.

IR (neat) ν : 3341 (N-H), 3340 (N-H), 3303 (N-H), 3120, 3026 (Aromatic C-H), 2957 (Alkyl C-H), 1654 (C=O), 1608, 1581, 1558, 1475, 1443, 1392, 1463, 1416, 1291 (C-N), 1189 cm⁻¹.

Melting point: 207.2 – 208.8°C

Yield: 1.9 g, 79 %

N-[(Z)-[amino-(3-fluoro-2-pyridyl)methylene]amino]-4-pentyl-benzamide (166)



¹H NMR (250 MHz, d₆-DMSO): 10.47 (s, 1H, **-NH**), 8.67 (m, 1H, **-a**), 8.01 (d, 2H, J = 8.2 Hz, **-d and g**), 7.84 (ddd, 1H, J = 12.9, 9.6, 4.8 Hz, **-b**), 7.42 (ddd, 1H, J = 7.3, 4.9, 1.3 Hz, **-c**), 7.21 (d, 2H, J = 8.3 Hz, **-e and f**), 6.69 (s, 2H, **-NH₂**), 2.60 (t, 2H, J = 7.5 Hz, **-CH₂CH₂(CH₂)₂ CH₃**), 1.85 1.44 (overlapping m, 2H, **-CH₂CH₂(CH₂)₂ CH₃**), 1.40 1.21 (overlapping m, 4H, **-CH₂CH₂(CH₂)₂ CH₃**), 0.85 (t, 3H, J = 6.8 Hz, **-CH₂CH₂(CH₂)₂ CH₃**) ppm.

¹⁹F NMR: -117.13 (s, **F**) ppm.

IR (neat) ν : 3356 (N-H), 3320 (N-H), 3252 (N-H), 3207, 3022 (Aromatic C-H), 2948 (Alkyl C-H), 1911, 1665 (C=O), 1634, 1547, 1470, 1438, 1393, 1247, 1170, 1057, 1012, 1002 cm⁻¹.

Melting point: 209.1 – 211°C

Yield: 1.83 g, 76 %

4.5.6 General procedure for trifluoromethylation of heteroaryl amidrazone compounds using Langlois reagent

The required carboxamidrazone (0.5 g, 1.69 mmol, 1 eq) was dissolved in a solution of DMSO (7 mL) and water (2.8 mL) along with 3 equivalents of sodium trifluoromethanesulfinate (0.79 g, 5.067 mmol) at 0°C, followed by dropwise addition of 5 equivalents of *tert*-butylhydroperoxide (1.15 g, 8.45 mmol) with vigorous stirring under argon. This reaction mixture was allowed to warm up to room temperature and the progress of the reaction was monitored with an hourly TLC check until the reaction goes to completion. The reaction mixture was then added to saturated NaHCO₃ solution with rapid foaming. The precipitate was collected by filtration and washed with water (three times, 15 mL). The obtained was vacuum dried and stored.

4.5.7 General procedure for trifluoromethylation of heteroaryl amidrazone compounds by photoredox catalysis method

A borosilicate tube was equipped with a small stirrer bar, iridium photocatalyst (Tris[2-(2,4-difluorophenyl)pyridine]iridium(III), Ir(Fppy)₃, 0.0076 g, 0.02 eq) and phosphate buffer (K₂HPO₄, 0.261 g, 3 eq) and sealed with a rubber cork. This system was then degassed with alternate vacuum suction and argon backfill (three times) before injecting the solvent anhydrous acetonitrile and required carboxamidrazone amide (4-pyridyl-4-octylbenzoyl carboxamidrazone amide, 0.13 g, 0.5 mmol, 1 eq). The resulting reaction mixture was again degassed with alternate vacuum suction and argon backfill (three times). To this triflyl chloride (0.213 mL, 4 eq) was injected and the tube was placed approximately 2 cm apart from the light bulb (in this case white light with the colour temperature of 6500 K and 1900 lumens output) with very slow stirring (< 4000 rpm), to allow more light penetration through the solution, for 24 hours. The reaction mixture was quenched with water (2 mL) and extracted with ethylacetate (two times) and DCM (one time), and the combined organic layers were dried over magnesium sulphate and evaporated under reduced pressure to give the desired product.

4.5.8 General procedure for trifluoromethylation of heteroaryl amidrazone compounds using the Togni reagent

4-cyano pyridine (0.3 mmol) was dissolved in anhydrous acetonitrile (2 mL) along with (0.6 mmol) of Togni reagent. The entire system was degassed by alternate vacuum suction and argon backfill (three times). This reaction mixture was stirred at 80°C for 96 hours under argon. The reaction was monitored by ¹⁹F NMR. The solvent was removed under reduced pressure and purified by column chromatography(hexane/DCM 30:1).

Chapter 5

Analogues of mycolic acids as potential inhibitors of mycobacterial cell wall synthesis

5.1 Introduction

The mycobacterial cell wall is unique in the sense that approximately 60% of the cell wall is constituted of high molecular weight hydroxy fatty acids called mycolic acid (MA), a term coined by Anderson & Chargaff (1929). In the cell wall the mycolic acid is covalently bound to the arabino-peptidogalactan layer with intercalation of free lipids (see Fig. 1.4). This complex structure is together referred to as mycolyl-arabinogalactan-peptidoglycan (mAGP) complex. This is discussed in detail in the introduction chapter (1.4). MA obtained from *M. tuberculosis* occurs in three forms: α -MA, methoxy-MA and keto-MA (see Fig. 1.5). The main function of MA is to provide integrity to the cell wall and form an extremely robust and impermeable envelope with high resistance to host-derived and therapeutic anti-bacterial agents.

The high degree of complexity in the structures of MA is attributed to its unique system as it employs fatty acid synthase (FAS) type I and II for its synthesis. FAS II is of special interest as this synthase is found exclusively in prokaryotic organisms and plants, but is absent in mammals. The detailed FAS I and II pathways are discussed in 1, see Fig. 1.10. The high complexity of the mycolic acids suggests that

many enzymes are involved in the bio-synthesis of this lipid. A detailed study of the this bio-synthesis can enable the scientists to identify the key intermediates and the enzymes associated with them, thus providing newer drug targets.

A detailed investigation was carried out by Takayama & Qureshi (1984) for *Mycobacterium tuberculosis* H₃7Ra (Takayama & Qureshi (1984)) who identified several intermediates. One such key intermediate was (*Z*)-tetracos-5-enoic acid. The authors suggested that the pathway involved in synthesis of α -mycolic acid in *M. tuberculosis* H₃7Ra involved desaturation of tetracosanoate to give (*Z*)-tetracos-5-enoic acid. The authors proposed that this step might explain the anti tubercular activity of the drug isoniazid (Takayama & Qureshi (1984), Winder (1982)), although an exact mechanism and the resistance to isoniazid by certain mycobacteria remains to be completely understood.

Besra et al. (1993) first synthesised the intermediate (*Z*)-tetracos-5-enoic acid, an ordinary fatty acid, an initial stage from where the bio-synthetic pathways diverge to form α -mycolates and oxygenated mycolates. An experiment which involved the incorporation of a radioactive label on to the mycolic acids in *M. smegmatis* confirmed its role in the bio-synthetic pathway of α -mycolic acid (Wheeler et al. (1993)). In a separate study it was shown that the process of desaturation of stearate to form oleate is inhibited by the cyclopropenyl analogue of the stearate (Fogerty et al. (1972), Jeffcoat & Pollard (1977)). With this principle in mind the authors decided to synthesise the cyclopropene analogue of (*Z*)-tetracos-5-enoate (methyl 4-(2-octadecylcyclopropen-1-yl)butanoate) as a potential inhibitor (Besra et al. (1993)) (see Fig. 5.1). The methyl 4-(2-octadecylcyclopropen-1-yl)butanoate was found to inhibit the mycolic acid bio-synthesis in the *M. smegmatis* extract, possibly by inhibiting the desaturase enzyme.

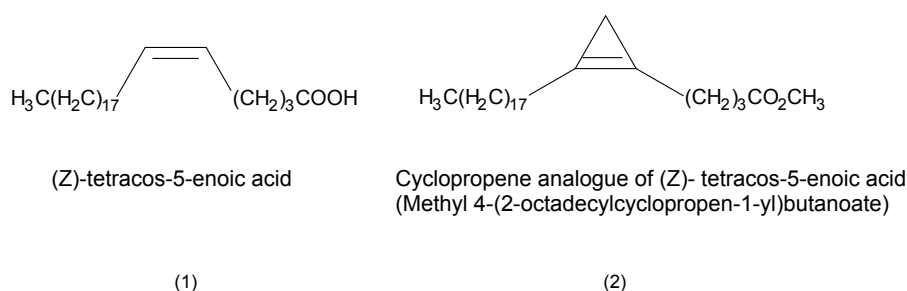
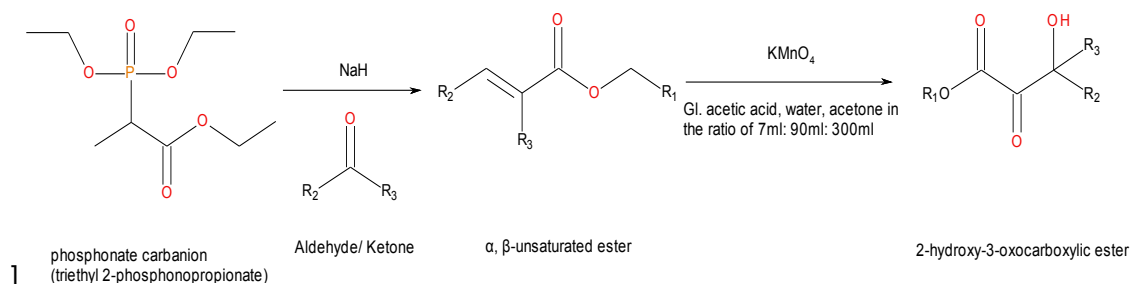


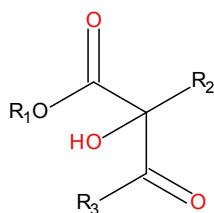
Figure 5.1: The key intermediate in mycolic acid pathway and its analogue

In this chapter, the concept of custom designed inhibitors is used. A set of long chain 2-hydroxy-3-oxocarboxylic esters were synthesised. The possible mechanism of action proposed for these compounds is the competitive direct uptake of the long alkyl chain esters in the FAS-II pathway instead of the precursors from the FAS-I pathway, thus disrupting the mycolic acid bio-synthesis.

5.2 Lead optimisation



Scheme 5.1: A complete synthetic scheme for the proposed target compounds



R_1 = ethyl or methyl groups
 R_2, R_3 = long alkyl chains

Figure 5.2: Generic structure of the proposed compounds

The synthesis of the 2-hydroxy-3-oxocarboxylic esters involves a two-step reaction sequence (see Scheme. 5.1). The first step is the synthesis of alkenes i.e. α, β -unsaturated esters. The respective aldehyde and ketones were reacted with the phosphonate carbanions to predominantly produce E-alkenes using HornerWadsworthEmmons modification to Wittig's reaction (Wadsworth & Emmons (1961), Wadsworth & Emmons (1965), Wadsworth (1977)). These compounds were then subjected to direct oxidation by potassium permanganate under mildly acidic conditions to yield 2-alkyl-2-hydroxy-3-oxocarboxylic esters (Crout & Rathbone (1989)). To synthesise a library of the target compound (see Fig. 5.2), aldehydes and ketones were selected of varying chain lengths. Table. 5.1 lists the aldehyde and ketones used for synthesis of the target compound.

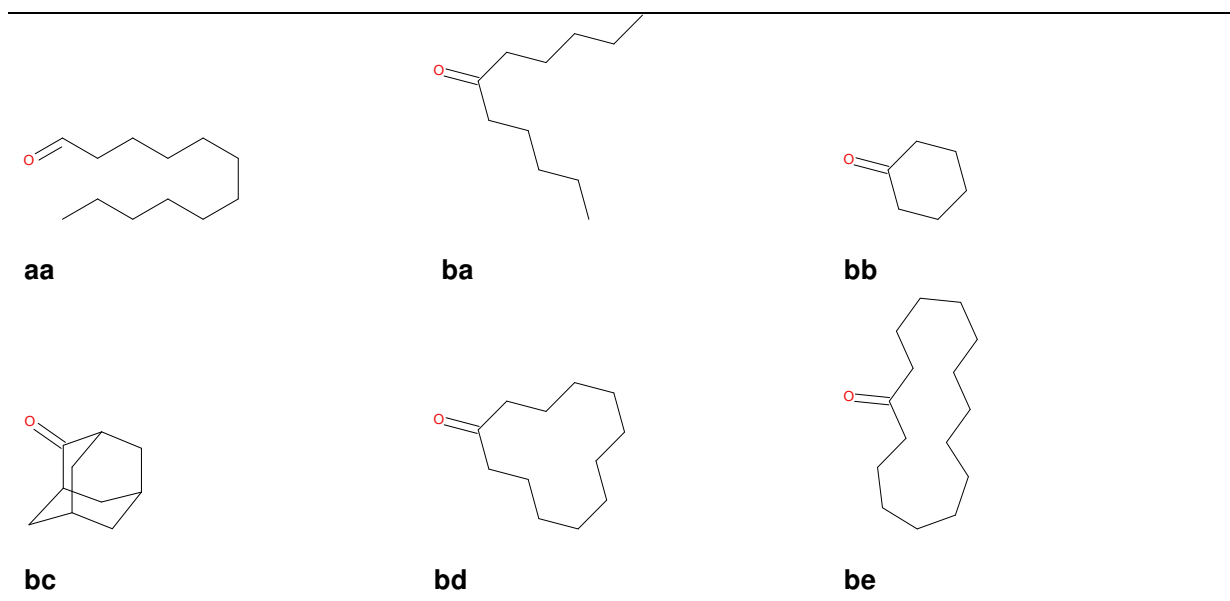
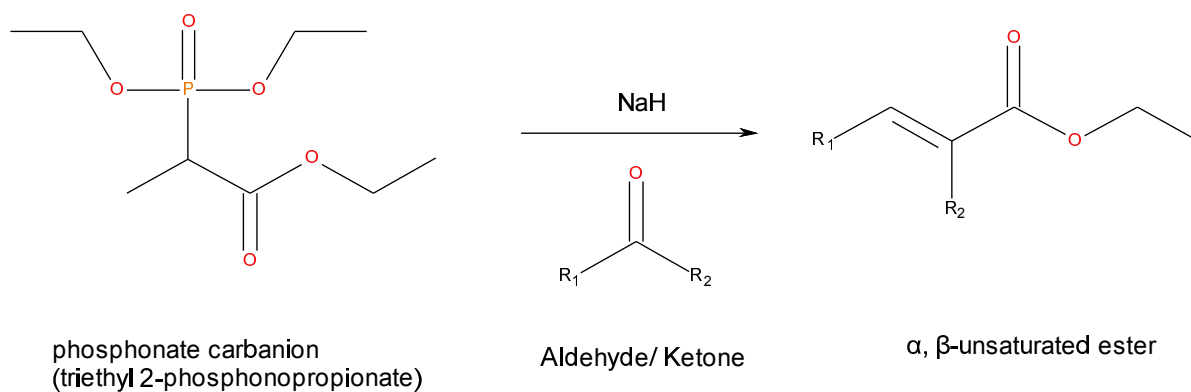


Table 5.1: Aldehyde and ketones used in synthesis of α, β -unsaturated esters

5.3 Results and Discussion

5.3.1 Synthesis of α, β -unsaturated esters (alkene) by HornerWadsworthEmmons modification to Wittig's reaction



Scheme 5.2: Scheme for synthesis of α, β -unsaturated esters (alkene) by HornerWadsworthEmmons modification to Wittig's reaction

The first step to synthesise the target compounds involved synthesis of α, β -unsaturated esters (alkene). As described in the Scheme. 5.2, sodium hydride (60% in mineral oil) was dispersed in DME (dimethyl ether), followed by drop wise addition of phosphonate carbanion (trimethyl phosphonoacetate, 1.1 eq), taking care that the temperature did not rise above 35°C by employing external cooling. It was observed

that the reaction mixture turned frothy and vigorous evolution of hydrogen was noted. The reaction mixture is stirred at room temperature for 30 mins, followed by drop wise addition of the ketone (6-undecanone, 1.1 eq) maintaining the temperature below 35°C. At this point it was observed that the reaction mixture gelled and the stirring was obstructed hence additional solvent (DME) was added to the reaction mixture to ensure smooth stirring. This reaction mixture was stirred at room temperature for 48 hours. The target α , β -unsaturated esters was obtained after an aqueous quenching and extractive work up Wadsworth & Emmons (1965). In this reaction care was taken that all the glassware used were oven-dried overnight and the reaction was carried out in dry conditions to avoid the contact of water or moisture with sodium hydride. The TLC analysis of the crude product suggested the presence of both alkene and ketone. A kugelrohr distillation apparatus was used for the purification. The individual proton NMR data obtained for the fractions showed that the first three flasks contained the mixture of ketone and alkene.

In an attempt to assist the reaction to go to the completion, the experiment was set up exactly the same with only changing the temperature parameter. The reaction mixture was stirred at 50°C for 48 hours. The work up for the experiment was the same as mentioned earlier. The TLC analysis of the crude product suggested that the reaction did not go to completion and instead a large amount of ketone was observed. Thus the rise in temperature decreased the yield of alkene.

Another optimisation was lowering the quantity of the ketone. The sodium hydride (1 eq) was dispersed in DME followed by addition of trimethyl phosphonoacetate (1.1 eq) with the temperature below 35°C. After stirring the reaction mixture at room temperature for 30 mins, the 6-undecanone was added (0.9 eq) and stirred at room temperature for 48 hours. The TLC of the crude product, obtained after the work up, suggested the presence of alkene and trimethyl phosphonoacetate.

To validate the procedure of the reaction, an example from the literature was performed Wadsworth & Emmons (1965). The experimental conditions for the new experiment were identical to the first experiment and the ketone used was cyclohexanone. The crude material was purified using kugelrohr distillation apparatus. The NMR data of the compound showed the pure product.

Hence for the next optimisation reaction using 6-undecanone was set up with the same quantities and conditions as the first experiment, but with increased reaction time. The reaction mixture was stirred for 7 days. Upon work up the crude product obtained was isolated using column chromatography. The desired alkene was obtained. However for ease of separating the alkene from the ketone, an

additional step was included in the work up. The bisulphite formation is a valuable chemoselective process which is often used for protection and/or purification of aldehyde and cyclic ketones. Sodium bisulphite when treated with aldehyde forms a sodium salt of the bisulphite adduct. These charged adducts can be removed via precipitation (Caron (2011), Kjell et al. (1999)). The next reaction was set up as usual and the crude product obtained was then stirred with freshly prepared sodium bisulphite solution for 48 hours. The white precipitate formed was filtered off and the aqueous layer was then extracted with ether. The organic layers collected were then evaporated under vacuum to give the desired alkene and some impurities, which was then subjected to the column separation. Using the same experimental conditions the aldehyde dodecanal was reacted to yield the respective alkene. The ketones adamantanone, cyclododecanone and cyclopentadecanone required 72 hours as reaction time. It was observed that the yields of the cyclododecanone and the cyclopentadecanone were significantly lower compared to the smaller carbon chain ketones and aldehydes. A pattern was observed that as the number of carbons increased in the compound the alkene yield decreased (see Table. 5.2).

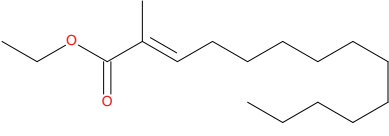
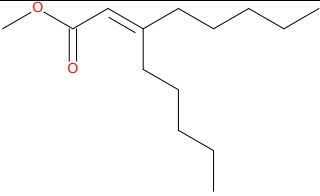
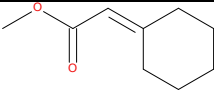
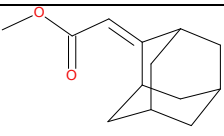
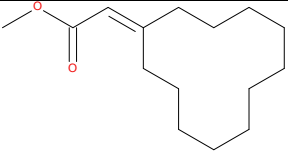
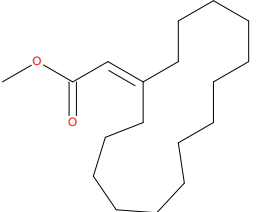
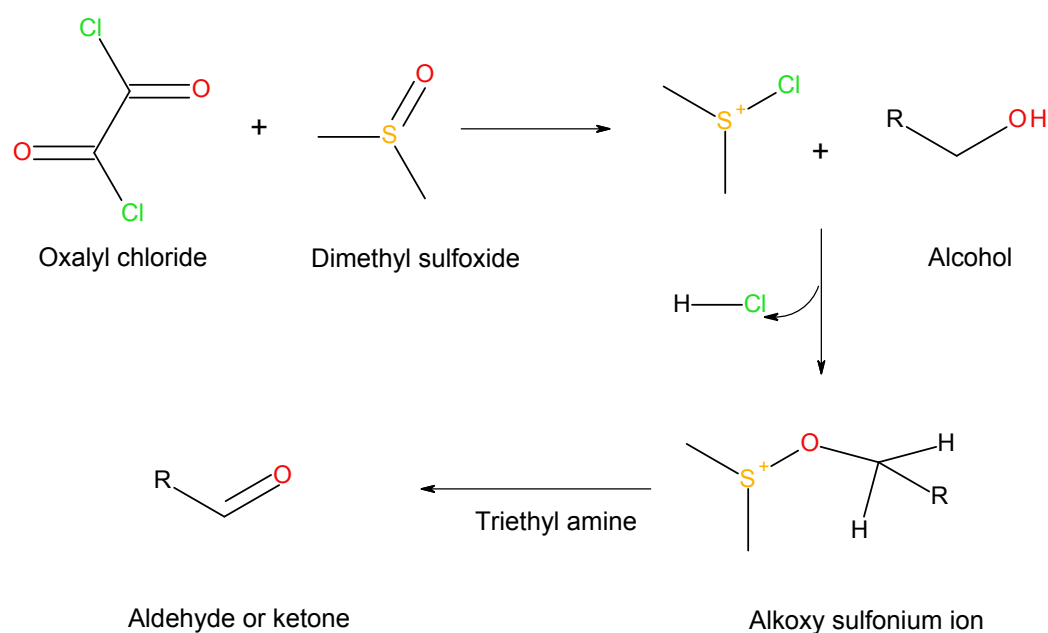
Compound number	Aldehydes and Ketones	Structure of alkenes	Yield in %	Number of days required for reaction to complete
(170)	Dodecanal		28.3	3
(171)	6-Undecanone		24.7	7
(172)	Cyclohexanone		60	overnight
(173)	Adamantanone		98.7	6
(174)	Cyclododecanone		12.53	7
(175)	Cyclopentadecanone		3	7

Table 5.2: Summary of alkenes prepared along with their yields

5.3.2 Synthesis of long chain aldehydes using Swern oxidation

All the ketones and aldehyde used in this project were purchased commercially. The cyclised or open chain aldehydes or ketones with the chain length above 15 carbons were not available commercially. Hence an attempt was made to synthesise long chain aldehydes from long chain alcohols using Swern oxidation, which can then be subjected to HornerWadsworthEmmons modification to Wittig's reaction (see Scheme. 5.3)



Scheme 5.3: Scheme for synthesis of long chain aldehydes and ketones from primary alcohols using Swern oxidation

This is a multi-step reaction sequence, where the oxalyl chloride and DMSO (dimethyl sulfoxide) are reacted at a controlled temperature of -78°C to give an intermediate product (sulfonium chloride) and releasing carbon dioxide and carbon mono-oxide. This sulfonium chloride then reacts with alcohol (1-docosanol) to yield alkoxy sulfonium ion intermediate which in turn deprotonates in excess organic base (triethyl amine) to give the corresponding aldehydes. The reaction mixture was stirred for one hour at room temperature before it was quenched with water and the aqueous layer was extracted with DCM three times. The organic extracts were then washed with 1M HCl. These washing were then dried over anhydrous MgSO_4 , and evaporated under pressure to give desired product (Omura & Swern (1978)). TLC analysis suggested formation of aldehyde, however the yield was low.

Hence to further optimise the reaction, another experiment was set up with a smaller alkyl chain alcohol (1-octadecanol), the experimental conditions were same as stated earlier. The TLC and NMR analysis of crude product shows a large amount of unreacted alcohol with traces of aldehyde. Hence in the next experiment the procedure remained the same as mentioned except the reaction time, which was increased to 3.5 hours maintaining the temperature at -70°C . The crude product yielded large amounts of unreacted alcohol. In the next set of experiments the quantities of the reagents were doubled except for the alcohol (1-octadecanol) and the reaction time was 3.5 hours at -70°C . After quenching the reaction with water the aqueous layer was extracted with petrol ether ($40-60^{\circ}\text{C}$) and washed with 1M HCl. The crude product obtained showed the presence of aldehyde. However, on the next day it was

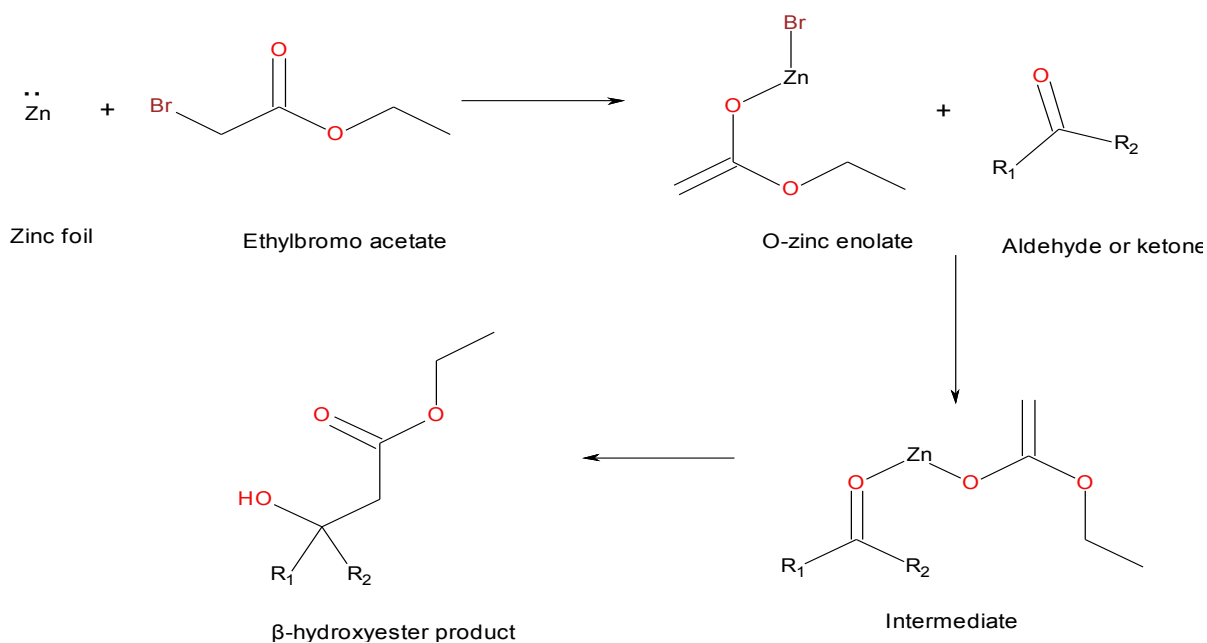
observed by TLC and NMR that the compound disintegrated and some impurities were observed. One of the possibilities is that the aldehyde synthesised in the presence of moisture might have reacted to give hemi-acetals or acetals.

Hence a scale up of the reaction was carried out in the next experiment and after a quick work up and TLC check, half of the product was taken to the next step i.e. HWE reaction to prepare alkene. The remaining half was dried thoroughly and stored in a freezer at 0°C for analysis. The HWE reaction did not progress after 72 hours and hence the reaction was stopped. In a similar way 1-docosanol was also converted to aldehyde using Swern oxidation. In the next set of experiments, both the aldehydes were prepared by Swern oxidation and after rapid work up were taken for HWE reactions. This reaction was monitored by TLC, however the reaction did not go to completion, hence after 14 days the reaction was stopped. Another set of experiment was set up with 1-octadecanol being converted to aldehyde and then taken to HWE reaction, however instead of stirring the reaction mixture at room temperature, it was heated up to 50-60°C. The reaction was monitored by TLC, however as the reaction failed to progress after 14 days, the reaction was stopped and traces of alkene were recovered along with a mixture of aldehyde and possible acetal by-products. Hence this reaction was not taken further.

It was therefore concluded that though the aldehyde formation occurred, the HWE reaction does not progress with large carbon chain compounds. It was also noted that the long chain aldehydes prepared by Swern oxidation were unstable at room temperature and required to be stored in a cold place away from moisture.

5.3.3 Synthesis of β -hydroxy esters by Reformatsky reaction

In an attempt to improve the yields of long carbon chain compounds a Reformatsky reaction was carried out. This reaction converts α -haloesters and aldehydes or ketones to β -hydroxy esters in the presence of zinc metal (see Fig. 5.4). These compounds can then be dehydrated to give α, β -unsaturated esters, which can then be oxidised by potassium permanganate to give the target compound.



Scheme 5.4: Scheme for synthesis of β hydroxy esters by Reformatsky reaction

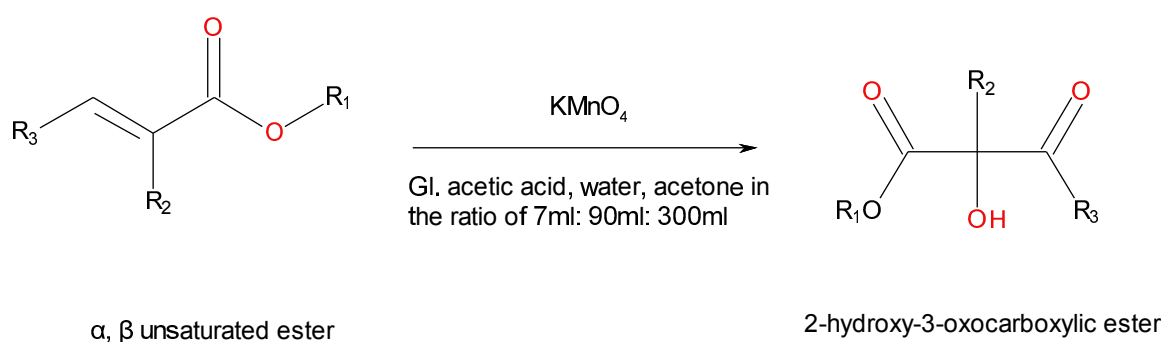
For this experiment, small pieces of zinc (1 equivalent) were added in the flask with anhydrous toluene, followed by 20% of the required α -haloester i.e ethylbromo acetate (20% of 1 equivalent) added drop wise in the flask. The remaining ethylbromo acetate was mixed with the ketone (cyclopentadecanone, 1 equivalent) along with the solvent (anhydrous toluene) and added to the mixture drop wise taking care that the temperature did not rise above 30-40°C. To avoid overheating external cooling was provided. After the complete addition of ketone or aldehyde, the reaction mixture was heated at reflux for 18 hours. This reaction mixture was then extracted with ethyl acetate. These layers were dried over magnesium sulphate and evaporated under reduced pressure to give the required product (Shriner (1942)). It is essential to maintain dry conditions throughout as moisture may cause decrease in yield. For the reaction to progress the zinc surface should be clean, the oily coating of the by-product can stop the reaction. A parallel reaction was set for cyclododecanone.

It was observed that the products obtained from the Reformatsky reaction did not improve the yield and hence products from both the ketones, cyclopentadecanone and cyclododecanone, were not taken for the next dehydration step. This reaction was validated by performing the experiment with a smaller carbon chain ketone like cyclohexanone. The experimental conditions remained same as mentioned in the earlier experiment. It was observed that the yield of the product obtained from the cyclohexanone was higher than products obtained from cyclopentadecanone and cyclododecanone. However on comparing the yields of the cyclohexanone product from both the reactions, the HWE reaction had a higher yield.

Hence the yields of cyclopentadecanone and cyclododecanone were not optimised any further.

From the synthetic chemistry point of view, the Reformatsky reaction not only constitutes a method for synthesis of β -hydroxy esters, but is also a valuable method for lengthening the carbon chain by two carbon atoms. Due to the presence of carbethoxy group, it is possible to further lengthen the chain through appropriate repetition of reaction sequence (Shriner (1942)). With this concept in mind, a new experiment was set up with ethyl-2-bromo caprylate and dodecyl aldehyde, with exact conditions as mentioned in the earlier reaction. However the reaction did not progress and large quantities of aldehyde were recovered. Hence this reaction was not taken any further.

5.3.4 Synthesis of 2-alkyl-2-hydroxy-3-oxocarboxylic esters



Scheme 5.5: Scheme for synthesis of 2-alkyl-2-hydroxy-3-oxocarboxylic esters by direct oxidation method by potassium permanganate

The α, β -unsaturated esters (alkene) prepared (see Scheme. 5.2) were oxidised using potassium permanganate under mildly acidic conditions following the method of Crout & Rathbone (1989) (see Scheme. 5.5). A solvent system was created by mixing glacial acetic acid, water, and acetone in the ratio of 7: 90: 300. The ratio in which the solvents are mixed is of importance for the reaction to progress. This solvent system was stirred along with the alkene (1eq) at -10°C in an ice bath with ice and salt (sodium chloride) mixture. To this reaction mixture solid $KMnO_4$ (in excess of alkene) was added slowly maintaining the temperature at -10°C . After the complete addition of $KMnO_4$, the reaction mixture was allowed to stir at -10°C for two hours. After the extractive work up with DCM, which upon evaporation gave desired 2-hydroxy-3-oxocarboxylic esters (Crout & Rathbone (1989)). The oxidised alkene compounds are sent for anti tuberculosis screening at NIAID, US. The microbiology results are still pending. The table 5.3 lists the compounds synthesised.

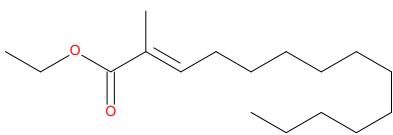
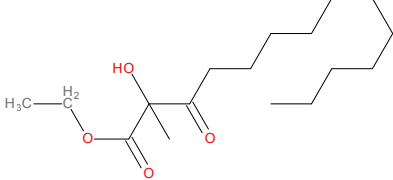
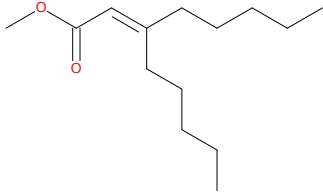
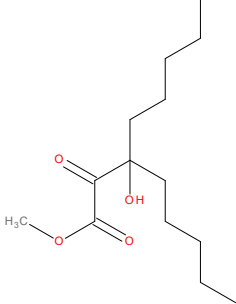
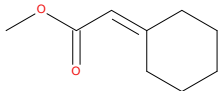
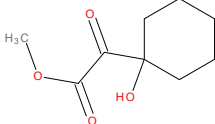
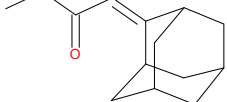
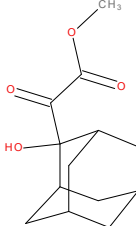
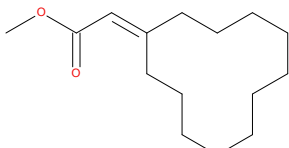
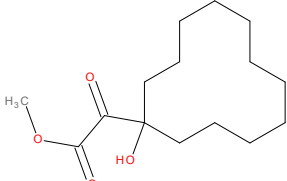
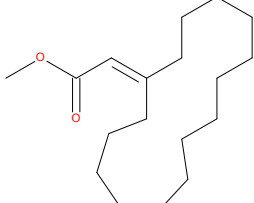
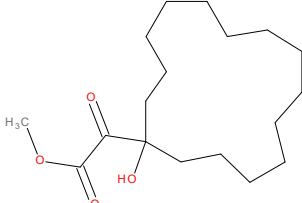
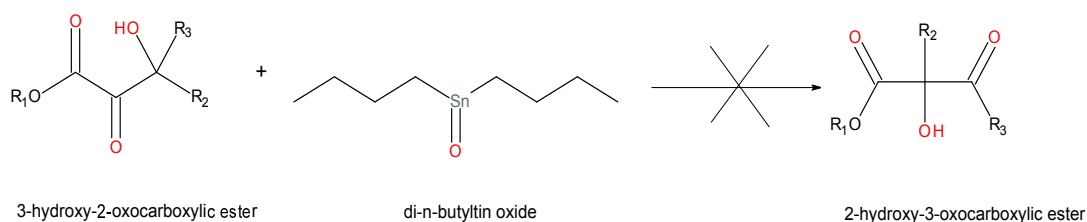
Compound number	Structure of alkene	Structure of final product	Yield (%)
(176)			74.7
(177)			79.2
(178)			87
(179)			75.3
(180)			30.2
(181)			49

Table 5.3: List of analogues of 2-alkyl-2-hydroxy-3-oxocarboxylic esters and 3,3-dialkyl-3-hydroxy-2-oxocarboxylic ester.

5.3.5 Attempted tertiary ketol rearrangement of 2-hydroxy-3-oxocarboxylic esters by di-n-butyltin oxide catalyst method

Schloss et al. (1985), isolated an enzyme acetolactate synthase, which catalyzes the first step formation of α -keto- β -hydroxy isomers, in the synthesis of the branched-chain amino acids (valine, leucine, and isoleucine). These intermediates undergo a tertiary ketol rearrangement to give β -keto- α -hydroxy isomers in presence of the enzyme reductoisomerase. Crout & Rathbone (1987) demonstrated the tertiary ketol rearrangement of α -keto- β -hydroxy compounds catalysed by di-n-butyltin oxide. The tertiary ketol rearrangement provided an added advantage of ring expansion by one carbon atom with particular examples (Crout & Rathbone (1987)). With this concept in mind, the tertiary ketol rearrangement was attempted on the 3-hydroxy-2-oxocarboxylic ester.

A small scale reaction was carried out in a glass vessel. The 3-hydroxy-2-oxocarboxylic ester was stirred in d_8 -toluene along with di-n-butyltin oxide (3 mol%). This tube was sealed and heated at a reflux at a controlled temperature in a heating block. A periodic NMR data was collected to check progress of the reaction. However as the reaction failed to progress, after two days the reaction was stopped. Another reaction was carried out with the chemicals and the experimental conditions remained same, except the reaction was allowed to stir for 7 days. However the reaction did not progress and hence the reaction was not taken further.



Scheme 5.6: Attempted scheme for synthesis of 2-alkyl-2-hydroxy-3-oxocarboxylic esters by catalytic rearrangement method

5.3.6 Microbiological results

The 2-alkyl-2-hydroxy-3-oxocarboxylic esters were sent to the Infectious Disease Research Institute (IDRI, US) for screening against *Mycobacterium tuberculosis* H37Rv strain. The Table. 5.4 presents the results obtained from IDRI.

Test Compounds			
Compound number	MIC (μM)	IC ₅₀ (μM)	IC ₉₀ (μM)
(178)	>200	>200	>200
(176)	53	30	48
(177)	>200	150	>200
(179)	>200	>200	>200
(180)	>200	>200	>200
(181)	200	150	180

Table 5.4: Table representing the first stage microbiological data for the 2-alkyl-2-hydroxy-3-oxocarboxylic esters.

As discussed in 2.4.8 in chapter 2, since it was observed that one of the compound was found to possess weak activity, the compound (176) was subjected to the high throughput screening (HTS) process (second stage evaluation).

In the microbiological second stage evaluation, MIC assays were performed in aerobic conditions and under low oxygen conditions and the compound was found to be active in both the assays (see Table. 5.5)

Assays	MIC under aerobic conditions	MIC under low oxygen
Compound number	(176)	
MIC (μM)	57	14
IC ₅₀ (μM)	32	28
IC ₉₀ (μM)	63	59

Table 5.5: The second stage MIC data summary of the 2-alkyl-2-hydroxy-3-oxocarboxylic esters.

The compound showed the bactericidal activity in the MBC assay. The minimum bactericidal concentration was found to be 13 μM and the bactericidal action was found to be concentration dependent but not time dependent. The compound (176) was also found to be cytotoxic with the IC₅₀ value of 16 μM , and also exhibited intracellular activity against *M. tuberculosis*. The compound (176) was tested against many *M. tuberculosis* resistant isolates and was found to be active (see Table.5.6)

Compound number	MIC (μM)	Resistant Isolate
(176)	95	INH-R1
	106	INH-R2
	95	RIF-R1
	99	RIF-R2
	98	FQ-R1

Table 5.6: The second stage MIC data summary of the fluorinated carboxamidrazone amides.

5.4 Summary and Conclusion

This study has explored the concept of custom designed inhibitors, and a range of α , β -unsaturated esters were prepared. The larger aldehydes and ketones proved problematic in preparation of the α , β -unsaturated esters. The permanganate oxidation of the α , β -unsaturated esters worked well except for the alkenes derived from the cyclic ketones having a ring size larger or equal to 12 carbons. With this set of α , β -unsaturated esters (alkenes) the Bu_2SnO catalysed tertiary ketol rearrangement was not observed.

It was observed that one of the α -keto, β -hydroxy esters have shown a weak activity. The future work might involve exploring various different ways to prepare stable long chain aldehydes and their subsequent conversion to α , β -unsaturated esters and oxidising it to derive the target compounds (α -keto, β -hydroxy esters). Another interesting fact that can be observed is that the compounds containing cyclised ring structures do not show any activity. The possible reason might be the constraints imposed on the rigid ring structure which make it difficult for the ligands to adapt to the binding site geometry of the protein.

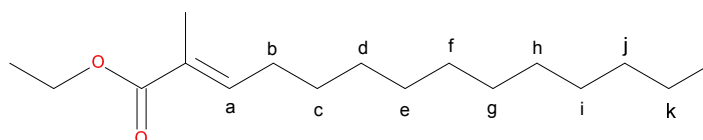
5.5 Experimental

The chemicals and instrumentations used are the same as discussed in 3.5.

5.5.1 General preparation of α, β -unsaturated esters

NaH (60% in mineral oil, 0.88 g, 22 mmoles) was dispersed in 10 mL of DME and stirred under argon. The reaction mixture was placed in an ice bath and the appropriate phosphonate (triethyl phosphonopropionate or trimethyl phosphonoacetate) (25 mmoles) was added drop wise into the mixture ensuring that the temperature remained below 35°C. After the addition of phosphono acetate the reaction mixture was allowed to stir at the room temperature for about 30 mins. The reaction mixture was again cooled to 10-15°C and the respective aldehyde or ketone (25 mmoles) was added drop wise again maintaining the temperature at 35°C. Following the addition, the reaction mixture was allowed to stir at room temperature for 2 days or as was required. The reaction mixture was quenched with water (20 mL) and extracted three times with DCM (15 mL). The organic layers collected were then evaporated under vacuum and the crude product was collected. The crude product obtained was then stirred with freshly prepared sat. sodium bisulphite solution for 48 hours. It was observed that a white precipitate was formed which was filtered off and the aqueous layer was then extracted with ether. The organic layers collected were then evaporated under vacuum to give the crude product, which was then subjected to column separation on silica using 1% ether in petrol 40-60°C as solvent system.

Ethyl (*E*)-2-methyltetradec-2-enoate (170)



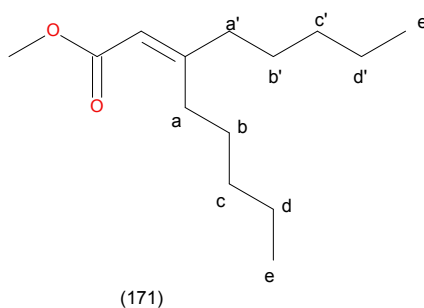
(170)

$^1\text{H NMR}$ (CDCl_3): 6.76 (m, 1H, $J = 7.5, 1.4$ Hz, **a**), 4.19 (q, $J = 7.1$ Hz, 2H, $\text{CH}_3\text{CH}_2\text{O-}$), 2.18 (s, 2H, **b**), 1.83 (s, 3H, CH_3), 1.65 (s, 3H, $\text{CH}_3\text{CH}_2\text{O-}$), 1.48 1.37 (overlapping m, 4H, **c and k**), 1.34 1.22 (overlapping m, 14H, **d, e, f, g, h, i and j**), 0.93 0.83 (t, 3H, $J = 6.7$ Hz, **l**) ppm.

IR (KBr disc) ν : 2958 (Alkyl C-H), 2949 (Alkyl C-H), 1663 (C=O), 1626, 1565, 1541, 1504, 1463, 1435, 1240, 1163, 1112, 1062 cm^{-1} .

Yield: 1.659 g, 24.7%.

Methyl 3-pentyloct-2-enoate (171)

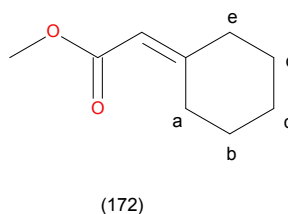


$^1\text{H NMR}$ (CDCl_3): 5.63 (s, 1H, **CH=C**), 3.68 (s, 3H, **-OCH₃**), 2.67–2.52 (overlapping m, 4H, **a and a'**), 2.16 (overlapping m, 4H, **b and b'**), 1.54–1.40 (overlapping m, 4H, **c and c'**), 1.31 (ddd, $J = 9.8, 6.7, 2.8$ Hz, 4H, **d and d'**), 0.90 (overlapping t, 6H, $J = 6.7$ Hz, **e and e'**) ppm.

IR (KBr disc) ν : 2946 (Alkyl C-H), 2925 (Alkyl C-H), 1636 (C=O), 1539, 1475, 1443, 1401, 1247, 1149 cm^{-1} .

Yield: 1.602g, 28.3%.

Methyl 2-cyclohexylideneacetate (172)

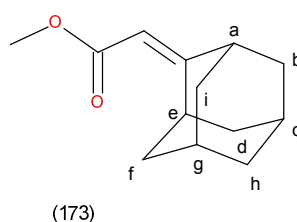


$^1\text{H NMR}$ (CDCl_3): 5.66 (s, 1H, **CH=C**), 3.78 (s, 3H, **-OCH₃**), 2.37–2.23 (overlapping m, 4H, **a and e**), 1.64–1.44 (overlapping m, 4H, **b and d**), 1.35 (dtt, 2H, $J = 11.7, J = 3.2, J = 2.430$, **c**) ppm.

IR (KBr disc) ν : 2934 (Alkyl C-H), 2856 (Alkyl C-H), 1705, 1663 (C=O), 1445, 1420, 1338, 1310, 1220, 1117 cm^{-1} .

Yield: 2.1 g, 60%.

Methyl 2-(2-adamantylidene)acetate (173)

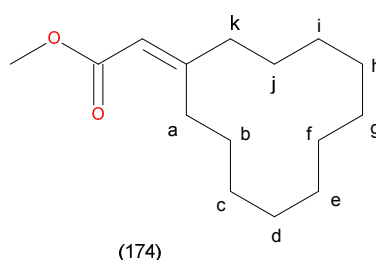


$^1\text{H NMR}$ (CDCl_3): 5.58 (s, 1H, **CH=C**), 3.67 (s, 3H, **-OCH₃**), 2.43 (overlapping m, 4H, **a and e**), 2.10 1.73 (overlapping m, 6H, **d, c and e**), 1.51 – 1.45 (overlapping m, 10H, **b, f, g, h and i**) ppm.

IR (KBr disc) ν : 2913 (Alkyl C-H), 2844 (Alkyl C-H), 1647 (C=O), 1584, 1547, 1470, 1435, 1392, 1167 cm^{-1} .

Yield: 5.095 g, 98.7%.

Methyl 2-cyclododecylideneacetate (174)

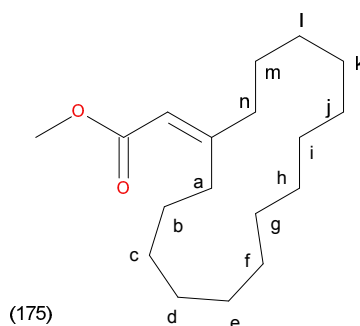


$^1\text{H NMR}$ (CDCl_3): 5.74 (s, 1H, **CH=C**), 3.81 (s, 3H, **-OCH₃**), 2.57 – 2.43 (overlapping m, 4H, **a and k**), 2.26 – 2.15 (ddd, 4H, $J=13.646$, $J=8.060$, $J=3.820$, **b and j**), 1.74 – 1.63 (overlapping m, 8H, **c, d, h and i**), 1.58 – 1.46 (overlapping m, 6H, **e, f and g**) ppm.

IR (KBr disc) ν : 2928 (Alkyl C-H), 2855 (Alkyl C-H), 2671, 1713 (C=O), 1469, 1446, 1416, 1377, 1347, 1320, 1282, 1268, 1166, 1148, 1076, 1052, 1019 cm^{-1} .

Yield: 0.747 g, 12.53%.

Methyl 2-cyclopentadecylideneacetate (175)



$^1\text{H NMR}$ (CDCl_3): 5.66 (s, 1H, **CH=C**), 3.67 (s, 3H, **-OCH₃**), 2.65 – 2.53 (overlapping m, 4H, **a and n**), 2.41 – 2.33 (overlapping m, 4H, **b and m**), 2.20 – 2.07 (overlapping m, 4H, **c and l**), 1.70 – 1.58 (overlapping m, 8H, **d, e, j and k**), 1.50 (dd, 2H, $J = 13.8, 6.0$ Hz, **h**), 1.45 – 1.21 (overlapping m, 6H, **f, g and i**) ppm.

IR (KBr disc) ν : 2900 (Alkyl C-H), 2875 (Alkyl C-H), 1652 (C=O), 1607, 1579, 1547, 1475, 1447, 1419, 1338, 1282, 1156, 1039 cm^{-1} .

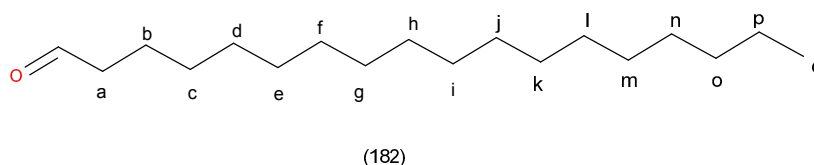
Yield: 0.12 g, 3%.

5.5.2 General procedure for synthesis of aldehydes using Swern oxidation

Oxalyl chloride (3 mmol) was stirred in anhydrous DCM (5 mL) at -78°C under argon. To this solution DMSO (6 mmol) was added drop wise taking care that the temperature was maintained below -65°C and the reaction mixture was stirred vigorously for 20 mins. To this reaction mixture, a solution of alcohol (2.1 mmol) in DCM (10 mL) was added drop wise maintaining the temperature below -65°C . This reaction mixture was then stirred for 1 hour, followed by the addition of triethylamine (12 mmol). The reaction mixture was stirred for one hour at room temperature before it was quenched with water (20 mL) and stirred for 30 mins and the aqueous layer was extracted with DCM three times (15 mL).

The organic extracts were then washed with 1M HCl (15 mL). These washing were then dried over anhydrous MgSO_4 , and evaporated under pressure to give crude product.

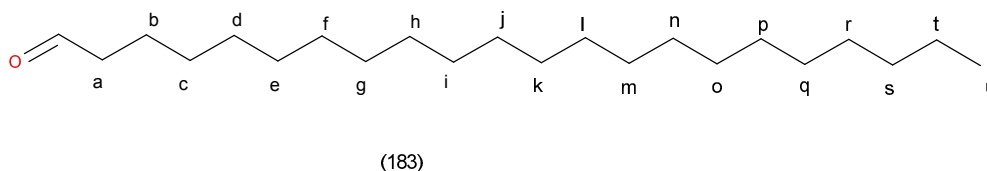
Octadecanal (182)



$^1\text{H NMR}$ (CDCl_3): 9.78 (s, 1H, $\text{O}=\text{C}-\text{H}$), 2.43 (overlapping m, 8H, **a, b, c and d**), 1.63 (overlapping m, 8H, **e, f, g and h**), 1.26 (overlapping m, 16H, **i, j, k, l, m, n, o and p**), 0.92–0.85 (t, 3H, $J=7.000$, **q**) ppm.

Yield: 0.37 g, 64%.

Docosanal (183)



$^1\text{H NMR}$ (CDCl_3): 9.76 (s, 1H, $\text{O}=\text{C}-\text{H}$), 2.63 (overlapping m, 2H, **a**), 1.58 (overlapping m, 2H, **b**), 1.26 (overlapping m, 36H, **c, d, e, f, g, h, i, j, k, l, m, n, o, p, q, r, s and t**), 0.94–0.83 (t, 3H, $J=7.000$, **u**) ppm.

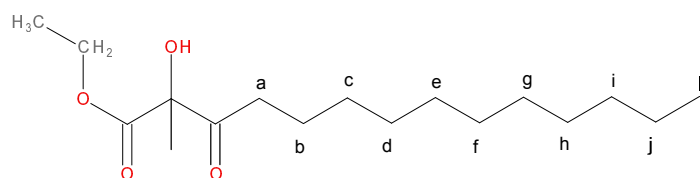
Yield: 0.42 g, 73.6%.

5.5.3 General procedure for oxidation of α, β -unsaturated carboxylic esters

A solvent system was prepared by mixing glacial acetic acid, water, and acetone in the ratio of 2.33 mL: 30 mL: 100 mL and stirred in an ice bath with salt and ice mixture at -10°C . To this solvent system alkene (2.6 mmol) was added and stirred at -10°C . To this reaction mixture solid KMnO_4 (in excess of alkene 4.5

mmol) was added slowly maintaining the temperature at -10°C . After the complete addition of KMnO_4 , the reaction mixture was allowed to stir at -10°C for two hours. The reaction mixture was then filtered off to remove the brown coloured manganese dioxide and the filtrate obtained was then evaporated under reduced pressure to remove acetone. The remaining solvent was then extracted with DCM (15 mL) three times and the organic layers were dried on magnesium sulphate, which upon evaporation gave desired 2-hydroxy-3-oxocarboxylic esters or 3-hydroxy-2-oxocarboxylic esters

Ethyl 2-hydroxy-2-methyl-3-oxo-tetradecanoate (176)



(176)

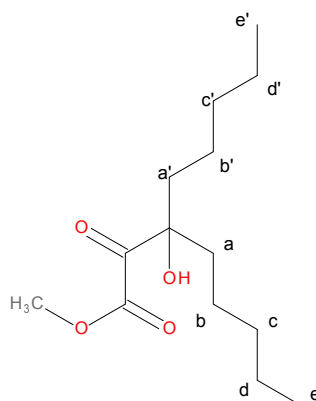
$^1\text{H NMR}$ (CDCl_3): 4.30–4.17 (q, 2H, $J = 7.115$, $\text{CH}_3\text{CH}_2\text{O}-$), 2.73–2.42 (complex m, 2H, **a**), 1.86 (complex m, 1H, **OH**), 1.61 (t, 3H, $J = 7.1$, CH_3), 1.57 (t, 3H, $J = 7.1$, $\text{CH}_3\text{CH}_2\text{O}-$), 1.32–1.21 (overlapping m, 18H, **b, c, d, e, f, g, h, i and j**), 0.90–0.83 (t, 3H, $J = 6.7$ Hz, **k**) ppm.

IR (neat) ν : 3045 (O-H), 2942 (Alkyl C-H), 2869 (Alkyl C-H), 1636 (C=O), 1446, 1427, 1389, 1324, 1283, 1267, 1131, 1092, 1047, 1019, 1010 cm^{-1} .

Mass spectrum(APCI +) **m/z**: Found 301.2373 ($\text{M}+\text{H}$) $^+$; calculated for $\text{C}_{17}\text{H}_{32}\text{O}_4$ 301.2300; 24.3 ppm.

Yield: 0.55g, 74.7%.

Methyl 3-hydroxy-2-oxo-3-pentyl-octanoate (177)



(177)

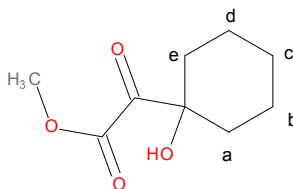
¹H NMR (CDCl₃): 9.74 (s, 1H, **OH**), 4.51 (s, 1H, **-OCH₃**), 2.32 (overlapping m, 4H, **a and a'**), 1.89 (overlapping m, 4H, **b and b'**), 1.29 (overlapping m, 8H, **c, c', d and d'**), 0.90 (overlapping t, 6H, J = 6.7 Hz, **e and e'**) ppm.

IR (neat) ν : 3044 (O-H), 2956 (Alkyl C-H), 2919 (Alkyl C-H), 1636 (C=O), 1496, 1479, 1462, 1412, 1390, 1283, 1247, 1149 cm⁻¹.

Mass spectrum(APCI +) m/z: Found 258.1826 (M+H)⁺; calculated for C₁₄H₂₆O₄ 258.1831; 1.9 ppm.

Yield: 0.53g, 79.2%.

Methyl 2-(1-hydroxycyclohexyl)-2-oxo-acetate (178)



(178)

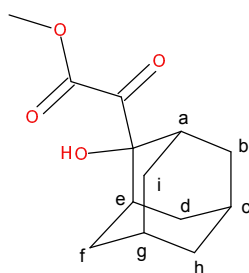
¹H NMR (CDCl₃): 9.72 (s, 1H, **OH**), 3.81 (s, 3H, **-OCH₃**), 2.31 (overlapping m, 4H, **a and e**), 1.52 (overlapping m, 4H, **b and d**), 1.34 (dtt, 2H, J=11.706, J=3.180, J=2.430, **c**) ppm.

IR (neat) ν : 3052 (O-H), 2946 (Alkyl C-H), 2925 (Alkyl C-H), 1624 (C=O), 1539, 1475, 1443, 1401, 1247, 1212, 1172, 1112, 1057, 1037, 1020, 1001 cm^{-1} .

Mass spectrum(APCI +) m/z: Found 186.0886 ($\text{M}+\text{H}$)⁺; calculated for $\text{C}_9\text{H}_{14}\text{O}_4$ 186.0892; 3.2 ppm.

Yield: 1.47g, 87%.

Methyl 2-(2-hydroxy-2-adamantyl)-2-oxo-acetate (179)



(179)

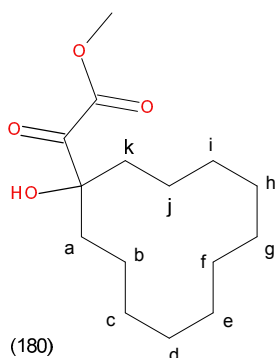
¹H NMR (CDCl₃): 9.74 (s, 1H, **OH**), 3.71 (s, 3H, **-OCH₃**), 2.31 (overlapping m, 4H, **a and e**), 1.84 (overlapping m, 6H, **d, c and e**), 1.40 (overlapping m, 10H, **b, f, g, h and i**) ppm.

IR (neat) ν : 3045 (O-H), 2956 (Alkyl C-H), 2919 (Alkyl C-H), 1631 (C=O), 1496, 1479, 1462, 1412, 1390, 1283, 1262, 1149, 1127, 1119, 1089, 1052, 1001 cm^{-1} .

Mass spectrum(APCI +) m/z: Found 237.1124 ($\text{M}-\text{H}$)⁺; calculated for $\text{C}_{13}\text{H}_{18}\text{O}_4$ 238.1205; 34.0 ppm.

Yield: 3.41g, 75.3%.

Methyl 2-(1-hydroxycyclododecyl)-2-oxo-acetate (180)



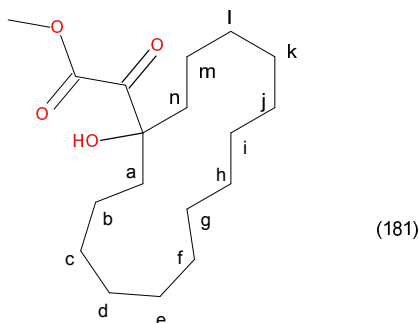
$^1\text{H NMR}$ (CDCl_3): 9.76 (s, 1H, **OH**), 3.89 (s, 3H, **-OCH₃**), 2.82–2.71 (overlapping m, 4H, **a and k**), 2.52–2.42 (overlapping m, 4H, **b and j**), 2.08–1.51 (overlapping m, 8H, **c, d, h and i**), 1.31 (overlapping d, 6H, $J = 26.4$ Hz, **e and f**), 0.87 (q, 2H, $J = 6.1$ Hz, **g**) ppm.

IR (*neat*) ν : 3100 (O-H), 2923 (Alkyl C-H), 2850 (Alkyl C-H), 1633 (C=O), 1611, 1539, 1314, 1298, 1248, 1183, 1145, 1109, 1075, 1048, 1011 cm^{-1} .

Mass spectrum(APCI +) m/z : Found 271.1903 ($\text{M}+\text{H}$)⁺; calculated for $\text{C}_{15}\text{H}_{26}\text{O}_4$ 270.1831; 26.6 ppm.

Yield: 0.24g, 30.2%.

methyl 2-(1-hydroxycyclopentadecyl)-2-oxo-acetate (181)



$^1\text{H NMR}$ (CDCl_3): 9.74 (s, 1H, **OH**), 3.62 (s, 3H, **-OCH₃**), 2.54–2.47 (overlapping m, 4H, **a and n**), 2.37–2.28 (overlapping m, 4H, **b and m**), 2.12 (overlapping m, 4H, **c and l**), 1.64 (overlapping m, 8H, **d, e, j and k**), 1.46 (dd, 2H, $J = 13.8, 6.0$ Hz, **h**), 1.32 (overlapping m, 6H, **f, g and i**) ppm.

IR (neat) ν : 3060 (O-H), 2951 (Alkyl C-H), 2885 (Alkyl C-H), 2832, 1629 (C=O), 1482, 1460, 1438, 1428, 1396, 1372, 1314, 1291, 1244, 1169, 1149, 1112, 1100, 1069, 1046, 1008 cm^{-1} .

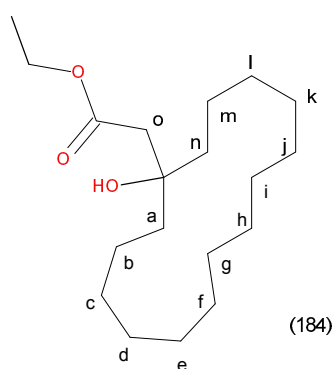
Mass spectrum(APCI +) m/z: Found 312.2200 (M+H)⁺; calculated for C₁₈H₃₂O₄ 312.2300; 32.0 ppm.

Yield: 0.0387g, 10%.

5.5.4 General procedure used for Reformatsky reaction

In an oven dried flask, anhydrous toluene was added (10 mL). To this fine pieces of zinc metal sheet were added (1 equivalent) followed by drop wise addition of 20% of the required ethylbromo acetate (20% of 1 equivalent) maintaining the temperature below 35°C using ice bath if required. The remaining ethylbromo acetate was mixed with the ketone (1 equivalent) along with anhydrous toluene (20 mL) and added drop wise again maintaining the temperature below 35°C. After the complete addition of ketone or aldehyde, the reaction mixture was heated at reflux for 18 hours. This reaction mixture was then extracted with ethyl acetate (15 mL) three times. These layers were dried over magnesium sulphate and evaporated under reduced pressure to give the desired product.

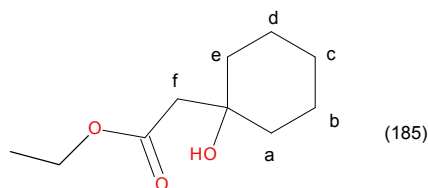
Ethyl 2-(1-hydroxycyclopentadecyl)acetate (184)



¹H NMR (CDCl₃): 4.20 (s, 3H, -OCH₂CH₃), 2.43 (s, 1H, OH), 2.28 (complex m, 2H, o), 1.84–1.56 (overlapping m, 4H, a and n), 1.43 (overlapping m, 8H, b, c, m and l), 1.34 (m, 3H, -OCH₂CH₃), 1.28 (overlapping m, 16H, d, e, f, g, h, i, j and k) ppm.

Yield: 0.12g, 8.9%.

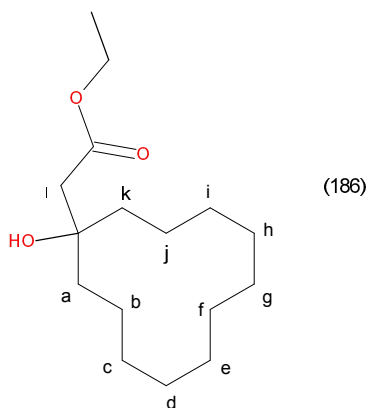
Ethyl 2-(1-hydroxycyclohexyl)peroxyacetate (185)



$^1\text{H NMR}$ (CDCl_3): 4.33–4.01 (complex m, 2H, $-\text{OCH}_2\text{CH}_3$), 2.45 (s, 1H, **OH**), 2.34 (complex m, 2H, **f**), 1.73–1.55 (overlapping m, 4H, **a and e**), 1.48–1.37 (overlapping m, 4H, **b and d**), 1.32 (m, 3H, $-\text{OCH}_2\text{CH}_3$), 1.26 (dtt, 2H, $J=11.706$, $J=3.180$, $J=2.430$, **c**) ppm.

Yield: 3.22g, 78%.

Ethyl 2-(1-hydroxycyclododecyl)acetate (186)



$^1\text{H NMR}$ (CDCl_3): 4.11 (complex m, 2H, $-\text{OCH}_2\text{CH}_3$), 2.47 (s, 1H, **OH**), 2.37 (complex m, 2H, **l**), 2.12 (overlapping m, 4H, **a and k**), 1.64 (overlapping m, 4H, **b and j**), 1.46 (overlapping m, 8H, **c, d, h and i**), 1.32 (m, 3H, $-\text{OCH}_2\text{CH}_3$), 1.25 (overlapping m, 6H, **e, f and g**) ppm.

Yield: 0.26g, 9.4%.

5.5.5 General procedure for tertiary ketol rearrangement using di-n-butyltin oxide catalyst

In an oven dried NMR glass tube, d_8 -toluene was added (0.8 mL). To this 3-hydroxy-2-oxocarboxylic ester was added (0.33 mmoles) followed by di-n-butyltin oxide (3 mol%, 0.01g). This tube was then sealed and heated at a controlled temperature in a heating block taking care that the toluene is just refluxing. At regular intervals (4 hours) NMR data was collected to check the progress of reaction.

References

- Abdel-Aal, M. T., El-Sayed, W. A., El-Kosy, S. M., & El-Ashry, E. S. H. (2008). Synthesis and antiviral evaluation of novel 5-(n-aryl-aminomethyl-1, 3, 4-oxadiazol-2-yl) hydrazines and their sugars, 1, 2, 4-triazoles, tetrazoles and pyrazolyl derivatives. *Archiv der Pharmazie*, *341*(5), 307–313.
- Aguilar, D., Infante, E., Martin, C., Gormley, E., Gicquel, B., & Hernandez Pando, R. (2007). Immunological responses and protective immunity against tuberculosis conferred by vaccination of balb/c mice with the attenuated mycobacterium tuberculosis (phop) so2 strain. *Clinical & Experimental Immunology*, *147*(2), 330–338.
- Alderwick, L., Birch, H., Mishra, A., Eggeling, L., Besra, G., et al. (2007). Structure, function and biosynthesis of the mycobacterium tuberculosis cell wall: arabinogalactan and lipoarabinomannan assembly with a view to discovering new drug targets. *Biochemical Society Transactions*, *35*(Pt 5), 1325.
- Almasirad, A., Tabatabai, S. A., Faizi, M., Kebriaeezadeh, A., Mehrabi, N., Dalvandi, A., & Shafiee, A. (2004). Synthesis and anticonvulsant activity of new 2-substituted-5- [2-(2-fluorophenoxy)phenyl]-1,3,4-oxadiazoles and 1,2,4-triazoles. *Bioorganic & Medicinal Chemistry Letters*, *14*(24), 6057 – 6059.
- Ananthan, S., Faaleolea, E. R., Goldman, R. C., Hobrath, J. V., Kwong, C. D., Laughon, B. E., Maddry, J. A., Mehta, A., Rasmussen, L., Reynolds, R. C., et al. (2009). High-throughput screening for inhibitors of *Mycobacterium tuberculosis* h37rv. *Tuberculosis*, *89*(5), 334–353.
- Anderson, R. & Chargaff, E. (1929). The chemistry of the lipoids of tubercle bacilli vi. concerning tuberculostearic acid and phthioic acid from the acetone-soluble fat. *Journal of Biological Chemistry*, *85*(1), 77–88.

- Andreocci, A. (1893). Ueber das santonin. *Berichte der deutschen chemischen Gesellschaft*, 26(3), 2985–2986.
- Asselineau, J., Lanéelle, G., et al. (1998). Mycobacterial lipids: a historical perspective. *Frontiers in Bioscience*, 3, e164–174.
- Astarie-Dequeker, C., Le Guyader, L., Malaga, W., Seaphanh, F.-K., Chalut, C., Lopez, A., & Guilhot, C. (2009). Phthiocerol dimycocerosates of *m. tuberculosis* participate in macrophage invasion by inducing changes in the organization of plasma membrane lipids. *PLoS pathogens*, 5(2), e1000289.
- Babudri, F., Farinola, G. M., Naso, F., & Ragni, R. (2007). Fluorinated organic materials for electronic and optoelectronic applications: the role of the fluorine atom. *Chemical Communications*, (10), 1003–1022.
- Barry III, C. E., Lee, R. E., Mdluli, K., Sampson, A. E., Schroeder, B. G., Slayden, R. A., & Yuan, Y. (1998). Mycolic acids: structure, biosynthesis and physiological functions. *Progress in Lipid Research*, 37, 143 – 179.
- Bayrak, H., Demirbas, A., Demirbas, N., & Karaoglu, S. A. (2009). Synthesis of some new 1, 2, 4-triazoles starting from isonicotinic acid hydrazide and evaluation of their antimicrobial activities. *European Journal of Medicinal Chemistry*, 44(11), 4362–4366.
- Behling, C., Perez, R., Kidd, M., Staton, G., & Hunter, R. (1993). Induction of pulmonary granulomas, macrophage procoagulant activity, and tumor necrosis factor-alpha by trehalose glycolipids. *Annals of Clinical & Laboratory Science*, 23(4), 256–266.
- Behr, M. A. (2002). BCG different strains, different vaccines? *The Lancet Infectious Diseases*, 2(2), 86–92.
- Belanger, A. E., Besra, G. S., Ford, M. E., Mikusová, K., Belisle, J. T., Brennan, P. J., & Inamine, J. M. (1996). The embab genes of mycobacterium avium encode an arabinosyl transferase involved in cell wall arabinan biosynthesis that is the target for the antimycobacterial drug ethambutol. *Proceedings of the National Academy of Sciences*, 93(21), 11919–11924.
- Belisle, J. T., Vissa, V. D., Sievert, T., Takayama, K., Brennan, P. J., & Besra, G. S. (1997). Role of the major antigen of mycobacterium tuberculosis in cell wall biogenesis. *Science*, 276(5317), 1420–1422.
- Ben, B. (2006). Interactions between mycobacterium tuberculosis and the immune system. Master's thesis, Davidson College.

- Besra, G. S., Minnikin, D. E., Wheeler, P. R., & Ratledge, C. (1993). Synthesis of methyl (z)-tetracos-5-enoate and both enantiomers of ethyl (e)-6-methyltetracos-4-enoate: possible intermediates in the biosynthesis of mycolic acids in mycobacteria. *Chemistry and Physics of Lipids*, 66(1–2), 23–34.
- Bhatt, A., Molle, V., Besra, G. S., Jacobs, W. R., & Kremer, L. (2007). The mycobacterium tuberculosis fas-ii condensing enzymes: their role in mycolic acid biosynthesis, acid-fastness, pathogenesis and in future drug development. *Molecular Microbiology*, 64(6), 1442–1454.
- Bühm, H.-J., Banner, D., Bendels, S., Kansy, M., Kuhn, B., Müller, K., Obst-Sander, U., & Stahl, M. (2004). Fluorine in medicinal chemistry. *ChemBioChem*, 5(5), 637–643.
- Billington, D. C., Lowe, P. R., Rathbone, D. L., & Schwalbe, C. H. (2000). A new amidrazone derivative with antimycobacterial activity. *Acta Crystallographica Section C*, 56, e211–e212.
- Bladin, J. A. (1885). Ueber die cyanverbindungen der aromatischen o-diamine. *Berichte der deutschen chemischen Gesellschaft*, 18(1), 666–674.
- Boese, R., Weiss, H. C., & Bläser, D. (1999). The melting point alternation in the short-chain n-alkanes: Single-crystal x-ray analyses of propane at 30 k and of n-butane to n-nonane at 90 k. *Angewandte Chemie International Edition*, 38(7), 988–992.
- Borders, C., Courtney, A., Ronen, K., Pilar Laborde-Lahoz, M., Guidry, T., Hwang, S.-A., Olsen, M., Hunter, R., Hollmann, T., Wetsel, R., et al. (2005). Requisite role for complement c5 and the c5a receptor in granulomatous response to mycobacterial glycolipid trehalose 6, 6'-dimycolate. *Scandinavian Journal of Immunology*, 62(2), 123–130.
- Brennan, P. J. & Nikaido, H. (1995). The envelope of mycobacteria. *Annual Review of Biochemistry*, 64(1), 29–63.
- Brewer, T. F. (2000). Preventing tuberculosis with bacillus calmette-guerin vaccine: a meta-analysis of the literature. *Clinical Infectious Diseases*, 31(Supplement 3), S64–S67.
- Buckler, R. T., Hartzler, H. E., Kurchacova, E., Nichols, G., & Phillips, B. M. (1978). Synthesis and anti-inflammatory activity of some 1,2,3- and 1,2,4-triazolepropionic acids. *Journal of Medicinal Chemistry*, 21(12), 1254–1260.
- Burguière, A., Hitchen, P. G., Dover, L. G., Kremer, L., Ridell, M., Alexander, D. C., Liu, J., Morris, H. R., Minnikin, D. E., Dell, A., et al. (2005). Losa, a key glycosyltransferase involved in the biosynthesis

- of a novel family of glycosylated acyltrehalose lipooligosaccharides from mycobacterium marinum. *Journal of Biological Chemistry*, 280(51), 42124–42133.
- Campbell, I. A. & Bah-Sow, O. (2006). Pulmonary tuberculosis: diagnosis and treatment. *BMJ: British Medical Journal*, 332(7551), 1194.
- Caron, S. (2011). *Practical Synthetic Organic Chemistry: Reactions, Principles, and Techniques*. Wiley.com.
- Case, F. H. (1965). The preparation of hydrazidines and as-triazines related to substituted 2-cyanopyridines. *The Journal of Organic Chemistry*, 30(3), 931–933.
- Chai, B., Qian, X., Cao, S., Liu, H., & Song, G. (2003). Synthesis and insecticidal activity of 1, 2, 4-triazole derivatives. *Arkivoc*, 2, 141–145.
- Chatterjee, D. (1997). The mycobacterial cell wall: structure, biosynthesis and sites of drug action. *Current opinion in Chemical Biology*, 1(4), 579–588.
- Chatterjee, D. & Khoo, K.-H. (2001). The surface glycopeptidolipids of mycobacteria: structures and biological properties. *Cellular and Molecular Life Sciences CMLS*, 58(14), 2018–2042.
- Chung, D. & Hubbard, W. (1969). Hyponatremia in untreated active pulmonary tuberculosis. *The American Review of Respiratory Disease*, 99(4), 595.
- Clader, J. W. (2004). The discovery of ezetimibe: a view from outside the receptor. *Journal of Medicinal Chemistry*, 47(1), 1–9.
- Colditz, G. A., Berkey, C. S., Mosteller, F., Brewer, T. F., Wilson, M. E., Burdick, E., & Fineberg, H. V. (1995). The efficacy of bacillus calmette-guerin vaccination of newborns and infants in the prevention of tuberculosis: meta-analyses of the published literature. *Pediatrics*, 96(1), 29–35.
- Coleman, M. D., Rathbone, D. L., Abberley, L., Lambert, P. A., & Billington, D. C. (1999). Preliminary in vitro toxicological evaluation of a series of 2-pyridylcarboxamidrazone candidate anti-tuberculosis compounds. *Environmental Toxicology and Pharmacology*, 7, 59–65.
- Coleman, M. D., Rathbone, D. L., Chima, R., Lambert, P. A., & Billington, D. C. (2001). Preliminary in vitro toxicological evaluation of a series of 2-pyridylcarboxamidrazone candidate anti-tuberculosis compounds iii. *Environmental Toxicology and Pharmacology*, 9, 99–102.

- Coleman, M. D., Rathbone, D. L., Endersby, C. R., Hovey, M. C., Tims, K. J., Lambert, P. A., & Billington, D. C. (2000). Preliminary in vitro toxicological evaluation of a series of 2-pyridylcarboxamidrazone candidate anti-tuberculosis compounds: ii. *Environmental Toxicology and Pharmacology*, *8*, 167–172.
- Collins, D. M., Skou, B., White, S., Bassett, S., Collins, L., Hurr, K., Hotter, G., de Lisle, G. W., et al. (2005). Generation of attenuated mycobacterium bovis strains by signature-tagged mutagenesis for discovery of novel vaccine candidates. *Infection and Immunity*, *73*(4), 2379–2386.
- Comstock, G. (2000). Epidemiology of tuberculosis. *Lung Biology in Health and Disease*, *144*, 129–156.
- Cox, H., Kebede, Y., Allamuratova, S., Ismailov, G., Davletmuratova, Z., Byrnes, G., Stone, C., Niemann, S., Rüscher-Gerdes, S., Blok, L., et al. (2006). Tuberculosis recurrence and mortality after successful treatment: impact of drug resistance. *PLoS Medicine*, *3*(10), e384.
- Cox, J. S., Chen, B., McNeil, M., & Jacobs, W. R. (1999). Complex lipid determines tissue-specific replication of mycobacterium tuberculosis in mice. *Nature*, *402*(6757), 79–83.
- Crellin, P. K., Luo, C.-Y., & Morita, Y. S. (2013). Metabolism of plasma membrane lipids in mycobacteria and corynebacteria.
- Crick, D. C., Mahapatra, S., & Brennan, P. J. (2001). Biosynthesis of the arabinogalactan-peptidoglycan complex of mycobacterium tuberculosis. *Glycobiology*, *11*(9), 107R–118R.
- Crout, D. & Rathbone, D. (1989). Synthesis of 2-hydroxy-3-oxocarboxylic esters from the corresponding α , β -unsaturated esters by a simple one-step procedure. *Synthesis*, *1989*(01), 40–42.
- Crout, D. H. & Rathbone, D. L. (1987). Catalysis by di-n-butyltin oxide of a tertiary ketol rearrangement: synthesis of intermediates and analogues of valine and isoleucine biosynthesis. *Journal of the Chemical Society, Chemical Communications*, (4), 290–291.
- Curtis, A. & Jennings, N. (2008). 5.02 - 1,2,4-triazoles. In A. R. Katritzky, C. A. Ramsden, E. F. Scriven, & R. J. Taylor (Eds.), *Comprehensive Heterocyclic Chemistry III* (pp. 159 – 209). Oxford: Elsevier.
- Daffe, M., Brennan, P. J., & McNeil, M. (1990). Predominant structural features of the cell wall arabinogalactan of mycobacterium tuberculosis as revealed through characterization of oligoglycosyl alditol fragments by gas chromatography/mass spectrometry and by ^1H and ^{13}C nmr analyses. *Journal of Biological Chemistry*, *265*(12), 6734–6743.

- Daffé, M. & Lanéelle, M. (1988). Distribution of phthiocerol diester, phenolic mycosides and related compounds in mycobacteria. *Journal of General Microbiology*, 134(7), 2049–2055.
- Daffe, M., Laneelle, M., & Lacave, C. (1991). Structure and stereochemistry of mycolic acids of *Mycobacterium marinum* and *Mycobacterium ulcerans*. *Research in Microbiology*, 142(4), 397–403.
- Daffé, M., Lanéelle, M., Puzo, G., & Asselineau, C. (1981). Acide mycolique epoxydique: un nouveau type d'acide mycolique. *Tetrahedron Letters*, 22(45), 4515–4516.
- Daffe, M., McNeil, M., & Brennan, P. J. (1991). Novel type-specific lipooligosaccharides from mycobacterium tuberculosis. *Biochemistry*, 30(2), 378–388.
- Doetsch, R. N. (1978). Benjamin marten and his "new theory of consumptions". *Microbiological Reviews*, 42(3), 521.
- Doyle, K. & Kurzer, F. (1976). Chemistry of amidrazones-iv: Addition-cyclisation of amidrazones with isocyanate esters and ethoxycarbonyl isothiocyanate. *Tetrahedron*, 32(19), 2347–2352.
- Dubnau, E., Chan, J., Raynaud, C., Mohan, V. P., Lanéelle, M.-A., Yu, K., Quemard, A., Smith, I., & Daffé, M. (2000). Oxygenated mycolic acids are necessary for virulence of mycobacterium tuberculosis in mice. *Molecular Microbiology*, 36(3), 630–637.
- Duran, A., Dogan, H., & Rollas, S. (2002). Synthesis and preliminary anticancer activity of new 1, 4-dihydro-3-(3-hydroxy-2-naphthyl)-4-substituted-5H-1, 2, 4-triazoline-5-thiones. *Farmaco II*, 57(7), 559–564.
- Ebrahim, O., Folb, P., Robson, S., & Jacobs, P. (1995). Blunted erythropoietin response to anaemia in tuberculosis. *European Journal of Haematology*, 55(4), 251–254.
- Eloy, F., Lenaers, R., & Moussebois, C. (1961). Synthesis of unsubstituted and monosubstituted 1, 2, 4-oxadiazoles. *Chemistry & Industry*, 292–292.
- Enomoto, Y., Sugita, M., Matsunaga, I., Naka, T., Sato, A., Kawashima, T., Shimizu, K., Takahashi, H., Norose, Y., & Yano, I. (2005). Temperature-dependent biosynthesis of glucose monomycolate and its recognition by cd1-restricted t cells. *Biochemical and Biophysical Research Communications*, 337(2), 452–456.
- Fischer, E. (1878). Ueber die hydrazinverbindungen; erste abhandlung. *Justus Liebigs Annalen der Chemie*, 190(1-2), 67–183.

- Fogerty, A., Johnson, A., & Pearson, J. (1972). Ring position in cyclopropene fatty acids and stearic acid desaturation in hen liver. *Lipids*, 7(5), 335–338.
- Foroumadi, A., Kiani, Z., & Soltani, F. (2003). Antituberculosis agents viii: Synthesis and in vitro antimycobacterial activity of alkyl α -[5-(5-nitro-2-thienyl)-1, 3, 4-thiadiazole-2-ylthio] acetates. *Farmaco II*, 58(11), 1073–1076.
- Fox, H. H. & Gibas, J. T. (1952). Synthetic tuberculostats. iv. pyridine carboxylic acid hydrazides and benzoic acid hydrazides. *The Journal of Organic Chemistry*, 17(12), 1653–1660.
- Foye, W. O., Lemke, T. L., & Williams, D. A. (2008). *Foye's principles of medicinal chemistry*. Lippincott Williams & Wilkins.
- Gastambide-Odier, M., Sarda, P., & Lederer, E. (1967). Biosynthesis of the aglycons of mycosides a and b]. *Bulletin de la Société de chimie biologique*, 49(7), 849.
- Georghiou, S. B., Magana, M., Garfein, R. S., Catanzaro, D. G., Catanzaro, A., & Rodwell, T. C. (2012). Evaluation of genetic mutations associated with mycobacterium tuberculosis resistance to amikacin, kanamycin and capreomycin: a systematic review. *PloS one*, 7(3), e33275.
- Ginsburg, A. S., Grosset, J. H., & Bishai, W. R. (2003). Fluoroquinolones, tuberculosis, and resistance. *The Lancet Infectious Diseases*, 3(7), 432–442.
- Goffin, C. & Ghuysen, J.-M. (2002). Biochemistry and comparative genomics of sxxk superfamily acyltransferases offer a clue to the mycobacterial paradox: presence of penicillin-susceptible target proteins versus lack of efficiency of penicillin as therapeutic agent. *Microbiology and Molecular Biology Reviews*, 66(4), 702–738.
- Goren, M. B., Brokl, O., Roller, P., Fales, H. M., & Das, B. C. (1976). Sulfatides of mycobacterium tuberculosis: the structure of the principal sulfatide (sl-i). *Biochemistry*, 15(13), 2728–2735.
- Grout, R. J. (1975). *Biological reactions and pharmaceutical uses of imidic acid derivatives*, (pp. 255–281). John Wiley & Sons, Ltd.
- Gülerman, N., Doğan, H., Rollas, S., Johansson, C., & Celik, C. (2001). Synthesis and structure elucidation of some new thioether derivatives of 1, 2, 4-triazoline-3-thiones and their antimicrobial activities. *Farmaco II*, 56(12), 953–958.
- Gurs, K. (1976). Method of separating isotopes. US Patent 3,951,768.

- Hann, M. M. & Keserü, G. M. (2012). Finding the sweet spot: the role of nature and nurture in medicinal chemistry. *Nature Reviews Drug Discovery*, 11(5), 355–365.
- Hanna, L. E., Bose, J. C., Nayak, K., Subramanyam, S., & Swaminathan, S. (2005). Short communication: Influence of active tuberculosis on chemokine and chemokine receptor expression in hiv-infected persons. *AIDS Research & Human Retroviruses*, 21(12), 997–1002.
- Hellmann, H., Piechota, H., & Schwiersch, W. (1961). Über 1.2. 4-oxdiazole, i: Synthese von 1.2. 4-oxdiazol-carbonsäure-(3)-estern. *Chemische Berichte*, 94(3), 757–761.
- Hemming, K. (2008). 5.04 - 1,2,4-oxadiazoles. In A. R. Katritzky, C. A. Ramsden, E. F. Scriven, & R. J. Taylor (Eds.), *Comprehensive Heterocyclic Chemistry III* (pp. 243 – 314). Oxford: Elsevier.
- Hershkovitz, I., Donoghue, H. D., Minnikin, D. E., Besra, G. S., Lee, O. Y., Gernaey, A. M., Galili, E., Eshed, V., Greenblatt, C. L., Lemma, E., et al. (2008). Detection and molecular characterization of 9000-year-old mycobacterium tuberculosis from a neolithic settlement in the eastern mediterranean. *PloS one*, 3(10), e3426.
- Herzog, B. H. (1998). History of tuberculosis. *Respiration*, 65(1), 5–15.
- Holla, B., Gonsalves, R., & Shenoy, S. (2000). Synthesis and antibacterial studies of a new series of 1,2-bis(1,3,4-oxadiazol-2-yl)ethanes and 1,2-bis(4-amino-1,2,4-triazol-3-yl)ethanes. *European Journal of Medicinal Chemistry*, 35(2), 267 – 271.
- Horwitz, M. A. (2005). Recombinant bcg expressing *Mycobacterium tuberculosis* major extracellular proteins. *Microbes and Infection*, 7(5), 947–954.
- Jalilian, A. R., Sattari, S., Bineshmarvasti, M., Shafiee, A., & Daneshtalab, M. (2000). Synthesis and in vitro antifungal and cytotoxicity evaluation of thiazolo-4h-1, 2, 4-triazoles and 1, 2, 3-thiadiazolo-4h-1, 2, 4-triazoles. *Archiv der Pharmazie*, 333(10), 347–354.
- Jeffcoat, R. & Pollard, M. (1977). Studies on the inhibition of the desaturases by cyclopropenoid fatty acids. *Lipids*, 12(6), 480–485.
- Ji, Y., Brueckl, T., Baxter, R. D., Fujiwara, Y., Seiple, I. B., Su, S., Blackmond, D. G., & Baran, P. S. (2011). Innate c-h trifluoromethylation of heterocycles. *Proceedings of the National Academy of Sciences*, 108(35), 14411–14415.

- Kan-Sutton, C., Jagannath, C., & Hunter, R. L. (2009). Trehalose 6, 6'-dimycolate on the surface of *Mycobacterium tuberculosis* modulates surface marker expression for antigen presentation and costimulation in murine macrophages. *Microbes and Infection*, 11(1), 40–48.
- Kappelman, J., Alçiçek, M. C., Kazancı, N., Schultz, M., Özkul, M., & Şen, Ş. (2008). First homo erectus from turkey and implications for migrations into temperate eurasia. *American Journal of Physical Anthropology*, 135(1), 110–116.
- Katsube, T., Matsumoto, S., Takatsuka, M., Okuyama, M., Ozeki, Y., Naito, M., Nishiuchi, Y., Fujiwara, N., Yoshimura, M., Tsuboi, T., et al. (2007). Control of cell wall assembly by a histone-like protein in mycobacteria. *Journal of Bacteriology*, 189(22), 8241–8249.
- Khan, N. B. (2008). *Design and synthesis of potential antimicrobial agents*. PhD thesis, Aston University, Birmingham.
- Kim, T. C., Blackman, R., Heatwole, K., Kim, T., & Rochester, D. (1984). Acid-fast bacilli in sputum smears of patients with pulmonary tuberculosis: prevalence and significance of negative smears pretreatment and positive smears post-treatment. *The American Review of Respiratory Disease*, 129(2), 264–268.
- Kitaev, Y. P., Buzykin, B. I., & Troepol'skaya, T. V. (1970). The structure of hydrazones. *Russian Chemical Reviews*, 39(6), 441–456.
- Kjell, D. P., Slattery, B. J., & Semo, M. J. (1999). A novel, nonaqueous method for regeneration of aldehydes from bisulfite adducts. *The Journal of Organic Chemistry*, 64(15), 5722–5724.
- Kobarfard, F. & Kauffman, J. M. (2003). Halogenated antituberculosis agents. US Patent 6,624,153.
- Kritsanida, M., Mouroutsou, A., Marakos, P., Pouli, N., Papakonstantinou-Garoufalias, S., Pan-necouque, C., Witvrouw, M., & De Clercq, E. (2002). Synthesis and antiviral activity evaluation of some new 6-substituted 3-(1-adamantyl)-1, 2, 4-triazolo [3, 4-b][1, 3, 4] thiadiazoles. *Farmaco II*, 57(3), 253–257.
- Küçükgülzel, İ., Güniz Küçükgülzel, Ş., Rollas, S., Ötük-Sarış, G., Özdemir, O., Bayrak, İ., Altuğ, T., & Stables, J. P. (2004). Synthesis of some 3-(arylalkylthio)-4-alkyl/aryl-5-(4-aminophenyl)-4h-1, 2, 4-triazole derivatives and their anticonvulsant activity. *Farmaco II*, 59(11), 893–901.

- Küçükgül, I., Küçükgül, S. G., Rollas, S., & Kiraz, M. (2001). Some 3-thioxo/alkylthio-1, 2, 4-triazoles with a substituted thiourea moiety as possible antimycobacterials. *Bioorganic & Medicinal Chemistry Letters*, *11*(13), 1703–1707.
- Kumar, P., Schelle, M. W., Jain, M., Lin, F. L., Petzold, C. J., Leavell, M. D., Leary, J. A., Cox, J. S., & Bertozzi, C. R. (2007). Papa1 and papa2 are acyltransferases essential for the biosynthesis of the mycobacterium tuberculosis virulence factor sulfolipid-1. *Proceedings of the National Academy of Sciences*, *104*(27), 11221–11226.
- Kumar, R. R., Perumal, S., Menéndez, J. C., Yogeeswari, P., & Sriram, D. (2011). Antimycobacterial activity of novel 1,2,4-oxadiazole-pyranopyridine/chromene hybrids generated by chemoselective 1,3-dipolar cycloadditions of nitrile oxides. *Bioorganic & Medicinal Chemistry*, *19*(11), 3444 – 3450.
- Kushner, S., Dalalian, H., Sanjurjo, J., Bach Jr, F., Safir, S., Smith Jr, V., & Williams, J. (1952). Experimental chemotherapy of tuberculosis. ii. the synthesis of pyrazinamides and related compounds. *Journal of the American Chemical Society*, *74*(14), 3617–3621.
- Labanauskas, L., Udrenaitė, E., Gaidelis, P., & Brukštus, A. (2004). Synthesis of 5-(2-, 3- and 4-methoxyphenyl)-4H-1, 2, 4-triazole-3-thiol derivatives exhibiting anti-inflammatory activity. *Farmaco*, *59*(4), 255–259.
- Lacave, C., Lanéelle, M.-A., Daffé, M., Montrozier, H., Rols, M.-P., & Asselineau, C. (1987). Etude structurale et métabolique des acides mycoliques de mycobacterium fortuitum. *European Journal of Biochemistry*, *163*(2), 369–378.
- Langlois, B. R., Laurent, E., & Roidot, N. (1991). Trifluoromethylation of aromatic compounds with sodium trifluoromethanesulfinate under oxidative conditions. *Tetrahedron Letters*, *32*(51), 7525 – 7528.
- Lenaers, R., Moussebois, C., & Eloy, F. (1962). Synthèse du dérivé diméthylé et de quelques dérivés monosubstitués de l'oxadiazole-1, 2, 4. *Helvetica Chimica Acta*, *45*(2), 441–446.
- Levy, S. & Andreocci, A. (1888). Ueber dichlorterephtalsäure und dichlordihydroterephtasäure. *Berichte der deutschen chemischen Gesellschaft*, *21*(1), 1959–1964.
- Libman, D. D. & Slack, R. (1956). Congeners of pyridine-4-carboxyhydrazide. part i. derivatives of 4-cyanopyridine and 2-cyanothiazole. *Journal of the Chemical Society*, 2253–2257.

- Lima, V. M., Bonato, V. L., Lima, K. M., Dos Santos, S. A., Dos Santos, R. R., Gonçalves, E. D., Faccioli, L. H., Brandão, I. T., Rodrigues-Junior, J. M., & Silva, C. L. (2001). Role of trehalose dimycolate in recruitment of cells and modulation of production of cytokines and no in tuberculosis. *Infection and Immunity*, 69(9), 5305–5312.
- Luquin, M., Roussel, J., Lopez-calahorra, F., Lanéelle, G., Ausina, V., & Lanéelle, M.-A. (1990). A novel mycolic acid in a mycobacterium sp. from the environment. *European Journal of Biochemistry*, 192(3), 753–759.
- Madigan, M. T. (2005). Brock biology of microorganisms, 11th edn. *International Microbiology*, 8, 149–152.
- Mamolo, M. & Vio, L. (1996). Synthesis and antimycobacterial activity of some indole derivatives of pyridine-2-carboxamidrazone and quinoline-2-carboxamidrazone. *Farmaco II*, 51, 65–70.
- Mamolo, M., Vio, L., Banfi, E., Predominato, M., Fabris, C., & Asaro, F. (1992). Synthesis and antimycobacterial activity of some 2-pyridinecarboxamidrazone derivatives. *Farmaco II*, 47(7), 1055–1066.
- Mamolo, M., Vio, L., Banfi, E., Predominato, M., Fabris, C., & Asaro, F. (1993). Synthesis and antimycobacterial activity of some 4-pyridinecarboxamidrazone derivatives. *Farmaco II*, 48(4), 529–538.
- McKeown, T., Lowe, C. R., et al. (1966). An introduction to social medicine. *An Introduction to Social Medicine*.
- McNeil, M., Daffe, M., & Brennan, P. J. (1990). Evidence for the nature of the link between the arabinogalactan and peptidoglycan of mycobacterial cell walls. *Journal of Biological Chemistry*, 265(30), 18200–18206.
- Mihina, J. S. & Herbst, R. M. (1950). The reaction of nitriles with hydrazoic acid: Synthesis of monosubstituted tetrazoles. *Journal of Organic Chemistry*, 15(5), 1082–1092.
- Miller, L. G., Asch, S. M., Emily, I. Y., Knowles, L., Gelberg, L., & Davidson, P. (2000). A population-based survey of tuberculosis symptoms: how atypical are atypical presentations? *Clinical Infectious Diseases*, 30(2), 293–299.
- Minnikin, D. & Polgar, N. (1967a). The methoxymycolic and ketomycolic acids from human tubercle bacilli. *Chemical Communications (London)*, (22), 1172–1174.
- Minnikin, D. & Polgar, N. (1967b). The mycolic acids from human and avian tubercle bacilli. *Chemical Communications (London)*, (18), 916–918.

- Minnikin, D. E. (1982). Lipids: complex lipids, their chemistry, biosynthesis and roles. *The Biology of the Mycobacteria*, 1, 95–184.
- Minnikin, D. E., Kremer, L., Dover, L. G., & Besra, G. S. (2002). The methyl-branched fortifications of *Mycobacterium tuberculosis*. *Chemistry & Biology*, 9(5), 545–553.
- Montgomery, J. A. & Hewson, K. (1957). Synthesis of potential anticancer agents. x. 2-fluoroadenosine1. *Journal of the American Chemical Society*, 79(16), 4559–4559.
- Moody, D. B., Reinhold, B. B., Guy, M. R., Beckman, E. M., Frederique, D. E., Furlong, S. T., Ye, S., Reinhold, V. N., Sieling, P. A., Modlin, R. L., et al. (1997). Structural requirements for glycolipid antigen recognition by cd1b-restricted t cells. *Science*, 278(5336), 283–286.
- Morrison, R. & Boyd, R. (1992). *Organic chemistry*. ORGANIC CHEMISTRY. Prentice Hall.
- Moussebois, C., Lenaers, R., & Eloy, F. (1962). Synthèse de l'oxadiazole-1, 2, 4. *Helvetica Chimica Acta*, 45(2), 446–449.
- Nagahara, K. & Takada, A. (1982). A synthesis of n-(4'-quinazolone-3'-yl)-2-pyridinecarboxamides and their conversion into 1,2,4-triazoles. *Heterocycles*, 19, 1565.
- Nagib, D. A. & MacMillan, D. W. (2011). Trifluoromethylation of arenes and heteroarenes by means of photoredox catalysis. *Nature*, 480(7376), 224–228.
- Neilson, D. G., Roger, R., Heatlie, J. W. M., & Newlands, L. R. (1970). The chemistry of amidrazones. *Chemical Reviews*, 70(1), 151–170.
- Obermeyer, Z., Abbott-Klafter, J., & Murray, C. J. (2008). Has the dots strategy improved case finding or treatment success? an empirical assessment. *PLoS One*, 3(3), e1721.
- Omura, K. & Swern, D. (1978). Oxidation of alcohols by "activated" dimethyl sulfoxide. a preparative, steric and mechanistic study. *Tetrahedron*, 34(11), 1651–1660.
- Organization, W. H. et al. (2010). Multidrug and extensively drug-resistant tb (m/xdr-tb): 2010 global report on surveillance and response. *Geneva: World Health Organization*.
- Organization, W. H. et al. (2011). Tuberculosis fact sheet n 104 november 2010.
- Papakonstantinou-Garoufalias, S., Pouli, N., Marakos, P., & Chytyroglou-Ladas, A. (2002). Synthesis antimicrobial and antifungal activity of some new 3-substituted derivatives of 4-(2, 4-dichlorophenyl)-5-adamantyl-1H-1, 2, 4-triazole. *Farmaco II*, 57(12), 973–977.

- Patterson, J. H., McConville, M. J., Haites, R. E., Coppel, R. L., & Billman-Jacobe, H. (2000). Identification of a methyltransferase from mycobacterium smegmatis involved in glycopeptidolipid synthesis. *Journal of Biological Chemistry*, 275(32), 24900–24906.
- Prasad, H. K., Mishra, R. S., & Nath, I. (1987). Phenolic glycolipid-i of mycobacterium leprae induces general suppression of in vitro concanavalin a responses unrelated to leprosy type. *The Journal of Experimental Medicine*, 165(1), 239–244.
- Prosser, G. A. & Carvalho, L. P. S. (2013). Kinetic mechanism and inhibition of mycobacterium tuberculosis d-alanine: d-alanine ligase by the antibiotic d-cycloserine. *FEBS Journal*, 280(4), 1150–1166.
- Qureshi, N., Takayama, K., Seydel, U., Wang, R., Cotter, R., Agrawal, P., Bush, C., Kurtz, R., & Berman, D. (1994). Structural analysis of the lipid a derived from the lipopolysaccharide of brucella abortus. *Journal of Endotoxin Research*, 1(3), 137–148.
- Rabea, S. M., El-Koussi, N. A., Hassan, H. Y., & Aboul-Fadl, T. (2006). Synthesis of 5-phenyl-1-(3-pyridyl)-1h-1, 2, 4-triazole-3-carboxylic acid derivatives of potential anti-inflammatory activity. *Archiv der Pharmazie*, 339(1), 32–40.
- Raman, K., Rajagopalan, P., & Chandra, N. (2005). Flux balance analysis of mycolic acid pathway: targets for anti-tubercular drugs. *PLoS Computational Biology*, 1(5), e46.
- Rao, V., Fujiwara, N., Porcelli, S. A., & Glickman, M. S. (2005). Mycobacterium tuberculosis controls host innate immune activation through cyclopropane modification of a glycolipid effector molecule. *The Journal of Experimental Medicine*, 201(4), 535–543.
- Rao, V., Gao, F., Chen, B., Jacobs, W. R., Glickman, M. S., et al. (2006). Trans-cyclopropanation of mycolic acids on trehalose dimycolate suppresses mycobacterium tuberculosis-induced inflammation and virulence. *Journal of Clinical Investigation*, 116(6), 1660–1667.
- Rathbone, D. L., Parker, K. J., Coleman, M. D., Lambert, P. A., & Billington, D. C. (2006). Discovery of a potent phenolic N1 -benzylidene-pyridinecarboxamidrazone selective against gram-positive bacteria. *Bioorganic & Medicinal Chemistry Letters*, 16, 879–883.
- Raviglione, M. C., Snider Jr, D. E., & Kochi, A. (1995). Global epidemiology of tuberculosis. *JAMA: The Journal of the American Medical Association*, 273(3), 220–226.
- Reading, C. L. & Wien, F. (2009). *Health Inequalities and the Social Determinants of Aboriginal Peoples' Health*. National Collaborating Centre for Aboriginal Health Prince George, BC.

- Reed, M. B., Domenech, P., Manca, C., Su, H., Barczak, A. K., Kreiswirth, B. N., Kaplan, G., & Barry, C. E. (2004). A glycolipid of hypervirulent tuberculosis strains that inhibits the innate immune response. *Nature*, *431*(7004), 84–87.
- Reed, S. G., Coler, R. N., Dalemans, W., Tan, E. V., Cruz, E. C. D., Basaraba, R. J., Orme, I. M., Skeiky, Y. A., Alderson, M. R., Cowgill, K. D., et al. (2009). Defined tuberculosis vaccine, mtb72f/as02a, evidence of protection in cynomolgus monkeys. *Proceedings of the National Academy of Sciences*, *106*(7), 2301–2306.
- Ren, J. (2009). *Computer-Aided Design, Synthesis and Screening of Potential Anti-Microbial Compounds*. PhD thesis, Aston University, Birmingham.
- Rothschild, B. M., Martin, L. D., Lev, G., Bercovier, H., Bar-Gal, G. K., Greenblatt, C., Donoghue, H., Spigelman, M., & Brittain, D. (2001). Mycobacterium tuberculosis complex dna from an extinct bison dated 17,000 years before the present. *Clinical Infectious Diseases*, *33*(3), 305–311.
- Rousseau, C., Winter, N., Pivert, E., Bordat, Y., Neyrolles, O., Avé, P., Huerre, M., Gicquel, B., & Jackson, M. (2004). Production of phthiocerol dimycocerosates protects mycobacterium tuberculosis from the cidal activity of reactive nitrogen intermediates produced by macrophages and modulates the early immune response to infection. *Cellular Microbiology*, *6*(3), 277–287.
- Rozwarski, D. A., Grant, G. A., Barton, D. H., Jacobs Jr, W. R., & Sacchettini, J. C. (1998). Modification of the nadh of the isoniazid target (inba) from mycobacterium tuberculosis. *Science*, *279*(5347), 98–102.
- Ryll, R., Kumazawa, Y., Yano, I., et al. (2001). Immunological properties of trehalose dimycolate (cord factor) and other mycolic acid-containing glycolipids—a review. *Microbiology and Immunology*, *45*(12), 801.
- Schatz, A., Bugle, E., & Waksman, S. A. (1944). Streptomycin, a substance exhibiting antibiotic activity against gram-positive and gram-negative bacteria?. In *Proceedings of the Society for Experimental Biology and Medicine*. Society for Experimental Biology and Medicine (New York, NY), volume 55, (pp. 66–69). Royal Society of Medicine.
- Schloss, J. V., Van Dyk, D. E., Vasta, J. F., & Kutny, R. M. (1985). Purification and properties of salmonella typhimurium acetolactate synthase isozyme ii from escherichia coli hb101/pdu9. *Biochemistry*, *24*(18), 4952–4959.

- Shafiee, A., Sayadi, A., Roozbahani, M. H., Foroumadi, A., & Kamal, F. (2002). Synthesis and in vitro antimicrobial evaluation of 5-(1-methyl-5-nitro-2-imidazolyl)-4h-1, 2, 4-triazoles. *Archiv der Pharmazie*, 335(10), 495–499.
- Sharma, S., Gangal, S., Rauf, A., & Zahin, M. (2008). Synthesis, antibacterial and antifungal activity of some novel 3, 5-disubstituted-1h-1, 2, 4-triazoles. *Archiv der Pharmazie*, 341(11), 714–720.
- Shivarama Holla, B., Veerendra, B., Shivananda, M., & Poojary, B. (2003). Synthesis characterization and anticancer activity studies on some mannich bases derived from 1, 2, 4-triazoles. *European Journal of Medicinal Chemistry*, 38(7), 759–767.
- Shriner, R. L. (1942). The reformatsky reaction. *Organic Reactions*.
- Sikdar, S. (2010). *Design and synthesis of potential antimicrobial agents*. PhD thesis, Aston University, Birmingham.
- Sorg, J. A. & Sonenshein, A. L. (2008). Bile salts and glycine as cogerminants for clostridium difficile spores. *Journal of Bacteriology*, 190(7), 2505–2512.
- Spotts, C. R. & Stanier, R. (1961). Mechanism of streptomycin action on bacteria: a unitary hypothesis. *Nature*, 192, 633–637.
- Suarez, J., Ranguelova, K., Jarzecki, A. A., Manzerova, J., Krymov, V., Zhao, X., Yu, S., Metlitsky, L., Gerfen, G. J., & Magliozzo, R. S. (2009). An oxyferrous heme/protein-based radical intermediate is catalytically competent in the catalase reaction of mycobacterium tuberculosis catalase-peroxidase (katg). *Journal of Biological Chemistry*, 284(11), 7017–7029.
- Sukhova, E. Need for psychological correction in patients with pulmonary tuberculosis]. *Problemy tuberkuleza i boleznei legkikh*.
- Takayama, K. & Kilburn, J. (1989). Inhibition of synthesis of arabinogalactan by ethambutol in mycobacterium smegmatis. *Antimicrobial Agents and Chemotherapy*, 33(9), 1493–1499.
- Takayama, K. & Qureshi, N. (1984). The mycobacteria: a sourcebook.
- Takayama, K., Wang, C., & Besra, G. S. (2005). Pathway to synthesis and processing of mycolic acids in mycobacterium tuberculosis. *Clinical Microbiology Reviews*, 18(1), 81–101.

- Tanaka, A., Motoyama, Y., & Takasugi, H. (1994). Studies on anti-platelet agents. iv: A series of 2-substituted 4, 5-bis (4-methoxyphenyl) pyrimidines as novel anti-platelet agents. *Chemical and Pharmaceutical Bulletin*, 42(9), 1828–1834.
- Tchilian, E., Desel, C., Forbes, E., Bandermann, S., Sander, C., Hill, A., & McShane, H. und kaufmann, sh (2009): Immunogenicity and protective efficacy of prime-boost regimens with recombinant (Δ) urec hly+ mycobacterium bovis bcg and modified vaccinia virus ankara expressing m. tuberculosis antigen 85a against murine tuberculosis. *Infect Immun*, 77(2), 622–31.
- Telenti, A., Philipp, W. J., Sreevatsan, S., Bernasconi, C., Stockbauer, K. E., Wieles, B., Musser, J. M., & Jacobs, W. R. (1997). The emb operon, a gene cluster of mycobacterium tuberculosis involved in resistance to ethambutol. *Nature Medicine*, 3(5), 567–570.
- Theodoridis, G. (2006). Chapter 4 fluorine-containing agrochemicals: An overview of recent developments. In A. Tressaud (Ed.), *Fluorine and the Environment Agrochemicals, Archaeology, Green Chemistry & Water*, volume 2 of *Advances in Fluorine Science* (pp. 121 – 175). Elsevier.
- Thiele, J. (1892). Nitroguanidine. *Liebigs Ann*, 270, 16.
- Tiemann, F. & Krüger, P. (1884). Ueber amidoxime und azoxime. *Berichte der deutschen chemischen Gesellschaft*, 17(2), 1685–1698.
- Tims, K. (2002). *Automated synthesis and evaluation of potential new anti-microbial agents*. PhD thesis, Aston University, Birmingham.
- Toman, K. & Frieden, T. (2004). *Toman's Tuberculosis: case detection, treatment, and monitoring: questions and answers*. Who.
- Toossi, Z. (2003). Virological and immunological impact of tuberculosis on human immunodeficiency virus type 1 disease. *Journal of Infectious Diseases*, 188(8), 1146–1155.
- Tozkoparan, B., Küpeli, E., Yeşilada, E., & Ertan, M. (2007). Preparation of 5-aryl-3-alkylthio-1, 2, 4-triazoles and corresponding sulfones with antiinflammatory–analgesic activity. *Bioorganic & Medicinal Chemistry*, 15(4), 1808–1814.
- Tripathi, K. (2013). *Essentials of medical pharmacology*. JP Medical Ltd.
- Turan-Zitouni, G., Kaplancıklı, Z. A., Yıldız, M. T., Chevallet, P., & Kaya, D. (2005). Synthesis and antimicrobial activity of 4-phenyl/cyclohexyl-5-(1-phenoxyethyl)-3-[N-(2-thiazolyl)acetamido]thio-4h-1,2,4-triazole derivatives. *European Journal of Medicinal Chemistry*, 40(6), 607 – 613.

- Turan-Zitouni, G., Sivacı, M., Kılıç, F. S., & Erol, K. (2001). Synthesis of some triazolyl-antipyrene derivatives and investigation of analgesic activity. *European Journal of Medicinal Chemistry*, 36(7), 685–689.
- Vachula, M., Holzer, T., & Andersen, B. (1989). Suppression of monocyte oxidative response by phenolic glycolipid i of mycobacterium leprae. *The Journal of Immunology*, 142(5), 1696–1701.
- van Heijenoort, J. (2001). Formation of the glycan chains in the synthesis of bacterial peptidoglycan. *Glycobiology*, 11(3), 25R–36R.
- van Roermund, C. W., Hetteema, E. H., Kal, A. J., van den Berg, M., Tabak, H. F., & Wanders, R. J. (1998). Peroxisomal β -oxidation of polyunsaturated fatty acids in *saccharomyces cerevisiae*: isocitrate dehydrogenase provides nadph for reduction of double bonds at even positions. *The EMBO journal*, 17(3), 677–687.
- Varvaresou, A., Siatra-Papastaikoudi, T., Tsotinis, A., Tsantili-Kakoulidou, A., & Vamvakides, A. (1998). Synthesis, lipophilicity and biological evaluation of indole-containing derivatives of 1, 3, 4-thiadiazole and 1, 2, 4-triazole. *Farmaco II*, 53(5), 320–326.
- Vereshchagina, N. N., Melkozerova, G. S., Frolova, N. N., Bedrin, A. V., & Postovskii, I. Y. (1973). Synthesis and tuberculostatic activity of some new 2-benzimidazolyl derivatives. *Pharmaceutical Chemistry Journal*, 7(6), 350–352.
- Villeneuve, C., Gilleron, M., Maridonneau-Parini, I., Daffé, M., Astarie-Dequeker, C., & Etienne, G. (2005). Mycobacteria use their surface-exposed glycolipids to infect human macrophages through a receptor-dependent process. *Journal of Lipid Research*, 46(3), 475–483.
- Wadsworth, W. & Emmons, W. D. (1965). Ethyl cyclohexylideneacetate. *Organic Syntheses*, 44–44.
- Wadsworth, W. S. (1977). Synthetic applications of phosphoryl-stabilized anions. *Organic Reactions*.
- Wadsworth, W. S. & Emmons, W. D. (1961). The utility of phosphonate carbanions in olefin synthesis. *Journal of the American Chemical Society*, 83(7), 1733–1738.
- Walker, K., Brennan, M., Ho, M., Eskola, J., Thiry, G., Sadoff, J., Dobbelaer, R., Grode, L., Liu, M., Fruth, U., et al. (2010). The second geneva consensus: Recommendations for novel live tb vaccines. *Vaccine*, 28(11), 2259–2270.

- Wang, F., Langley, R., Gulten, G., Dover, L. G., Besra, G. S., Jacobs, W. R., & Sacchettini, J. C. (2007). Mechanism of thioamide drug action against tuberculosis and leprosy. *The Journal of Experimental Medicine*, *204*(1), 73–78.
- Wang, J.-Y., Hsueh, P.-R., Jan, I.-S., Lee, L.-N., Liaw, Y.-S., Yang, P.-C., & Luh, K.-T. (2006). Empirical treatment with a fluoroquinolone delays the treatment for tuberculosis and is associated with a poor prognosis in endemic areas. *Thorax*, *61*(10), 903–908.
- Wang, L., Slayden, R. A., Barry III, C. E., & Liu, J. (2000). Cell wall structure of a mutant of mycobacterium smegmatis defective in the biosynthesis of mycolic acids. *Journal of Biological Chemistry*, *275*(10), 7224–7229.
- Waters, W. R., Palmer, M. V., Nonnecke, B. J., Thacker, T. C., Scherer, C. F. C., Estes, D. M., Jr., W. R. J., Glatman-Freedman, A., & Larsen, M. H. (2007). Failure of a mycobacterium tuberculosis Δ rd1 Δ pancd double deletion mutant in a neonatal calf aerosol m. bovis challenge model: Comparisons to responses elicited by m. bovis bacille calmette guerin. *Vaccine*, *25*(45), 7832 – 7840.
- Wehrli, W. (1983). Rifampin: mechanisms of action and resistance. *Review of Infectious Diseases*, *5*(Supplement 3), S407–S411.
- Wheeler, P. R., Besra, G. S., Minnikin, D. E., & Ratledge, C. (1993). Stimulation of mycolic acid biosynthesis by incorporation of cis-tetracos-5-enoic acid in a cell-wall preparation from mycobacterium smegmatis. *Biochimica et Biophysica Acta (BBA) - Lipids and Lipid Metabolism*, *1167*(2), 182 – 188.
- Wheeler, P. R. & Ratledge, C. (1994). Metabolism of mycobacterium tuberculosis. *Tuberculosis: Pathogenesis, Protection, and Control*, 353–385.
- White, S. W., Zheng, J., Zhang, Y.-M., & Rock, C. O. (2005). The structural biology of type ii fatty acid biosynthesis. *Annual Review of Biochemistry*, *74*, 791–831.
- WHO (2009). *Global tuberculosis control 2009: epidemiology, strategy, financing*. World Health Organization.
- WHO (2013). *Global Tuberculosis Report 2012*. WORLD HEALTH ORGN.
- Winder, F., Collins, P., & Whelan, D. (1971). Effects of ethionamide and isoxyl on mycolic acid synthesis in mycobacterium tuberculosis bcg. *Journal of General Microbiology*, *66*(3), 379–380.
- Winder, F. G. (1982). Mode of action of the antimycobacterial agents and associated aspects of the molecular biology of the mycobacteria. *The Biology of the Mycobacteria*, *1*, 353–438.

- Yasuda, K. (1999). Mycobacterium tuberculosis and rhodococcus ruber. *Osaka City Medical Journal*, 45(2), 159–174.
- Zahajska, L., Klimešová, V., Kočí, J., Waisser, K., & Kaustova, J. (2004). Synthesis and antimycobacterial activity of pyridylmethylsulfanyl and naphthylmethylsulfanyl derivatives of benzazoles, 1, 2, 4-triazole, and pyridine-2-carbothioamide/-2-carbonitrile. *Archiv der Pharmazie*, 337(10), 549–555.
- Zhang, Y. & Yew, W. (2009). Mechanisms of drug resistance in mycobacterium tuberculosis [state of the art series. drug-resistant tuberculosis. edited by cy. chiang. number 1 in the series]. *The International Journal of Tuberculosis and Lung Disease*, 13(11), 1320–1330.
- Zimhony, O., Cox, J. S., Welch, J. T., Vilchèze, C., & Jacobs, W. R. (2000). Pyrazinamide inhibits the eukaryotic-like fatty acid synthetase i (fasi) of mycobacterium tuberculosis. *Nature Medicine*, 6(9), 1043–1047.
- Zimhony, O., Vilchèze, C., Arai, M., Welch, J. T., & Jacobs, W. R. (2007). Pyrazinoic acid and its n-propyl ester inhibit fatty acid synthase type i in replicating tubercle bacilli. *Antimicrobial Agents and Chemotherapy*, 51(2), 752–754.
- Zink, A. R., Sola, C., Reischl, U., Grabner, W., Rastogi, N., Wolf, H., & Nerlich, A. G. (2003). Characterization of mycobacterium tuberculosis complex dnas from egyptian mummies by spoligotyping. *Journal of Clinical Microbiology*, 41(1), 359–367.